INTEGRATED ANALYSIS OF LOWER CRETACEOUS STRATIGRAPHY AND DEPOSITIONAL SYSTEMS: THE ESSAOUIRA-AGADIR BASIN OF MOROCCO.

A thesis submitted to the University of Manchester for the degree of Doctor of Philosophy (Ph.D.) in the Faculty of Science and Engineering

2017

Tim L. Luber

School of Earth and Environmental Sciences

TABLE OF CONTENTS

Additonial Material is supplied on a CD medium at the end of this thesis and includes:

- Distribution charts for foraminifera of the Tiskatine section
- Distribution charts for calcareous nannofossils of the Tiskatine section
- Distribution charts for calcareous nannofossils of DSDP borehole 370
- $\delta^{13}C$ data for the Tiskatine section

Final word count (including references): 57,279

LIST OF FIGURES

LIST OF TABLES

LIST OF ABBREVIATIONS

BML – Below mud line

CAM – Central Atlantic Margin

CC – Correlative Conformity

EAB – Essaouira-Agadir Basin

Fm. – Formation

FO – First Occurence

FSST – Falling Stage Systems Tract

GDE – Gross Depositional Environment

HST – Highstand Systems Tract

HUF – Horizon of Faunal Uniformity

ITS – Initial Transgressive Surface

LST – Lowstand Systems Tract

MAM – Massif Ancien de Marrakech

MFS – Maximum Flooding Surface

RSME – Regressive Surface of Marine Erosion

SB – Sequence Boundary

SMAS – Standard Mediterranean Ammonite Scale

SU – Subaerial Unconformity

TSE – Transgressive Surface of Erosion

TST – Transgressive Systems Tract

WAM – West Moroccan Arch

ABSTRACT

INTEGRATED ANALYSIS OF LOWER CRETACEOUS STRATIGRAPHY AND DEPOSITIONAL SYSTEMS: THE ESSAOUIRA-AGADIR BASIN OF MOROCCO.

This multi-disciplinary study integrates high-resolution field sedimentological analysis, biostratigraphy and chemostratigraphy to build a sequence stratigraphic and bio-chronostratigraphic framework of the Lower Cretaceous in the Essaouira-Agadir Basin (EAB) of Morocco. The results provide insight into the controls on coarse siliciclastic sediment delivery along the Northwest African passive continental margin.

This area lies inboard of an underexplored but potentially prolific hydrocarbon province of the Central Atlantic Margin. Recent and past drilling activity has failed to locate commercial reservoirs, highlighting the poor understanding of timing, location, and controls of sediment distribution.

Low-temperature geochronological studies of the hinterland show that provenance terranes have experienced kilometre-scale exhumation during the Late Jurassic and Early Cretaceous. This opens the potential for delivery of a substantial amount of coarse clastic material into the basin. The Lower Cretaceous strata of the west-central EAB, however, is overall characterised by a mud-dominated shelf succession. During the late Barremian to early Aptian, a major shoreline shift placed the shallow marine fluvial transition zone close to the shelf edge. No similar event was recorded throughout the Cretaceous, opening questions on the relative role of eustasy versus tectonics as a driving mechanism along passive margins.

Detailed sequence stratigraphic assessment on the migration of the shoreface and deltaic depositional environments across the shelf identified tectonic control in the hinterland as the main factor for progradation of the shoreline. The amplification through a subsequent eustatic sea-level fall shifted the shoreline even further basinward and leads to the development of forced regressive deposits. The upper Barremian to lowermost Aptian is the key interval for coarse siliciclastic sediment delivery offshore in the EAB.

Detailed correlations, constrained by the high-resolution biostratigraphy, also give important insight into pre-existing structural domains in the basin. The work reveals the presence of palaeohighs throughout the study area, which interacted with fluvial sedimentation during the regression and influenced sediment dispersal.

This work underscores the need for integrated and multi-disciplinary stratigraphic studies to decipher basin evolution and controls on changes in depositional environments. It also questions the paradigm for a largely eustatic control on base-level change along the NW Atlantic margin, adding to the growing body of published literature that identifies a more complex post-rift tectonic history for passive margins.

DECLARATION

No portion of the work referred to in the thesis has been submitted in support of an application for another degree or qualification of this or any other university or other institute of learning.

Tim Leo Luber

September 2017

COPYRIGHT STATEMENT

i. The author of this thesis (including any appendices and/or schedules to this thesis) owns certain copyright or related rights in it (the "Copyright") and s/he has given The University of Manchester certain rights to use such Copyright, including for administrative purposes.

ii. Copies of this thesis, either in full or in extracts and whether in hard or electronic copy, may be made only in accordance with the Copyright, Designs and Patents Act 1988 (as amended) and regulations issued under it or, where appropriate, in accordance with licensing agreements which the University has from time to time. This page must form part of any such copies made.

iii. The ownership of certain Copyright, patents, designs, trademarks and other intellectual property (the "Intellectual Property") and any reproductions of copyright works in the thesis, for example graphs and tables ("Reproductions"), which may be described in this thesis, may not be owned by the author and may be owned by third parties. Such Intellectual Property and Reproductions cannot and must not be made available for use without the prior written permission of the owner(s) of the relevant Intellectual Property and/or Reproductions.

iv. Further information on the conditions under which disclosure, publication and commercialisation of this thesis, the Copyright and any Intellectual Property and/or Reproductions described in it may take place is available in the University IP Policy (see http://documents.manchester.ac.uk/DocuInfo.aspx?DocID=24420), in any relevant Thesis restriction declarations deposited in the University Library, The University Library's regulations (see http://www.library.manchester.ac.uk/about/regulations/) and in The University's policy on Presentation of Theses.

ACKNOWLEDGEMENTS

This study was sponsored by the North Africa Research Group (NARG) and the author would like to acknowledge the support of the sponsoring companies. L'Office National des Hydrocarbures et des Mines (ONHYM), in particular, the Exploration Director Mr Mohammed Nahim, is thanked for their continued logistical and scientific support.

For supervision, during the PhD I would like to thank Dr. Jonathan Redfern, Dr. Luc Bulot, Dr. Giovanni Bertotti and Dr. Stefan Schröder.

Stéphane Bodin, Camille Frau, Jason Jeremiah, Mike Simmons and Moussa Masrour are thanked for their valued input and extensive discussions that improved this work.

The reviewers Miguel Company and Josep A. Moreno Bedmar of the manuscript for chapter 3 are acknowledged for constructive comments and improvements.

Thank you to David Gelsthorpe, Kate Sherburn and the team of the Manchester Museum for curation of all the figured material of this publication.

The Natural History Museum in London is thanked for allowing access to their SEM facility.

Prof. Paul Bown at University College London is thanked for access to nannofossil photographic equipment.

Thank you to all field assistants for their tireless efforts in the field and discussions.

A special thank you to Mark Anderton and Carmen Luber for constructive comments and help in the editing of this thesis.

THESIS PRESENTATION

This thesis has been prepared in the alternative format, according to the standards of the University of Manchester and chapters 3, 4 and 5 have been written for publication in technical journals.

Chapter 1: Introduction

This chapter introduces the aims and rationale for this thesis and outlines the research questions addressed. It is followed by a review of concepts and methods used to answer these questions.

Chapter 2: Geological setting

This chapter introduces the research area and the wider geological setting.

Chapter 3: A revised ammonoid biostratigraphy for the Aptian of NW Africa: Essaouira-Agadir Basin, Morocco

This chapter was published in Cretaceous Research. It establishes a regional biostratigraphic scale based on ammonoids. It forms the foundation for subsequent work establishing a stratigraphic reference section for the Aptian in NW Africa (chapter 4).

Contribution of Co-Authors: Dr. Luc G. Bulot (ammonoid identification, manuscript review), Dr. Jonathan Redfern (discussion, manuscript review), Camille Frau (ammonoid identification, manuscript review), Angel Arantegui (fieldwork assistance, discussion), Dr. Moussa Marour (regional geology, manuscript review)

Chapter 4: A Stratigraphic Reference Section for the Aptian of NW Africa

This chapter was submitted for publication to Cretaceous Research. It establishes a stratigraphic reference section for the Aptian in NW Africa that enables us to time important stratigraphic events and correlate them on a regional and inter-regional scale (chapter 5).

Contribution of Co-Authors: Dr. Luc G. Bulot (ammonoid identification, manuscript review), Dr. Jonathan Redfern (discussion, manuscript review), Dr. Mohammed Nahim (regional geology and manuscript review), Dr. Jason Jeremiah (calcareous nannofossil identification, manuscript review, core investigation), Dr. Mike Simmons (foraminifera identification, manuscript review), Dr. Stéphane Bodin ($\delta^{13}C$ analysis, manuscript review) Camille Frau (ammonoid identification, manuscript review), Dr. Mike Bidgood (foraminifera identification, discussion), Dr. Moussa Marour (regional geology, manuscript review)

Chapter 5: Tectonic control on the development of forced regressive systems along a passive continental margin.

This chapter is pending submission to Basin Research. It applies the biostratigraphic investigation (chapter 3, 4 and 5) and utilizes it for sequence stratigraphic interpretation and palaeogeographic reconstruction. It gives insight into controls on sediment delivery along passive margins.

Contribution of Co-Authors: Dr. Jonathan Redfern (discussion, manuscript review), Dr. Luc G. Bulot (ammonoid identification, manuscript review), Dr. Giovanni Bertotti (structural geology discussion, manuscript review), Remi Charton (low-temperature geochronology)

Chapter 6: Synthesis, conclusion and future work

This final chapter gives a synthesis of the work presented. It reviews the initial research questions and gives an outlook on future work.

CHAPTER 1: INTRODUCTION

1.1 Introduction to the Lower Cretaceous project

The Moroccan Atlantic Margin is currently the focus of exploration for commercial hydrocarbon reservoirs to extend the success achieved to the south in the Mauritania-Senegal-Gambia-Bissau-Conakry (MSGBC) region. One key area of interest is the Essaouira-Agadir Basin (EAB). Past and recent drilling activity offshore has failed to find commercial reservoirs in the basin, with the main targets being the Jurassic and Lower Cretaceous clastics. A key factor is the lack of understanding regarding timing, location and controls on sediment delivery and distribution of siliciclastic material along the margin, or wether or not coarse sediments were delivered at all. These are the key applied research questions that prompted the establishment of a large source-to-sink study in collaboration with the Technical University of Delft, designed to address the evolution of the Moroccan Atlantic margin throughout the Mesozoic. This PhD forms part of this broader source-to-sink study and focuses on the investigation of the shelfal and shallow-marine to fluvial transition zone of the system in the Lower Cretaceous. A multi-disciplinary stratigraphic approach was chosen to investigate timing, sequence stratigraphic evolution, and palaeogeography of the upper Barremian to Lower Albian in the Essaouira-Agadir Basin of Morocco. This time interval records the migration of the shallow-marine fluvial transition zone to the Cretaceous shelf edge and subsequent re-establishment of the shelfal depositional environment.

In addition to the applied aims, this study also addresses fundamental questions about the evolution of passive margins. These key aims are outlined below and build on recent work on the massifs in the hinterland (Ghorbal et al., 2008, Saddiqi et al., 2009, Bertotti and Gouiza, 2012) that have recognised km-scale exhumation in the Jurassic and Cretaceous, showing that the “passive” margin had a significant post-rift tectonic activity.

1.2 Aims of the PhD project

The principal aims of this PhD project were:

- Characterisation of the Lower Cretaceous depositional systems.
- Identification of the main coarse clastic intervals in the EAB.

- Improvement of the biostratigraphic resolution and timing of any coarse clastic intervals.
- Understanding of the relative control of eustasy, climate, and tectonics as drivers for sequence development along passive margins.

After reconnaissance work carried out in March 2014 (Fig. 1.1) along the northern Moroccan Atlantic margin, the EAB was chosen as the core study area for this project. This basin can be subdivided into three sub-basins, the Essaouira, Haha and Agadir sub-basins (see chapter 2.2). Previous studies carried out in the basin had focused mainly on two east-west transects, one in the Agadir sub-basin and one in the Essaouira sub-basin. The west-central part, the Haha sub-basin, had received very limited attention. The Barremian to Albian strata in the Haha sub-basin offers outstanding outcrop quality and includes the most prominent regressive phase in the Lower Cretaceous. Following the reconnaissance work, it was apparent that to study this regressive phase a comprehensive investigation of the upper Barremian to Lower Albian strata was necessary. This included high-resolution biostratigraphic sampling for the upper Barremian to Lower Albian section and the establishment of a new reference section for the Aptian of NW Africa. Biostratigraphic work and ammmnoid identification was carried out in close collaboration with Dr. Luc Bulot. The outcrops are particularly rich in macrofossils and microfossils and an integrated stratigraphic assessment was undertaken. This included integration of lithostratigraphy, key biostratigraphic markers (ammonoids, foraminifera and calcareous nannofossils), chemostratigraphy (total organic carbon, carbonate content, $\delta^{13}C_{carb}$ and $\delta^{13}C_{org}$), and sequence stratigraphy. The work carried out in the Aptian forms the foundation for chapters 3 and 4. This work provides high-resolution timing of the studied interval and provides valuable data about the depositional environments. It also gives an invaluable insight of the general basin architecture. Chapter 5 develops a sequence stratigraphic framework and examines the palaeogeographic evolution of the Haha and Agadir sub-basins during the upper Barremian to lower Aptian. It assesses the relative control of eustasy, climate and tectonics as drivers for sequence development along this passive margin.

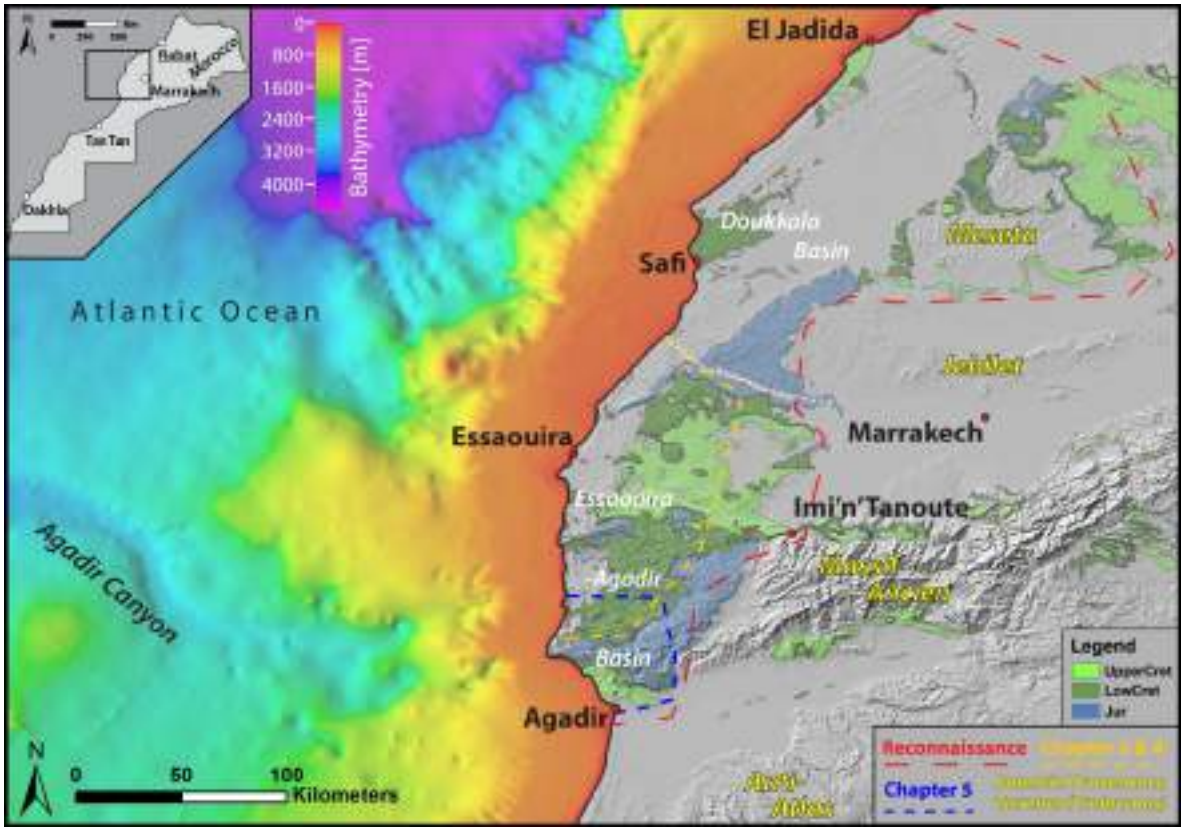

Figure 1.1: A geographic overview of the study area.
An offshore bathymetry data set (GEBCO, 2014) and digital elevation model (USGS, 2004) overlain by a summary geological map showing Jurassic and Cretaceous outcrops (Saadi et al., 1985). (Study areas for individual chapters are indicated by dashed lines).

1.3 Objectives of the PhD project

The following objectives for this thesis were defined after the reconnaissance work:

1. Improving the dating resolution of the upper Barremian and Aptian strata in the Haha sub-basin of the EAB, to better constrain the coarse clastic sediment delivery phase of the upper Bouzergoun Formation.
2. Building a bio-chronostratigraphic framework and sequence stratigraphic interpretation for the Aptian in the EAB enabling regional and inter-regional correlation.
3. Investigating the coarse clastic sediment delivery system in the upper Barremian to lower Aptian through detailed and integrated stratigraphy.
4. Reconstructing the sequence stratigraphy and palaeogeography of this key interval through field mapping and logging.
5. Identifying the mechanisms and controls on forced regressions in a passive margin setting.

1.4 Methods and dataset

Prior to fieldwork, a comprehensive review of all previous literature for the study area was undertaken. This included French, German and Moroccan PhD studies, available well data and company reports. This material is referenced throughout the text. Data in the field was collected primarily through detailed sedimentary logging of 27 stratigraphic sections (Fig. 1.2, Table 1.1) and the investigation of additional intermediate outcrops. The scale of logging depended upon the aim of the individual field season but was mainly at bed-by-bed scale. Handheld gamma-ray measurements were performed in key outcrops. For the biostratigraphic publications (chapters 3 and 4) a bed-by-bed collection of ammonoids and sample material for other biostratigraphic and chemostratigraphic analysis were made from seven sections. For chapter 5 detailed sedimentological and stratigraphic observations were made from 20 sections. Photographic panels were utilised to trace horizons in inaccessible areas and to aid interpretation. Observed lithofacies were grouped into lithofacies associations. Geographic overview maps with locations of studied outcrops and details on the techniques used are given in the individual chapters.

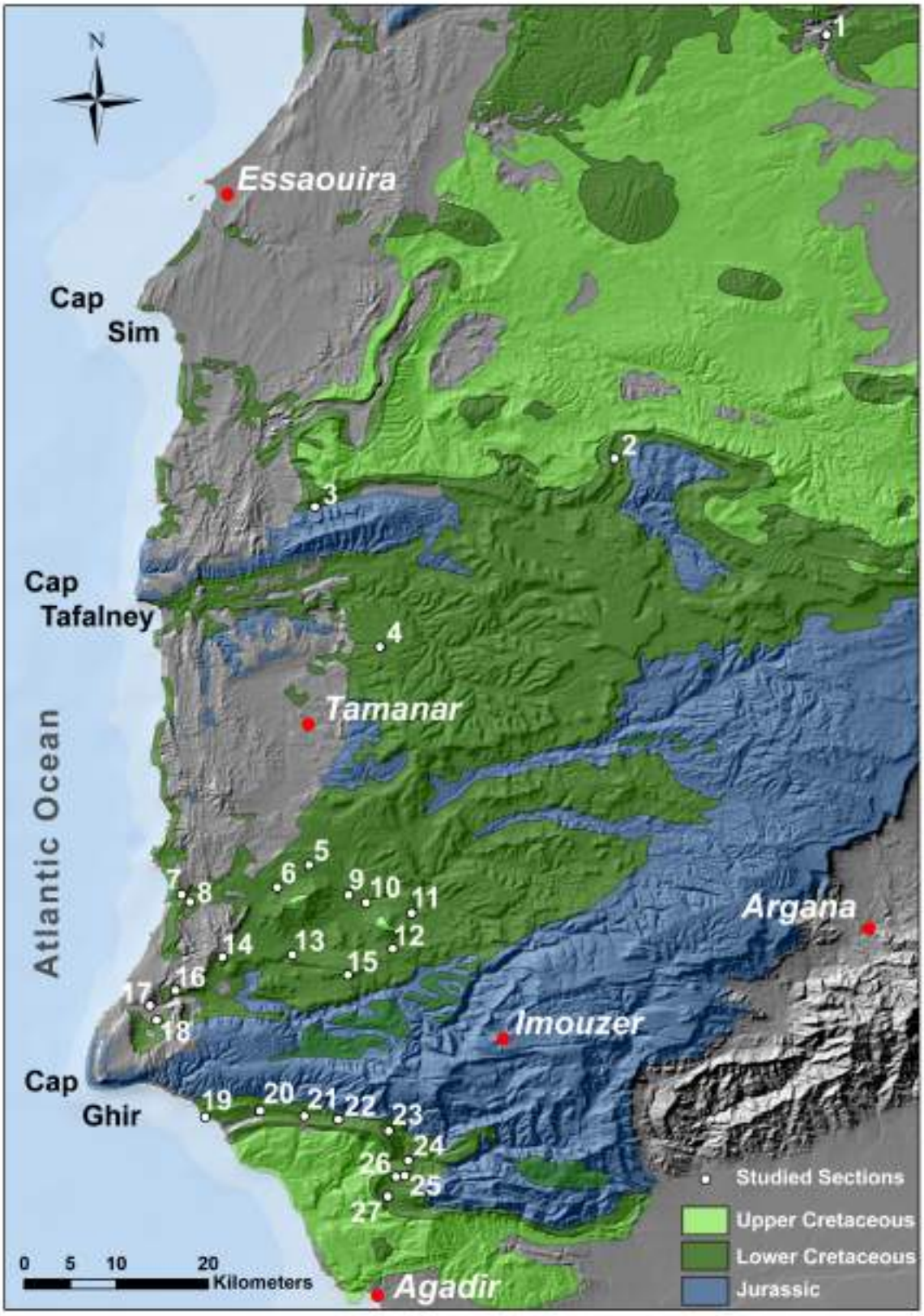

Figure 1.2 Location of studied sections.
Outcrop identifiers correspond to numbers in table 1.1, next page. Digital elevation model (USGS, 2004) overlain by a summary geological map showing Jurassic and Cretaceous outcrops (Saadi et al., 1985).

Table 1.1: Studied sections
Summary of sections studied, geographic location and data collected.

Map ID	Location	Latitude [°]	Longitude [°]	Data-type available	Chapter
1	Mramer (1)	31.657033	-9.164205	Stratigraphic log, biostratigraphic collection	3
	Mramer (2)	31.666118	-9.153251	Stratigraphic log, biostratigraphic collection	3
2	Zem Zem	31.241846	-9.372052	Stratigraphic log, biostratigraphic collection	3
3	Oued Tlit	31.194306	-9.665616	Stratigraphic log, biostratigraphic collection	3
4	Tamanar	31.057403	-9.601503	Stratigraphic log, biostratigraphic collection	3
5	Tiskatine N	30.843396	-9.671297	Stratigraphic log, palaeocurrent measurements	5
6	Tiskatine (1)	30.821463	-9.702555	Stratigraphic log, biostratigraphic collection	3, 4
	Tiskatine (2)	30.810477	-9.739966	Stratigraphic log, biostratigraphic collection	3, 4
7	Assaka	30.81437	-9.796262	Stratigraphic log, biostratigraphic collection, palaeocurrent measurements, gamma ray	5
8	Assaka (Top)	30.807297	-9.787837	Stratigrahic log, biostratigraphic collection	4
9	Ilmer Ichemerarn	30.814195	-9.631806	Stratigrahic log, palaeocurrent measurements	5
10	Aziar North	30.807532	-9.61515	Stratigraphic log, palaeocurrent measurements	5
11	Id Amran	30.796026	-9.571094	Stratigraphic log, biostratigraphic collection	4
12	Aziar South	30.760975	-9.589397	Stratigraphic log, palaeocurrent measurements, biostratigraphic collection	5
13	Barrage	30.75305	-9.75609	Stratigraphic log, palaeocurrent measurements	5
14	Akerkaou	30.754941	-9.687529	Stratigraphic log, palaeocurrent measurements, biostratigraphic collection	5
15	Tinkert	30.735477	-9.633326	Stratigraphic log, palaeocurrent measurements, biostratigraphic collection	5
16	Mahmout	30.720219	-9.802239	Stratigraphic log, palaeocurrent measurements	5
17	Tamri Cliff	30.705638	-9.827041	Stratigraphic log, palaeocurrent measurements	5
18	Tamri South	30.691054	-9.820617	Stratigraphic log, palaeocurrent measurements	5
19	Aghroud	30.596237	-9.772992	Stratigraphic log, palaeocurrent measurements	5
20	Addar	30.602799	-9.719271	Stratigraphic log, palaeocurrent measurements	5
21	Adenz	30.597151	-9.675501	Stratigraphic log, palaeocurrent measurements	5
22	Aouerga	30.593486	-9.642455	Stratigraphic log, palaeocurrent measurements	5
23	East of Aouerga	30.582605	-9.592904	Stratigraphic log, palaeocurrent measurements	5
24	Inrarne	30.55339	-9.573838	Stratigraphic log, palaeocurrent measurements	5
25	Fossil Shop Road Cut	30.538927	-9.577312	Stratigraphic log, palaeocurrent measurements	5
26	Alma East	30.537621	-9.58645	Stratigraphic log, palaeocurrent measurements	5
27	Alma	30.518663	-9.593786	Stratigraphic log, palaeocurrent measurements	5

1.5 Review of concepts

1.5.1 Biostratigraphy and lithostratigraphy

During the Early Cretaceous ammonoids provide the primary standard for biochronology. Ammonoids achieve the highest refinement, but they are not present in all environments or locations. Additionally, the more refined the subzones are, the more they are constrained geographically (Callomon, 1994). Therefore, it is important to define other chronometers (such as foraminifera, calcareous nannofossils and $\delta^{13}C$). This study develops a bio- and chemo-chronological framework against the primary standard and thereby defines local markers based on well-known species and extends the range of cosmopolitan markers.

This approach of developing local standard chronozones based on other fossil groups and chemostratigraphy against the primary standard was outlined by Callomon (1994) as the key to building reproducible regional and inter-regional chronostratigraphic reference scales. A case study highlighting the application of integrated stratigraphy in previously poorly-constrained areas is the work by Vincent et al. (2010) in Iran. A similar approach was chosen in the study, detailed in chapters 3 and 4.

The definition of a revised lithostratigraphic framework for the study area follows the international stratigraphic guidelines outlined by Murphy and Salvador (1999).

1.5.2 Sequence stratigraphy

Mitchum et al. (1977) defined depositonal sequences as stratigraphic units composed of a relatively conformable succession of genetically related strata. Observations at different scales may lead to the assignment to different hierarchical orders of depositonal sequences and their bounding surfaces (Cantuneanu et al., 2011). Vail et al. (1977) defined first-, second-, and third-order sequences based on seismic interpretation with durations of 200-300 Myr, 10-80 Myr, and 1-10 Myr, respectively (Strasser et al., 2000). Subsequent work has assigned variable durations to 3rd-order sequences (e.g. Haq et al., 1987; Vail et al., 1991; Hardenbol 1998) and Strasser et al. (2000) has shown the possible link to 400-kyr Millankovitch cycles. Vail et al. (1991) argued more for a combined effect of eustasy and tectonics in the evolution of 3rd-order cycles. In this thesis, we assign

3rd-order sequences and their associated bounding surfaces to sequences ranging between 1-10 Ma.

The sequence stratigraphic scheme and definition of individual surfaces and different approaches are summarised in Catuneanu et al. (2011). The application and recognition of individual surfaces and tracts on clastic shelvess are discussed in Zecchin and Catuneanu (2013) and Zecchin et al. (2017). An interesting historic evolution of stratigraphic concepts paving the way for sequence stratigraphy and discussion of condensed sections and their application is given in Loutit et al. (1988). Sequence stratigraphic nomenclature used here is closely related to the depositional sequence IV (Catuneanu et al., 2009) based on Hunt and Tucker (1992 and 1995), Helland-Hansen and Gjelberg (1994), and Plint and Nummedal (2000). More details on sequence stratigraphic nomenclature and on the definition of key surfaces and systems tracts are given in chapter 5.

CHAPTER 2: GEOLOGICAL SETTING

2.1 Regional setting

The northern and central part of Morocco can be subdivided into four major tectonic domains: (*i*) the Rif, (*ii*) the Meseta, (*iii*) the Atlas system, and (*iv*) the Anti-Atlas (Fig. 2.1). The Rif to the north is part of the western Mediterranean alpine mountain belt and mainly composed of post-Palaeozoic rocks. To the south, along the Atlantic margin, lies the plateau of the western Meseta comprising Palaeozoic rocks and in places a thin post-Palaeozoic cover, which is of significant economic interest and yields the abundant phosphorous deposits of the Upper Cretaceous. The western Meseta is separated from the eastern Meseta (the Oran Meseta) by the middle Atlas, representing the northern extension of the next major tectonic domain: the Atlas system. The Atlas system is composed of two arms - the Middle Atlas and the High Atlas - and both are mainly composed of Mesozoic sediments. To the south of the High Atlas is the Anti-Atlas at the northern end of the Saharan plateau. The Anti-Atlas is mainly composed of Palaeozoic sedimentary rocks but includes Precambrian rocks along its core. Between those major tectonic domains, large east-west trending Cenozoic sediment basins are exposed.

Two minor tectonic domains of particular importance for this study are the Jebilet, forming the southern extension of the western Meseta, and the Massif Ancien de Marrakech (often referred to as the Massif Ancien or MAM). During Jurassic and Cretaceous times the Western Meseta and Massif Ancien are interpreted to have formed the West Moroccan Arch (WMA, Fig. 2.1). Frizon de Lamotte et al. (2008) interpreted this region as being a high during the Mesozoic, separating the High Atlas rift (a failed rift arm) to the east from the Atlantic rift to the west. Recent geochronology studies support the interpretation that the WMA was actively uplifting during the Late Jurassic and Early Cretaceous (Ghorbal et al., 2008; Saddiqi et al., 2009; Bertotti and Gouiza, 2012). It separated the Tethyan domain to the east and the Atlantic domain to the west. How much these two domains were in connection during times of relative sea-level highstand is still an ongoing debate, but affinities with the Tethyan domains that are apparent in biostratigraphic studies suggest at least periodic drowning and connection (e.g. Wippich, 2001; Company et al., 2008; Peybernes et al, 2013 and Luber et al., 2017). During times of relative sea-level lowstand the domains were probably separated (Frizon de Lamotte et al., 2008), and again the biostratigraphic data supports this, with clear evidence of endemism.

Vast areas of Cretaceous strata associated with the Tethyan domain crop out on the eastern and northern part of the High Atlas system, but the west coast of Morocco is one of the few places where a rare glimpse into the Atlantic Mesozoic basin is given. Here favourable conditions for the development of a Mesozoic basin west of the WAM and inversion of the Atlas rift system during the Atlas/Alpine orogeny exposes a continuous Triassic to Upper Cretaceous succession. This is the key area for the study of Mesozoic history in the eastern Central Atlantic Margin (CAM). It is composed of the Argana Valley (Fig. 2.2) comprising Permian to Triassic strata and the Essaouira-Agadir Basin (EAB) with outcropping Jurassic and Cretaceous strata, which is the focus of this study.

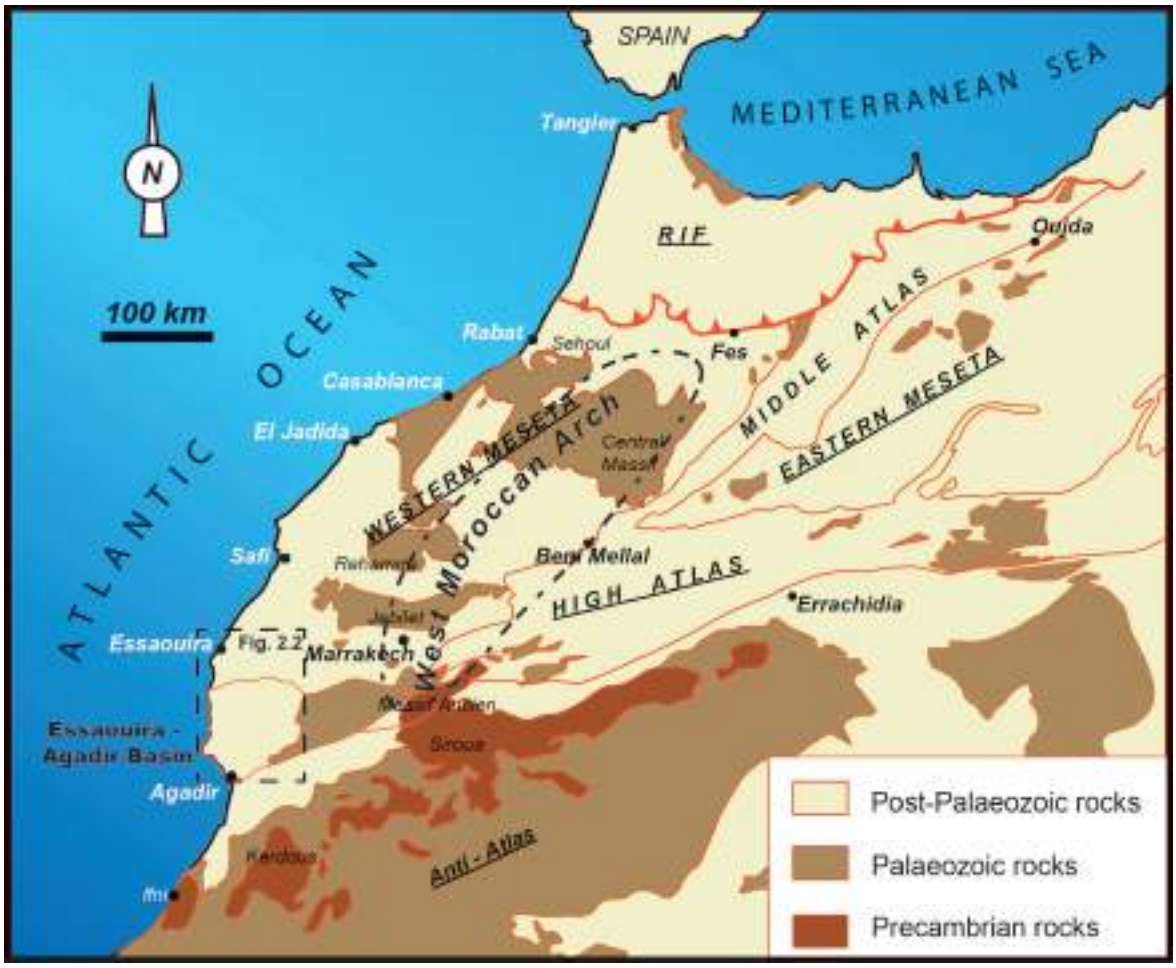

Figure 2.1: Major tectonic domains of northern and central Morocco and westernmost Algeria (modified after Michard et al. 2008).
The Western Moroccan Arch was a palaeohigh during the Jurassic and Cretaceous.

2.2 The Essaouira-Agadir Basin

The Essaouira-Agadir Basin (EAB) is located to the west of the High Atlas, where Lower Cretaceous strata crop out adjacent to the Moroccan Atlantic coast (Fig. 2.2). It forms the most continuous succession of Mesozoic strata along the Central Atlantic Margin (CAM).

Rifting was initiated in the Permo-Triassic and separated Africa and North America (Le Roy and Piqué, 2001) (Fig. 2.3). Following rifting, extensive Jurassic carbonate platforms established along the NW African margin (Jansa and Wiedmann, 1982). During the Lower Cretaceous, the EAB was bound by the following highs/provenance terranes: by the Meseta to the north and its southern extension the Jebilet, to the south by the Anti-Atlas, and to the east by the Massif Ancien de Marrakech (Fig. 2.1). During most of the Lower Cretaceous the area of the EAB was covered by a gulf-like embayment, termed the "Atlas Gulf", opening out to the west into the Proto-Atlantic Ocean (Behrens et al., 1978). The basin can be subdivided from north to south into the Essaouira, Haha, and Agadir sub-basins (Fig. 2.2). Cretaceous to Cenozoic inversion and uplift linked to the Atlasic/Alpine orogeny (Laville et al., 2004) led to the present-day exposure of the Mesozoic basin fill and neighbouring basement terrains.

Pioneering work on the Jurassic and Cretaceous successions was carried out by Roch (1930), Ambroggi (1963) and Duffaud et al. (1966). Two other important phases of basin-scale research in the area were undertaken in the late 70's to early 80's and this work is compiled in Von Rad et al. (1982). During the late 80's the most significant work is that of Rey et al. (1986a and b, 1988). Specific local studies, mainly biostratigraphy and sedimentology, have since been published and are mentioned in the text where appropriate.

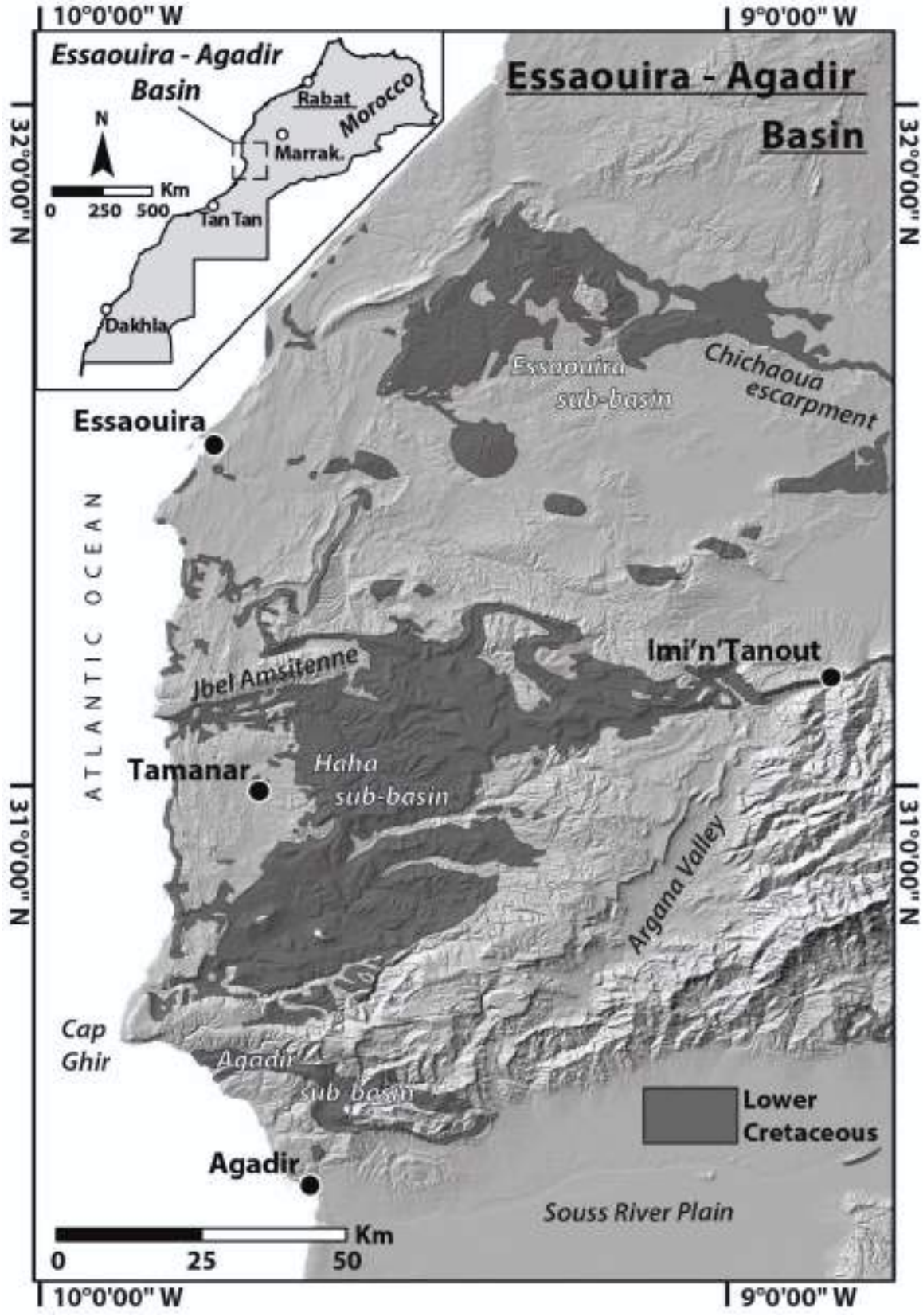

Figure 2.2: Geographical overview of the Essaouira-Agadir Basin.
Digital elevation model (USGS, 2004) overlain by a summary geological map showing Lower Cretaceous outcrops (Saadi et al., 1985).

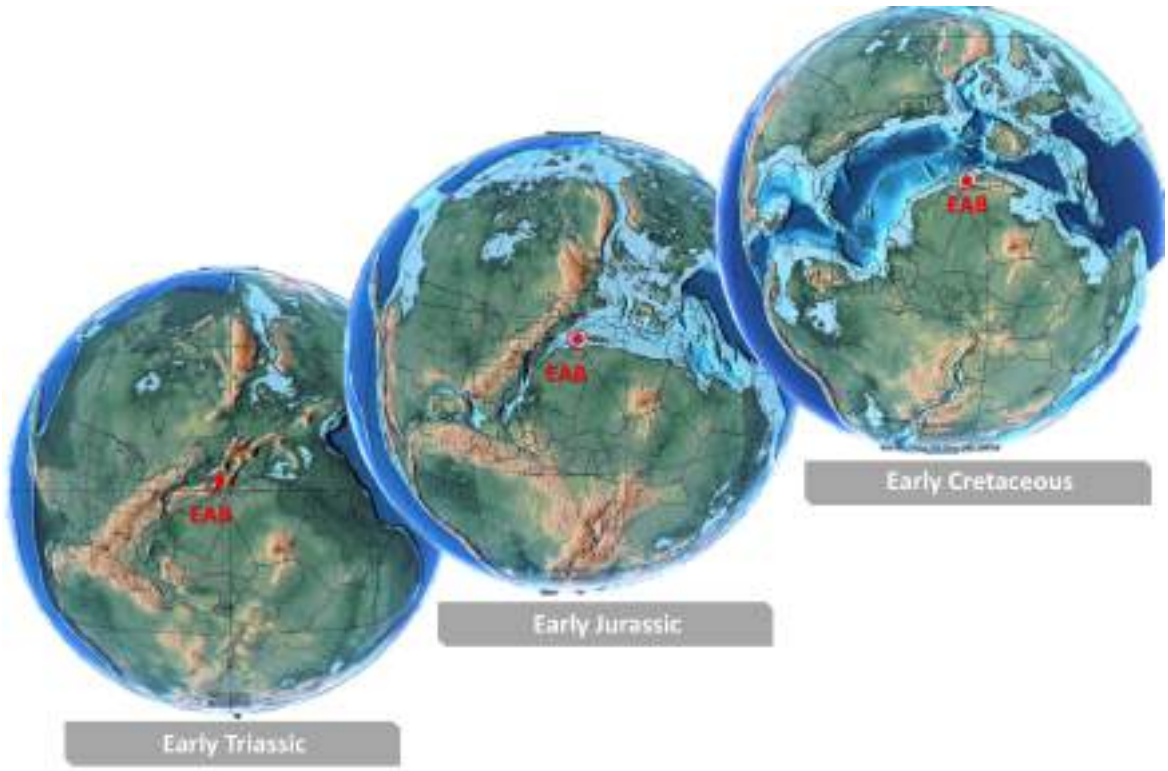

Figure 2.3 Palaeoglobes
Paleoglobe for the Early Triassic to Early Cretaceous, after Scotese and Dreher (2012), PALEOMAP Project

2.3 Lower Cretaceous stratigraphy of the Essaouira-Agadir Basin

Sedimentation during the Lower Cretaceous in the EAB took place on a shallow-dipping shelf, which inherited its palaeotopography from the carbonate ramp developed in the Upper Jurassic to Lowermost Cretaceous (Berriasian) (Behrens et al., 1978; Canerot et al., 1986; Rey et al. 1988; Ettachfini, 1998, 2004). The Lower Cretaceous sediments in the western part of the basin are mud-dominated, with only discrete intervals of coarse clastic material delivery (Fig. 2.4). Overall carbonate production in the EAB was significantly reduced in the Lower Cretaceous compared to the Jurassic (Wiedmann et al., 1978). The thickness of Lower Cretaceous deposits increases to the west and some formations disappear to the east due to coastal onlap (Rey et al., 1988). Significant thickness reductions are also recognized close to salt diapir structures (e.g. Tidzi diapir) and pre-existing, palaeotopographic-positive features (e.g. Cap Ghir and Jbel Amsittene), previously reported by Rey et al. (1986a, 1988).

The following is an abridged description of the main lithostratigraphic formations of the Lower Cretaceous (Fig. 2.4) with key biostratigraphic information. It focuses on the west-central part of the EAB and closely follows the nomenclature of Duffaud et al. (1966) and Rey et al. (1986a and 1988).

Tithonian to Berriasian: The Cap Tafalney Fm. was originally introduced by Duffaud et al. (1966). Taj-Eddine (1992) reported the Jurassic–Cretaceous boundary at the top of the Cap Tafaleney Fm. based on calpionellids but the exact stratigraphic position is still the subject of debate. The top of the Cap Tafalney Fm. is likely to be diachronous. Deposits mainly include algae mats, ooid-rich grainstones and cross-bedded calcareous sandstones (Wippich, 2001). A significant reduction in thickness is reported from the Oued Tidzi diapir, linked to syn-sedimentary salt tectonics (Rey et al., 1986a). The transition from the Jurassic to Cretaceous is marked by subtidal and intertidal shallow-marine to lagoonal deposits (Rey et al., 1988).

Rey et al. (1986a) defined the Agroud Ouadar Fm. and assigned it to the Valanginian, but subsequent work of Ettachfini (2004) has clearly shown that this formation is Berriasian in age. It consists of limestones and marls rich in ammonites and echinoids. Deposition took place on the inner to middle shelf (Canerot et al., 1986; Rey et al, 1988; Rossi et al., 2003).

Valanginian: The Sidi Lhousseine Fm. was introduced by Duffaud et al. (1966). Its base is diachronous but located within the lower Valanginian (Ettachfini, 2004) and the formation ranges into the lower Hauterivian. The ammonite biostratigraphy of the Valanginian to basal Hauterivian interval is discussed in the PhD thesis of Ettachfini (2004). The Sidi Lhousseine Fm. is mainly composed of extensive green marls with common sandstones interbeds towards the top. The overall depositional environment is the inner to middle shelf (Rey et al., 1988; Rossi et al., 2003; Wippich, 2001).

Hauterivian: The deposits of the Tamanar Fm. (Duffaud et al., 1966) are attributed to the lower Hauterivian (Rey et al., 1988; Ettachfini, 2004). These deposits show a reefal character, composed of coral-bearing limestones and bioclastic-rich carbonates (Duffaud, 1966; Rey et al., 1988). The upper part of the Tamanar Fm., especially in more proximal settings, includes lagoonal deposits composed of oolitic shoals and increased siliciclastic influx (Rey et al., 1988).

The Talmest Fm. was defined by Duffaud et al. (1966). Rey et al. (1988) assigned the formation, without direct paleontological evidence, to the late Hauterivian. It is now clearly established that the Talmest Fm. belongs to the Hauterivian (Ettachfini, 2004; findings of this study). The Talmest Fm. in the study area is composed of green marls, often interbedded with bioclastic-rich sandstones. The sandstones decrease in abundance upwards, where marls dominate. The main depositional environment was the inner shelf with a deepening trend into the Barremian (Zühlke et al, 2004).

Barremian: The Taboulouart Fm. was originally introduced by Duffaud et al. (1966) and its age was poorly-constrained until the detailed biostratigraphic study of Company et al. (2008). The contact with the underlying Talmest Fm. is composed of yellow to green marls with minor sandstone beds. The Taboulouart Fm. is of early to early late Barremian age (*T. hugii* to *T. vandenheckii* zones) (Company et al., 2008; this study). It is mainly composed of marls interbedded with bundles of ammonite-rich limestones. The Taboulouart Fm. was deposited in the middle to outer shelf (Rey et al, 1986, 1988; Witam 1998).

The Bouzergoun Fm. (Duffaud et al., 1966) was until recently assigned to the upper Barremian, despite the lack of palaeontological evidence (Canerot et al., 1986a; Rey et al., 1988; Witam, 1998). Company et al. (2008) identifyed a condensed horizon that marks the boundary between the Taboulouart Fm. and the Bouzergoun Fm.; of upper Barremian age (early to middle part of the *Gerhardtia sartousiana* Zone). An early Aptian age for the uppermost part of the Bouzergoun Fm is shown by Witam (1998).

The Bouzergoun Fm. is composed of mudstones, siltstones and minor sandstones in the lower part and sandstones (often bioclastic-rich), conglomerartes, red-green mudstones and sandy limestones in the upper part (Duffaud et al., 1966; Rey et al, 1988; Nouidar and Chellai 2001, 2002). The lower part of the Bouzergoun Fm. is interpreted as shelfal mudstone-deposits (Nouidar and Chellai, 2002). The upper part is interpreted as transitioning from lower shoreface/lower deltafront environments to upper shoreface/upper deltafront shoreline sandstones during the advance of a wave-dominated shoreline/deltaic system (Nouidar and Chellai, 2002). Conglomerates and red-green mudstones have been interpreted as fluvial to paralic deposits (Nouidar and Chellai, 2001).

Aptian: The Tamzergout Fm. was originally introduced by Duffaud et al. (1966). Rey et al. (1986a) restricted its age to the early Aptian (Bedoulian in regional French stratigraphy) and limited its occurrence to the west and central part of the EAB. The formation is mainly made up of fossiliferous alternating blue-grey marls and grey limestones with abundant marine fauna (Duffaud et al., 1966; Rey et al. 1988). Deposition took place in mid to outer shelf conditions with a deepening trend (Rey et al., 1988; Peybernes et al., 2013).

Albian: The Oued Tidzi Fm. was initially described by Duffaud et al. (1966) and Rey et al. (1988) assigned an uppermost (Clansayesian in regional French stratigraphy) to Albian age for this formation. The Oued Tidzi Fm. shows a clear change from blue marls and limestones of the Aptian Tamzergout Fm. to green marls with minor bioclastic-rich sandstone interbeds in the Albian Oued Tidzi Fm (Duffaud et al., 1966; Rey et 1988). Overall deposition took place on an open-marine, middle shelf for the lower part of the formation (Rey et al. 1988, Peybernes et al., 2013).

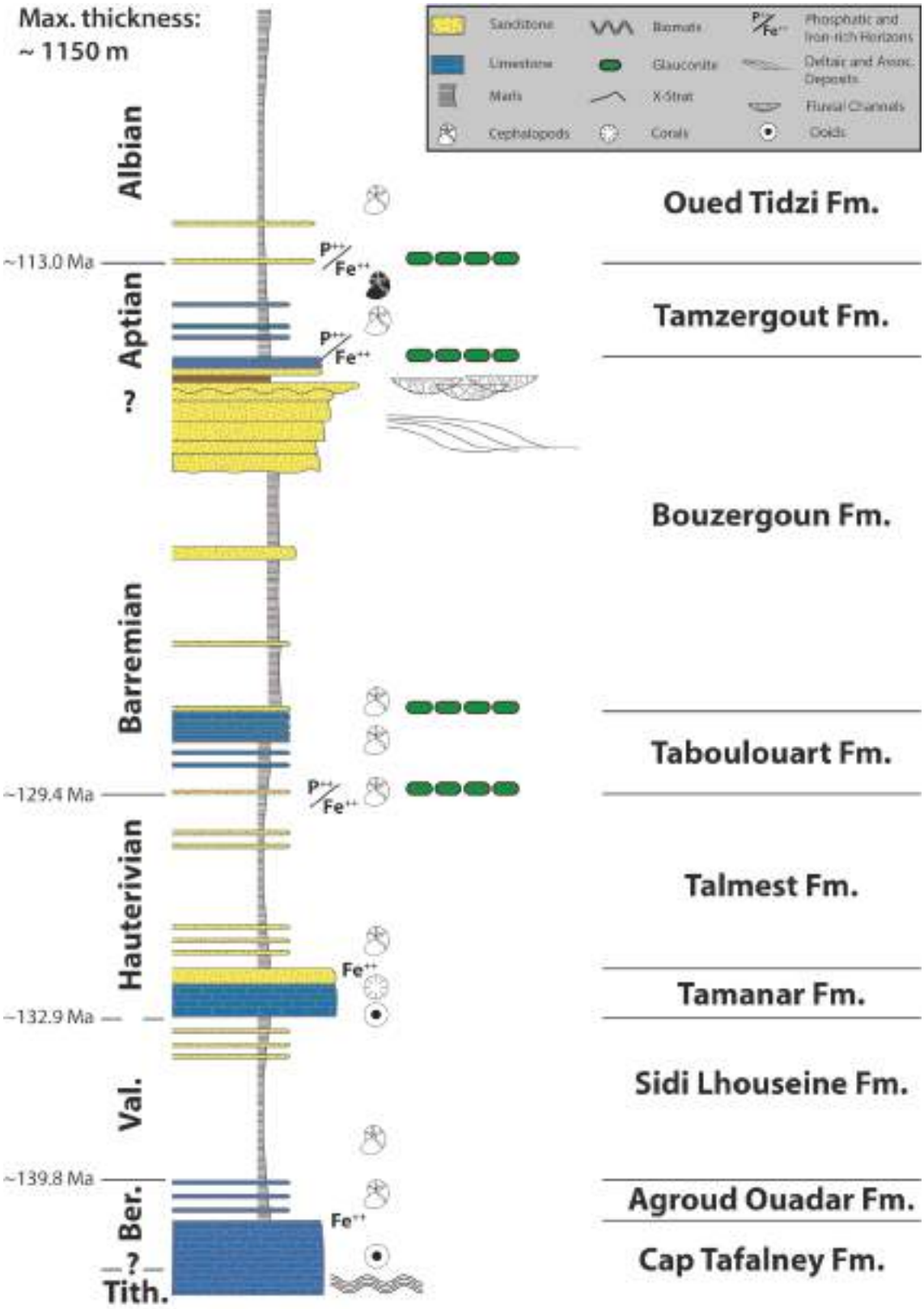

Figure 2.4: Schematic profile of the Lower Cretaceous stratigraphy in the west-central EAB.
Numerical ages after Cohen et al. (2013, updated) from the international commission of stratigraphy. Note that the Lower Cretaceous has no ratified GSSPs or constrained numberical ages. Maximum thickness from the reference profil of the Cretaceous near Agadir after Wiedmann et al. (1978).

CHAPTER 3: A REVISED AMMONOID BIOSTRATIGRAPHY FOR THE APTIAN OF NW AFRICA: ESSAOUIRA-AGADIR BASIN, MOROCCO

This chapter has been published in Cretaceous Research.

Authors: Luber, T.L., Bulot, L.G., Redfern, J., Frau, C., Arantegui, A., Masrour, M.

Available online: 01/07/2017

DOI: https://doi.org/10.1016/j.cretres.2017.06.020

Keywords: Ammonite, Biostratigraphy, Aptian, Essaouira-Agadir Basin, Morocco

3.1 Abstract

A revised ammonoid biostratigraphy is presented for the Aptian of NW Africa, Essaouira-Agadir Basin (EAB), Morocco, based on detailed analysis of 5 key sections. A number of bio-events are documented and 26 genus and 43 species fully documented, forming the largest published Aptian ammonite collection made from NW Africa. The section at Tiskatine is documented as the type section, and 8 zones and subzones are defined, of which 5 are new. This work allows correlation of the Aptian of the EAB to the Standard Mediterranean Ammonite Scale (SMAS).

Two main hiatuses are identified at the scale of the basin: a major one that includes most of the lower Aptian and the base of the upper Aptian and a second one encompass the top of the upper Aptian and the base of the Lower Albian. The ammonite fauna displays a clear Tethyan palaeobiogeographic character affected by a fairly high degree of endemism at the genus and species level. The new genus and species *Elsaisabellia tiskatinensis* is introduced.

3.2 Introduction

Aptian to lowermost Albian ammonite biostratigraphy across the northwest African Atlantic margin remains poorly-documented compared to counterparts of the Mediterranean Tethys; such as in Spain (Moreno Bedmar et al., 2008, 2009, 2010, 2012a, 2014), France (Delanoy, 1995; Cecca et al., 1999; Ropolo et al., 1999; Kennedy et al., 2000; Ropolo et al., 2000a-c; Dauphin, 2002; Dutour, 2005; Ropolo et al. 2006; Ropolo et al., 2008a-b; Frau et al., 2015), Tunisia (Lehmann et al., 2009; Chihaoui et al., 2010; Latil, 2011), and Iran (Raisossadat, 2004, 2006; Bulot in Vincent et al., 2010; Seyed-Emami and Wilmsen, 2016); or on the opposite side of the Central Atlantic Margin (CAM), e.g. Mexico (Barragán-Manzo and Méndez-Franco, 2005; Moreno Bedmar et al., 2012b, 2013, 2015, Barragán et al., 2016).

The Aptian Stage contains some globally significant events, recording a time of high sea-level during the mid-Cretaceous greenhouse period (Larson and Erba, 1999; Leckie et al., 2002). It also records some of the most wide-spread and best studied oceanic anoxic events (Schlager and Jenkyns, 1976; Scholle and Arthur, 1980; Arthur et al., 1990; Bralower et. al, 1994; Weissert et al., 1998; Föllmi et al., 2006; Föllmi, 2012).

In this study, we present a new high-resolution dataset from NW Morocco, discussed within a broader regional/global context and with special reference to the standard ammonite zonal scheme of the Mediterranean Tethys (Reboulet et al., 2011, 2014). In Morocco, the Aptian successions of the west-central part of the Essaouira-Agadir Basin (EAB) is part of one of the most complete and best-constrained successions of the Lower Cretaceous in NW Africa. The Aptian succession is characterized by ammonite-rich, shallow-marine (Bouzergoun Formation) to shelf deposits (Tamzergout and Oued Tidzi formations), that crop out in a corridor along the Moroccan coast between the cities of Agadir and Essaouira (Fig. 3.1). The aim of the present contribution is to improve the biostratigraphic frame of the Aptian and lowermost Albian of the EAB based on the detailed analysis of the bed-by-bed distribution of ammonoids at five key sections (Fig. 3.1).

Our results document the specific character of the ammonoid fauna of the EAB and discuss its similarities and differences with equivalent ammonite faunas of Mediterranean-Caucasian Subrealm of the Tethyan Realm. The results of this study develop a strong reference framework for the Aptian to earliest Albian for the northwest African Atlantic margin.

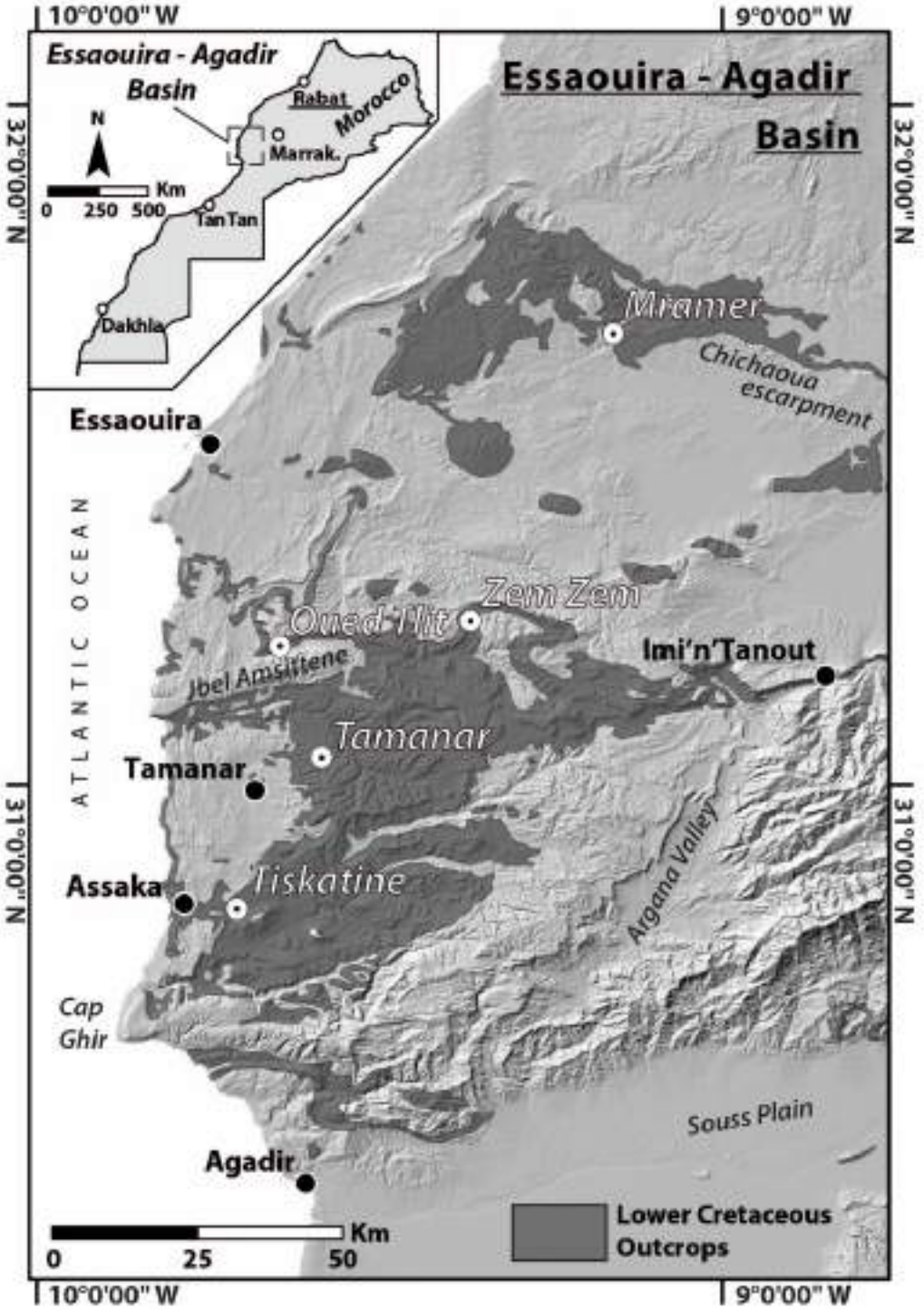

Figure 3.1: An overview map of the Essaouira-Agadir Basin.
Digital elevation model (USGS, 2004) with sub-crop of a geological map (Saadi et al., 1985), showing Lower Cretaceous outcrops, studied sections and key locations.

3.3 Regional setting and stratigraphy

Lower Cretaceous strata crops out over an area 100 km wide and 150 km long, adjacent to the Moroccan Atlantic coast; the only continuous succession of Mesozoic fill of the Central Atlantic Margin (CAM) (Fig. 3.1). Following Permo-Triassic rifting that separated Africa and North America (Le Roy and Piqué, 2001), extensive Jurassic carbonate platforms developed all along the NW Africa (Jansa and Wiedmann, 1982). Later deposition shared this inherited regional physiography, but also record distinct sub-basins with variable subsidence, evolving throughout the Early Cretaceous (Rey et al., 1988; Davison, 2005; Wenke et al., 2011).

During this time, the EAB, the focus of this study, was limited to the north by the Meseta and the Jebilet, to the south by the Souss Basin and to the east by the Massif Ancien de Marrakech. The general physiography formed a large gulf-like embayment opening out to the west into the Atlantic Ocean (Behrens et al., 1978). Present-day exposure of the Mesozoic basin fill and adjacent basement terrains reflects the Cretaceous to Cenozoic inversion and uplift linked to the Atlasic/Alpine orogeny (Laville et al., 2004) and associated salt tectonics (Tari and Jabour, 2013).

This study focuses on the outcrops in the west-central part of the EAB, located between the prominent Cretaceous Essaouira and Chichaoua escarpment to the north and the broad Cap Ghir anticline to the south (Fig. 3.1). Strata are mainly flat-lying, only exhibiting folding with steep flanks close to fault zones and associated with salt diapirs (Hafid et al., 2000, 2006). The maximum thickness of the entire Cretaceous post-rift succession is estimated to be 1300 m (Behrens et al., 1982) (Zem Zem section). The Lower Cretaceous reaches approximately 800 m in thickness but varies dramatically and thinning toward salt diapirs suggests Cretaceous syn-sedimentary activity (Hafid et al., 2000; Le Roy and Pique, 2001; Zühlke et al., 2004).

The Early Cretaceous represents a time of major change from the carbonate-dominated system in the Middle- to Late Jurassic to a mixed carbonate-siliciclastic or purely siliciclastic systems in the Cretaceous, following the drowning of the Jurassic carbonate platform. Cretaceous deposits in the EAB are dominated by shelfal mudstone successions with discrete intervals of coarse clastic sediment delivery in the late Valanginian, late early Hauterivian and late Barremian to earliest Aptian (Ambroggi, 1963; Behrens et al., 1978).

During the Aptian, the palaeogeography of the EAB was dominated by an open marine shelf. Arid climatic conditions are indicated by low nannofossil productivity (Herrle, 2002; Peybernes et al., 2013) and clay mineral composition (Daoudi and Deconinck, 1994). The EAB is thought to have been located away from the main upwelling zone, which existed during Aptian and early Albian times around the Mazagan Plateau to the north (Herrle, 2002). A cooling climatic trend has been recognized from the late Aptian – early Albian, evidenced by southward migration of high-latitude/boreal nannofossil into mid- and low-latitudes (Jeremiah, 1996, 2001; Herrle and Mutterlose, 2003; Rueckenheim et al., 2006). This trend was also observed in the EAB by Peybernes et al. (2013).

Overall the Aptian to Albian transition is a time of global eustatic sea-level rise (Hardenbol et al., 1998; Haq, 2014). In the EAB shallow-marine conditions were widespread during the early Aptian, with a transgression recognised in the late Aptian, the establishment of outer shelf conditions, and the reoccurrence of the Atlas Gulf (Behrens et al., 1978).

Most of the formation names for the Lower Cretaceous were introduced by Duffaud et al. (1966), later revised by Rey et al. (1986a and b, 1988). The reference sections are mainly located along an east-west trending transect in the northern part of the EAB (Essaouira to Imi'n'Tanoute). There are no stratigraphic units at group level defined in the EAB. Previous sedimentological and stratigraphic work on the Lower Cretaceous in the areas was carried out by Ambroggi (1963), Duffaud et al. (1966), Wiedmann et al. (1978, 1982), Adams et al. (1980), Behrens et al. (1982) and Rey et al. (1986a and b, 1988). More recent studies have mainly focused on the ammonite biostratigraphy of the Berriasian to Hauterivian interval (Ettachfini, 1991, 2004; Wippich, 2001, 2003) and the integrated stratigraphy of the Barremian/Aptian interval (Witam et al., 1993; Witam, 1998; Nouidar and Chellai, 2001, 2002; Company et al., 2008; Peybernes et al., 2013).

3.3.1 Barremian to Albian lithostratigraphic framework

The first attempt to subdivide the lithostratigraphic succession of the EAB was made by Duffaud et al. (1966). For the Barremian to Albian interval, those authors introduced five lithostratigraphic units: the "Calcaires lumachéliques de Taboulaourt", the "Grès et marnes rouges du Bou Zergoun", the "Marno-calcaires de Tamzergout", the "Grès marneux du Lemgo" and the "Marnes de l'Oued Tidsi". This synoptic lithostratigraphic chart was

introduced without formal description, a definition of boundaries or designation of reference sections.

Subsequent works by Rey et al. (1986a and b, 1988), Andreu (1989), Witam et al. (1993) and Witam (1998) led to refining the litho- and biostratigraphic framework of the EAB, but little attention was paid to the formal description and definition of the formations. Despite Witam's (1998) attempt to propose reference sections for the lithostratigraphic units introduced by Duffaud et al. (1966), a unified lithostratigraphic nomenclature for the EAB is still lacking. This drastically limits the value of the lithostratigraphic units for the correlation of the Barremian to Albian strata and also reflects the limited published work on regional stratigraphic relationships. Revising the lithostratigraphic framework of the EAB is beyond the scope of the present contribution and in this study, we have utilised the existing scheme of Duffaud et al. (1966) that best applies to our observations in the west-central part of the basin (Fig. 3.2).

3.3.1.1 Bouzergoun Formation

The Bouzergoun Fm., composed of sandstones and red mudstones, was introduced by Duffaud et al. (1966). Rey et al. (1986a, 1988), describes them as margino-littoral deposits made of sands, varicoloured clays, dolomites and bioclastic-rich limestones with large cross-stratification; and topped by a major disconformity.

There is no agreement in the literature about the age of the Bouzergoun Fm. Rey et al. (1986a) proposed a late Barremian age, based on the occurrence of early Barremian ammonites in the underlying Taboulouart Fm. and early Aptian ammonites in the overlying Tamzergout Fm. This was amended by Nouidar and Chellaï (2001) who assigned the upper part of the Bouzergoun Fm. (red beds) to the lower Aptian, based on the occurrence of *Salpingoporella? dinarica* Radoičić. However, it is unclear if the occurrence is derived from new data obtained by the authors or from a misinterpretation of Canérot et al. (1986), who never reported these dasyclad algae from the EAB. In any case, the occurrence of *Salpingoporella? dinarica* does not allow discrimination between the Barremian and Aptian stages.

Analysis of outcrops for this new study identifies the Bouzergoun Fm. as being composed of a thick succession of shelfal muds with minor sandstones at the base, truncated by coarsening and thickening-upward shallow-marine and deltaic sand-rich

deposits and fluvial deposits. In places, erosional channels and valley features are in-filled by coarse clastic material and green to red-coloured mudstones with interbedded sandstones. The uppermost part of the formation is made of sandstones, sandy limestones and mudstone interbeds bearing marine fauna and often oyster-rich beds to the top (Fig. 3.2). The unit reaches a maximum thickness of 84 metres at Assaka.

Ammonites collected from Assaka identify a condensed horizon that marks the boundary between the Taboulouart and the Bouzergoun formations, of early late Barremian age (early to middle part of the *Gerhardtia sartousiana* Zone) (see also discussion in Company et al., 2008). In most sections studied the occurrence of *Prochelonicerasdechauxi* (Kilian and Reboul, 1915) firmly establish an earliest Aptian age (see discussion below) for the uppermost beds of the Bouzergoun Fm. (see discussion below). At Tiskatine, the top of the formation is marked by two beds of siltstones that contain a rich early late Aptian ammonite fauna (lower part of the *Colombiceras tobleri* Zone) (see discussion below). This indicates that the top of the Bouzergoun Fm. is diachronous and ranges in age from earliest to early late Aptian (base of the *Deshayesites forbesi* to lower part of the *Colombiceras tobleri* zones).

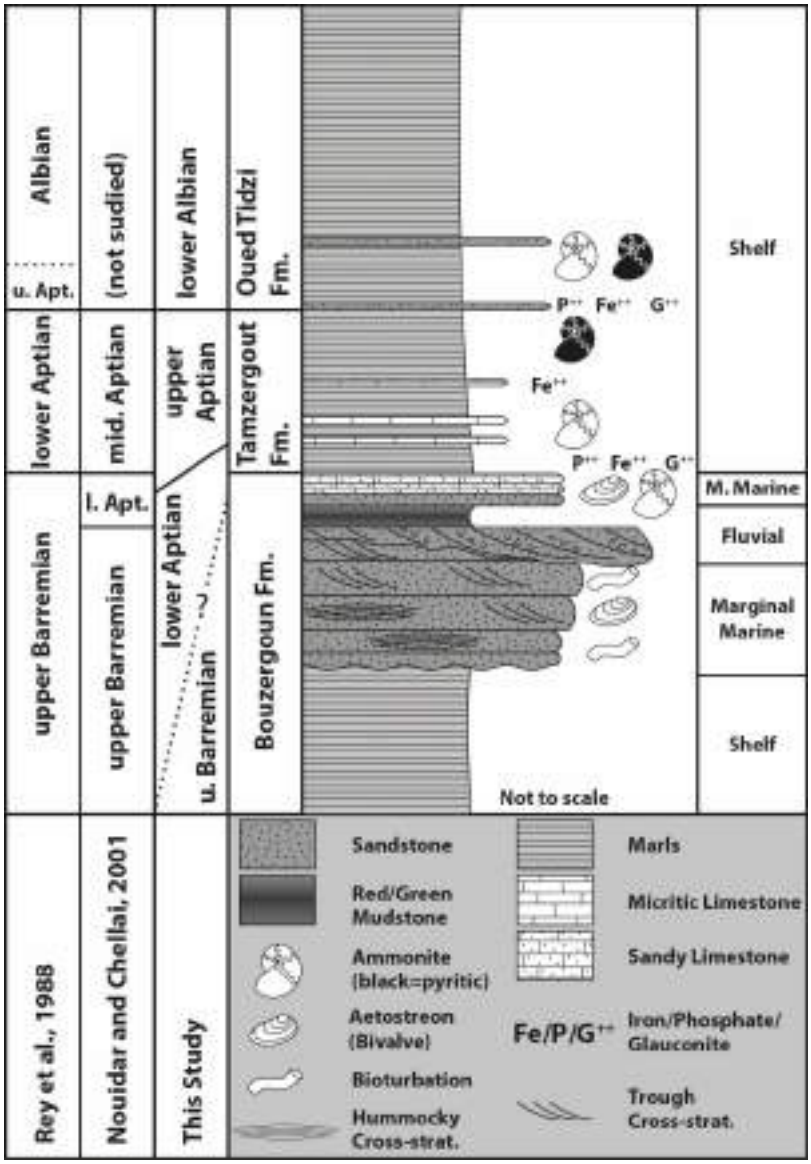

Figure 3.2: Generalised lithostratigraphy of the study interval.
The upper Bouzergoun to lower Oued Tidzi formations and their main depositional environments in the west-central part of the EAB.

3.3.1.2 Tamzergout Formation

The Tamzergout Fm. was defined by Duffaud et al. (1966) as a succession of marls and limestones. The vertical and lateral extension of this unit has been variously interpreted by subsequent authors (see discussion in Witam, 1998, p. 153-154).

The formation is mainly made up of fossiliferous alternating blue-grey marls and grey limestones that correspond to shallow-marine to shelfal deposits (Fig. 3.2). Rey et al. (1986a) restricted its age to the early Aptian (Bedoulian in regional French stratigraphy) and limited its occurrence to the west and central part of the EAB. Rey et al. (1986a) also

introduced the Tadhart Fm. of late Aptian age (Gargasian in regional French stratigraphy), sitting between the Tamzergout and subsequent Oued Tidzi Fm. In this study, we propose a different age range for the Tamzergout Formation (see below), from the early to latest Aptian. We, therefore, consider the Tadhart Fm. a time-equivalent unit for parts of the upper Tamzergout Fm. that is restricted to the eastern and more proximal parts of the basin. In the western and central part of the basin, it cannot be discriminated from the Tamzergout Fm. In the studied area, the top of the Tamzergout Fm. is marked by a regional unconformity that was previously reported from Agadir (discontinuity **D4** of Peybernes et al. 2013). The formation reaches a maximum thickness of 33 metres at Tiskatine.

In most sections studied, the lower part of the formation contains the base of the *Deshayesites forbesi* Zone (lowermost Aptian). *Procheloniceras dechauxi* is abundant but first appears in the underlying Bouzergoun Fm. At Tiskatine, the first limestone bed of the Tamzergout Fm. is marked by the First Occurrence (**FO**) of "*Epicheloniceras*" *marocanus* (Roch, 1930) that indicates the base of the upper part of the *Colombiceras tobleri* Zone (see discussion below). The assigned ages further highlight the diachronicity of the top Bouzergoun Formation and base Tamzergout Formation. The upper part of the formation is usually rich in small pyritic ammonites that indicate a latest Aptian age (*Elsaisabellia tiskatinensis* Zone, see definition and discussion below).

3.3.1.3 Lemgo Formation

The Lemgo Fm. was introduced by Duffaud et al. (1966) and subsequently re-interpreted by Rey et al. (1986b) to include a complex of green marls, yellow sandy marls and sandy dolomites at the top. It is named after the Jbel Lemgo ridge, to the east of Imi'n'Tanoute.

Based on our field observations and microfacies analysis in the Mramer section, the Lemgo Fm. is composed of argillaceous sandstones and bioclastic-rich sandy limestones. Regional correlations suggest that the Lemgo Fm. represents the proximal equivalent of the upper Tamzergout Formation and is not present in the western central part of the basin (see discussion below).

Rey et al. (1988) assigned the formation to the uppermost Aptian (Clansayesian in regional French stratigraphy) based on the occurrence of ammonite assemblages that characterized the *Nolaniceras nolani* and *Hypacanthoplites jacobi* zones. Material collected

in this study of what is exposed of the Lemgo Fm. at the Mramer section indicates a latest Aptian to earliest Albian age (*Acanthohoplites aschiltaensis* to *Mellegueiceras chihaouiae* zones, see discussion below).

3.3.1.4 Oued Tidzi Formation

Described by Duffaud et al. (1966) as marls, it was redefined by Rey et al. (1988) as a complex of green marls bearing small pyritic ammonites, intercalated with marly limestones and sandy dolomites.

The unit is easily recognized in the west-central part of the EAB where it reaches a maximum thickness of 340 m and forms extensive recessive slopes in the landscape. Our field observations and microfacies analysis, focused on the lower part of this formation, show a clear change from blue marls and limestones of the Tamzergout Fm. to a complex of green marls with minor bioclastic-rich sandstone interbeds (Fig. 3.2). The early Albian age of the basal sandstones is established by the occurrence of the diagnostic ammonite genus *Douvilleiceras*.

3.3.2 Previous work on Aptian biostratigraphy

Pioneering work reporting and describing ammonites in the EAB was undertaken by Kilian and Gentil (1906), Roch (1930) and Ambroggi (1963). The work of Ambroggi (1963) has to be highlighted, as it established the first regional biostratigraphic framework for the Lower Cretaceous. The ammonite biostratigraphy of the Berriasian - Barremian interval was subsequently refined by Ettachfini (1991, 2004), Wippich (2001, 2003) and Company et al. (2008). Yet, despite the good accessibility of sections and abundance of ammonites, no recent studies have focused on the detailed ammonite palaeontology and biostratigraphy of the Aptian – Albian interval.

Following the work of Roch (1930) and Ambroggi (1963), extensive faunal lists of Aptian and Albian ammonites were published by Bergner et al. (1982), Rey et al. (1986a and b, 1988), Witam et al. (1993) and Witam (1998). Unfortunately, the precise stratigraphic position of the material within the formations was not documented and only a very limited number of specimens were illustrated in the literature. As a consequence,

the available previously published data sets do not fulfil the standards of modern biostratigraphic studies and it is difficult to reinterpret them in the light of our own results.

Most recently a detailed biostratigraphic framework based on bed-by-bed collections from a transect along the Agadir segment of the EAB was published by Peybernes et al. (2013). A fairly high degree of endemism was suggested by the introduction of many new species and genus names that are unfortunately not formally described or illustrated. The authors chose not to introduce new biostratigraphic units but pointed out the necessity for a local ammonite zonal scheme. The published zonation is an attempt to apply the upper lower Aptian to Lower Albian ammonite zonal scheme of northern Tethys (Reboulet et al., 2011) to the EAB. This interval is described as being strongly affected by condensation and temporal hiatuses. According to these authors, the co-occurrence of *Cheloniceras sp.* and *Deshayesites sp.* indicates an early Aptian age for the base of the Tamzergout Fm. (tentatively assigned the *Deshayesites deshayesi* Zone). Condensation and merging of unconformities across the lower/upper Aptian boundary is supported by the mixing of *Dufrenoyia furcata* and *Epicheloniceras martini* zones assemblages. The upper Aptian *Epicheloniceras martini*, *Parahoplites melchioris*, *Acanthohoplites nolani* and *Hypacanthoplites jacobi*, zones are identified on the basis of characteristic ammonites assemblages, even so it is highlighted that the extension of the *P. melchioris* Zone is uncertain, as the index fossil is absent and indicative taxa are scarce. The lower Albian *Leymeriella tardefurcata* Zone and *Douvilleiceras mammillatum* Superzone are recognized throughout most of the basin even though the index species are absent. It should be noted that a bed-by-bed distribution of ammonites is only documented in the Addar section and the authors do not provide photographic plates to substantiate the ammonite systematics used in their contribution.

3.4 Studied sections

The present publication is focused on five Aptian-Albian sections (Fig. 3.1). Locations were chosen to reinvestigate previously studied sections for reference and further to add new sections for better spatial constraints and coverage of the western, central and the northern part of the basin.

3.4.1 Tiskatine

Tiskatine (Fig. 3.3) - Lat.: 30.821463° Long.: -9.702555° (Tiskatine 1) and Lat.: 30.810477° Long.: -9.739966° (Tiskatine 2).

The lower part of the succession (beds **TK 159 to 206,** Fig. 3.3) is best exposed 6.5 Km to the east of the village of Assaka (Tiskatine 1), northwest of Adrar (mountain) Tiskatine. The upper beds (**TK 206 to 249**) are better exposed 3 Km to the east of Assaka (Tiskatine 2). The two sections were correlated using the marker bed **TK 206**. Section Tiskatine 1 starts in the riverbed south of the road from Assaka to Tazzougart and continues to the north. At Tiskatine 2 the beds crop out on both sides of the road. Tiskatine 1 was previously studied by Roch (1930) and Ambroggi (1963). A detailed sedimentary log with field photographs of key intervals and surfaces are shown in appendix C11 and C14.

3.1 m of the upper part of the Bouzergoun Fm. are exposed at Tiskatine. The first bed (**TK 157**) is a well-consolidated oyster-rich, ammonite-barren, sandy limestone topped by an iron-rich crust (see App. C11). It is followed by yellow sandstones interbedded with yellow to green mudrock partings (beds **TK 158-162**). The sandstones are fine-grained and show low angle cross-bedding and laterally extensive undulating surfaces. They are often topped by iron-enriched crusts, yielding phosphatic, glauconitic pebbles and fossils. The fossil content comprises ammonites, belemnites, echinoids, gastropods, and rare solitary coral fragments. The top surface of bed **TK 161** is marked by a belemnite accumulation that suggests transport and winnowing by currents (type 4 condensation accumulates of Doyle and Macdonald (1993)). The deposits represent a deepening-upward shallow marine succession. Wave-influenced shoreface sedimentation dominates at the base (bed **TK 157**) with a subsequent transition into lower shoreface to offshore sedimentation (bed **TK 158-162**). The contact with the overlying Tamzergout Fm. is marked by well-developed marls in bed **TK 163** (App. C11). The contact is abrupt and marks the change to shelfal conditions below storm wave base.

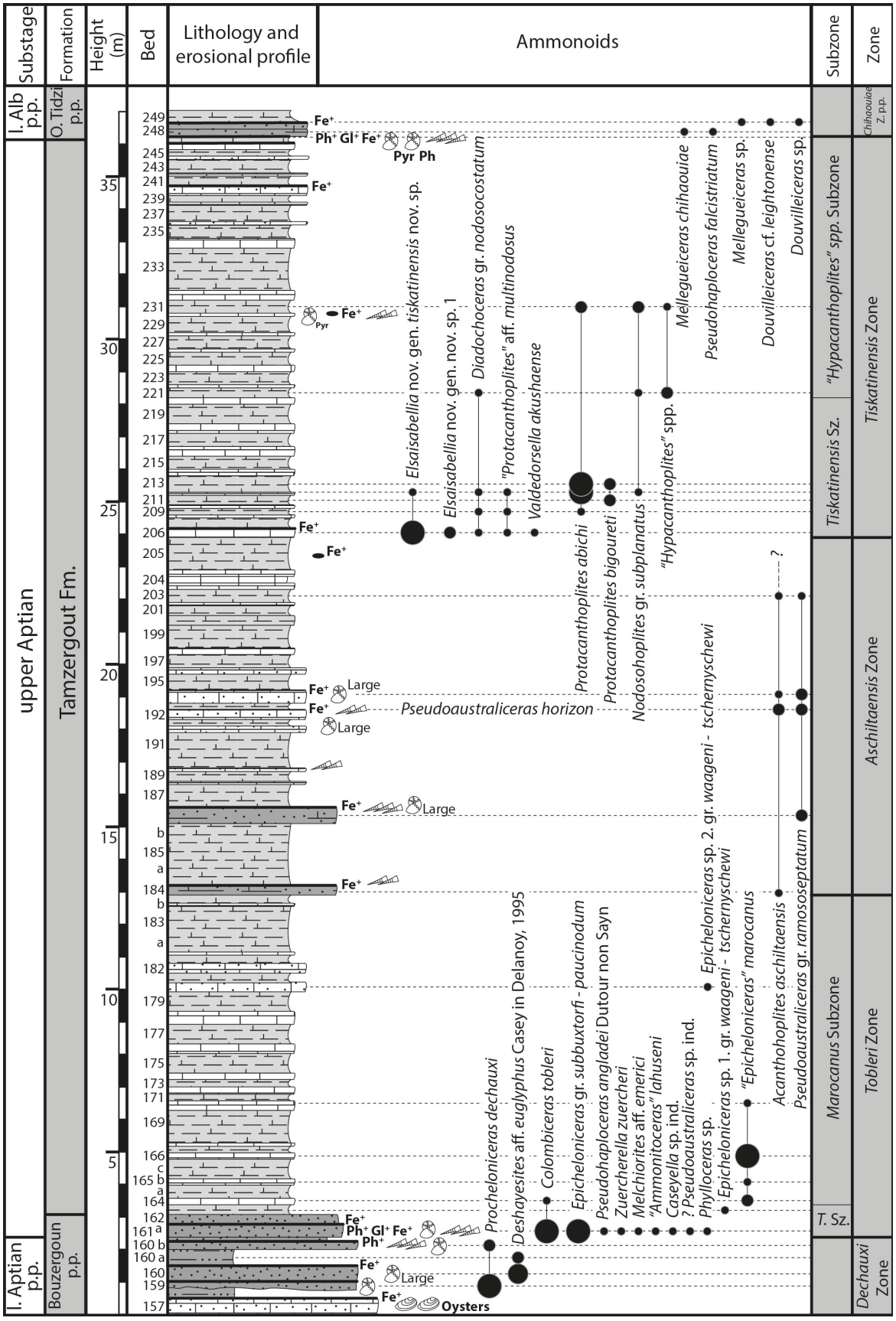

Figure 3.3: Tiskatine section. Ammonoid distribution and biostratigraphic interpretation. Legend in Fig. 3.2.

The alternating blue-grey marls and grey limestones of the Tamzergout Formation develop from bed **TK 163** to bed **TK 247** (App. C14). The marls are laminated, forming decimetre- to metre-thick beds. Limestones are 10 to 20 centimetres thick and appear massive. Contacts between alternating beds are mostly sharp and planar. In the middle part of the succession, some limestones beds have a detrital component (**TK 180, 182, 192** and **194**) and two prominent fine-grained sandstone beds (**TK 184** and **TK 186**) are recognised. The sandstones are topped by ferruginous crusts. From bed **TK 197** to bed **TK 246** the succession is characterized by a fairly monotonous alternation of marls and limestones. **TK 206** is a prominent extremely fossiliferous marker bed, with a well-developed iron-crust on the top. Above, the marls are rich in pyritic nodules and ammonites, and some minor detrital input was observed toward the top of the Tamzergout Fm. that ends at a distinct glauconitic horizon (bed **TK 247**) rich in phosphate nodules. The total thickness of the Tamzergout Fm. is 33.15 metres. Sedimentation of the Tamzergout Fm. is mainly through suspension fall out. Sandstone beds **TK 184** and **TK 186** are interpreted as gravity flow deposits.

The base of the Oued Tidzi Fm. is marked by a fossil-rich sandstone bed **TK 248** (App. C11 and C14) that contains reworked phosphatic pebbles and glauconitic fossils (including ammonites). It is capped by a well-developed iron crust directly overlain by distinctive green to yellow marls of the Oued Tidzi Fm. Bed **TK 248** is interpreted as a shelf gravity flow.

Ammonite abundance and diversity vary throughout the succession. This discontinuous palaeontological record may partially reflect collection failure, despite an intensive search of the barren intervals. Based on our present knowledge, the following sequence of bio-events is recognised as regionally significant following comparison with the other sections studied:

- Bio-event 1: sudden mass occurrence of *Prochelonicerasin* bed **TK 159**, followed by the first observed occurrence of *Deshayesites* in bed **TK 160**;
- Bio-event 2: peak of diversity in bed **TK 161a** dominated by *Colombiceras* and *Epicheloniceras*;
- Bio-event 3: first apparition datum of the endemic species "*Epicheloniceras*" *marocanus* at the top of bed **TK 162**, followed by its acme in bed **TK 166**;
- Bio-event 4: lowest occurrence of *Acanthohoplites* in bed **TK 184**;

- Bio-event 5: peak of abundance of *Pseudoaustraliceras* in beds **TK 192** and **TK 194**;
- Bio-event 6: sudden mass occurrence of *Elsaisabellia* gen. nov. in bed **TK 206**;
- Bio-event 7: radiation of the Acanthohoplitidae (*Nodosohoplites*, *Protacanthoplites* and "*Hypacanthoplites*") from bed **TK 206** to bed **TK 221**;
- Bio-event 8: lowest occurrence of *Douvilleiceras* in bed **TK 248**.

Tiskatine is the only studied section where the complete succession of events was recognized and documented. It has, therefore, been selected as the reference section for the ammonite biostratigraphy of the west-central part of the EAB.

3.4.2 Tamanar

Tamanar (Fig. 3.4) - Lat.: 31.057403° Long.: -9.601503°

This outcrop is 10 Km northeast of Tamanar and the section is also known as Ida Ou Shak named after the nearby village. It can be reached via an unmade track that leaves National road 1 approximately 8 Km north of Tamanar. This section has not been previously described in the literature.

Fine-grained laminated sandstones with interbedded calcareous mudstones make up the lower 8 metres (beds **TM 49** to **58**) of the studied section and comprise the uppermost part of the Bouzergoun Fm. Oysters and other large bivalves are abundant throughout. The lower part of the logged section is affected by soft sediment deformation. The first occurrence of ammonites is recognised on top of the slumped interval. The deposits of the Bouzergoun Fm. here are interpreted as lower shoreface to offshore shelf transition.

The base of the Tamzergout formation is marked by the change to limestones and interbedded marls, both containing abundant open-marine fauna (e.g. ammonites and belemnites). The formation encompasses beds **TM 59** to **TM 80**. Compared to the interval exposed at Tiskatine, the limestones here have a stronger siliciclastic detrital component. The succession is fairly monotonous, but a few beds have notable features. From bottom to top, these are:

- Bed **TM 69** contains very abundant ammonites (dominantly *Prochelonicerasdechauxi*) associated with a high ferruginous content;

- Bed **TM 70a** is a slumped complex marked the only occurrence of upper lower Aptian ammonites (*Cheloniceras*) identified in this study;

- Bed **TM 71** contains a phosphatic, glauconitic and ferruginous fossil assemblage rich in ammonites, belemnites, bivalves, and brachiopods.

- Bed **TM 73** contains belemnites and bivalves and is marked by a well-developed and prominent iron crust.

- Bed **TM 76** is rich in ammonites and marks an increase in diversity of the ammonite fauna

- Bed **TM 80** yields abundant pyritic ammonites.

The sandstone of bed **TM 81** is interpreted to define the base of the Oued Tidzi Formation, displaying a similar depositional environment to Tiskatine.

The Tamzergout Formation has a total thickness of 19.20 metres. At this location it is interpreted to be mixed shelfal pelagic marls, with changes in siliciclastic sediment influx transported by wave and current supported gravity flows, forming the sandy limestones.

Compared to the succession of bio-events recognized at Tiskatine, several points should be outlined:

- Bio-event 1 is marked by a less sudden appearance of *Prochelonicerasin* bed **TM 55**;

- Bio-event 2 is not well expressed due to poor outcrop conditions but merely lies at the top of bed **TM 71**;

- Bio-event 3 is marked by the spot occurrence of "*Epicheloniceras*" *marocanus* in bed **TM 72**;

- Bio-event 4 and 5 are not recorded;

- Bio-event 6 and 7 are identified in beds **TM 76** to **TM 80** with a slightly different expression due to condensation combine with temporal hiatus.

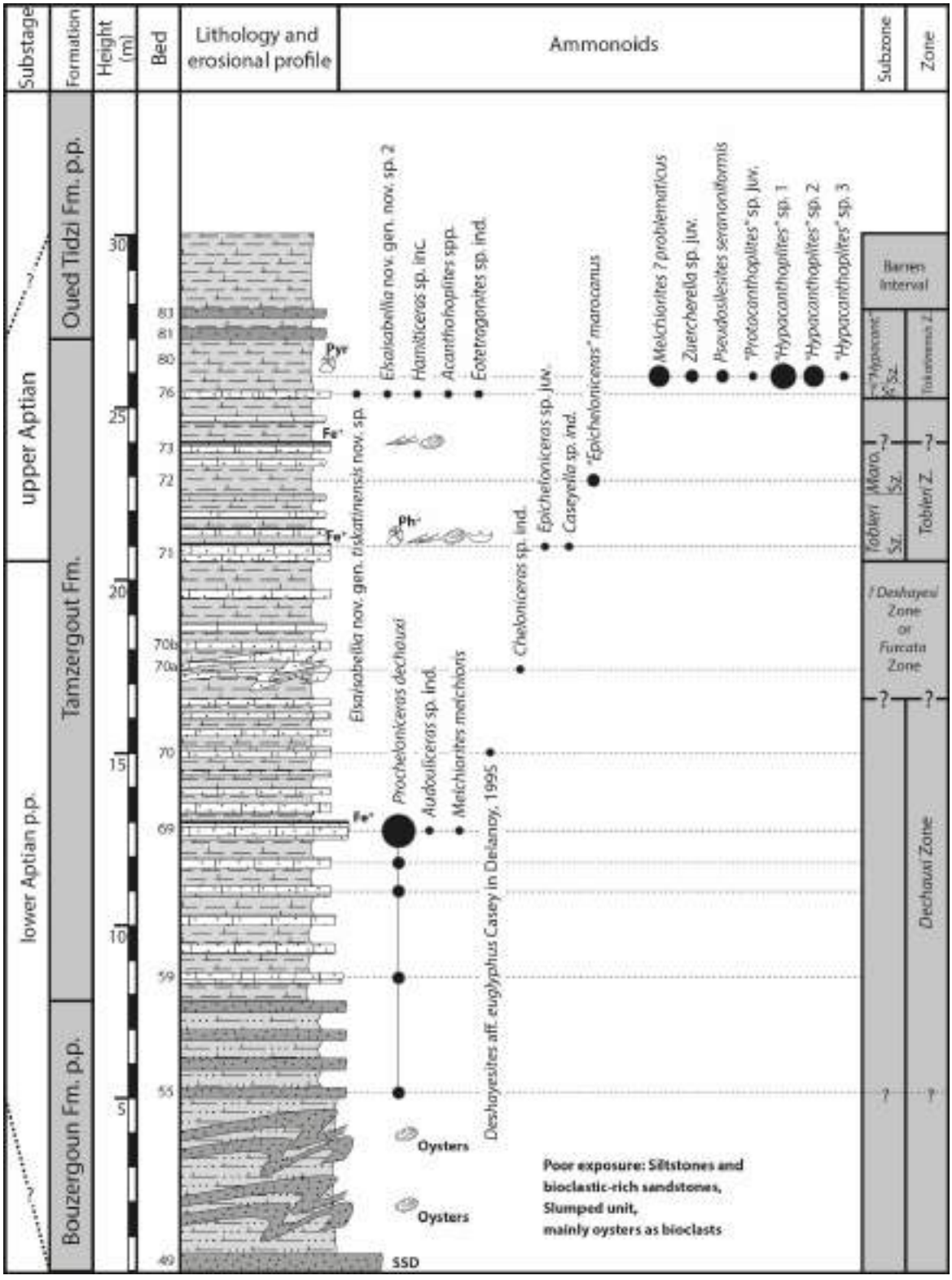

Figure 3.4: Tamanar section. Ammonoid distribution and biostratigraphic interpretation. Legend in Fig. 3.2.

3.4.3 Zem Zem

Zem Zem (Fig 3.5) - Lat.: 31.241846° Long.: -9.372052°

Located about 17 Km to the south-southeast of Meskala, this outcrop can be reached via an unmade road leaving the main road between Bizdad and Ait Daoud, approximately 2 Km south-southeast of Bizdad. Nearby sections have been studied by Roch (1930), Butt (1982), Rey et al. (1986a, 1988) and Witam (1998).

The Bouzergoun Fm. reaches a thickness of 12 metres at Zem Zem (up to bed **ZZ 60**).The upper part is composed of sandy rudstones, sandstones and minor wackestones with marls interbedded. Fauna is dominated by brachiopods, oysters, ammonites and echinoderms, pointing towards open-marine conditions. Horizon **ZZ 59** is a prominent ferruginous surface just below the topmost bed of the formation, containing abundant fossils with phosphatic preservation. Deposition overall took place in a shoreface to carbonate-rich subtidal environment with higher energy index, on a shallow shelf.

The Tamzergout Fm. is interpreted to extend from bed **ZZ 61** to **ZZ 68** and is dominated by marls with two prominent limestone beds (**ZZ 61** and **ZZ 65**) and a sandstone bed topped by an iron crust (**ZZ 67**). The thickness of the Tamzergout Fm. is approximately 20 metres, and the presence of laterally extensive marls with limestone interbeds containing open marine fauna and reduced siliciclastic input suggests a low-energy shelf environment, similar to that at Tiskatine.

The base of the Oued Tidzi Fm. is defined as a prominent sandstone horizon, and continues to the top of the measured section, with a minimum thickness of 10 metres.

At Zem Zem, the palaeontological record shows that bio-event 1 (mass occurrence of *Prochelonicera*s) is well expressed and almost directly overlain by the sudden appearance of *Elsaisabellia* gen. nov., followed by the radiation of the Acanthohoplitidae (bio-events 6 and 7). Bio-event 2 is suspected in the condensed horizon at the top of the Bouzergoun Fm. (spot occurrence of *Epicheloniceras* with reworked *Deshayesites* at the top of bed **ZZ 60**). Bio-events 3, 4 and 5 are not recorded and outline the existence of a major temporal hiatus at the base of the Tamzergout Fm.

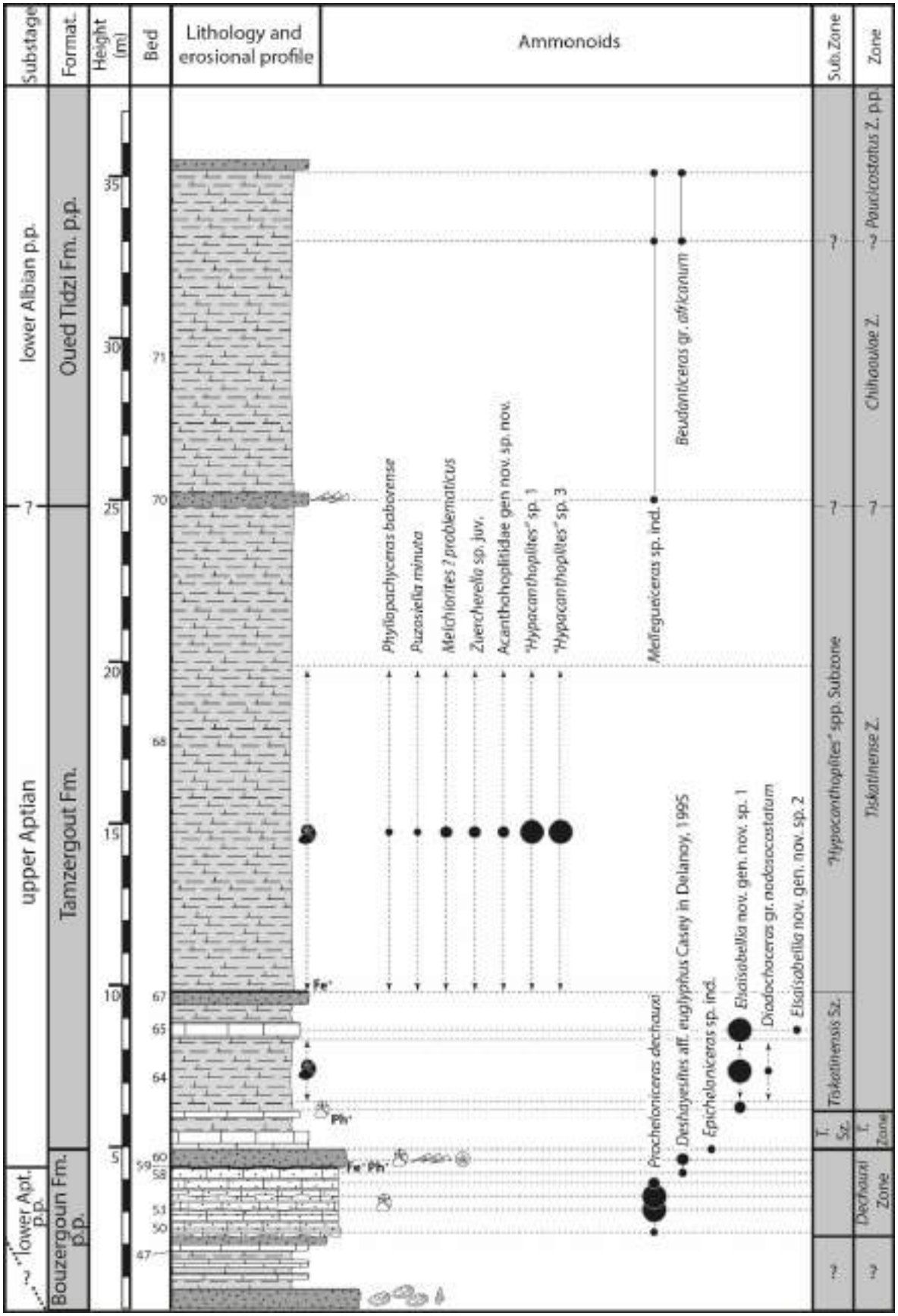

Figure 3.5: Zem Zem section. Ammonoid distribution and biostratigraphic interpretation. Legend in Fig. 3.2.

3.4.4 Oued Tlit

Oued Tlit (Fig. 3.6) - Lat.: 31.194306° Long.: -9.665616°

The section is located 4 Km southeast of Smimou, on the northern flank of the Djebel Amsittene anticline, north of the road between Smimou and Imi'n'Tlit. This locality has previously been studied by Roch (1930), Rey et al. (1986a, 1988) and Witam (1998).

The top of the Bouzergoun Formation comprises the lowermost 2.10 metres. It is composed of fine to medium-grained non-amalgamated sandstones interbedded with mudstones. The sandstones exhibit hummocky cross-stratification and are often affected by in-situ soft sediment deformation. The upper part is formed by a very prominent set of oyster rudstones. The depositional environment is interpreted as shoreface to subtidal. Ammonites occur immediately above the set of oyster rudstones and the remaining 11.70 m are interpreted to as part of the Tamzergout Formation. It comprises alternating marls and micritic limestones. A well-expressed hardground surface marked by iron crust and glauconite, associated with belemnite accumulation and phosphatic ammonites, occurs at the top of bed **OT 11**. The upper part of the Tamzergout Fm. has not been investigated in this study.

The succession of bio-event 1 (sudden appearance of *Prochelonicera*s) and bio-event 2 (peak abundance of *Epicheloniceras* and *Colombiceras*) are recognized in the lower part of the Tamzergout Fm. Our findings also question the identification of the *Dufrenoyia* and *Epicheloniceras* illustrated by Witam (1998) from this section (see discussion below).

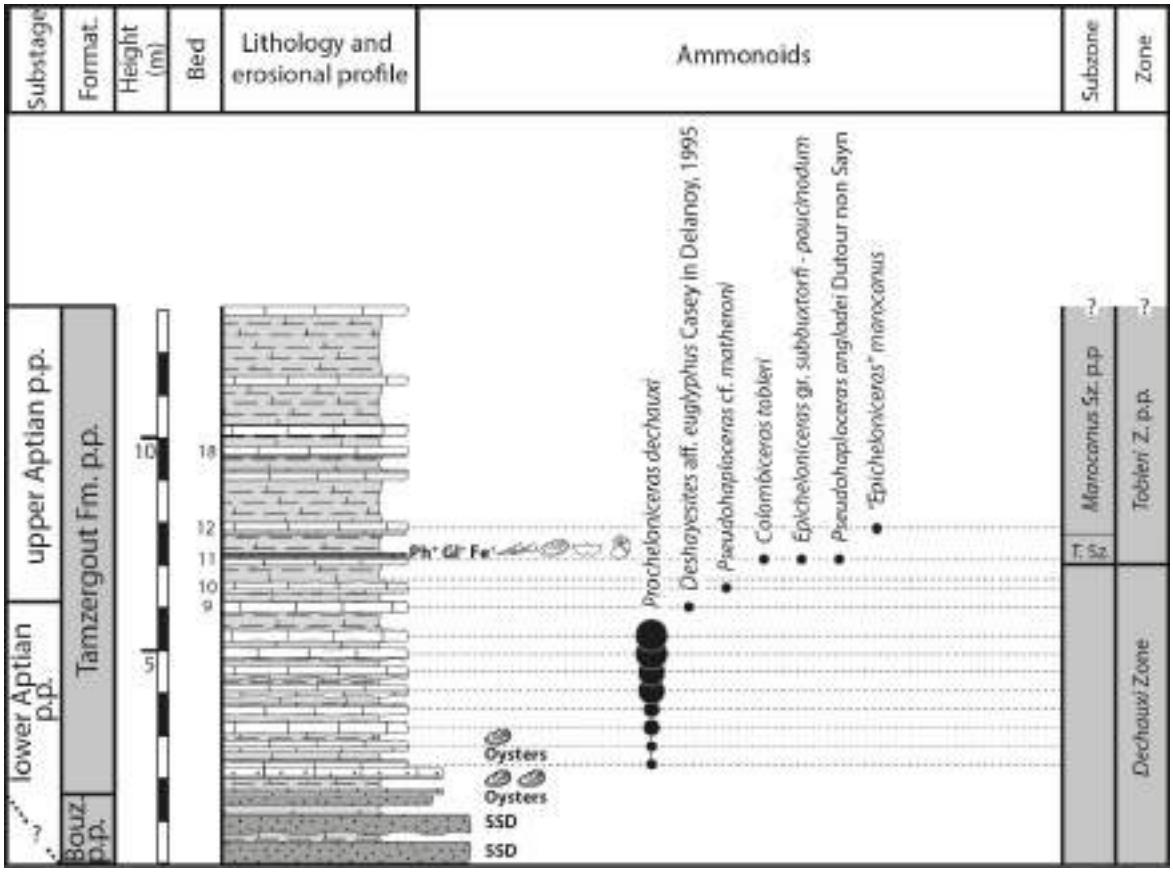

Figure 3.6: Oued Tlit section. Ammonoid distribution and biostratigraphic interpretation. Legend in Fig. 3.2.

3.4.5 Mramer

Mramer (Fig. 3.7) - Lat.: 31.657033° Long.: -9.164205° (Mramer 1) and Lat.: 31.666118° Long.: -9.153251° (Mramer 2).

Mramer represents the northernmost section studied in the EAB. It is located approximately 60 Km to the ENE of Essaouira and 12 Km NE of Tafetachte. The Mramer section is a composite section, both locations cropping out in a river bed. Mramer 1 is located about 1.5 Km to the northeast of the market in Mramer and location Mramer 2 is at the base of a steep slope south of the market. This outcrop was mentioned by Roch (1930) but not reported in detail.

The upper 3.50 metres of the Bouzergoun Fm. are exposed at this locality. Strata are dominated by sandstones and siltstones. The fauna is rich in oyster fragments, and further includes scarce ammonites; towards the top echinoderm fragments are common. The medium to fine-grained sandstones exhibit in-situ soft sediment deformation

structures and common bioturbation, they are dominated by low-angle cross lamination, interpreted to have been deposited under shoreface conditions.

The following interval (beds **MR 9a** to **9f**) comprises part of the Tamzergout Fm., here composed of sandy limestones and marls interbedded. The limestones contain belemnites, bivalves, and echinoderms and exhibit prominent iron crusts at the tops. The exposed part of the Tamzergout Fm. records a return to shelfal, open water, and lower-energy depositional environments. This interval is capped by a zone of poor exposure that is 17.5m thick and likely composed of limestones and interbedded marls with increasing abundance of ammonites.

It is overlain by the Lemgo Fm., the proximal equivalent to the upper Tamzergout Fm. The base of the Lemgo Fm. is not exposed in the study area. It is composed of yellow argillaceous sandstones and sandy limestones obtaining a minimum thickness of 4.50 metres. Fossil-rich sandy limestones at the base (beds **MR 9x** to **9z**) are laterally continuous. Beds **MR 10** to **MR 17** comprise very fine- to fine-grained sandstones interbedded with floatstones. Sandstones exhibit large-scale, higher energy dune bed forms and often rework the interbedded limestones. Limestones have well-developed iron crusts and are rich in fossils containing brachiopods, ammonites, gastropods, and belemnites. These fossils often occur in phosphatic and glauconitic preservation, pointing to a reoccurrence of anoxia.

This mixed siliciclastic-carbonate succession is interpreted to represent shelfal carbonates being reworked by sandstones deposited during intermittent, wave-influenced sedimentation. The Abundance of ammonites and cosmopolitan taxa imply an open–marine connection but the reoccurrence of anoxia and absence of indicative, open-marine fauna is pointing towards a periodic development of a restricted environment. Overall, this represents a shallowing-up succession with a higher energy index than other time-equivalent sections studied of the central and western part of the basin. The Lemgo Fm. is overlain by marls and minor sandy limestones of the Oued Tidzi Fm. that starts at bed **MR 20** and marks the return into lower-energy shelfal sedimentation.

At Mramer, the Lemgo Fm. records the local expression of bio-events 6 to 8. The ammonite succession is characterized by the radiation of the Acanthohoplitidae from bed **MR 10m** to **MR 15**, followed the lowest occurrence of *Douvilleiceras* in bed **MR18**. Noteworthy is the occurrence of a well preserved and abundant fauna of *Mellegueiceras*, a genus that was so far only known from Central Tunisia (Latil, 2011).

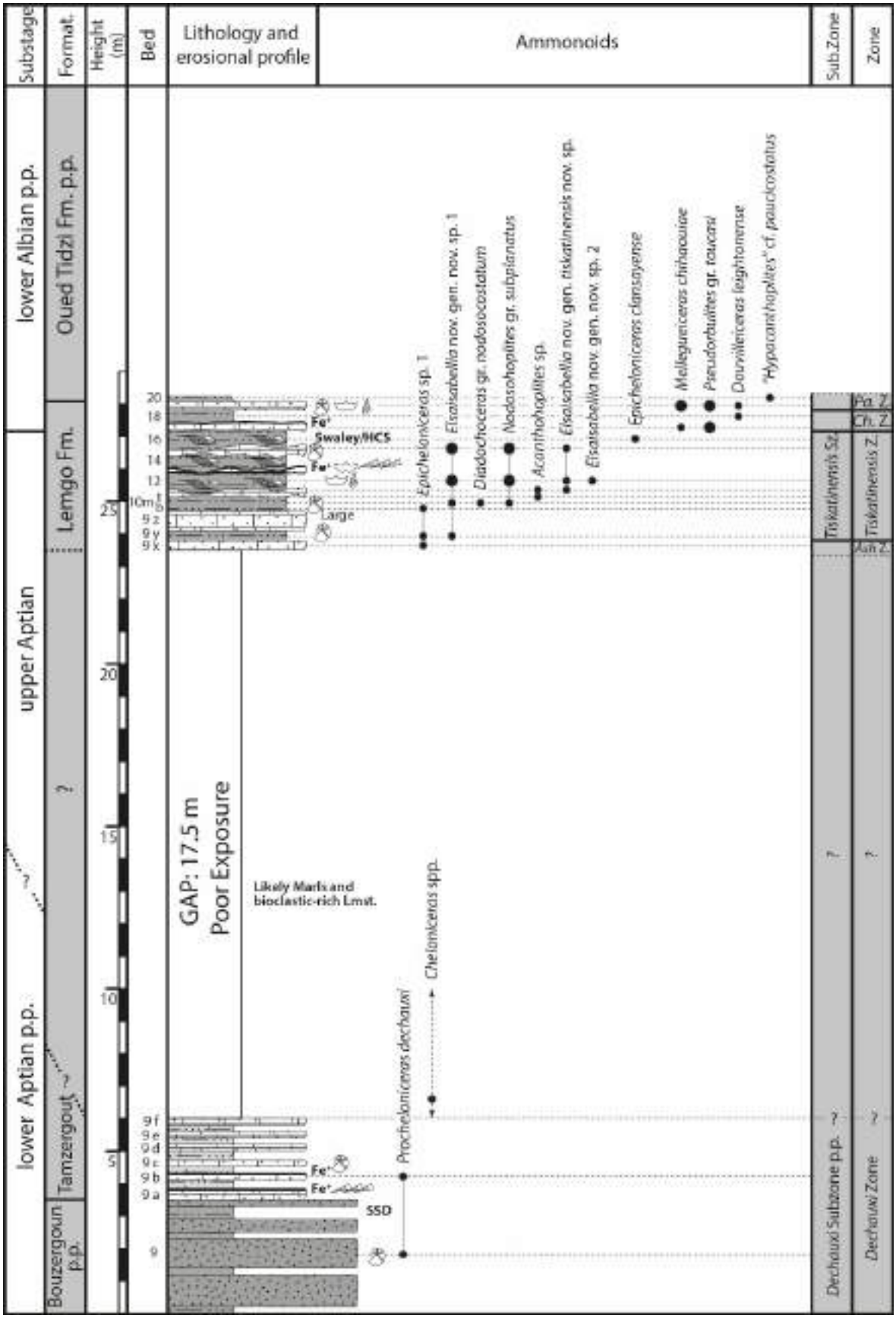

Figure 3.7: Mramer section. Ammonoid distribution and biostratigraphic interpretation. Legend in Fig. 3.2.

3.5 Systematic palaeontology

More than 1000 ammonite specimens were collected during two field sessions in 2015 and 2016. To our knowledge, the material collected represents the largest bed-by-bed collection made from the Bouzergoun and Tamzergout formations of the central and northern part of the EAB. The preservation of the material is variable and includes internal calcareous, phosphatic and pyritic moulds. Abundance varies considerably throughout the studied sections and high diversity is observed in specific horizons, some of which can be correlated at the scale of the EAB.

As already outlined in the faunal lists given by our predecessors (Roch, 1930; Ambroggi, 1963; Rey et al., 1986a), the ammonite assemblages are largely dominated by the Douvilleiceratidae Parona and Bonarelli, 1897 and Acanthohoplitidae Stoyanow, 1949. The Deshayesitidae Stoyanow, 1949, Desmoceratidae Zittel, 1895 and Ancyloceratidae Gill, 1871 are minor elements of the faunas. Aconeceratidae Spath, 1923, Phylloceratidae Zittel, 1884 and Tetragonitidae Hyatt, 1900 are even rarer.

Despite an extensive list of published work, the systematics of the Aptian Ammonoidea is still at a very preliminary stage due to the lack of modern taxonomic revision taking in consideration intraspecific variation and sexual dimorphism. This is especially true for the Douvilleiceratidae and Acanthohoplitidae, for which a plethora of typological species was introduced over the years (see lists in Klein and Bogdanova, 2013). Moreover, there is hardly any agreement among authors regarding the limits and content of *Colombiceras* Spath, 1923, *Acanthohoplites* Sinzow, 1908; *Protacanthoplites* Tovbina, 1970; *Nolaniceras* Casey, 1961a; *Hypacanthoplites* Spath, 1923; *Prochelonicera*s Spath, 1923; *Diadochoceras* Hyatt, 1900; *Nodosohoplites* Egoian, 1965 and *Epicheloniceras* Casey, 1954.

Finally, a large number of species are based on material that was collected from condensed beds. This is the case for many key taxa from South-Eastern France (Seunes, 1887; Jacob, 1905) and Switzerland (Jacob and Tobler, 1906); and the great majority of the late Aptian faunas from western Caucasus (Egoian, 1965, 1969), northern Caucasus (Sinzow, 1906, 1913; Nikchitch, 1915), Dagestan (Anthula, 1900; Kazansky, 1914), Georgia (Kvantaliani, 1971, 1972), Turkmenistan (Glazunova, 1953; Tovbina, 1968, 1970, 1982) and Mangyschlak (Sinzow, 1908; Glazunova, 1953). Although the recent contribution of Bogdanova and Mikhailova (2016) clarifies the biostratigraphic distribution of the early late

Aptian ammonites of the northern Caucasus and Transcaspia to some extent, the precise range of the latest Aptian faunas remain poorly understood.

The palaeontological study of the Aptian ammonite faunas from the EAB deserve extensive taxonomic descriptions that are beyond the scope of the present paper. Selected elements of the fauna that are crucial for the definition of the biostratigraphic scheme are illustrated (Figs. 3.8 to 3.11) and their taxonomic assignments are briefly discussed. In most cases, the identifications are based on direct comparison with the originals or plaster casts of the type material from SE France (Seunes, 1887; Jacob, 1905; Kilian and Reboul, 1915), Switzerland (Jacob and Tobler, 1906), Dagestan (Anthula, 1900) and Mexico (Burckhardt, 1925; Humphrey, 1949). A deliberate choice has been made to reduce synonymies to a limited number of key specimens. Emphasis has been taken on material from Morocco previously illustrated in the literature. Unless otherwise mentioned the suprageneric classification retained herein follows the nomenclature of Wright et al. (1996).

Order Ammonoidea Zittel, 1884
Suborder Ancyloceratina Wiedmann, 1966
Superfamily Douvilleiceratoidea Parona and Bonarelli, 1897
Family Douvilleiceratidae Parona and Bonarelli, 1897

Comment. For the reasons exposed by Bulot in Vincent et al. (2010, p. 184), Cheloniceratinae Spath, 1923 is herein considered as a junior subjective synonym of the subfamily Douvilleiceratinae.

Subfamily Douvilleiceratinae Parona and Bonarelli, 1897
Genus *Procheloniceras* Spath, 1923

Type species. Ammonites stobieckii d'Orbigny, 1850, p. 113.

Procheloniceras dechauxi (Kilian and Reboul, 1915)
Figure 3.8.7–12

Holotype. *Douvilleiceras Martinii* var. *Dechauxi* Kilian and Reboul, 1915, p. 56, pl. 1, fig. 3.7, 7b, pl. 7, fig. 3.2. The specimen is housed in the Université de Grenoble collections (catalogue number UJF-ID.1084).

Remarks. The genus *Prochelonicerας* was reported on various occasions from the Tamzergout Fm. of the EAB. According to Roch (1930), *Prochelonicerας pachystephanum* (Uhlig, 1883) is the most common species with *P. albrechtiaustriae* (Uhlig, 1883). Additionally, *P. stobieckii* (d'Orbigny, 1850) was reported by Rey et al. (1986a, 1988). None of the specimens quoted by those authors were illustrated. The well-preserved and abundant material collected at Tamanar and Zem Zem questions those identifications. Even though a full revision of the genus is needed, the recent contributions of Delanoy (1995, 1998) and Delanoy et al. (2008) has helped to clarify the systematics of *Prochelonicerας*. Our material differs from *P. pachystephanum* and *P. albrechtiaustriae* by its smaller umbilicus, more depressed whorl section, and rigid and regular ornamentation. Most Moroccan specimens (Fig 3.8.7–10) match the holotype of *Prochelonicerας dechauxi* well. The variability of the populations includes a slender morphology (Fig. 3.8.11–12) that superficially matches the lectotype of *P. stobieckii* illustrated by Conte (1981) and Ropolo et al. (2008a).

Genus *Epichelonicerας* Casey, 1954

Type species. *Douvilleiceras Tschernyschewi* Sinzow, 1906, by original designation.

Epichelonicerας* gr. *subbuxtorfi – paucinodum (Burckhardt, 1925)
Figure 3.9.1–8.

v 1930. *Douvilleiceras buxtorfi* Jacob and Tobler; Roch, p. 381, pl. 19, fig. 1a–d.
v 1930. *Douvilleiceras aequicostatum* Burckhardt; Roch, p. 381, pl. 20, fig. 1a–b.
1998. *Cheloniceras (Epichelonicerας)* gr. *martinioides* Casey; Witam, p. 356, pl. 7, fig. 2–6.

Remarks. Epichelonicerας is a fairly common element of the late Aptian ammonite faunas of the EAB. It is noteworthy that the large population from Tiskatine (bed **TK 161A**) can easily be distinguished from the *Epichelonicerας* of the *martini* (d'Orbigny, 1841) and

buxtorfi (Jacob and Tobler, 1906) groups by the early loss of the ventral tubercles, simplified ornamentation and highly distinctive subrounded whorl section. The various morphotypes show close similarities with *Epicheloniceras paucinodum* (Burckhardt, 1925), *E. subbuxtorfi* (Burckhardt, 1925) and *E. aequicostatum* (Burckhardt, 1925). This affinity with the Mexican taxa was already recognised by Roch (1930, p. 381).

"*Epicheloniceras*" *marocanus* (Roch, 1930)
Figure 3.9.25–28.

v 1930. *Parahoplites* (?) *marocanus* Roch, p. 378, pl. 16, fig. 5–6.

Lectotype. *Parahoplites* (?) *marocanus* Roch, 1930, pl. 16, fig. 5 (UJF-ID.1601), herein designated.

Type locality. Tiskatine (Djebel Tissakatine in Roch, 1930).

Description. Small–sized planulate ammonites (Dmax ≤ 50mm) with a moderate evolute coiling. Earliest ontogeny unknown. On the adult whorl, the whorl section is depressed, sub-rounded and becomes progressively compressed, sub-rectangular and is higher than it is wide. The venter is moderately flattened and becomes rounded near the aperture. The umbilical wall is rounded and tends to become steep in the adult. The suture line is unknown. Two ornamental stages on the adult whorl:

(*i*) Alternation of tuberculate primary and one to two atuberculate secondary ribs. Small rounded tubercles occur on the upper part of the flank and divide into two branches. All ribs cross the venter but the adoral branches bear small thickenings on the ventrolateral margin;

(*ii*) Abrupt change toward spaced, simple ribs with rare secondaries. Ribs are slightly flexuous or straight with a marked apertural bending on the upper part of the flank. All ribs cross the venter forming an elevated proverse bending.

Remarks. This micromorphic species is provisionally assigned to *Epicheloniceras*. Derivation from an *Epicheloniceras* stock is based on the similarity of its early ontogenetic stages with

the juveniles of the *Epicheloniceras* of the *waageni* (Anthula, 1900) – *tschernyschewi* (Sinzow, 1906) group that occur in underlying level (see Fig. 3.9.29-32).

Family Deshayesitidoidea Stoyanow, 1949

Family Deshayesitidae Stoyanow, 1949

Genus *Deshayesites* Kazansky, 1914

Type species. *Ammonites Deshayesi* d'Orbigny, 1841, by original designation.

Deshayesites* aff. *euglyphus Casey, 1964 *in* Delanoy (1995)

Figure 3.8.1–6.

Microconchs

v 1995. *Deshayesites* aff. *euglyphus* Casey, Delanoy, p. 77, pl. 1, fig. 4, pl. 4, fig. 4.

v 1998. *Deshayesites* aff. *euglyphus* Casey, Delanoy, pl. 6, fig. 2, pl. 24, fig. 2 (Delanoy, 1995, pl. 1 ,fig. 4, pl. 4, fig. 4).

1998. *Deshayesites* aff. *luppovi* Bogdanova, Witam, p. 357, pl. 8, fig. 2.

Macroconchs

v 1995. *Deshayesites* aff. *evolvens* Luppov, Delanoy, p. 77, pl. 3, fig. 1.

Remarks. The Moroccan material includes both microconchs and macroconchs. The microconch forms show an intermediate morphology between *Deshayesites luppovi* Bogdanova, 1983 and the coarser morphotypes of the *D. forbesi* Casey, 1961a group such as *D. euglyphus* Casey, 1964. They match well the specimens illustrated by Delanoy (1995) as *D.* aff. *euglyphus*. The larger macroconchs compares with specimens from South East France that were most often misidentified as *Deshayesites consobrinus* (d'Orbigny, 1841) (Ropolo et al., 2000a, p. 162-163, fig. 3.2 and 4; Ropolo et al.,2006, pl. 6, fig. 6). The Moroccan specimens are left in open nomenclature and their species assignment will be addressed in a forthcoming contribution once the ongoing revision of the material from South-Eastern France is completed.

Superfamily Acanthohoplitoidea Stoyanow, 1949

Remark. Our ongoing revision of the Acanthohoplitidae supports the view that it has no phyletic link with the Parahoplitidae, even so both families derivate iteratively from the Douvilleiceratidae.

Family Acanthohoplitidae Stoyanow, 1949

Genus *Colombiceras* Spath, 1923

Type species. *Ammonites crassicostatus* d'Orbigny, 1841, by original designation.

Colombiceras tobleri (Jacob and Tobler, 1906)

Fig. 3.9.9-12

v 1930. *Parahoplites teffryanus* Karsten in Anthula; Roch, p. 377, pl. 16, fig. 7.

? 1998. *Colombiceras* aff. *tobleri* Jacob and Tobler; Witam, p. 362, pl. 10, fig. 5.

Remarks. Among the material from Morocco, two morphologies can be distinguished. The most common is a compressed and finely ribbed morphotype with a rectangular section and tabulate venter (Fig. 3.9.9–10). It somewhat bears a similarity to *Colombiceras crassicostatum* (d'Orbigny, 1841) and *Gargasiceras gargasense* (d'Orbigny, 1841) but the early ontogeny differs by having a distinct ribbing pattern where all the ribs appears single or by pairs on the umbilical margin and cross the venter without weakening. The other morphotype is a coarsely ribbed form that shows a rounded rectangular whorl section higher than wide and a widely spaced alternation of primary and intercalatory ribs. It closely matches the lectotype of *Colombiceras discoidale* (Sinzow, 1908, pl. 5, fig. 17–18) at similar growth stages. In our opinion, the slender and coarse morphotypes are conspecific and are linked by intermediate forms such as the specimen illustrated on Figure 3.9.9–11. Since the examination of a large number of specimens from South-Eastern France has convinced us that *Colombiceras discoidale* represent a compressed morphotype of *C. tobler*i, the Moroccan specimens are considered to fall within the range of variation of the

later species. It should be noted that the lectotype of *C. tobleri* notably differs from our material by its rounded section throughout ontogeny.

Genus *Acanthohoplites* Sinzow, 1908

Type species. *Parahoplites aschiltaensis* Anthula, 1900, by subsequent designation (Roman, 1938).

Remarks. Re-examination of Anthula's type material leaves no doubt that the lectotype designated by Dimitrova (1967, p. 185) is the microconch of the large specimen illustrated by Anthula (1900, pl. 10, fig. 4, pl. 11, fig. 1). Our material includes a series of individuals that match the macroconch well. Even though the large specimen illustrated on Figure 3.11.1-2 does not show the characteristic juvenile ornamental stage of *A. aschiltaensis*, complete material from other sections support its specific identification. The very large adult body chambers, which are characterized by a rigid adult ornamentation, and were collected from bed **MR 10t** and **11** at Mramer, are left in open nomenclature.

Genus *Protacanthoplites* Tovbina, 1970

Type species. Parahoplites abichi Anthula, 1900, by original designation.

Remarks. The genus has been variously interpreted since its introduction by Tovbina (1970) and some authors suggest that it could be a junior subjective synonym of *Acanthohoplites* (Wright et al., 1996, Bogdanova and Mikhailova, 2016). Comparison of the lectotypes of *A. aschiltaensis* and *P. abichi* shows that the two species are fairly close but the material at our disposal does not allow yet a definitive conclusion regarding synonymy. For the time being, we maintain the genus *Protacanthoplites* to accommodate the Moroccan specimens, that occur above the last occurrence *Acanthohoplites aschiltaensis*, and closely match *P. abichi* (Fig. 9.17–20), *P. bergeroni* (Seunes, 1987) and "*Protacanthoplites*" aff. *multinodosus* Tovbina, 1982 (Fig. 9.13–16).

Genus *Diadochoceras* Hyatt, 1900

Type species. *Ammonites nodosocostatus* d'Orbigny, 1841, by original designation.

Remarks. Specimens of *Diadochoceras* from the type locality of *D. nodosocostatum* are fairly numerous in the French historical collections (Obata, 1975), but our understanding of the genus is largely handicapped by the condensed character of faunas and the absence of a proper revision of the type species that is based on a single poorly preserved juvenile specimen (neotype designed by Guerin-Franiatte in Gauthier et al., 2006). Examination of the topotype material strongly suggest that the large number of new taxa introduced by Glazunova (1953), Mikhailova (1963), Egoian (1965, 1969) and Kvantaliani (1971, 1972) merely represent sexual dimorphism and intraspecific variation. This high variability is reflected by the Moroccan specimens and assignment to a *Diadochoceras nodosocostatum* group was preferred to the identification of specific typologic taxa (Fig. 3.9.21-22).

Genus *Nodosohoplites* Egoian, 1965

Type species. *Nodosohoplites subplanatus* Egoian, 1965, by original designation.

Remarks. As pointed out by Klein and Bogdanova (2013), there is no agreement in the literature about the validity and content of *Nodosohoplites*. Wright et al. (1996) consider that the genus is a junior subjective synonym of *Diadochoceras*. Szives et al. (2007) suggest that some of the specimens that were placed in *Nodosohoplites* by Egoian (1965) are sexual dimorphs of *Diadochoceras*. Our material shows that the planulate forms with a reduced trituberculate ornamental stage similar to *Nodosohoplites subplanatus* and *N. multispinatus* (Anthula, 1900) appear at a slightly younger stratigraphical level than the first occurrence of *Diadochoceras* of the *nodosocostatum* group. Pending a global revision of *Diadochoceras* and *Nodosohoplites* based on abundant and stratigraphically well-documented populations we prefer to keep the two genera separate.

Genus *Elsaisabellia* gen. nov.

Derivation of the name. Dedicated to Elsa Schnebelen-Bulot for her participation in our field investigations in Morocco and continuous support to one of us (L.G.B.) during the preparation of this work.

Type species. *Elsaisabellia tiskatinensis* sp. nov., by monotypy.

Diagnosis. Small–sized (D ≤ 45–50 mm), planulate ammonite with a moderate evolute coiling. Sub-rounded whorl section in the juvenile becomes sub-rectangular as growth increases. Venter is rounded throughout ontogeny. The umbilical wall is low to moderately steep at the adult stage. Two ornamental stage (*i*) irregular alternation of simple or bifurcate primary ribs and simple secondaries (D ≤ 15 mm); (*ii*) Uniform and dense ribs originates by pairs or bundles from periumbilical bullae. Bullae strengthen as growth increases and the ribs are more spaced on the outer part of the body chamber. All ribs cross the venter without interruption and slightly bend forward. Aperture is simple. Acanthohoplitid suture line.

Discussion. The genus *Immunitoceras* (type species: *I. immunitum* Stoyanow, 1949) compares superficially to *Elsaisabellia*. The original description and the re-examination of the holotype leave no doubt that the primary ribs are bituberculated at the younger stages and do not compare with the equivalent ontogenetic stages of *Elsaisabellia*. The only other acanthohoplid genus that can be compared with *Elsaisabellia* gen. nov. is *Nolaniceras*. Differences between the type species of the two genera are discussed below.

***Elsaisabellia tiskatinensis* sp. nov.**

Fig. 3.10.1-16.

1998. *Nolaniceras nolani* Seunes, Witam, p. 361, pl. 9, fig. 7a-b, pl. 10, fig. 1-2 (sol).

1998. *Nolaniceras nolani* var. *planulata* Egoian, Witam, p. 361, pl. 10, fig. 3a-b (sol).

Holotype. (MANCH) LL.16123, (Fig. 3.10.1-2).

Paratypes. (MANCH) LL.16124 – LL.16131, (Fig. 3.10.3-16).

Type locality. Tiskatine, Essaouira-Agadir Basin, Morocco.

Type strata. Bed **TK206**, *Elsaisabellia tiskatinensis* Zone (see definition below), upper Aptian.

Diagnosis. As for the genus.

Discussion. *Elsaisabellia tiskatinensis* sp. nov. has been misidentified as *Nolaniceras nolani* in the Moroccan literature (Rey et al. 1986a, 1988, Witam 1998, Peybernes et al. 2013). In a recent revision, Bulot et al. (2014) have shown that *Nolaniceras nolani* differs from all other uppermost Aptian Acanthohoplitidae by its highly distinctive low and convex umbilical wall and most unusual ornamental style. Compared to *Elsaisabellia tiskatinensis* sp. nov., *Nolaniceras nolani* can be distinguished by its compressed suboval whorl section throughout ontogeny, the absence of umbilical bullae and attenuation of the ribbing on the venter.

Remarks. The late upper Aptian Moroccan faunas also includes coarser and larger forms of *Elsaisabellia* that compare with *Acanthoceras bigoti* Seunes (1887) and *Acanthoceras migneni* Seunes (1887). These two species have been diversely interpreted in the literature and remain poorly understood since it seems that the originals from the Mignen collection are lost. The coarser forms of *Elsaisabellia* that dominate the assemblages at Mramer and Zem Zem are provisionally referred as *Elsaisabellia* sp. 1 and sp. 2. More work is needed to determine if these forms represent ecological morphotypes of *E. tiskatinensis* or new taxa.

Geographical and stratigraphical distribution. Since *E. tiskatinensis* is a very common ammonite in the lower part of the late upper Aptian of the EAB, it is selected herein as the index species of the *E. tiskatinensis* Zone. Outside Morocco, and despite an extensive survey of the literature, none of the specimens previously referred to *Nolaniceras nolani* in the literature can be assigned with certainty to our new species.

Genus *Hypacanthoplites* Spath, 1923

Type species. *Acanthoceras Milletianum* Var. *plesiotypica* Fritel, 1906, by original designation.

Remarks. Problems with the systematics of the genus *Hypacanthoplites* have been addressed at length by Bulot (2010). The genus was reported on many occasions in the Moroccan literature (Rey et al. 1986a, 1988, Witam 1998, Peybernes et al. 2013). Our new

collection shows that hypacanthoplid-like ammonites occur at two different levels in the EAB.

The older fauna is preserved as small pyritic internal moulds that occur above the *Elsaisabellia* beds at Tiskatine, Tamanar, and Zem Zem. Those forms are provisionally placed in "*Hypacanthoplites*" and left in open nomenclature as sp. 1, sp. 2 and sp. 3. They all show a very clear tabulate venter associated with a weakening of the ribs on the siphonal line. Even though there is a reinforcement of the ribs on both sides on the ventral shoulder; this feature is not as marked as in true *Hypacanthoplites*. The ornamental style of the very finely ribbed "*Hypacanthoplites*" sp. 1 (Fig. 3.11.15-25) suggests evolution from *Elsaisabellia tiskatinensis*. To the difference "*Hypacanthoplites*" sp. 3 (Fig. 3.11.3-11) shows a very distinct bituberculate ontogenetic stage that somehow recalls the ornamentation of *Hypacanthoplites tuberculatus* Egoian, 1969 and *H. microtuberculatus* Egoian, 1969.

Higher up in the succession, a collection of specimens that match the type material of *Mellegueiceras chihaouiae* Latil, 2011 and "*Hypacanthoplites*" *paucicostatus* Breistroffer in Dubourdieu, 1953 was made. This fauna will be described in a separate paper and its early Albian age is established by the co-occurrence of the genus *Douvilleiceras*. It should be noted that the fragments identified by Witam (1998, pl. 9, fig. 4-6) as *Hypacanthoplites* gr. *jacobi* (Collet, 1907) are merely misidentified "*Hypacanthoplites*" *paucicostatus*.

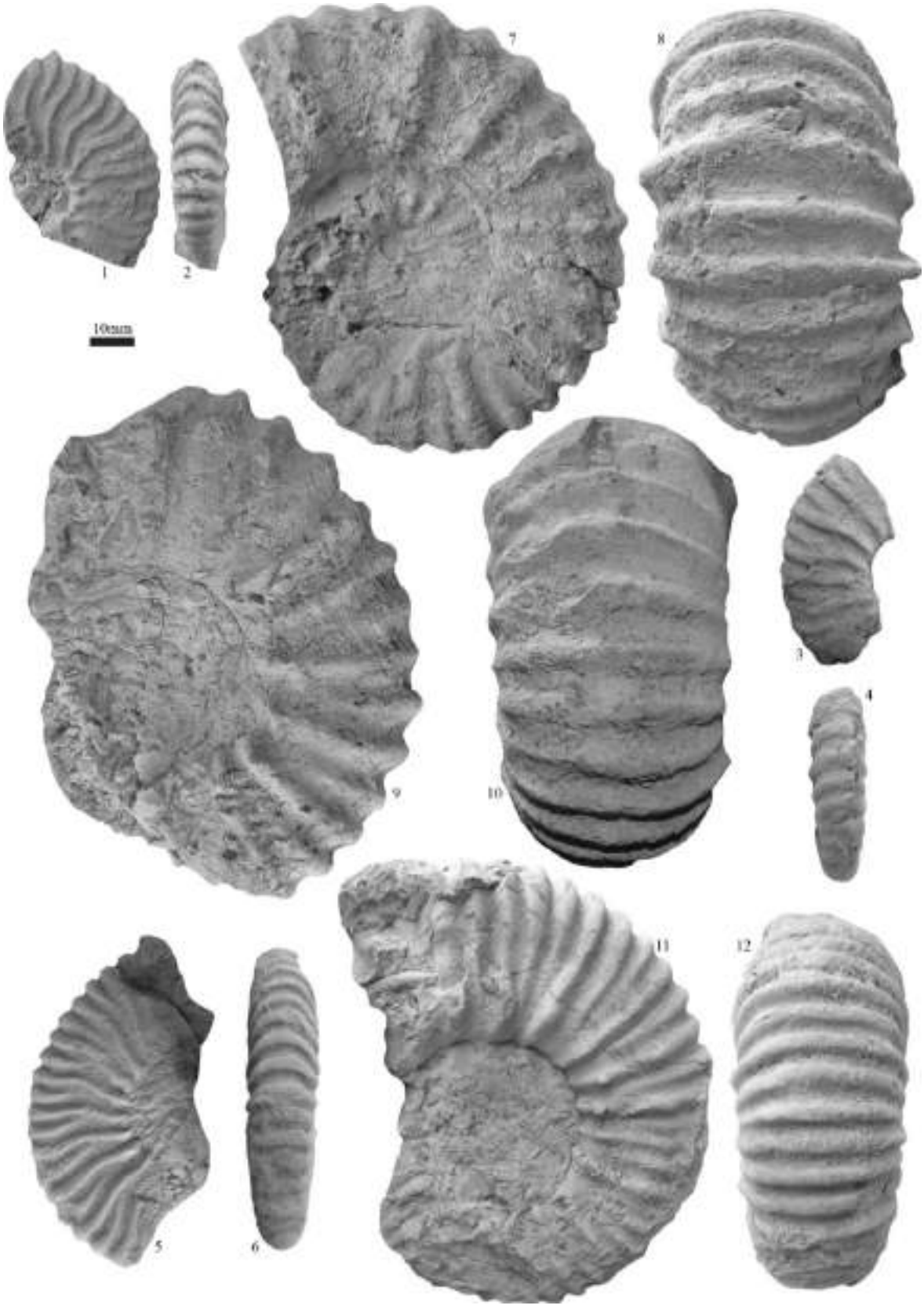

Figure 3.8: Ammonite plate 1.
(1–6) *Deshayesites* aff. *euglyphus* (Casey, 1964) *in* Delanoy (1995) – (1–2) and (5–6) from bed **TK 160** ((MANCH) LL.16103 and (MANCH) LL.16105), (3–4) from bed **TR 70** (MANCH) LL.16104; (7–12) *Prochelonicerasdechauxi* (Kilian and Reboul, 1915) from bed **TR 69** ((MANCH) LL.16106 – (MANCH) LL.16108). All specimens coated with ammonium chloride prior to photography. Scale bar is 10mm.

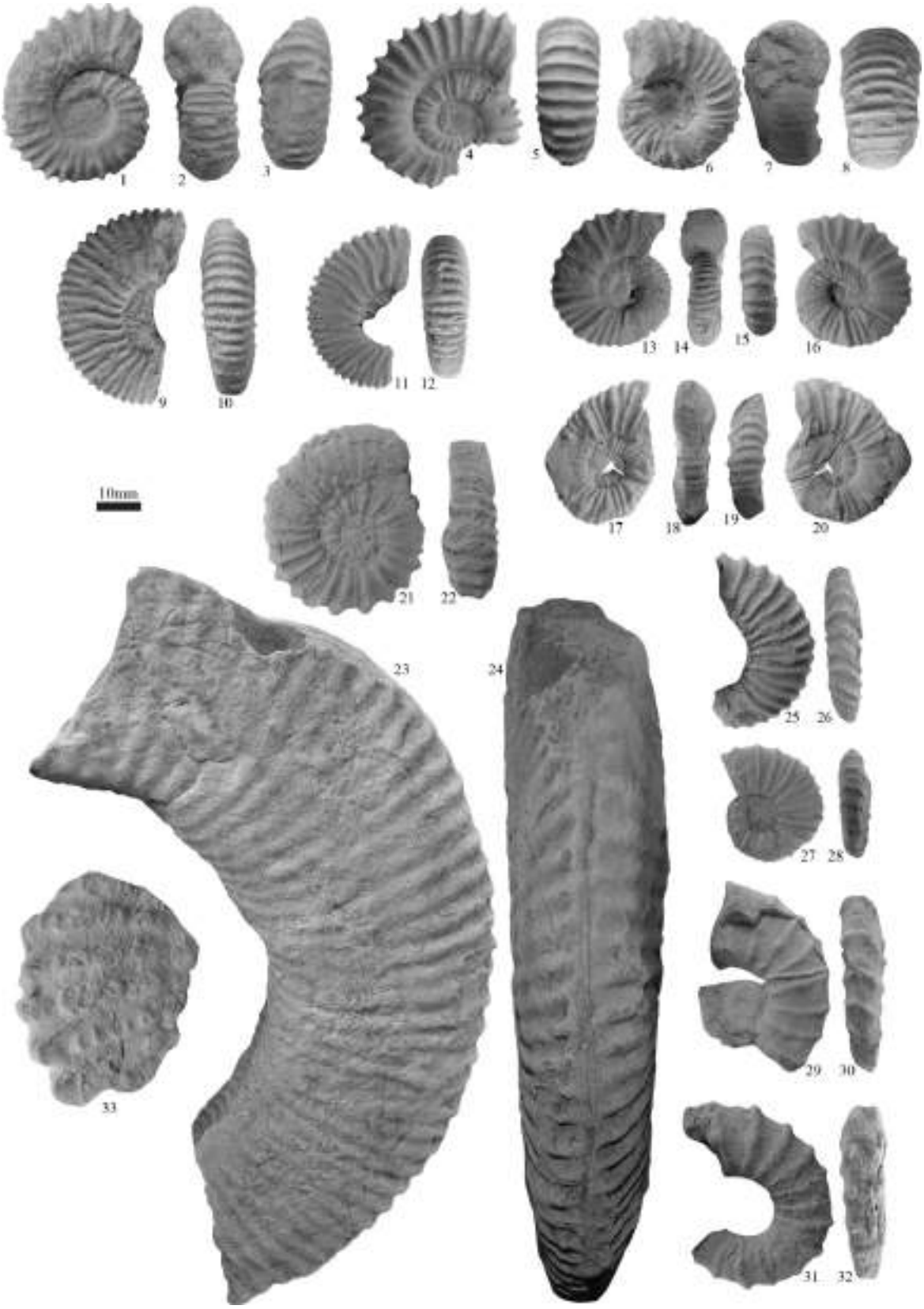

Figure 3.9: Ammonite plate 2.
(1–8) *Epicheloniceras* gr. *subbuxtorfi* – *paucinodum* (Burckardt, 1925) from bed **TK 161A** ((MANCH) LL.16109 – (MANCH) LL.16111); (9–12) *Colombiceras tobleri* (Jacob and Tobler, 1906) from bed **TK 161A** ((MANCH) LL.16112 and (MANCH) LL.16113); (13–16) "*Protacanthoplites*" aff. *multinodosus* (Tovbina, 1982) from bed **TK 206** ((MANCH)

LL.16114); (17–20) *Protacanthoplites abichi* (Anthula, 1900) from **TK 212/213** ((MANCH) LL.16115); (21–22) *Diadochoceras* gr. *nodosocostatum* (d'Orbigny, 1841) from bed **TK 206**((MANCH) LL.16116); (23–24) *Pseudoaustraliceras* gr. *ramososeptatum* (Anthula, 1900) from **TK 196** ((MANCH) LL.16117); (25–28) "*Epicheloniceras*" *marocanus* (Roch, 1930) from bed **TK 166** ((MANCH) LL.16118 and (MANCH) LL.16119); (29–32) *Epicheloniceras* sp. juv. 1 gr. *waageni* (Anthula, 1900) – *tschernyschewi* (Sinzow, 1906) from bed **TK 163** (MANCH) LL.16120 and (MANCH) LL.16121); (33) *Douvilleiceras* cf. *leightonense* (Casey, 1962) from bed **TK 248** ((MANCH) LL.16122). All specimens coated with ammonium chloride prior to photography. Scale bar is 10mm.

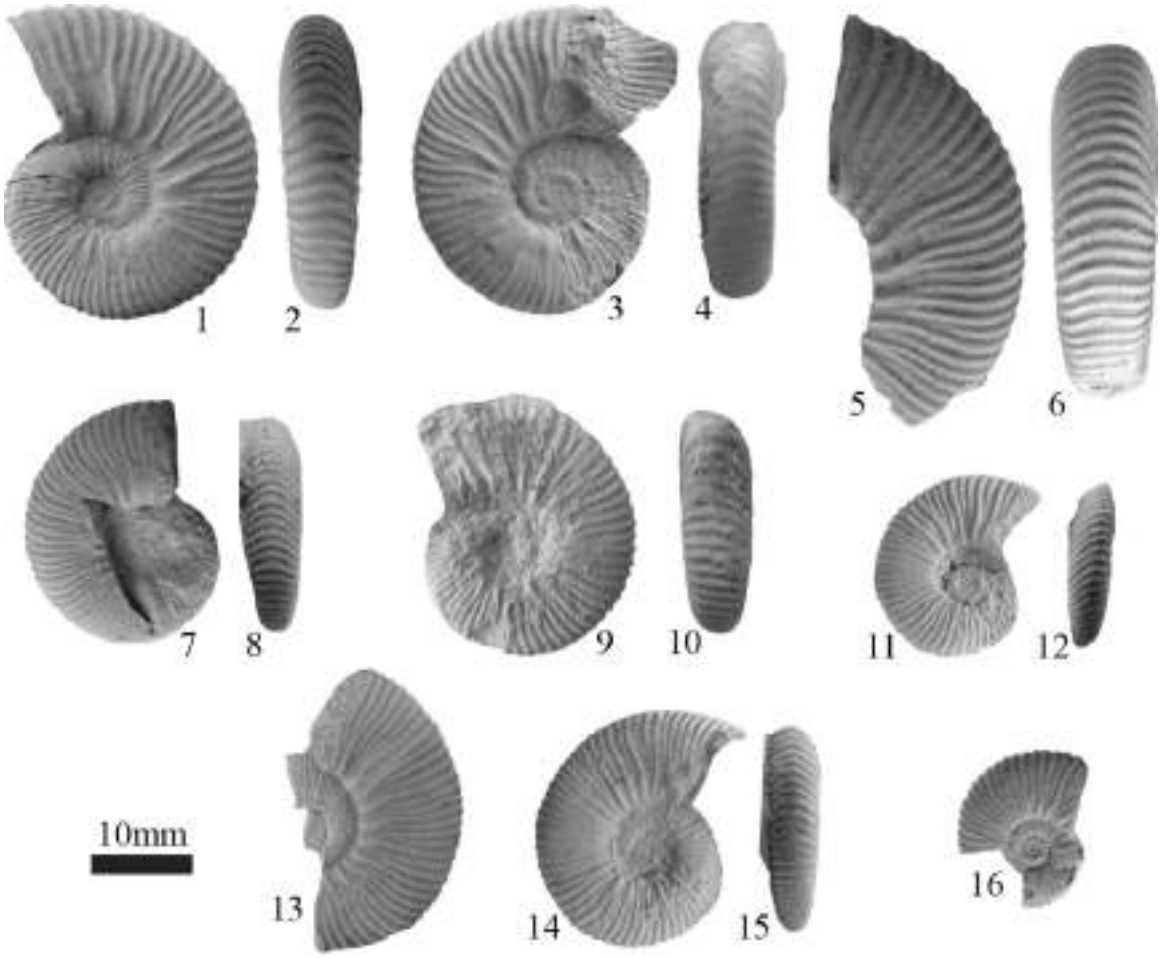

Figure 3.10: Ammonite plate 3.
Elsaisabellia tiskatinensis gen. and sp. nov. from bed **TK 206** – (1–2) holotype ((MANCH) LL.16123), (3–16) paratypes (MANCH) LL.16124 – (MANCH) LL.16131). All specimens coated with ammonium chloride prior to photography. Scale bar is 10mm.

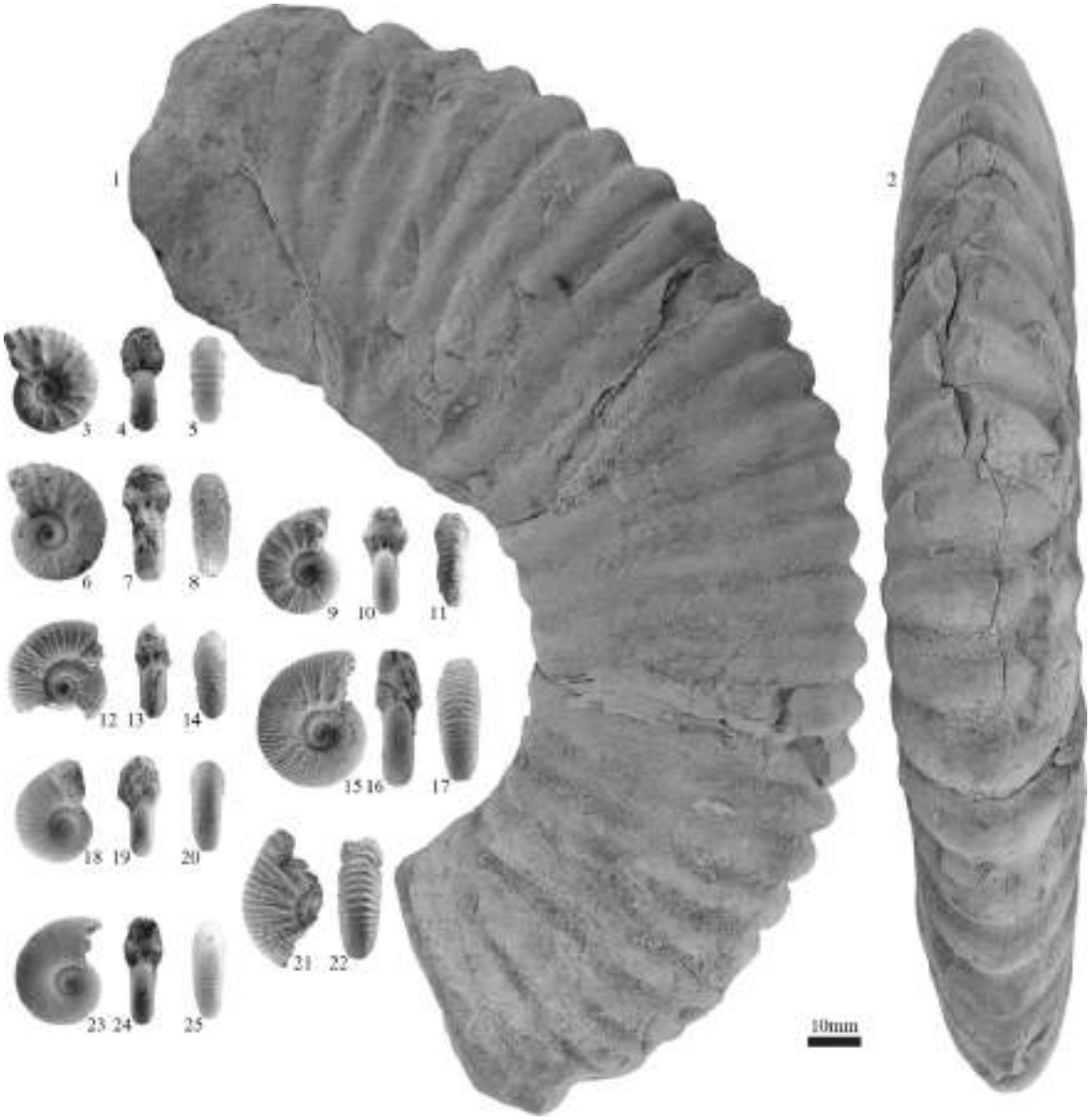

Figure 3.11: Ammonite plate 4.
(1–2) *Acanthohoplites aschiltaensis* (Anthula, 1900) from bed **TK 192** ((MANCH) LL.16132); (3–11) "*Hypacanthoplites*" sp. 3 – (3–8) are from bed **ZZ 68** ((MANCH) LL.16133 and (MANCH) LL.16134), (9–11) from bed **TM 80** ((MANCH) LL.16135); (12–14); *Pseudosilesites seranoniformis* (Egoian, 1969) from bed **TM 80** ((MANCH) LL.16136); (15–25) "*Hypacanthoplites*" sp. 1 from bed **TM 80** ((MANCH) LL.16137 – (MANCH) LL.16140). All specimens coated with ammonium chloride prior to photography. Scale bar is 10mm.

3.6 Ammonite biostratigraphy and correlation to the Standard Mediterranean Ammonite Scale (SMAS)

As shown by the systematic notes, the ammonite faunas from the EAB have a distinct character that is most certainly linked to the palaeogeography of the basin. Although the successive assemblages are clearly of Tethyan affinity, none of the index species of the Standard Mediterranean Ammonite Scale (SMAS) of Reboulet et al. (2011, 2014) were found in the course of our study. As a consequence, we have chosen to introduce a regional biostratigraphic scale based on the main bio-events recognized at basin-scale (Fig. 3.12) and a correlation panel showing all studied sections is included in appendix C9. When possible, correlations with the SMAS are proposed, the precision of these correlations is handicapped by the fact, that for the upper part of Aptian Stage, the biostratigraphic subdivision of the SMAS is largely based on assemblage zones and subzones originally defined in the former Soviet Union (Bogdanova and Tovbina, 1995) for which detailed successions are still poorly documented.

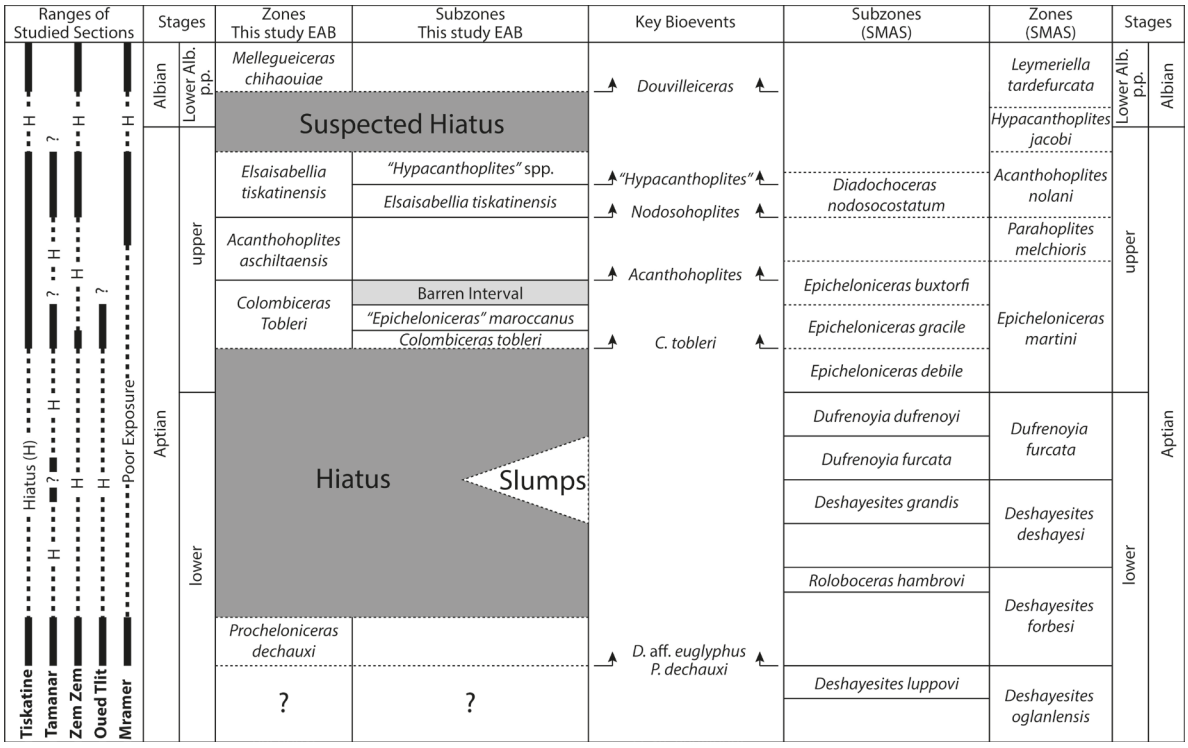

Figure 3.12: Chart showing correlation between the EAB and SMAS ammonite scales (SMAS zones and subzones after Reboulet et al. 2011, 2014).

Lower Aptian – *Prochelonicerasdechauxi* Zone, new, this paper

Index species. *Prochelonicerasdechauxi* (Kilian and Reboul, 1915)
Reference section. Tiskatine – bed **TK 159** to **TK 160b**.

Definition. The base of the zone is defined by the first occurrence of the index–species that largely dominates the assemblage in all studied sections. The diversity is low but some beds are rich in *Deshayesites* aff. *euglyphus* Casey in Delanoy (1995). It should be noted that *P. dechauxi* and *D.* aff. *euglyphus* are most often mutually exclusive. *Audouliceras* sp. ind., *Pseudohaploceras* cf. *matheroni* (d'Orbigny, 1841) and *Melchiorites melchioris* (Tietze, 1872) are minor elements of the fauna.

Correlations. Correlation with the SMAS is based on the occurrence of *P. dechauxi* and *D.* aff. *euglyphus*. These two taxa are known to occur in the lower part of the *Deshayesites forbesi* Zone in South-East France (Delanoy, 1995, 1998; Pictet, 2012).

Upper Aptian – *Colombiceras tobleri* Zone, Eristavi (1960) emended.

Index species. *Colombiceras tobleri* (Jacob and Tobler, 1906)
Reference section. Tiskatine – bed **TK 161a** to **TK 183c**.

Definition. Since its first introduction, the *Colombiceras tobleri* Zone was variously interpreted in the literature (see discussion in Bogdanova and Mikhailova, 2016). As herein understood, the zone is defined by the first occurrence of its index–species. Two subzones can be distinguished in the EAB.

Colombiceras tobleri Subzone, new, this paper

Index species. As for the zone.
Reference section. Tiskatine – bed **TK 161a** to **TK 163**.

Definition. The base of the subzone is defined by the first occurrence of the index–species. The diversity of the fauna is fairly high. Together with the index species, the various

Epicheloniceras of the s*ubbuxtorfi – paucinodum* group are the most common elements of the faunal assemblage. Desmoceratids are unusually common compared to the rest of the succession. *Pseudohaploceras angladei* Dutour, 2005 non (Sayn, 1891), *Zuercherella zuercheri* (Jacob and Tobler, 1906), *Melchiorites* aff. *emerici* (Raspail, 1831) and *Caseyella* sp. ind. were identified. The heteromorph taxa "*Ammonitoceras*" *lahuseni* (Sinzow, 1906) and ? *Pseudoaustraliceras* sp. are minor elements of the fauna. A single phylloceratid tentatively assigned to *Phylloceras* sp. was collected.

"*Epicheloniceras*" *marocanus* Subzone, new, this paper

Index species. "*Epicheloniceras*" *marocanus* (Roch, 1930)
Reference section. Tiskatine – bed **TK 164** to **TK 183c**.

Definition. The base of the subzone is defined by the first occurrence of the index–species. The diversity of the fauna is very low. The lower part of the subzone is marked the acme of "*Epicheloniceras*" *marocanus* and its upper part correspond to a barren interval. The last occurrence of *C. tobleri* is to be noted at the base of the subzone. In the barren interval, spot occurrence of *Epicheloniceras* of the *waageni* (Anthula, 1900) – *tschernyschewi* (Sinzow, 1906) group was identified.

Correlations. Because of the highly endemic character of the fauna, a precise correlation with the SMAS is hard to establish. A provisional correlation between the base of the *C. tobleri* Zone of Morocco and the base of the *E. gracile* Subzone (*E. martini* Zone) can be proposed on the basis of the evolution of the genus *Colombiceras* in SE France (Bulot in Dauphin 2002), Caucasus and Transcaspia (Bogdanova and Mikhailova, 2016). Due to the somehow “primitive” character of the Moroccan *C. tobleri*, a slightly older position in the *E. martini* Zone cannot be excluded. An ongoing study of the large collection of *Epicheloniceras* should allow more precise correlation in the future.

Upper Aptian – *Acanthohoplites aschiltaensis* Zone, Mordvilko (1960) emended.

Index species. *Acanthohoplites aschiltaensis* (Anthula, 1900). First
Reference section. Tiskatine – bed **TK 184** to **TK 205**.

Definition. Since its introduction, the *Acanthohoplites aschiltaensis* Zone has had a number of interpretations in the literature (see discussion in Bogdanova and Mikhailova, 2016). As herein understood the zone is defined by the first occurrence of the index–species. The diversity is very low but a distinctive horizon rich in *Pseudoaustraliceras* of the *ramososeptatum* (Anthula, 1900) group (Fig. 3.9.23 – 24) was identified in the middle part of the zone. The geographical extension of this bio-event at the scale of the basin remains unknown. In the marginal areas of the EAB, the occurrence of large *Epicheloniceras* that do not match any species of the literature is also to be noted. The precise range and affinities of those specimens are still to be documented.

Correlations. The precise range of *A. aschiltaensis* has never been precisely calibrated with the SMAS zones. Data from South-Eastern France suggests that the lowest occurrence of the *Acanthohoplites* of the *aschiltaensis* group occurs in the uppermost part of the *E. martini* Zone close to its boundary with the *P. melchioris* Zone (Bulot in Dauphin, 2002; Frau and Bulot, unpublished data). According to Russian literature, *A. aschiltaensis* is a common element of the *P. melchioris* Zone (Bogdanova and Mikhailova, 2016, with references).

Upper Aptian – *Elsaisabellia tiskatinensis* Zone, new this paper

Index species. *Elsaisabellia tiskatinensis* gen. nov. sp. nov.
Reference section. Tiskatine – bed **TK 206** to **TK 247**.

Definition. The zone is defined by the first occurrence of the genus *Elsaisabellia*. Two subzones can be distinguished.

Elsaisabellia tiskatinensis Subzone, new this paper

Index species. As for the zone.
Reference section. Tiskatine – bed **TK 206** to **TK 220**.

Definition. The first occurrence of the genus *Elsaisabellia* marks the base of the subzone. In all studied sections the fauna is marked by the evolutive radiation of the Acanthohoplitidae.

The various morphologies of *Elsaisabellia* dominate in the lower part of the subzone. In the upper part of the subzone a fairly diverse assemblage of Acanthohoplitidae develops and includes *Diadochoceras* of the *nodosocostatum* group, *Nodosohoplites* of the *subplanatus* group, and various species of P*rotacanthoplites*. *Epicheloniceras clansayense* (Jacob, 1905) is a secondary element of the fauna in the marginal parts of the EAB.

"*Hypacanthoplites*" spp. Subzone, new this paper

Index species. Hypacanthoplitids with a tabulate venter ("*Hypacanthoplites*" sp. 1, "*H.*" sp. 2 and "*H.*" sp. 3).
Reference section. Tiskatine – bed **TK 221** to **TK 247**.

Definition. The fauna is dominated by "*Hypacanthoplites*" sp. 1, "*H.*" sp. 2 and "*H.*" sp. 3 but also contains relict elements from the underlying subzone such as *Protacanthoplites abichi* and *Nodosohoplites gr. subplanatus*. Other noteworthy taxa are *Pseudosilesites seranoniformis* Egoian, 1969 (Fig. 3.11.12-14), *Puzosiella minuta* Egoian, 1969 and *Melchiorites* ? *problematicus* (Fallot and Termier, 1923).

Correlations. The detailed range of the ammonite faunas of the *A. nolani* Zone of the SMAS is still not documented. Nevertheless, it seems reasonable to consider that the first occurrence of *Diadochoceras* in the lower part of the *E. tiskatinensis* Zone suggests a correlation with a level close to the base *D. nodosocostatum* Subzone. Co-occurrence of primitive "*Hypacanthoplites*" spp. and *Pseudosilesites seranoniformis* in the upper part of the *A. nolani* Zone was reported from North-Eastern Spain by Robert et al. (2001). This suggests that the base of the *Hypacanthoplites* spp. The subzone is likely older than the base of the *H. jacobi* Zone even so correlation with a slightly younger level cannot be excluded.

In agreement with Latil (2011), the base of the Lower Albian (*M. chihaouiae* Zone) is marked by the co-occurrence of first representatives of the genus *Douvilleiceras* (Fig. 3.9.33) with *Mellegueiceras chihaouiae*. This boundary is clearly documented at Tiskatine and Mramer. At Mramer, the index species of the overlying lower Albian "*Hypacanthoplites*" *paucicostatus* Zone was also identified.

It should be noted that the beds that contain the first Lower Albian faunas with *Douvilleiceras* (see details below) directly overlie the "*Hypacanthoplites*" spp. Subzone. As a consequence, we suspect a hiatus that would embrace the uppermost part of the *H. jacobi* Zone and lower part of the *L. tardefurcata* Zone.

3.7 Conclusions

A high-resolution bed-by-bed sampling of five sections in the west-central Essaouira Agadir Basin (EAB) has yielded the largest Aptian published ammonite collection in NW Africa. The results provide new information on the age range of previously defined formations, and a type section with fully-documented collections correlated against type species. In addition, new species have been identified and the collections provide new insights into the regional endemism of species in this part of NW Africa.

The main conclusions from the study are:

- A diverse Aptian and Early Albian ammonite fauna is documented, comprising 26 different genera and 43 species.
- The global palaeobiogeographic character of the fauna is Tethyan, however a high degree of endemism is recognised at the genus and species level.
- A new genus and species *Elsaisabellia tiskatinensis* is described.
- New material also allows re-examination of *Parahoplites marocanus,* provisionally included in the genus *Epicheloniceras*.
- Based on the ammonite distribution a regional biostratigraphic scale is introduced for the Aptian of the EAB. 8 zones and subzones are recognised, 5 of which are new.
- The section at Tiskatine [Lat.: 30.821463° Long.: -9.702555° (Tiskatine 1) and Lat.: 30.810477° Long.: -9.739966° (Tiskatine 2)] is selected as the type section for the Aptian in the west-central part of the EAB. Key taxa are documented, illustrated with collection references. A correlation based on first occurrence of common taxa with the Standard Mediterranean Ammonite Scale (SMAS) is proposed when possible.

- Two basin-scale regional hiatuses are identified. The lower one encompasses the time equivalent of the middle part of the *D. forbesi* Zone to lower part of the *E. martini* Zone of the SMAS. The upper one includes the *H. jacobi* Zone and the lowermost part of the *L. tardefurcata* Zone equivalent.
- The age of the Tamzergout Fm. has been clearly defined, ranging from the local and newly introduced *P. dechauxi* to the *E. tiskatinensis* zones.
- The top Bouzergoun / base Tamzergout Fm. is identified as being diachronous, ranging in age from the early to late Aptian (*P. dechauxi* to *C. tobleri* zones).
- The improved age dating of the Lemgo Fm. (based on collection from the Mramer section) indicates a range from middle upper Aptian *A. aschiltaensis* Zone to the lowermost Albian "*H.*" *paucicostatus* Zone.
- An early Albian age for the base of the Oued Tidzi Fm. is established by the lowest occurrence of the genus *Douvilleiceras*.

CHAPTER 4: A STRATIGRAPHIC REFERENCE SECTION FOR THE APTIAN OF NW AFRICA

This chapter has been submitted for publication in Cretaceous Research.

Authors: Luber, T.L., Bulot, L.G., Redfern, J., Nahim, M., Jeremiah, J., Simmons, M., Bodin, S., Frau, C., Bidgood, M., Masrour, M.

Submitted: 12/09/2017

Keywords: Foraminifera, Calcareous Nannofossils, Ammonoids, Carbon Isotopes, Integrated Stratigraphy, Sequence Stratigraphy, Aptian, Essaouira-Agadir Basin, Morocco, Atlantic Margin

4.1 Abstract

This paper documents the first high-resolution, multi-disciplinary stratigraphic reference section for the Aptian to Lower Albian on the NW African Atlantic Margin. Distribution of ammonoids, foraminifera and calcareous nannofossils are reported from a bed by bed collection and a type section for the Aptian of NW Africa is proposed at Tiskatine in the Essaouira-Agadir Basin of Morocco (EAB). The reference section also includes $\delta^{13}C_{carb}$, $\delta^{13}C_{org}$ and total organic carbon (TOC) curves, the first documented for the Aptian of the onshore NW African margin, integrated with the biostratigraphic data and compared to reference material from the Provençal and Vocontian basins. Analysis of a diverse foraminiferal and calcareous nannofossil assemblage enables correlation to standard zonation schemes; but also highlights the urgent need of revision and future work on the integration of these zonation schemes across disciplines.

Two previously undocumented sections for the Aptian to Lower Albian are introduced (Assaka and Id Amran) and their regional sequence stratigraphic correlation with the Tiskatine section is presented. They are key in identifying the control on sequence development by local tectonics, with recognition of an north-south-orientated palaeotopographic high located along the modern coastline of Morocco.

The work at Id Amran further complements the local ammonoid zonation and introduces two additional ammonoid faunas that characterise the middle part of the *D. forbesi* Zone and the middle part of the *D. furcata* Zone. These observations are further supported by calcareous nannofossil analysis at Id Amran.

The onshore sections are correlated offshore to the section in DSDP borehole 370, where a revised biostratigraphic analysis of the upper Barremian to Lower Albian is presented. A basal Albian unconformity is recognised in this well, which can be correlated to the regional basal Albian sequence boundary recognized onshore in all sections studied.

This combined high-resolution litho-, bio-, chemo- and sequence stratigraphic analysis establishes a robust chronostratigraphic framework for regional and super-regional correlation.

4.2 Introduction

This study presents the first high-resolution integrated multi-disciplinary stratigraphic study for the Lower Cretaceous of NW Africa. We present combined high-resolution litho-, bio-, chemo- and sequence stratigraphic analysis using a multi-disciplinary approach that establishes a robust chronostratigraphic framework for regional and super-regional correlations. It also sheds light on the calibration of various stratigraphic schemata, both against one another and against regional and global standards.

The analyses have been undertaken on a number of outcrops in the Essaouira-Agadir Basin (EAB), Morocco (Fig.4.1), comprising the most complete and best age-constrained succession of the Lower Cretaceous along the NW African Atlantic Margin. Previous work established a regional biochronologic ammonoid scale for the Aptian of the EAB (Luber et al., 2017) and this contribution extends the analysis to include key micropalaeontological groups and stable isotope stratigraphy, as well as placing the succession in a sequence stratigraphic context.

A critical section is exposed at Tiskatine (Fig. 4.1) [Lat.: 30.821463° Long.: -9.702555° (Tiskatine 1) and Lat.: 30.810477° Long.: -9.739966° (Tiskatine 2)], and proposed as a reference section for the Aptian of the NW African Margin. Here, excellent outcrop affords a bed-by-bed collection for combined ammonoid, calcareous nannofossil and foraminiferal analysis and biostratigraphic calibration. This is integrated with chemostratigraphic data, including the first Aptian $\delta^{13}C_{carb}$ and $\delta^{13}C_{org}$ curves and total organic carbon (TOC) analysis for the onshore NW African Atlantic Margin. This study offers insight into the stratigraphic evolution of the margin, and also has significant applied importance in subsurface studies offshore for hydrocarbon resources, to improve age constraint and aid prediction of key play elements.

Data from each discipline is presented, followed by a regional interpretation of the palaeoenvironment and sequence stratigraphy. We then address the correlation to the successions of the Provençal and Vocontian basins, key locations for establishing the standard biostratigraphy of Mediterranean-Caucasian Subrealm of the Tethyan Realm via the Standard Mediterranean Ammonite Scale (SMAS of Reboulet et al., 2011, 2014) (Bergen, 2000; Kennedy et al. 2000; Moullade et al. 2000; Dauphin, 2002; Herrle and Mutterlose, 2003; Herrle et .al, 2004; Kuhnt and Moullade, 2007; Baudin et al., 2008;

Kennedy et al. 2014; Frau et al. 2015). New ammonoid findings and key foraminifera and calcareous nannofossil species are fully illustrated for future reference with photographic plates.

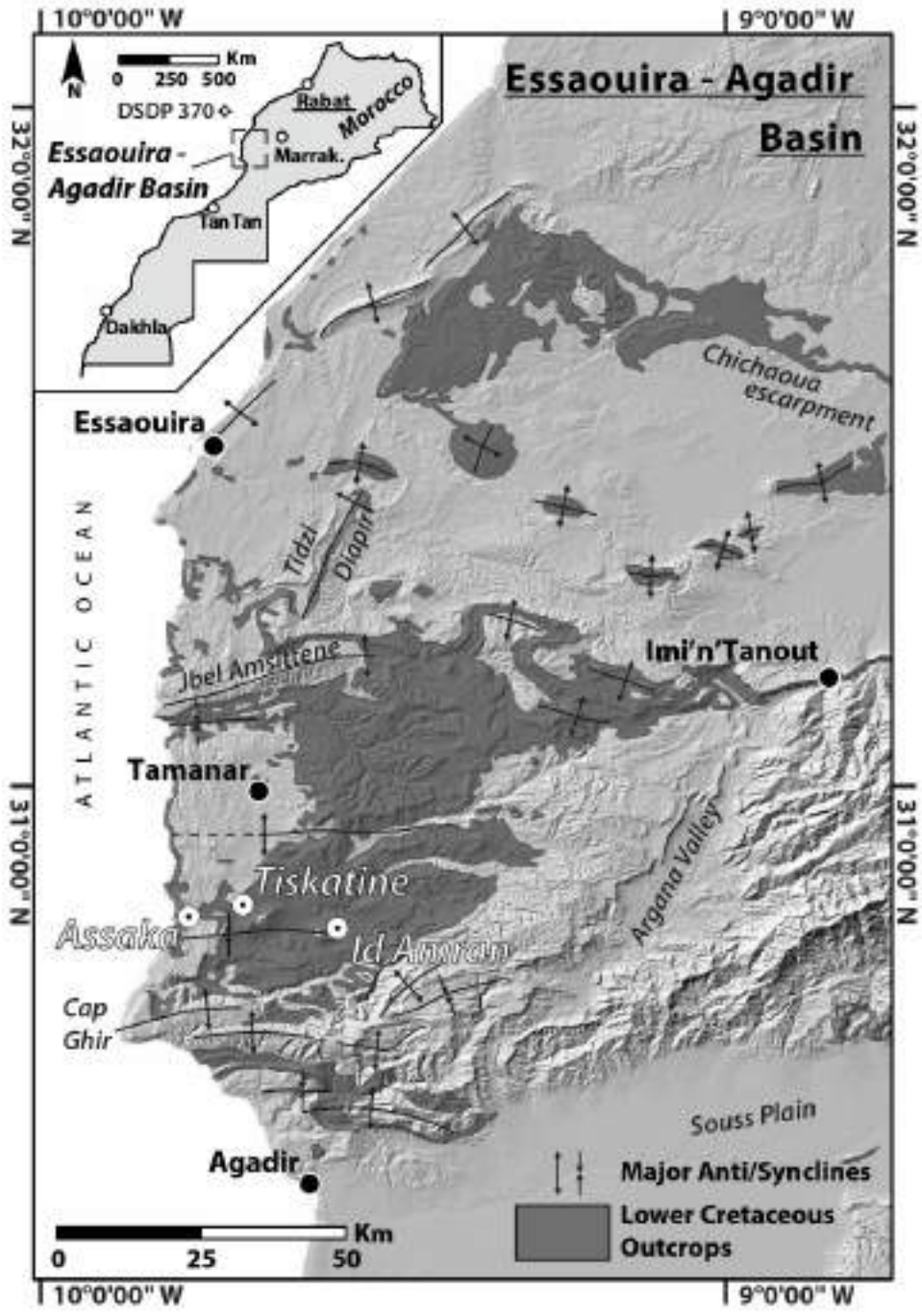

Figure 4.1: Overview map Essaouira-Agadir Basin.
Inset: Location map of Morocco and position of the DSDP well 370 offshore (reference coordinate system WGS 84). Main: Digital elevation model of the Essaouira-Agadir Basin (USGS, 2004) with sections studied and sub-crop of the geological map showing Lower Cretaceous outcrops (Saadi et al., 1985) and main anticlines and synclines.

4.3 Regional setting and stratigraphy

The Mesozoic strata of the Argana Valley and the EAB form the most extensive and complete succession of syn- and post-rift sediments outcropping on the flanks of the Central Atlantic Margin **(CAM)**. The onset of synrift deposition in the Argana Valley is marked by a non-conformity between Palaeozoic basement and Permian to Earliest Jurassic synrift deposits (T1 to T10 of Tixeront, 1973; Brown et al., 1980; Hofmann et al. 2000). Synrift deposition in the Argana Valley is dominated by clastic sedimentation forming extensive continental red beds. Basalt flows associated with the Central Atlantic Magmatic Province (CAMP) (Verati et al., 2007) separate the Permo-Triassic (T1-T8) from the earliest Jurassic (T9 and 10).

During the Jurassic, carbonate sedimentation dominated not only in the EAB but all along the NW African margin, with the formation of widespread carbonate platforms (Jansa and Wiedmann, 1982). Carbonate platform sedimentation continued into the earliest Cretaceous but was curtailed through flooding of the basin margin in the early Valanginian (Rey et al., 1988; Ettachfini et al., 1998). It was marked by the first establishment of the "Atlas Gulf" above the Berriasian shelf opening out to the west into the Atlantic (Behrens et al., 1978).

In the Cretaceous the EAB was limited to the north by the Meseta and the Jebilet, to the south by the Souss Basin and to the east by the Massif Ancien de Marrakech. The modern day exposure of the Mesozoic succession in the EAB occurs mainly along E-W trending anticlines and synclines linked to the Late Cretaceous to Cenozoic Atlasic orogeny (Laville et al., 2004) and combined salt tectonics (Tari and Jabour, 2013) (Fig. 4.1).

This work focuses on the Aptian of the EAB**.** The studied sections are located within the Tiskatine syncline north of the prominent Cap Ghir anticline in the west-central part of the EAB (Fig. 4.1). In the upper Barremian to lower Aptian the west-central and southern part of the EAB experienced a significant regressive phase (middle Bouzergoun Fm., Fig. 4.2) with widespread exposure. Later during the Aptian, the depositional environments of the west-central EAB transitioned from shallow-marine to open-marine shelfal representing an overall transgressive trend. During the early Aptian (*P. dechauxi* Zone and potentially older) shoreface to shallow shelf conditions were dominant (upper Bouzergoun to lower Tamzergout Fm.). In the upper Aptian, mid- to outer shelf conditions record the re-establishment of the Atlas Gulf (Behrens et al., 1978). The Aptian - Albian boundary is

marked by an important regressive phase, followed by a return to shelfal conditions that persisted throughout the early Albian.

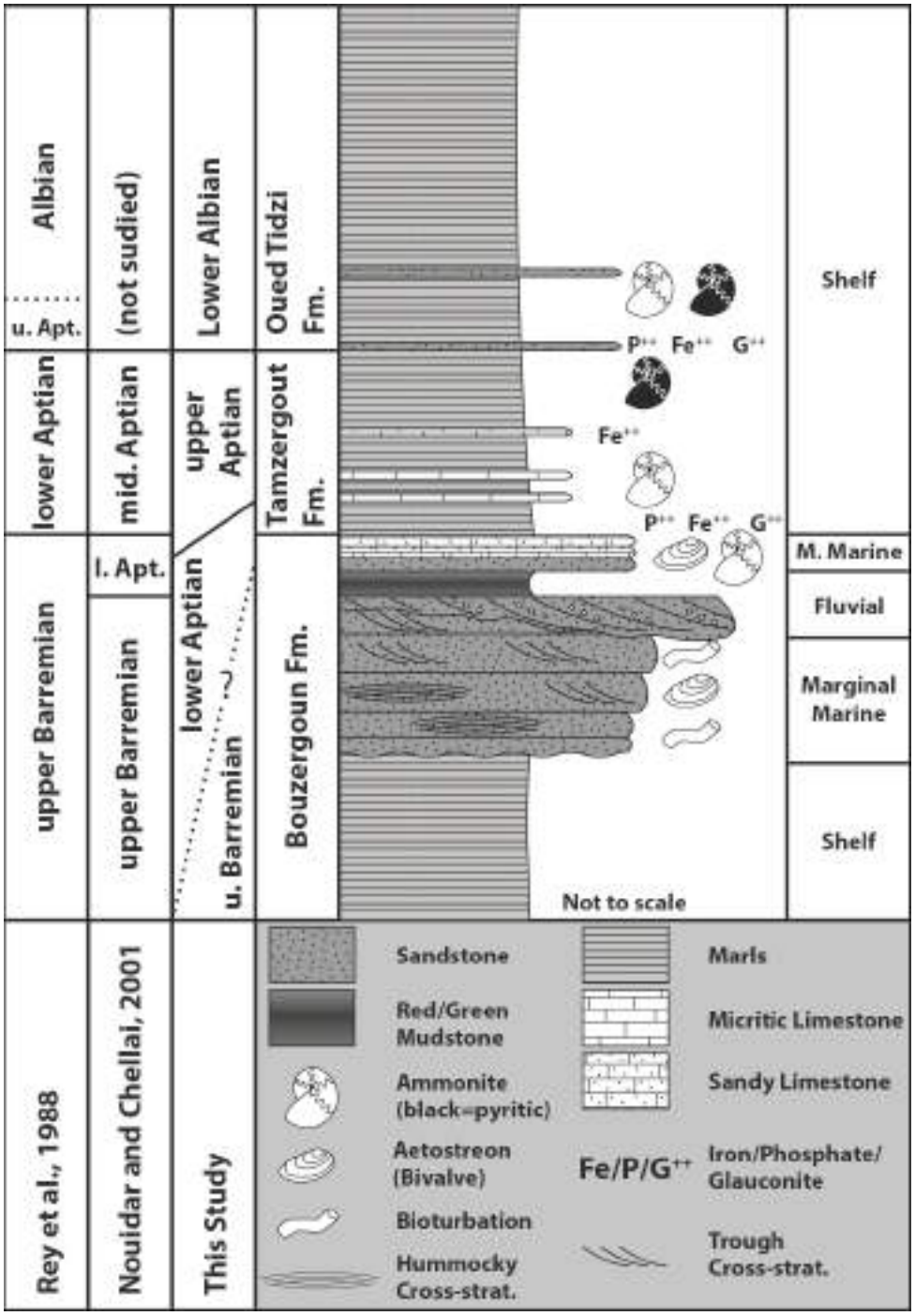

Figure 4.2: Generalised lithostratigraphy of the upper Barremian to Lower Albian strata in the west-central part of the EAB.

4.3.1 Upper Barremian to Lower Albian lithostratigraphy

The following is an abridged version of the lithostratigraphic framework and the reader is referred to Luber et al. (2017) for more detailed information. In this study, we follow a modified scheme based on Duffaud et al. (1966).

4.3.1.1 Bouzergoun Fm.

This unit was originally introduced by Duffaud et al. (1966) and subsequent revisions were made by Rey et al. (1986, 1988). In this study, we only investigated the upper part of the Bouzergoun Formation, which consists of mostly fine-grained sandstones, sandy limestones (mainly oyster-rich grainstones and rudstones) and minor mudstone interbeds. Sandstones and limestones often exhibit low-angle cross-bedding and are commonly topped by iron-, glauconite- and phosphatic-rich horizons. Marine macrofossils are very abundant and include bivalves (dominated by oysters), belemnites, ammonoids and brachiopods.

Previous work by Company et al. (2008), supported by our own findings, has shown that in the Assaka section the base of the Bouzergoun Fm. is erosive and overlies a condensed horizon of early late Barremian age (early to middle part of the *Gerhardtia sartousiana* Zone). Furthermore, it is now established that the upper limit of the Bouzergoun Fm. is diachronous and ranges in age from early Aptian to early late Aptian (base of the *P. dechauxi* to lower part of the *C. tobleri* zones, as understood by Luber et al. (2017)).

4.3.1.2 Tamzergout Fm.

The Tamzergout Fm. was also defined by Duffaud et al. (1966). Based on the initial description of the formation we assign it to fossiliferous alternating blue-grey marls and grey limestones. Its age was re-defined by Luber et al. (2017), ranging from the earliest Aptian *P. dechauxi* Zone to the latest Aptian *E. tiskatinensis* Zone. As discussed above the base of the formation is diachronous.

4.3.1.3 Oued Tidzi Fm.

The Oued Tidzi Fm. was first described by Duffaud et al. (1966) and was redefined by Rey et al. (1988). The lower part of this formation is composed of green marls with minor bioclastic-rich sandstone interbeds, showing a clear change from the blue marls and limestones of the underlying Tamzergout Fm.

The Early Albian age of the basal sandstones is established by the occurrence of the diagnostic ammonite genus *Douvilleiceras* (Luber et al., 2017).

4.3.2 Previous biostratigraphic studies

Pioneering work carried out by Kilian and Gentil (1906), Roch (1930), and Ambroggi (1963), outlined the abundance of the ammonoid faunas in the EAB. Roch (1930) was the first author to suggest that the Tissakatine (herein Tiskatine) section could stand as a reference for the Aptian of the EAB. Nevertheless, neither the works by Rey et al. (1986a, 1988) nor the investigations by Witam (1998) provided any high-resolution biostratigraphy for the Aptian Stage of the central EAB. Yamina et al. (2002) provided a preliminary account on the distribution of planktonic foraminifera in the Western High Atlas in Morocco, although lacking systematic descriptions or illustration. The work by Peybernes et al. (2013) was focused on the Agadir segment of the EAB and correlations to the SMAS (Reboulet et al., 2011). It is discussed at length in Luber et al. (2017).

4.3.3 Biostratigraphic framework of the Aptian in the EAB

A high-resolution biostratigraphic ammonoid biozonation was recently established for the EAB by Luber et al. (2017) and correlations with the Standard Mediterranean Ammonite Scale (SMAS) were proposed. As shown below this local zonation is reproducible at the scale of the Essaouira-Agadir Basin. A detailed account of the correlation to the type sections in SE France is presented in the discussion below.

4.4 Integrated stratigraphy of the Tiskatine section

Lat.: 30.821463° Long.: -9.702555° (Tiskatine 1) and Lat.: 30.810477° Long.: -9.739966° (Tiskatine 2).

The lithostratigraphy, main depositional environments and ammonoid biostratigraphy of the Tiskatine section have been described comprehensively by Luber et al. (2017) and a detailed log with field photographs and interpreted depostional environments is shown in appendix C11 and C14. The following builds on this framework and integrates the results of a high-resolution study of foraminifera, calcareous nannofossils and carbon isotopes, calibrated to the reference ammonoid scale of the EAB. A detailed map showing the location of the Tiskatine and all other sections studied for chapter 4 is provided in appendix C10.

4.4.1 Foraminifera biostratigraphy

96 samples from the Tiskatine section were examined for their foraminiferal content. The majority of samples were from the Tamzergout Fm., with a few samples from the underlying upper Bouzergoun Fm. and the overlying lowermost Oued Tidzi Fm.

The samples were prepared by dissolution in a 10% solution of hydrogen peroxide, dried and the residues concentrated by the use of a nest of sieves. Foraminifera (and also ostracoda and other miscellaneous microfossils) were then transferred to slides for examination with a binocular microscope.

In general, microfossil recovery was good to very good (specimens numbers typically in excess of 100 and sometimes over 500) but variable. Preservation was generally good.

The taxa present comprise a diverse assemblage of calcareous and agglutinating benthic foraminifera and planktonic foraminifera. The taxa are identifiable with reference to the extensive literature on age-equivalent cosmopolitan, Mediterranean and North-West European material (e.g. Bartenstein and Bettenstaedt, 1962; Damotte and Magniez-Jannin, 1973; Premoli Silva and Verga, 2004). The identification of key planktonic

foraminifera follows the taxonomy of Verga and Premoli Silva (2003a, b) and Premoli Silva and Verga (2004).

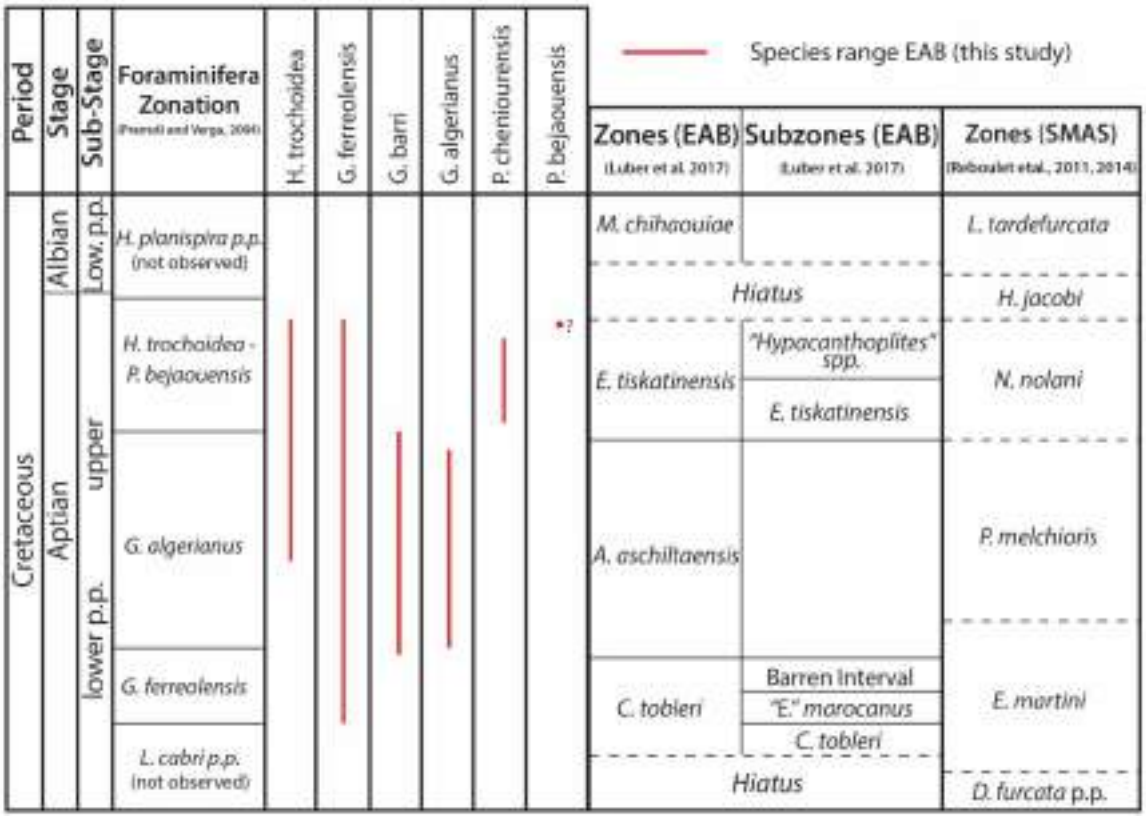

Figure 4.3: Distribution of key planktonic foraminifera species.
Formanifera zonation (after Premoli and Verga, 2004) against the local ammonoid zonation scheme in the EAB of Luber et al. (2017) and the Standard Mediterranean Ammonite Scale (SMAS) of Reboulet et al. (2011, 2014).

4.4.1.1 Zonation and key events (Figs. 4.3, 4.4)

Planktonic foraminifera are common in much of the studied material, often forming 50% or more of the total foraminiferal assemblage (Fig. 4.4 and App. C1). Planktonic foraminifera have long been known to have stratigraphic utility within the later part of the Early Cretaceous (e.g. Moullade, 1966) with a series of evolutionary inceptions and extinctions forming the basis for a standard planktonic foraminiferal zonation (e.g. Caron, 1985; Robaszynski and Caron, 1995; Premoli Silva and Verga, 2004; Ogg and Hinnov, 2012) that can be applied to the studied section (Fig. 4.3). Notwithstanding considerable discussion of the taxonomy of Early Cretaceous planktonic foraminifera (BouDagher-Fadel

et al., 1997; Moullade et al., 2002; Bellier and Moullade, 2002; Verga and Premoli Silva 2003a, b; Premoli Silva and Verga, 2004; Ando et al., 2013) and remaining uncertainties regarding precise stratigraphic range, their fundamental stratigraphic utility remains. Although the nomenclature of the zonation varies between authors (e.g. use of *Hedbergella infracretacea* Zone or *Pseudoplanomalina cheniourensis* Zone instead of *Hedbergella trochoidea* Zone), the basic series of defining events is well understood, although direct calibration to other stratigraphic tools (e.g. the SMAS and carbon isotope record) is still at a very preliminary stage and remains a subject of ongoing research.

***Globigerinelloides ferreolensis* Zone*:* samples MTTK 164 – MTTK 186**

This zone was defined by Moullade (1966) as the interval from the extinction of *Leopoldina cabri* (Sigal, 1952) (*Schackoina cabri*) to the inception of *Globigerinelloides algerianus* Cushman and Ten Dam, 1948. Whilst rare specimens of *Globigerinelloides ferreolensis* (Moullade, 1961) can be found within the *L. cabri* Zone (Robaszynski and Caron, 1995; Verga and Premoli Silva, 2003b; Premoli Silva and Verga, 2004) extinction of *L. cabri* and the inception of common *G. ferreolensis* can be considered to be synchronous (Aguado et al., 1999; Moullade et al., 2002, 2005), so that the inception of common *G. ferreolensis* is also an effective marker for the base of the zone. In the Tiskatine section the lowest records of *G. ferreolensis* occurs at almost the base of the Tamzergout Fm. in sample **MTTK 164** (Fig. 4.4). No species restricted to the *L. cabri* Zone or older were found, supporting the assignment of the lowest samples yielding planktonic foraminifera to the *G. ferreolensis* Zone. *G. ferreolensis* is illustrated in figure 4.16.4-6. The zone extends to sample **MTTK 186** since the overlying sample **MTTK 187** contains *G. algerianus*, the index for the subsequently younger biozone. The uppermost part of the zone contains forms transitional between *G. ferreolensis* and *G. algerianus* (Fig. 4.16.7-8) as well as specimens of *Globigerinelloides barri* (Bolli, Loeblich and Tappan, 1957).

***Globigerinelloides algerianus Zone:* samples MTTK 187 – MTTK 208**

This zone was defined by Moullade (1966) as encompassing the total range of the nominate species (Fig. 4.16.9-11). In the Tiskatine section, this occurs between samples **MTTK 187** and **MTTK 203**, but the top of the zone can be extended to sample **MTTK 208**

(Fig. 4.4) which contains *G. barri* (Fig. 4.16. 1-3), a species that does not extend above the *G. algerianus* zone. Although a range chart within Premoli Silva and Verga (2004) shows a minute extension of *G. barri* above the *G. algerianus* zone, Verga and Premoli Silva (2003a) stated that "*Globigerinelloides barri* disappears at the top of the *Globigerinelloides algerianus* Zone". The local inception of *Hedbergella trochoidea* (Gandolfi, 1942) occurs midway within this zone.

***Hedbergella trochoidea* - *Paraticinella bejaouensis* zones undifferentiated*: s*amples MTTK 210 – MTTK 247**

The *Hedbergella trochoidea* Zone is, according to Sigal (1977), the interval from the extinction of *G. algerianus* to the inception of *Paraticinella bejaouensis* (Sigal, 1966). The *Paraticinella bejaouensis* Zone is defined (Robaszynski and Caron, 1995) as the total range of the nominate species. Since *P. bejaouensis* (Fig. 4.17.1) does not definitely occur in our studied material (a questionable occurrence occurs in sample **MTTK 247**), the interval above the *G. algerianus* Zone with planktonic foraminiferal recovery (samples **MTTK 210** – **MTTK 247**) must be assigned to an undifferentiated *H. trochoidea – P. bejaouensis* Zone (Figs. 4.3, 4.4). This is supported by the presence of *Pseudoplanomalina cheniourensis* (Sigal, 1952) (Fig. 4.16.12-15), a species that ranges no higher than the lower part of the *P. bejaouensis* Zones (Moullade et al., 2002; Bellier and Moullade, 2002; Ando et al., 2013). Additional taxa include *G. ferreolensis* and *H. trochoidea* (Fig. 4.17.2-4), two species that range throughout the upper Aptian (Moullade et al., 2002). The name *P. bejaouensis* is retained for reference to the standard literature, although proposals exist to correct the name of this species and its nominate zone to *Paraticinella rohri* (Ando et al., 2013).
Other key specimens not mentioned here but supporting our interpretations are illustrated in figure 4.17.

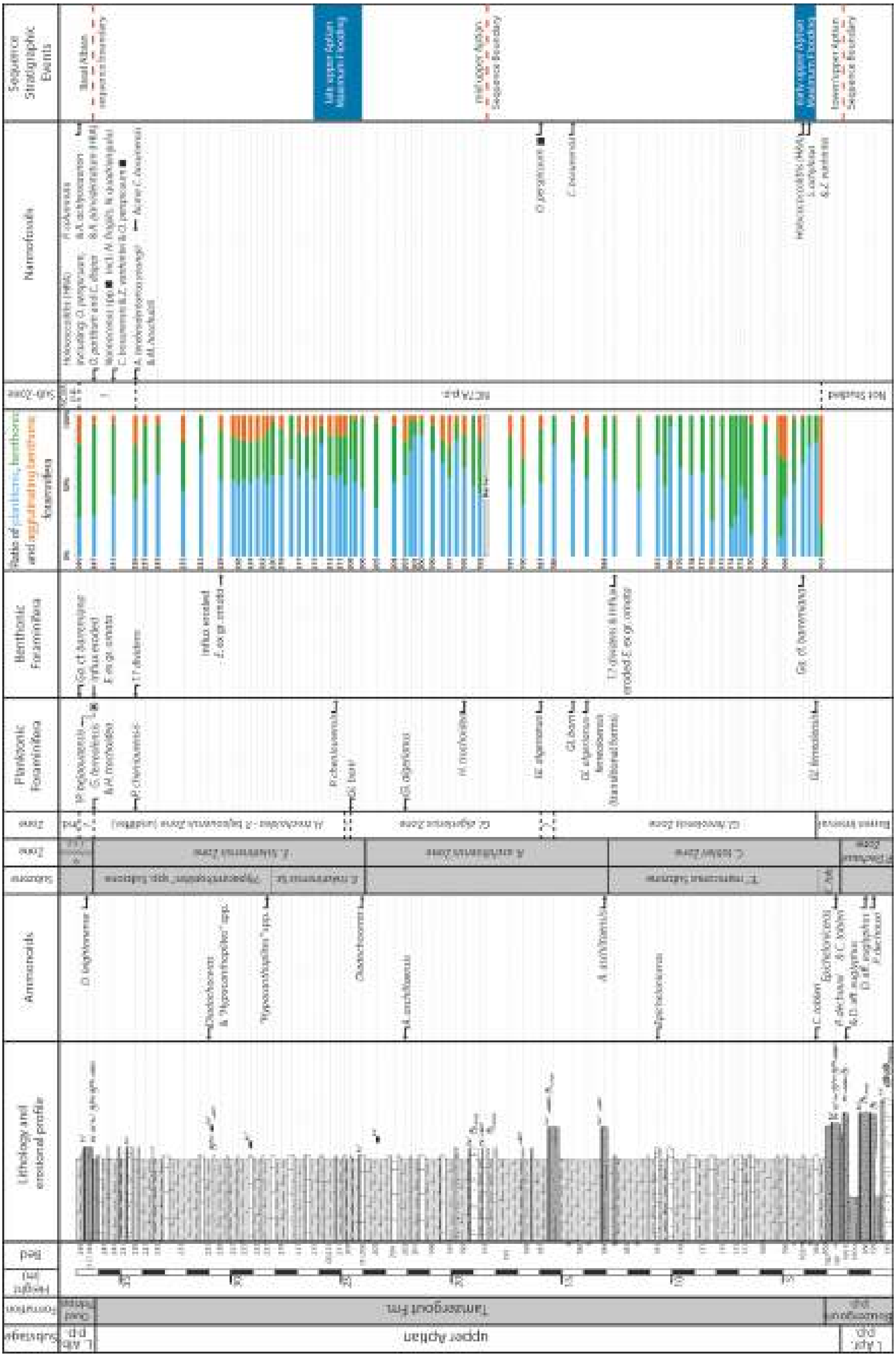

Figure 4.4: Integrated biostratigraphic chart of the Tiskatine section, EAB.
Local ammonoid zonation scheme of Luber et al. (2017), foraminifera zonation after Premoli and Verga (2004) and calcareous nannofossil zonation after Roth (1978) and Bralower et al. (1993). Distribution charts for foraminifera and calcareous nannofossil can be found in the supplementary data. An A3 version is provided in Appendix C1.

4.4.2 Calcareous nannofossil biostratigraphy

Forty-four samples from the Tiskatine section were examined for their nannofossil content. The majority of samples were from the Tamzergout Fm., with a few samples from the underlying upper Bouzergoun Fm. and the overlying lowermost Oued Tidzi Fm (Fig. 4.4). Calcareous nannofossils were analysed using simple smear slides and standard light microscope techniques (Bown and Young, 1998), the sediment distributed on the slides utilising the picking brush method of Jeremiah (1996). Samples were analysed semi-quantitatively, with the first 30 fields of view (FOV) counted and the remaining portion of the slide scanned for rare specimens outside of the count. A taxonomic list for calcareous nannofossils can be found in Appendix A.

The following relative abundance categories which are widely used in industry are also utilised in the present study:

Rare: specimen found outside of the initial 30FOV.

Occasional: 1-2 specimens per 30FOV.

Common: 3-10 specimens per 30FOV.

Abundant: 11-30 specimens per 30FOV

Influx: individuals are a major component of assemblage and > 29 specimens per 30 FOV i.e. 1 or more specimens per FOV.

The nannofossil biostratigraphy is described with reference to the Lower Cretaceous NC Zones of Roth (1978, 1983) and subzones after Bralower et al. (1993). All samples analysed from the Bouzergoun Fm. proved barren of nannoplankton (**MTTK 160**-**MTTK 162**). The basal 0.5m (**MTTK 163** – **MTTK 164**) mudstone section of the Tamzergout Fm. yielded low diversity and abundance assemblages with diversity and abundance markedly increased from sample **MTTK 165b** upwards.

4.4.2.1 Zonation and key events

The Aptian nannofossil bearing sediments at Tiskatine are entirely of late Aptian age. Key markers in the Tiskatine section are shown in Fig. 4.4 and appendix C1.

The standard Aptian nannofossil zonations are, however, in urgent need of revision, the nominate species utilised in the cosmopolitan NC zonation (Roth 1978; Bralower et al., 1993) either showing diachronism (FAD *Prediscosphaera columnata* (Stover, 1966), figure 4.18), difficulty of identification (differentiation of *Hayesites albiensis* Manivit, 1971 from *Hayesites irregularis* (Thierstein *in* Roth and Thierstein, 1972)) or a sporadic LAD (*Micrantholithus hoschulzii* (Reinhardt, 1966), figure. 4.18). As a consequence, the calibration of nannofossil zones as shown in standard texts (e.g. Ogg and Hinnov, 2012) is incorrect.

Although an attempt has been made to calibrate the NC zonation, an endemic zonation calibrated to ammonite / foraminiferal data for the NW African Atlantic margin should be established from a complete Aptian, nannofossil-bearing sequence. A potential cosmopolitan upper Aptian marker, *Crucibiscutum bosunensis* Jeremiah, 2001 (Fig. 4.18), not previously utilised outside of the North Sea could help establish a calibration datum between the Boreal and Tethyan realms.

The Aptian nannofloras record few regional stratigraphic events. Quantitative variations in holococcoliths are potentially of local correlative value. The FAD of *C. bosunensis* is the only event that is of potential inter-regional correlative value within the sequence. The occurrences of *Zebrashapka vanhintei* Covington and Wise, 1987 (Fig. 4.18), rare *Assipetra terebrodentarius youngii* Tremolada and Erba, 2002 (Fig. 4.18) and *Stoverius achylosus* (Stover, 1966) are recorded throughout the studied, nannofossil-bearing sequence, their true FADs and LADs not recorded. Sporadic occurrences of *M. hoschulzii* are reported throughout most of the Aptian sequence, uncertainty remaining on whether its last local occurrence at **MTTK 239** is its true LAD, or a result of truncation at the basal Albian unconformity (Fig. 4.4)

A marked nannofloral turnover is seen at sample **MTTK 249** where Lower Albian nannofossils yielding both *Rhagodiscus achlyostaurion* (Hill, 1976) (Fig. 4.18), *P. columnata* and a local correlative incursion of the cold-water form, *Repagulum parvidentatum* (Deflandre and Fert, 1954) (Fig. 4.18) is recorded (Fig. 4.4).

Subzone NC7A: samples MTTK 163 – MTTK 239

Definition: Interval from FAD of *Eprolithus floralis* (Stradner, 1962) to LAD of *M. hoschulzii* (Bralower et al., 1993).

Discussion: *M. hoschulzii*, the marker for NC7A is found sporadically throughout the Tamzergout Formation. The top of this subzone is placed at **MTTK 239** (Fig. 4.4) but is probably an artificial top due to the sporadic local range of this form. The LAD of *M. hoschulzii* has been classically calibrated (Bralower et al., 1993; Ogg and Hinnov, 2012) to a position slightly above the base of the upper Aptian, at a level close to the base of the *E. martini* Zone. Studies by Bergen (2000) from the historical stratotype of the Bedoulian in SE France recorded *M. hoschulzii* from the top beds (**MTTK 175b**); its true LAD not seen. The classic calibration for the top of Subzone NC7A (Ogg and Hinnov, 2012) appears depressed to more recent records from northwestern Europe (Jeremiah, 2000; Supplementary SUP 18155; Jeremiah, 2001), the Gulf of Mexico (Phelps et al., 2015; Supplementary document) and the EAB (Tiskatine section, studied herein).
In the North Sea the LAD of consistent *M. hoschulzii* appears close to the top of the *P. nutfieldiensis* ammonite Zone where it is associated with the LAD of a quantitative influx of *C. bosunensis* (Jeremiah, 2000; Supplementary SUP 18155; Jeremiah, 2001). Recent studies from the Bexar Member of onshore Texas also indicate a LAD within upper Aptian sediments (Phelps et al., 2015; Supplementary document). *Kazanskyella spathi* (Stoyanow, 1949) was reported from the Bexar shales at Magnolia Oil Co. well (Span #1) (Young, 1974) and a late Aptian age (*K. minima* ammonite Zone) has been since established by Young (1986). Ongoing research in Mexico and Texas suggest that the *K. minima* Zone lies within the middle part of the upper Aptian (Moreno-Bedmar et al. in progress). These studies however also illustrate the inconsistent and sporadic nature of *M. hoschulzii*, a consistent LAD utilised instead of a true LAD. Where found it indicates an age no younger than the middle part of the upper Aptian but should be utilised with caution without supporting stratigraphic markers. Many of the key, ammonoid constrained supporting nannofossil datums from the upper Aptian of the Boreal Realm are, however not recorded in the Morocco sections. This includes the presence of the *Farhania varolii* (Jakubowski, 1986) and *Lithraphidites moray-firthensis* Jakubowski, 1986. Another boreal marker, *C. bosunensis* is, however, recorded from the Tiskatine section. Its FAD at Tiskatine is recorded

from bed **MTTK 185b** (Fig. 4.4). In the boreal North Sea, *C. bosunensis* has a short stratigraphic acme range constrained to the *P. nutfieldiensis* and uppermost beds of the *E. martinoides* ammonite Zone (Jeremiah, 2000). Its true LAD appearance appears more sporadic, rare occurrences ranging up into the lowermost Albian of the North Sea (Jeremiah, 2001). *C. bosunensis* has not been widely recorded outside of the North Sea but recent studies (Phelps et al., 2015; supplementary document) show that this form is much more widely distributed than previously described. Further studies are required from the type French outcrops to resolve the stratigraphic range of this intra upper Aptian quantitative event. At Tiskatine the acme of *C. bosunensis* is at bed **MTTK 239** (Fig. 4.4). This acme only 2m below the basal Albian unconformity suggests that sediments equivalent to the latest Aptian *H. jacobi* Zone are either extremely condensed or eroded. In the North Sea, *C. bosunensis* is only recorded rarely from *H. jacobi* dated sediments (Jeremiah, 2001; Jeremiah et al., 2010).

Within the Tiskatine section, there are a number of nannofossil events that are of potential local correlative events. *Z. vanhintei* is found throughout the upper Aptian but does not range up into the Lower Albian (Fig. 4.4). *Z. vanhintei* has only been recorded from Tethyan locations, this form is unknown from the Boreal realm to date (Street and Bown, 2000). At Tiskatine, the upper Aptian records are probably very close to the worldwide LAD of *Z. vanhintei*. There are currently no records of *Z. vanhintei* from Albian sediments and the occurrences here in upper Aptian sediments extends the range of this form from its published LAD in the early Aptian (Bown et al., 1998).

A. terebrodentarius ssp *youngii* is found sporadically throughout the Tiskatine section. Elsewhere in Tethys, the LAD of *A. terebrodentarius* ssp *youngii* also appears to span the Aptian/Albian boundary where it is found together with NC8 marker, *P. columnata* (Tremolada and Erba, 2002). This observation is supported by the association of common *A. terebrodentarius ssp youngii* with NC8 markers *P. columnata* and *R. achlyostaurion* in the Gulf of Mexico (Jeremiah, pers. obs.).

Holococcoliths are particularly prevalent in the Aptian Tiskatine section. In the lower beds (**MTTK 165b – MTTK 185a**) *Calculites dispar* Varol *in* Al-Rifaiy et al., 1990 (Fig. 4.18) predominates. From bed **MTTK 187** above *Orastrum perspicuum* Varol *in* Al-Rifaiy et al., 1990 (Fig. 4.18) dominates the holococcolith assemblage with *Owenia partitum* (Varol *in* Al-Rifaiy et al., 1990) also showing quantitative influxes between beds **MTTK 200** and **MTTK 218**. These events may be of local correlative importance but due to their prevalence

as neritic taxa (Street and Bown, 2000; Bown, 2005) subject to palaeo-environmental changes at a more regional basin context.

Subzone NC8A: sample MTTK 249

Definition: Interval from FAD of *P. columnata* to FAD of *H. albiensis* (Bralower et. al., 1993)

Discussion: Subzones NC7B and NC7C are not utilised in the current study. These subzones are based on a differentiation of the FAD of *R. achlyostaurion* from that of the FAD of *P. columnata*. Current studies indicate that the base of *R. achlyostaurion* lies close to the base of the Albian where it appears together with *P. columnata* (Kennedy et al. 2000, 2014). At the Gorgo a Cerbera section, Italy (Bralower, 1987; Bralower et al., 1993) the FAD's of both *P. columnata* and *R. achlyostaurion* are recorded together within the Lower Albian. Similar records are seen from the Lower Albian of the Gulf of Mexico (J.J. pers. obs) and here recorded at the Tiskatine section (Fig. 4.4). At Tiskatine, however, a clear basal Albian unconformity does not yield the true FAD's of both these species. Further complications when utilising the base of this zone is the published diachronicity for the FAD of *P. columnata*. In the current study, the usage of *P. columnata* is strictly allocated to circular forms of *Prediscosphaera*. In the UK onshore, *P. columnata* has a FAD stratigraphically high within the Lower Albian *D. mammillatum* ammonite Zone (Jeremiah, 1996, Jeremiah et al., 2010). In contrast, the elliptical variation, *Prediscosphaera spinosa* (Bramlette and Martini, 1964) is prevalent and recorded in sediments ranging down to the to the lower/upper Aptian boundary (Jeremiah, 2001; Jeremiah et al., 2010). This intra Lower Albian FAD of *P. columnata* is supported by the absence of circular *P. columnata* from older Albian sediments (*L. tardefurcata* Zone) from the German south-western Saxony Basin (Jeremiah, 1996; Mutterlose et al., 2003), Dutch western Saxony Basin (Jeremiah et al., 2010) and the UK Yorkshire Speeton Cliff outcrops (Jeremiah, 2001). The diachronous radiation and FO of *P. columnata* appears even further delayed in northern boreal waters (UK Central and Northern North Sea), the FO of *P. columnata* not occurring here until the base of the Middle Albian (core data J. Jeremiah, pers. obs, 2010).

The top of Subzone NC8A is based on the FAD of *H. albiensis*. In Tethyan sections, both *H. irregularis* and *H. albiensis* are found with their ranges potentially overlapping. Due to the

difficulty of differentiating *H. albiensis* from *H. irregularis* the base of *H. albiensis* is not considered a reliable subzonal marker, a view that has already been expressed by Kennedy et al. (2000).

In the boreal Realm, the FAD of *Broinsonia viriosa* (Jeremiah, 1996) followed by the FAD of *Seribiscutum primitivum* (Thierstein, 1974) are recorded within the lowermost Albian (Jeremiah, 2001; Jeremiah et al., 2010) and are also important datum boundaries recorded from SE France (Kennedy et al., 2014). Neither of these species have yet to be recorded southwards along the Moroccan Atlantic Margin and are absent from the Lower Albian sediments at Tiskatine.

Sample **MTTK 249**, whilst yielding both the FAD of NC8A marker *P. columnata* together with *R. achlyostaurion* also records a quantitative acme of the predominantly boreal species *R. parvidentatum* (Fig. 4.4). There is a major nannofloral turnover at the Aptian – Albian boundary section at Tiskatine. Holococcoliths and nannoconids are rare compared to the underlying upper Aptian, diversity and abundance of the nannofloras as a whole reduced. The FAD of abundant *R. parvidentatum* is a potentially important local correlative event marking the base of the Albian along the Moroccan Atlantic Margin.

At Id Amran (Fig. 4.1) a sample from the base of the Oued Tidzi Formation (**MTIA 156**), above the basal Albian unconformity was analysed. The sample yielded *P. columnata* and *R. achlyostaurion* together with *C. bosunensis*. *R. parvidentatum* was not recorded in this sample. It appears that *C. bosunensis* ranges into basal Albian sediments, the presence here at Id Amran suggesting that the lowermost Albian sediments here above the basal Albian unconformity are slightly older than those preserved at Tiskatine where the LAD of *C. bosunensis* is truncated. A more expanded sequence of events including the Lower Albian LAD of *C. bosunensis* and *A. terebrodentarius youngii* is recorded at DSDP 370 (see discussion below).

4.4.3 Carbon isotope stratigraphy

4.4.3.1 Methodology

We here present the first carbon isotope data from the Lower Cretaceous in the EAB and the onshore Moroccan Atlantic Margin. A total of 75 bulk rock samples were run from a bed-by-bed collection of the Tiskatine section (Fig. 4.5). Remaining reference material is stored at the University of Manchester. Sampled material is almost exclusively

composed of shelf marls and limestones, with few exceptions of calcareous sandstones. The $\delta^{13}C$ analysis was performed at the Friedrich-Alexander Universität in Erlangen, Germany. All values are reported in per mil relative to V-PDB.

For carbonate $\delta^{13}C$ analyses, powders were reacted with 100% phosphoric acid at 70°C using a Gasbench II connected to a ThermoFisher Delta V Plus mass spectrometer. Reproducibility and accuracy were monitored by replicate analysis of laboratory standards calibrated by assigning $\delta^{13}C$ values of +1.95‰ to NBS19 and -46.6‰ to LSVEC and $\delta^{18}O$ values of -2.20‰ to NBS19 and -23.2‰ to NBS18. Reproducibility for $\delta^{13}C$ and $\delta^{18}O$ was ±0.04 and ±0.05 std. dev., respectively.

Prior to bulk organic matter $\delta^{13}C$ analyses, the sample powders were treated in order to remove inorganic carbonate phases. Hence, for each sample, around 2 g of powder was treated twice with 25 ml of 6N HCl. Following centrifugation, the supernatant was removed. Residues were thoroughly rinsed several times with distilled water and finally dried at 60 C. Weighting of dried powder prior to and after decarbonisation permits to calculate the mass lost and subsequently the carbonate content of each sample. Carbon isotope analyses of organic carbon were performed with a Flash EA 2000 elemental analyser connected online to ThermoFinnigan Delta V Plus mass spectrometer. Accuracy and reproducibility of the analyses were checked by replicate analyses of laboratory standards calibrated to international standards USGS 40 and 41. Reproducibility for $\delta^{13}C_{org}$ was ±0.07‰ (1σ).

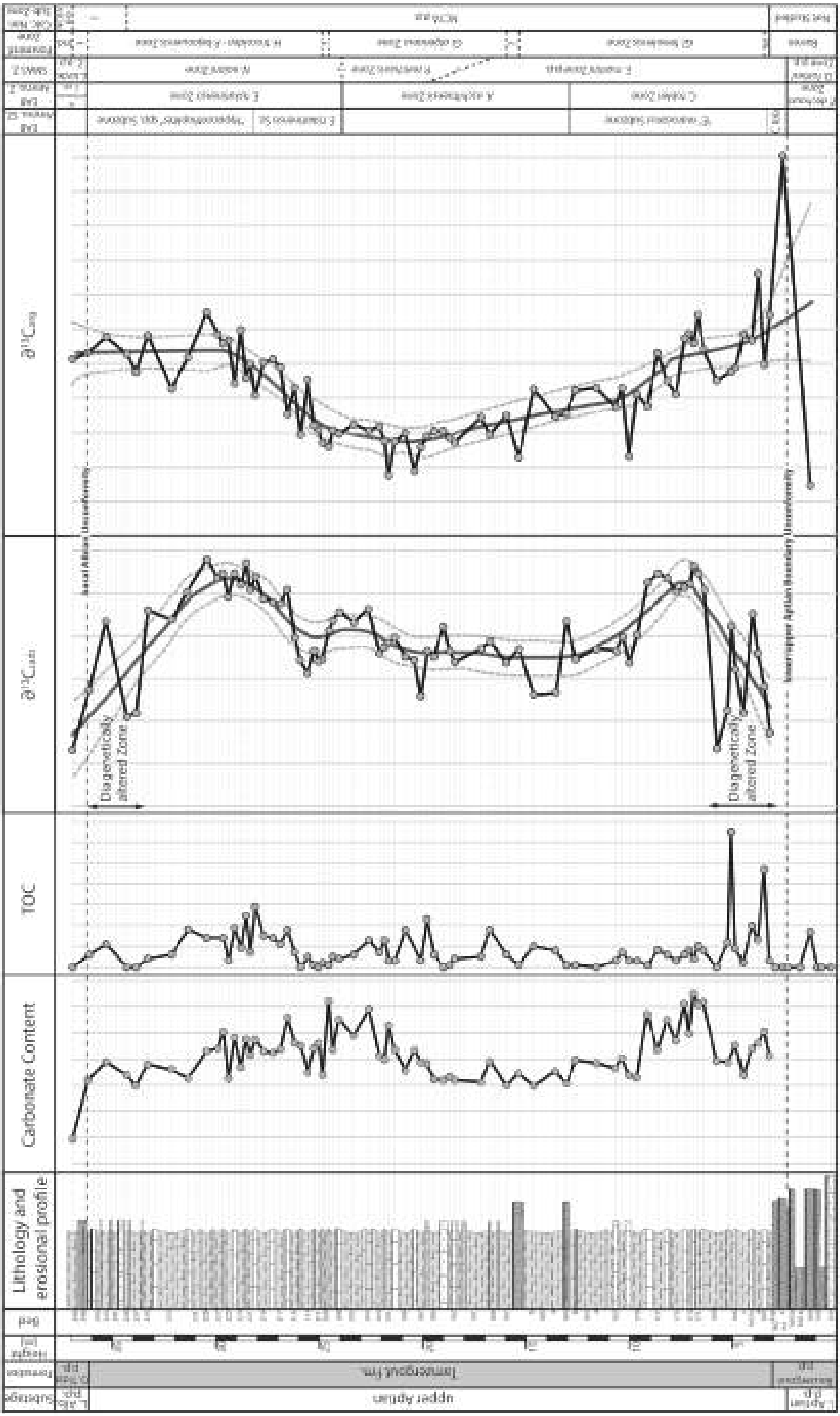
Carbonate Content
Carbonate (%)
TOC
TOC (%)
Lithology and erosional profile
Diagenetically altered Zone
Diagenetically altered Zone
Basal Albian Unconformity
Intra-upper Aptian Boundary Unconformity
Bed
Height [m]
Formation
Substage
upper Aptian
Jamwergout Fm.

Figure 4.5: Carbonate content, total organic carbon (TOC), δ13 Ccarb and δ13 Corg (‰ VDPB) of the lower Aptian to Lower Albian at Tiskatine, EAB.
Chemostratigraphic data is referenced against the local ammonoid zonation scheme in the EAB of Luber et al. (2017), the Standard Mediterranean Ammonite Scale (SMAS) of Reboulet et al. (2011, 2014), standard planktonic foraminiferal zonation of Premoli and Verga (2004) and Lower Cretaceous NC Zones of Roth (1978, 1983) and subzones after Bralower et al. (1993).

4.4.3.2 Results

The $\delta^{13}C_{carb}$ values of the Tiskatine section between **MTTK 163** and **MTTK 249** (Fig. 4.5) range between -0.34‰ (**MTTK 249**) and 1.9‰ (**MTTK 229**). The upper Aptian to lowermost Albian carbonate carbon isotope results ($\delta^{13}C$) in the Tiskatine section can be grouped into 5 major segments.

- **Segment 1**: Overall increase of δ^{13} C_{carb} values from -0.13‰ to 1.83 ‰ between **MTTK 163** to **MTTK 172**, with wide scatter of values between **MTTK 163** to **MTTK 169**.
- **Segment 2**: Decreasing trend of δ^{13} C_{carb} values following **MTTK 172** to 0.31‰ in **MTTK 185b**.
- **Segment 3**: Overall plateau of δ^{13} C_{carb} values from **MTTK 186** to **MTTK 206/208**, oscillating between 0.29 (**MTTK 197**) and 1.32‰ (**MTTK 204**). A small long-term increasing trend can be observed within the segment. On top of segment 3, a short-lived negative excursion (from **MTTK 206** to **MTTK 213**) can be observed.
- **Segment 4**: Rapid increasing trend in δ^{13} C_{carb} values from **MTTK 213** to **MTTK 216** followed by an attenuated increase towards a maximum value in the section of 1.90‰ in **MTTK 229**.
- **Segment 5**: Pronounced decreasing trend of δ^{13} C_{carb} values following **MTTK 229** to the minimum value in the section of -0.34‰ in **MTTK 249**.

According to the segmentation presented above, the following prominent positive δ^{13} C_{carb} peaks have been recognized in the Tiskatine section and correlate to the SMAS as noted below:

- **δ^{13} C_{carb} peak 1: MTTK 170** and **MTTK 178** ranging between 1.52‰ to 1.83 ‰. This interval falls within the "*E". marocanus* Subzone in the EAB (middle *E. martini* Zone

equivalent) around the NNC 2 interval of the Vocontian basin.

- **$\delta^{13}C_{carb}$ peak 2: MTTK 216** to **MTTK 232** ranging between 1.56‰ to 1.52‰. This interval falls within the *E. tiskatinensis* to "*Hypacanthoplites*" spp. subzones in the EAB (upper *N. nolani* Zone equivalent)

$\delta^{13}C_{carb}$ peak 1 falls within an interval barren of ammonoids and further marked by low recovery of foraminifera but increased percentage of calcareous benthic foraminifera. This interval, as discussed above, is linked to multiple parasequences and shallowing events culminating around bed **MTTK 192**. $\delta^{13}C_{carb}$ peak 2 falls into an interval of high ammonoid abundance and diversity, as well as high foraminifera recovery.

The $\delta^{13}C_{org}$ values of the Tiskatine section between **MTTK 160** and **MTTK 249** (Fig. 4.5) range between -27.27‰ (**MTTK 160**) and -22.49‰ (**MTTK 161**). The Aptian organic matter carbon isotope results in the Tiskatine section can be grouped into 4 major segments.

- **Segment 1**: Decreasing trend of $\delta^{13}C_{org}$ values from **MTTK 161** (-22.49‰) to -26.86‰ in **MTTK 186**.
- **Segment 2**: Overall plateau of $\delta^{13}C_{org}$ values from **MTTK 186** to **MTTK 206** (-26.5‰).
- **Segment 3**: Increasing values until **MTTK 226** (-25.21‰).
- **Segment 4**: Overall plateau until the basal Albian unconformity.

4.5 Additional sections

A number of additional sections were logged and correlated with the Tiskatine section to assess the regional sequence stratigraphic framework. These include the Id Amran (Fig. 4.6) and Assaka sections (Fig. 4.7), which form an E-W transect. A detailed log of sections with field photographs for the Id Amran and Assaka sections are shown in appendix C12 and C13, respectively.

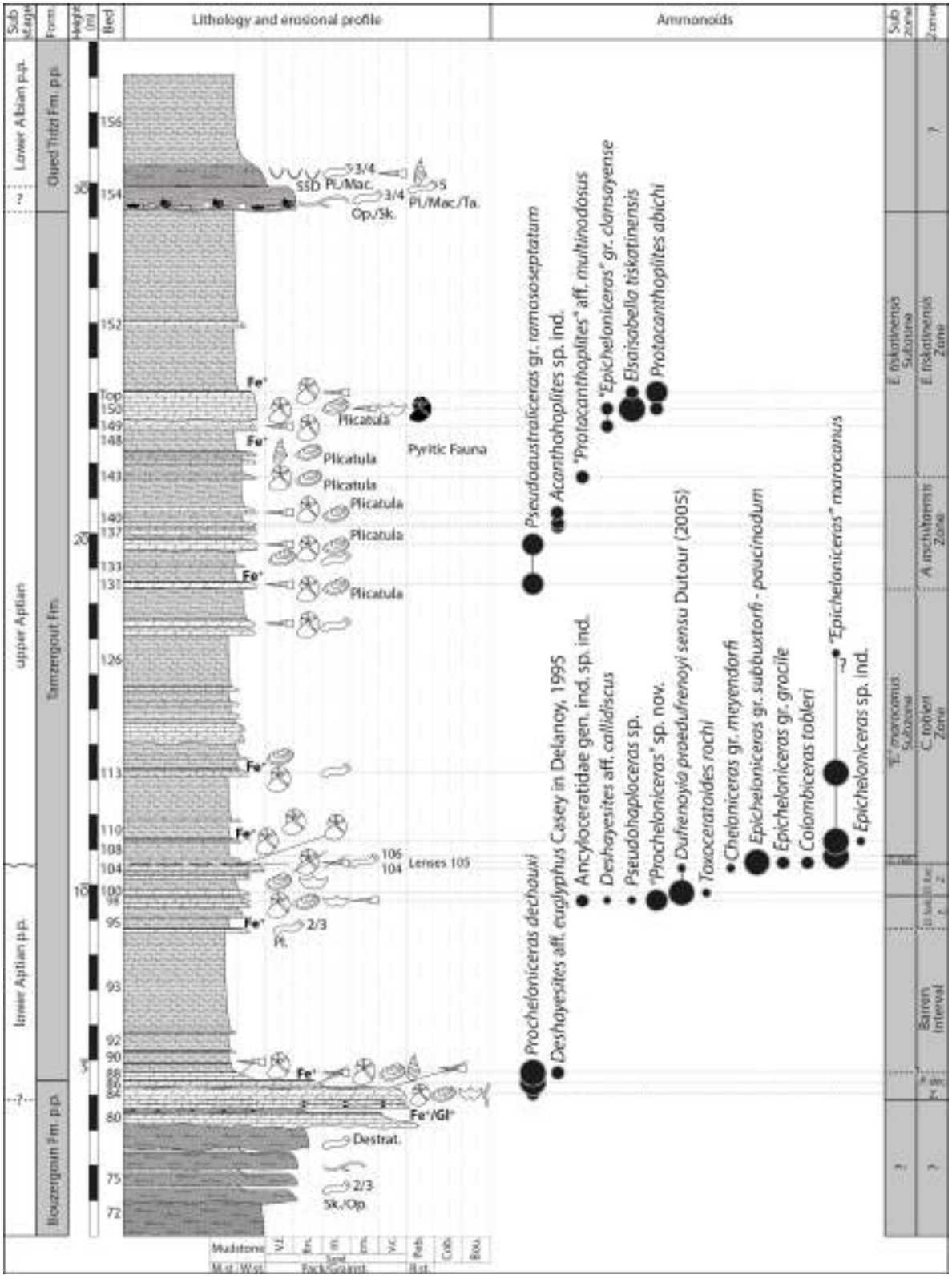

Figure 4.6: Id Amran section. Distribution of ammonoids, and biostratigraphic interpretation.

Legend in Fig. 4.2. An annotated version with depositonal environment interpretation and field photographs is provided in appendix C12.

4.5.1 Id Amran section

Id Amran (Fig. 4.6) Lat.: 30.796026° Long.: -9.571094°

This section is located 26.5 Km northeast of Tamri (Fig. 4.1). Access is by tarmac road driving east from Tamri to Azziar and then north for approximately 3 Km. There has been no previous publication about this section.

A log of the section is presented in figure 4.6 and an annotated version with interpreted depositonal environment and field photographs is provided in appendix C12.

The lower 3.2 metres (beds **MTIA 72 – 79**) of the studied sections start with a prominent meter-thick dolomitic siltstone. It is followed by very fine- to fine-grained, cm- to dm-sized and laterally continuous sandstones interbedded with calcareous mudstones. Bioturbation in the sandstones are common to abundant and the top sandstone is destratified. Internally sandstones exhibit a lenticular architecture on dm to m-scale that is made of planar lamination to low-angle cross-stratification and common hummocky cross-stratification. The interval is macrofossil free. Beds **MTIA 80 – 87** are composed of sand-rich rudstones with minor interbedded sandstones. The contact with the underlying succession is erosive. Rudstones are rich in oysters, brachiopods and serpulids. The first occurrence of ammonoids is in bed **MTIA 83**. This **MTIA 81 – 83** contain glauconite pebbles likely derived from a distinct iron and glauconite-rich horizon on top of **MTIA 80**. Other distinct features are macrofossil rich lenses infilling relief on the top of bed **MTIA 85**, which itself exhibits a belemnite-rich horizon to the top, belemnites often appear abraded. **MTIA 86** is similar, topped by an iron-rich horizon exhibiting abraded belemnites. **MTIA 72 – 87** comprise the upper part of the Bouzergoun Formation. This part of the succession is interpreted to represent a shallow-marine shelfal interval with the transition from lower shoreface to inner shelf conditions with the accumulation of bioclastic material along a barrier island/bar.

MTIA 88 – 153 comprises of the Tamzergout Formation. The succession is made of alternating cm- to dm-sized limestones and dm- to m-sized blue to grey-coloured marls. Most beds in this succession are ammonoid-bearing. Other macrofossils include common belemnites and various bivalves (basal section mostly *Aetostreon*; from bed **MTIA 131 – 153** dominated by *Plicatula*). Certain intervals (**MTIA 94 – 104**, **113 – 118**, **127 – 131**, **135 – 147** and **149 / 150**) show an increased siliciclastic input producing sandy limestones.

Overall this succession was deposited in inner to mid shelfal environments with shallowing pulses or times of higher siliciclastic runoff into the basin.

MTIA 154 – 156 are part of the Oued Tidzi Formation and display a basal erosional unconformity. The contact with the marls below exhibits clear scouring and the distinct basal surface of bed **MTIA 154** is rich in fauna including pyritic ammonites, belemnites and further rip-up clasts from the succession below. The rest of the bed is macrofossil free. This very fine- to fine-grained sandstone bed exhibits low-angle cross-stratification and hummocky cross-stratification. Bioturbation is common within the bed (*Ophiomorpha, Skolithos* ichnotaxa) to abundant at the top (*Planolites, Macronicus* ichnotaxa). **MTIA 155 – 156** represents the abrupt return into mud-dominated sedimentation. Interval **MTIA 154 – 156** is interpreted to represent a significant shallowing event and the advance of the shoreface onto the shelf with abrupt flooding and re-establishment of shelfal conditions in **MTIA 156**.

Compared to the reference succession established at Tiskatine the following ammonoid bio-events are recognised:

- Bio-event 1: occurrence of *P. dechauxi* (Kilian and Reboul) in **MTIA 84**
- Bio-event 2: peak of diversity dominated by *Colombiceras* and *Epicheloniceras* **MTIA 105**
- Bio-event 3: first appearance datum of the endemic species "*Epicheloniceras*" *marocanus* (Roch) in **MTIA 106**
- Bio-event 5: peak of abundance of *Pseudoaustraliceras* in beds **MTIA 131** and **135**
- Bio-event 6: sudden mass occurrence of *Elsaisabellia* in bed **MTIA 150**

By comparison to the ammonoid succession at Tiskatine, it should be noted that two additional ammonoid faunas are recognized. In bed **MTIA 98** the assemblage is dominated by *"Prochelonicerasʺ* sp. nov. (Fig. 4.14.11-17), large ancyloceratids associated with *Deshayesites* aff. c*allidiscus* Casey, 1961a (Fig. 4.14.1-2). Slightly above bed **MTIA 100** contains an abundant fauna dominated by *Dufrenoyia praedufrenoyi* Casey, 1964 *sensu* Dutour (2005) (Fig. 4.14.3-9). The occurrence of *Toxoceratoides rochi* Casey, 1961b (Fig., 4.14.10) at this level is noteworthy. By comparison with the ammonoid successions of SE France the fauna from **MTIA 98** indicates the middle part of the *D. forbesi* Zone *sensu* Frau et al. (2015). The assemblage from **MTIA 100** is indicative of the middle part of

the *D. furcata* Zone *sensu* Dutour (2005). As a consequence, these two early Aptian ages demonstrate the existence of a hiatus that spans the upper part of the *D. forbesi* Zone, the *D. deshayesi* Zone and the lower part of the *D. furcata* Zone on top of bed **MTIA 98**, time equivalent of the OAE1a-related culmination and succeeding recovery. These ages are further supported by the occurrence of the calcareous nannofossil association of *E. floralis* and *Nannoconus circularis* Deres and Achéritéguy, 1980 (Fig. 4.18) in **MTIA 104.** The early lower Aptian nannofloras (**MTIA 89 – 95**) investigated from Id Amran have extremely rich nannofloras yielding *Diazomatolithus lehmanii* Noël, 1965 (Fig. 4.18), high relative abundances of *Cyclagelosphaera margerelii* Noël, 1965 (Fig. 4.18) and *Assipetra terebrodentarius* (Applegate et al. *in* Covington and Wise, 1987) (Fig. 4.18) (with *Pickelhaube furtiva* (Roth, 1983), events all occurring below the FAD of *E. floralis*. This assemblage is characteristic of other lower *D. forbesi* Zone ammonite dated assemblages (Atherfield Clay, UK, Fischschiefer UK North Sea; Jeremiah, 2000; Jeremiah et al., 2010; Lehmann et al., 2012, 2016). At Id Amran a rich nannoconid association also occurs with the wide canal forms *N. circularis* and *Nannoconus vocontiensis* Deres and Achéritéguy, 1980 predominant. The Id Amran *D. forbesi* Zone dated sediments investigated between **MTIA 97** and **MTIA 110** are stratigraphically younger than the sediments immediately below the basal Albian unconformity at DSDP 370 and 416A. Here the samples also yield *Zeugrhabdotus scutula* (Bergen, 1994) (Fig. 4.18), a nannofossil not recorded from Id Amran.

Other important calcareous nannofossil bio-events recorded are: (*i*) The occurrence of *C. bosunensis* and *M. hoschulzii* was recorded from two selected samples from the Id Amran outcrop, at beds **MTIA 151** and beds **MTIA 153** (*E. tiskatinensis* Zone); additionally at bed **MTIA 153** *C. bosunensis* was common and an incursion of common *Z. vanhintei* (Fig. 4.18) (*E. tiskatinensis* Zone) was also recorded. (*ii*) *P. columnata*, *R. achlyostaurion* and rare *C. bosunensis* are recorded from **MTIA 156**, confirming a basal Albian age.

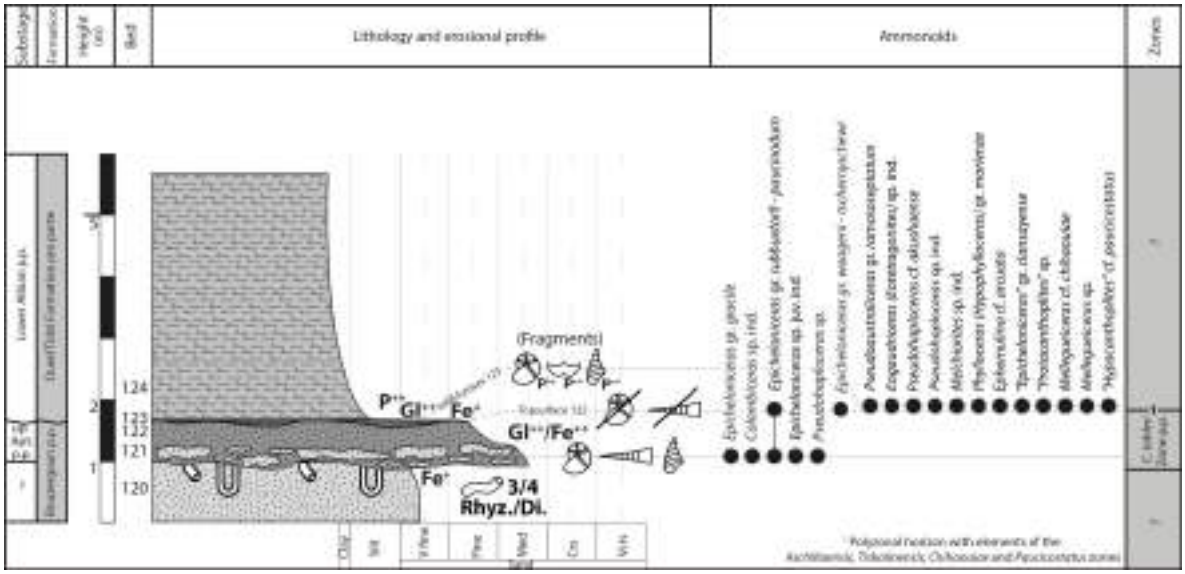

Figure 4.7: Assaka section. Ammonoid distribution and biostratigraphic interpretation. Legend in Fig. 4.2. An annotated version with depositonal environment interpretation and field photographs is provided in appendix C13.

4.5.2 Assaka section

Assaka (Fig. 4.7) Lat.: 30.807297° Long.: -9.787837°

Located 1.8 Km southwest of the village Assaka (Fig. 4.1), this section can be reached by following an unmade track leaving Assaka, towards Teldi, opposite the mosque in the bend of the national road 1.

A log of the section is presented in figure 4.7 and an annotated version with interpreted depositional environment and field photographs is provided in appendix C13. **MTAS 121 – 122** represent the uppermost part of Bouzergoun Fm. **MTAS 121** is a well-sorted, very fine-grained and macrofossil free sandstone with intense bioturbation at the top. Main ichnotaxa present include abundant *Rhizocorallium* and ?*Diplocraterion.* **MTAS 122** has an erosive base and includes reworked clasts from the **MTAS 121**. It is a glauconite-rich sandstone with a massive appearance and a finning-upward profile. Macrofossils include ammonoids, belemnites and gastropods, among others. The larger ammonoid shells are infilled by glauconitic sand and other macrofossils, pointing to a poly-phased condensation horizon. The top forms an erosional surface with abraded, large ammonoids and belemnites. The fauna from **MTAS 122** is dominated by the genus *Epicheloniceras*. **MTAS 120** is interpreted to represent shallow-marine sandstones deposited in the

shoreface zone and **MTAS 121/122** a condensed interval deposited on a palaeotopographic high with constant reworking of the deposits and enrichment in glauconite.

The contact with the overlying Oued Tidzi Fm. is marked by lenses of macrofossil-rich, very glauconite-rich, very fine-grained silty sandstone of **MTAS 123**. Macrofossils include belemnites, ammonoids, brachiopods and gastropods, typically in phosphatic preservation. Most material occurs as fragments and infilled with glauconite sand pointing to a poly-phased horizon. The ammonoid fossil assemblage further proves **MTAS 123** to be polyzonal (see discussion below). We prefer not to assign a formation name to **MTAS 123** as deposition took place on a palaeotopographic high leading to condensation and constant winnowing/reworking of the deposits. It should be noted that the Tamzergout Fm. is absent at this location.

MTAS 124 marks a shift into mud-dominated deposition. Marls are of prominent green to yellow colour and **MTAS 124** is part of the Oued Tidzi Fm. Marls are laminated and macrofossil recovery is poor including occasional belemnites. The change from sand-dominated deposits below to marls shows a significant increase in water depth. The deposition took place through pelagic fall out in shelfal conditions.

Compared to the reference succession established at Tiskatine: (*i*) the co-occurrence of *Epicheloniceras* and *Colombiceras* in **MTAS 121** indicates the early late Aptian *C. tobleri* Zone and Subzone; (*ii*) the mass occurrence of *Epicheloniceras* in **MTAS 122** suggests a similar age, even though occurrence of elements from the "*E." marocanus* Subzone cannot be excluded; (*iii*) the fauna collected from **MTAS 123** contains reworked upper Aptian ammonites from the *A. aschiltaensis* Zone [*Pseudoaustraliceras* gr. *ramososeptatum* (Anthula, 1900)], from the *E. tiskatinensis* Zone ["*Epicheloniceras*" gr. *clansayense* (Jacob, 1905)] together with *Melleguieiceras* and "*Hypacanthoplites*" that are diagnostic of the Lower Albian (Latil, 2011; Luber et al., 2017). The key ammonoid material is illustrated in figure 4.15.

The early Albian age of the uppermost part of the section (**MTAS 124**) is established by the co-occurrence of the calcareous nannofossils *P. columnata* and ?*R. achlyostaurion.*

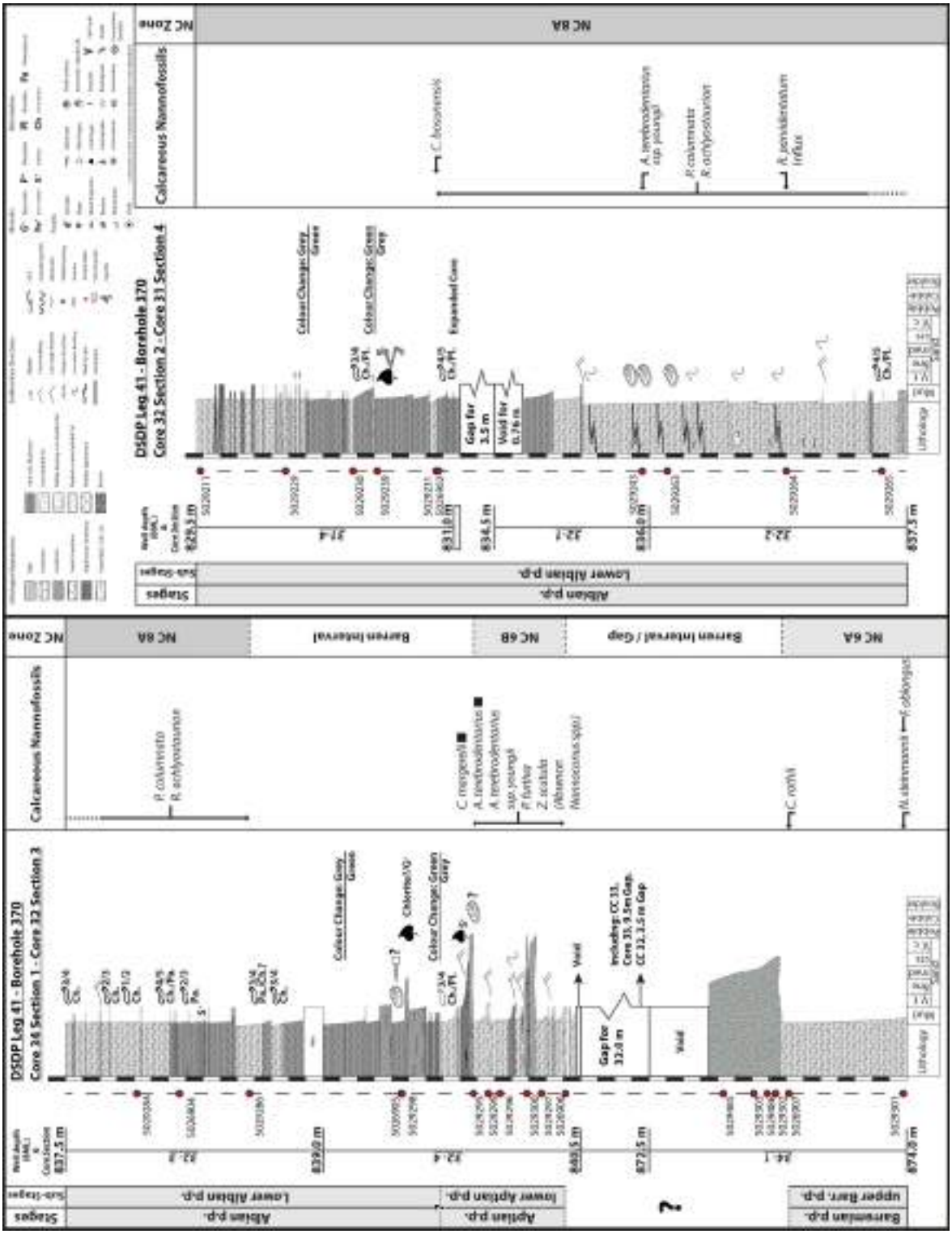

Figure 4.8: DSDP borehole 370: Lithostratigraphic log and calcareous nannofossil distribution.

Distribution charts for calcareous nannofossil can be found in the supplementary data (compact disc). An A3 version is provided in appendix C2.

4.5.3 DSDP Leg 41 borehole 370: The offshore record

To compare the onshore work in the EAB with the offshore in Morocco the upper Barremian to Lower Albian strata (Fig. 4.8) of the DSDP Leg 41 – borehole 370 was investigated and sampled for calcareous nannofossil analysis (request number: 049055-IODP and 049614-IODP). DSDP well 370 is located about 155 kilometres offshore the modern Moroccan coastline, northwest of the city Safi in water depths of 4214 m (Fig. 4.1). No ammonoid specimens were encountered or reported from the interval of interest in the borehole.

The main target interval for this study was the upper Barremian to Lower Albian strata from the base of core 34-section 1 to top of core 32-section 4 (839.0 m – 874.0 m below mud line (BML)). A summary log is shown in Fig. 4.8 and an A3 version is provided in appendix C2.

4.5.3.1 Lithostratigraphy, sedimentology

The investigated interval is predominantly composed of alternating calcareous and non-calcareous mudstones but also includes the following prominent coarse clastic intervals and erosion surfaces. Some of the coarse clastic deposits have previously been investigated by Meyer et al. (1978). All depth values are in meters below mud line (BML).

- **872.85 – 873.26 m:** sharp-based, erosive, coarse-grained, sandy grainstone forming a basal lag and exhibiting a grain size break with normal-graded, medium- to very fine-grained sandy grainstone above (microfacies C of Meyer et al. 1978)
- **840.43 m:** Mud-draped scour surface
- **840.16 – 840.23 m:** sharp-based, erosive, well-sorted sandy rudstones (microfacies E2 of Meyer et al. 1978) overlain by pebble-bearing mudstones and topped by well-sorted fine-grained, cross-laminated calcareous sandstone
- **839.78 – 839.87 m:** sharp-based, erosive, poorly-sorted rudstone overlain by a thin mudstone unit rich in plant debris separating the coarse basal layer from a medium-grained, well-sorted sandstone (up to here microfacies E1 of Meyer et al., 1978) which in turn is overlain by a siltstone bearing a large lignite clast and is topped by interbeds of laminated very fine-grained sandstones interbedded with mudstones

- **839.68 m:** erosional surface overlain by laminated, calcareous, very fine-grained sandstones interbedded with non-calcareous mudstone marking a prominent colour change from dark grey to green mudstones

The majority of core **32-2** and lower part of **32-1** (837.02 – 835.61 m) is composed of a mud-dominated unit that exhibits prominent contorted beds made of mudstone clasts, retaining original lamination. Occasionally mudstones develop poor sorting with cm-sized sandy grainstone clasts and shell fragments.

4.5.3.2 Calcareous nannofossil bio-events

The following key bio-events have been recognised (Fig. 4.8 and App. C2):

- 1. LAD of common nannoconids and *Micrantholithus obtusus* Stradner, 1963*; presence of Flabellites oblongus* (Bukry, 1969) (Fig. 4.18) at 874.81m indicating an age no older than latest Barremian (Zone NC6A).
- 2: *LAD of Nannoconus steinmannii* Kamptner, 1931 (Fig. 4.18) at 873.98 m
- 3: LAD of *Conusphaera rothii* (Thierstein, 1971) (Fig. 4.18) with common *Z. scutula* at 873.31m indicating an age no younger than latest Barremian. In this study the LAD of *C. rothii* is utilised as an approximation for top Barremian (Zone NC6A).
- 4. LAD of *Z. scutula* at 840.03 indicating an age no younger than earliest Aptian (Zone NC6B).
- 5: LAD of HRA of *C. margerelii* with an influx of *A. terebrodentarius* and LAD consistent *P. furtiva* in the absence of *E. floralis* indicating an age no younger than early Aptian intra *D. forbesi* ammonite zone equivalent age at 839.87m (Zone NC6B).
- 6. FAD of *R. achlyostaurion*, presence of *C. bosunensis* and *A. terebrodentarius youngii* indicates a basal Albian age at 838.57m (Zone NC8A).
- 7. FAD of *P. columnata* at 837.90m (Zone NC8A).
- 8. LAD of *A. terebrodentarius youngii* at 835.95m (Zone NC8A). *A. terebrodentarius youngii* is more extensively recorded from the oceanic DSDP 370 than at the shallower shelf outcrop at Tiskatine, a result of this form's preference to deeper waters (Street and Bown, 2000).
- 9. FAD of an influx of *R. parvidentatum* at 836.80 m.

- 10. LAD of *C. bosunensis* at 830.89m (Zone NC8A).
- In the DSDP 370 borehole *C. bosunensis* is found from 830.89m down to the basal Albian sample analysed at 838.57m.

At the DSDP 370 borehole both *C. bosunensis* and *A. terebrodentarius youngii* are found to have LAD's extending into the basal Albian.

4.6 Interpretation – discussion

4.6.1 Age interpretation foraminifera

All of the planktonic foraminifera present suggest a late Aptian age for the Tamzergout Fm. at Tiskatine (Fig. 4.3). Lower Aptian taxa such as the distinctive *L. cabri* are absent and the lowest significant planktonic foraminifera occurring in the section, *G. ferreolensis* is restricted to the upper Aptian according to some authors (e.g. Moullade et al. 2002). The occurrence of this species in the highest part of the Tamzergout Fm. (Fig. 4.4) indicates a late Aptian age (along with the presence of *H. trochoidea* and, just below these occurrences, *P. cheniourensis*) (Premoli Silva and Verga, 2004). Taxa indicative of a Lower Albian age such as *T. primula* are absent from the Tamzergout Fm. at Tiskatine. Ammonoid and calcareous nannofossil occurrences demonstrate an Albian age for the overlying Oued Tidzi Fm.

This interpretation contrasts with that of Yamina et al. (2002) who described, but did not illustrate, a variety of lower Aptian planktonic foraminifera species from the lower part of the Tamzergout Fm. at localities north of the Amsittene Anticline. Luber et al. (2017) highlighted that the base of the Tamzergout Fm., as originally defined by Duffaud et al. (1966) is markedly diachronous being the lower part of the lower Aptian at some localities and lower upper Aptian at others (Fig. 4.2). Rey et al. (1988) also regarded the Tamzergout Fm. as lower Aptian, although their Tadhart Fm., regarded herein as part of the Tamzergout Fm., was assigned an upper Aptian age. A possibility to explain the discrepancies in age interpretation, in addition to the difficulties in applying lithostratigraphy, is that the Tiskatine section represents deposition in proximity of a local high, such that the well-established intra-Aptian hiatus (sequence boundary) (Peybernes et al., 2013; Luber et al., 2017) is most expansive there.

The late Aptian age interpretation of the Tamzergout Fm. at Tiskatine provided by the planktonic foraminifera is in broad agreement with the age interpretations provided here from the occurrences of ammonoids and calcareous nannofossils (Fig. 4.4), as well as the stable carbon isotope record (Fig. 4.5). It is very likely that the uppermost Aptian ("*H*". *jacobi* Zone) is missing in the Tiskatine section as *P. cheniourensis* occurs near the top of the formation, a species with a Last Appearance Datum (LAD) well below the top of the Aptian (Ando et al., 2013) or reported to be "uppermost Gargasian" (Moullade et al., 2002). Ammonoid, calcareous nannofossils and carbon isotope records support this interpretation (Figs. 4.4, 4.5).

The calibration of the standard planktonic foraminiferal zonation to the Standard Mediterranean Ammonite Scale (SMAS) remains a work in progress as, regrettably, there are few publications that clearly document the co-occurrence of planktonic foraminifera alongside ammonoid occurrences from the classic sections in the Mediterran – Caucasian Realm of the Tethyan Superrealm (Westermann, 2000). The data from the Tiskatine section (Figs. 4.3, 4.4) may be helpful in this respect as the local ammonoid zonation of Luber et al. (2017) can be calibrated to the SMAS and the $\delta^{13}C$ record and calcareous nannofossils provide additional constraint.

The oldest ammonites found in the Tamzergout Fm. at Tiskatine are assigned to the local *C. tobleri* Zone. This is calibrated (Luber et al., 2017) to a position midway within the *E. martini* Zone of the SMAS (the oldest standard zone of the late Aptian, a time-equivalent to the *E. martinoides* Zone *sensu* Casey et al., 1998). The recognition of the *G. ferreolensis* planktonic foraminiferal zone for the same samples is intriguing in that for some authors the *G. ferreolensis* Zone is regarded as occurring at the base of the upper Aptian, in the lowest part of the *E. martini* Zone (Ogg and Hinnov, 2012). Our data would suggest that positioning the base of *G. ferreolensis* Zone above the base of the upper Aptian, within the *E. martini* Zone (Figs. 4.3, 4.4) would be preferable as indicated by Robaszynski and Caron (1995) and Dauphin (2002). The δC^{13} record points to calibration with the Ap9 segment of the standard $\delta^{13}C$ curve from the Vocontian Trough. Ap9 is low within the *E. martini zone* and calibrates with the *G. ferreolensis* zone.

The local *A. aschiltaensis* ammonite Zone found in the middle part of the Tamzergout Fm. at Tiskatine is calibrated (Luber et al., 2017) to straddling the upper *E. martini* to *P. melchioris* zones of the SMAS. The portion of the Tiskatine section assigned to the *A. aschiltaensis* Zone is also assigned to the *G. algerianus* planktonic foraminifera Zone

and the upper part of the *G. ferreolensis* Zone. Although these zones are calibrated by some authors to levels within the *E. martini* Zone (e.g. Ogg and Hinnov, 2012) the data from Tiskatine (Figs. 4.3, 4.4) would suggest that placement of the top of the *G. algerianus* zone extends to the *P. melchioris* Zone as suggested by Robasynski and Caron (1995) and Dauphin (2002).

4.6.2 Biostratigraphic correlation to the Standard Mediterranean Scale (SMAS)

As already outlined by Luber et al. (2017) correlation between the ammonoid scale developed in the EAB and the SMAS of Reboulet et al. (2011, 2014), is largely handicapped by: (*i*) the endemism that characterise the EAB assemblages; (*ii*) the absence of most SMAS index species in Morocco; (*iii*) the limited published data on the ranges of key taxa that would allow correlation between both scales; and (*iv*) the lack of precise definition of the Aptian and Lower Albian biochrono-zones and subzones of the SMAS. This latter point was already addressed by Owen (1996), Dauphin (2002), Bulot (2010), Bulot et al. (2014), Frau et al. (2015, 2016). As a consequence, the high-resolution integrated stratigraphy of the Aptian Stage is at a far more preliminary stage than advocated by many authors in recent years (see also discussions in Frau et al., 2017b).

It should be kept in mind that the Aptian zonal subdivision of the SMAS is originally based on the ammonoid successions of the Caucasian and Transcaspian Republics of the former USSR (Hoedemaeker and Bulot, 1990; Hoedemaeker et al., 1993). This choice was imposed by the lack of detailed data on the ammonoid succession in the Aptian historical type sections of south-eastern France. The condensed nature of the Caucasian and Transcaspian sections is clearly outlined by the descriptions of the lithological successions by Bogdanova and Prozorovsky (1999) and Bogdanova and Mikhailova (2016). In the meanwhile an extensive survey of the ammonoid successions of the Provençal and Vocontian basins has been carried out and is still in progress (Dauphin, 2002; Dutour, 2005; Ropolo et al., 2006, 2008a, with references; Frau et al., 2015, 2016; Frau and Bulot, in preparation). A state of the art of the integrated ammonoid, planktonic foraminifer, and calcareous nannofossils in the reference sections of the Provençal and Vocontian basins are presented in figures 4.9 to 4.11 and A3 versions are provided in appendix C3 to C5. These synthetic figures include both published (Bergen, 2000; Kennedy et al., 2000, 2014; Moullade et al., 2000, 2005; Dauphin, 2002; Herrle and Mutterlose, 2003; Dutour, 2005;

Kuhnt and Moullade, 2007; Frau et al., 2015) and unpublished data by two of us (CF and LGB). The bio-events selected are the ones that have proved to be the more reliable to correlate the EAB and the SMAS successions (Luber et al., 2017). Formal revision of the SMAS is far beyond the scope of the present contribution. This work is currently in progress and will be published elsewhere.

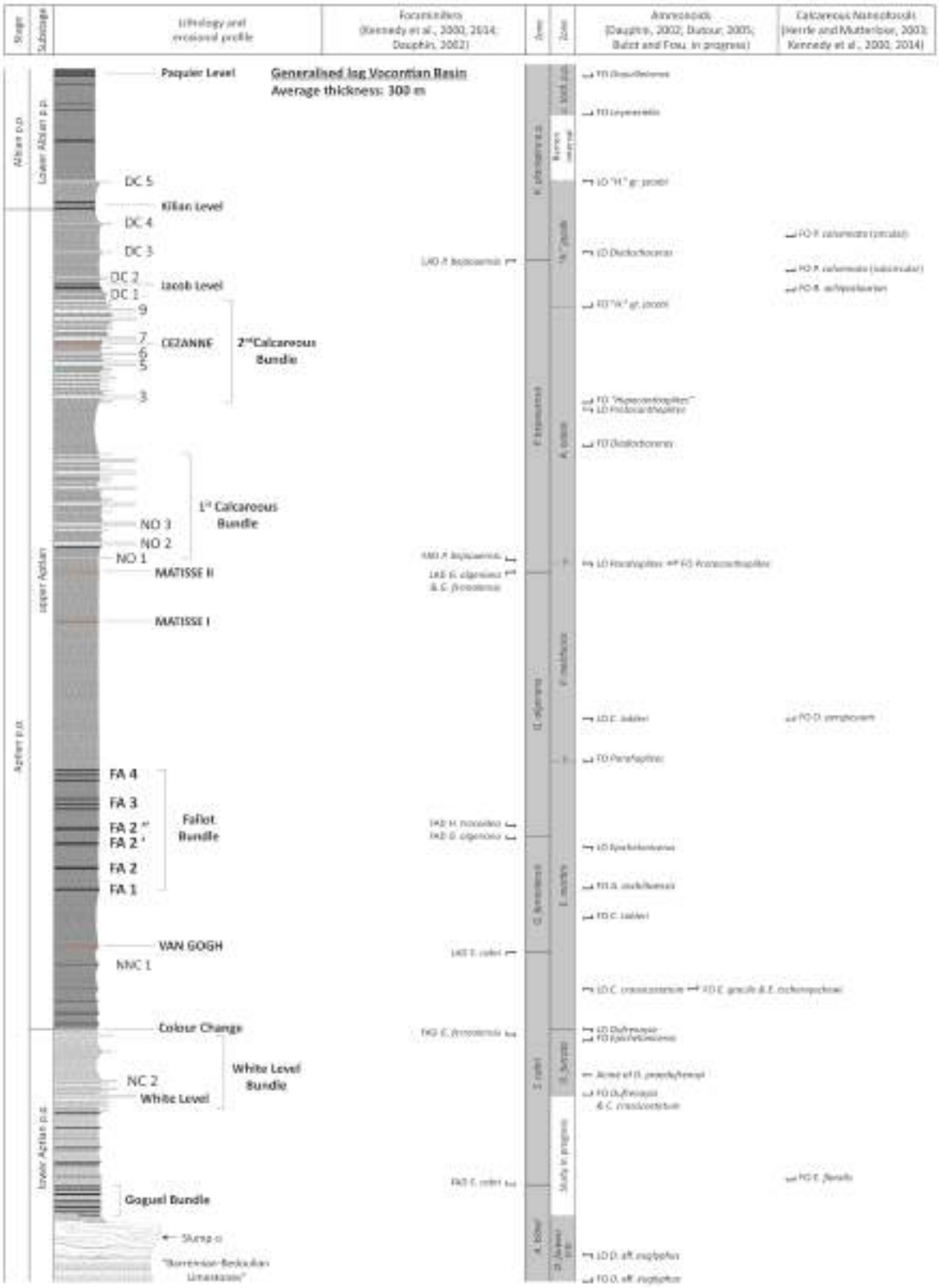

Figure 4.9: Generalised log Vocontian Basin.
Distribution of key ammonoid (Dauphin, 2002; Dutour, 2005; Bulot and Frau, in progress), foraminifera (Kennedy et al., 2000, 2014; Dauphin, 2002) and calcareous nannofossils (Herrle and Mutterlose, 2003; Kennedy et al., 2000, 2014) of the Vocontian Basin in SE France. An A3 version is provided in appendix C3.

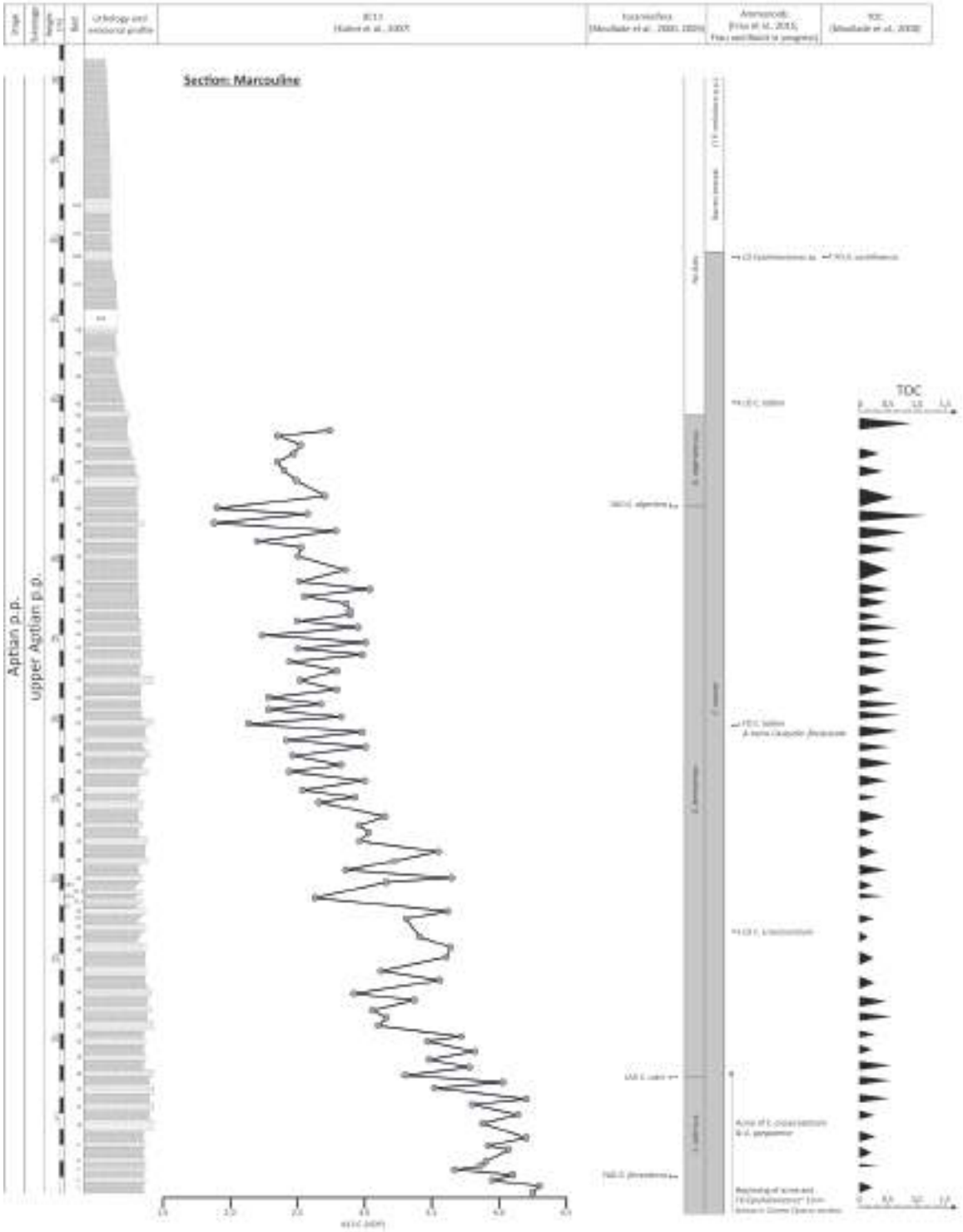

Figure 4.10: Marcouline Section.
Distribution of key ammonoids (Frau et al., 2015; Frau and Bulot in progress), foraminifera (Moullade et al., 2000, 2005) and calcareous nannofossils (Bergen, 2000) of the Marcouline section, Provençal Basin. δ13C data from Kuhnt et al. (2007) and TOC data from Moullade et al. (2000). An A3 version is provided in appendix C4.

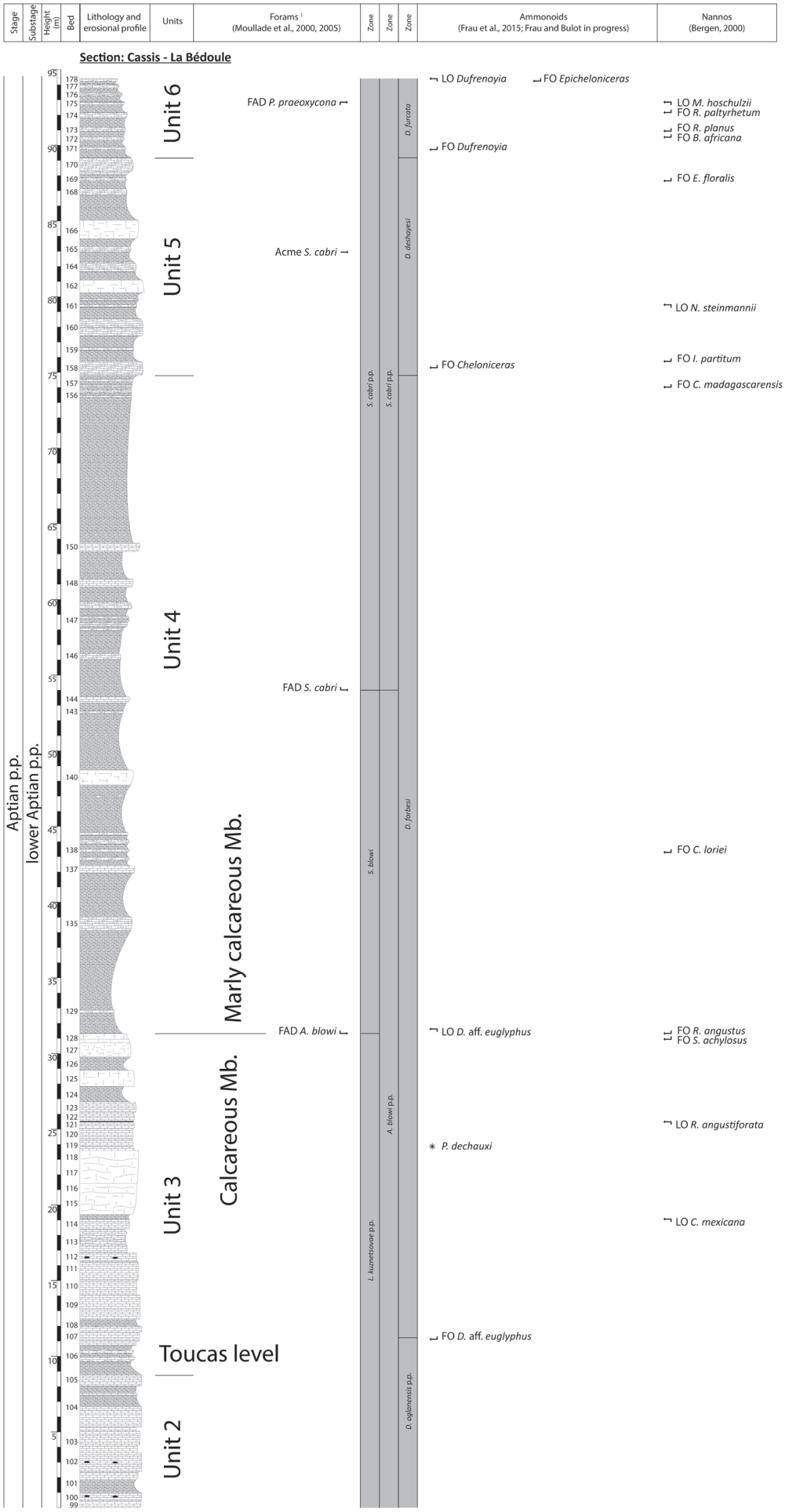
Stage
Substage
Height (m)
Bed
Lithology and erosional profile
Units
Forams [1] (Moullade et al., 2000, 2005)
Zone
Zone
Zone
Ammonoids (Frau et al., 2015; Frau and Bulot in progress)
Nannos (Bergen, 2000)
Section: Cassis - La Bédoule
Aptian p.p.
lower Aptian p.p.
Unit 6
Unit 5
Unit 4
Unit 3
Unit 2
Marly calcareous Mb.
Calcareous Mb.
Toucas level
FAD P. praeoxycona
Acme S. cabri
FAD S. cabri
FAD A. blowi
LO Dufrenoyia
FO Epicheloniceras
FO Dufrenoyia
FO Cheloniceras
LO D. aff. euglyphus
P. dechauxi
FO D. aff. euglyphus
LO M. hoschulzii
FO R. paltyrhetum
FO R. planus
FO B. africana
FO E. floralis
LO N. steinmannii
FO I. partitum
FO C. madagascarensis
FO C. loriei
FO R. angustus
FO S. achylosus
LO R. angustiforata
LO C. mexicana
S. cabri p.p.
S. cabri p.p.
S. blowi
A. blowi p.p.
L. kuznetsovae p.p.
D. furcata
D. deshayesi
D. forbesi
D. oglanensis p.p.

Figure 4.11: Cassis section.
Distribution of key ammonoid (Frau et al., 2015; Frau and Bulot in progress), foraminifera (Moullade et al., 2000, 2005) and calcareous nannofossil (Bergen, 2000) specimen from the Cassis section, Provençal Basin. An A3 version is provided in appendix C5.

4.6.3 Carbon isotope chemostratigraphic correlation

The following paragraph provides interpretation on the preservation of the $\delta^{13}C$ curve in the Tiskatine section. Further, we attempt to correlate the observations of the EAB**,** well-constrained by biostratigraphic data, to the Tethyan sections in the Vocontian (Fig. 4.12) and Provençal basins (Fig. 4.10) in SE France, considered as standard sections for the Tethyan realm and reference locations for the SMAS.

4.6.3.1 Interpretation of the $\delta^{13}C$ trend in the Tiskatine section

Marine $\delta^{13}C$ values are primarily linked to phytoplankton productivity (Weissert, 1989), leading to an enrichment of ^{13}C in the upper water column and consequently higher $\delta^{13}C$ values in marine carbonate and organic matter formed within these waters. On a geological timescale, short- and long-term changes in marine $\delta^{13}C$ values have been linked to global change in the ratio between the burial flux of organic matter and carbonates as well as changes in the isotopic composition of the input fluxes into the atmosphere-ocean reservoir. Assuming a constant isotopic input flux to the atmosphere-ocean reservoir, a global relative increase of organic matter burial compared to carbonates will lead to higher carbonate or organic matter $\delta^{13}C$ values on a global scale (Kump and Arthur, 1999). Pending confirmation that local factors or diagenetic alteration have not overprinted the global $\delta^{13}C$ signal in the analysed material, the variations of $\delta^{13}C$ values can thus be used to correlate sections across the globe, an exercise known as carbon isotopic chemostratigraphy. This approach has been widely employed in Mesozoic strata (e.g. Huck et al., 2011; Trecalli et al., 2012; Navarro-Ramirez et al., 2016; Tedeschi et al., 2017), relying on the establishment of reference curves in biostratigraphically-constrained sections (Menegatti et al., 1998; Herrle et al., 2004; Föllmi et al., 2006; Jarvis et al., 2006; Bodin et al., 2015; Scott 2016).

As such, in order to employ and discuss our $\delta^{13}C$ dataset for chemostratigraphic purposes, it must first be assessed that local water cycling processes or diagenesis have had no significant influence on the analysed material so that the observed $\delta^{13}C$ trends are

mainly representative of the global change in the carbon cycle. Given that the here-analysed carbonate samples are made of bulk micrite (either from carbonate mudstones or marls) deposited in an open shelf setting, open ocean water masses are expected (Immenhauser et al., 2002) and resetting of $\delta^{13}C_{carb}$ values by late diagenetic processes are unlikely since the abundance of carbonates act as a strong buffer against significant isotopic exchange with C-poor fluids (e.g. Marshall, 1992). The absence of major diagenetic resetting of our $\delta^{13}C_{carb}$ dataset is confirmed by the fact that the measured values are typical for Aptian oceanic signature, as reported from numerous studies (e.g. Herrle et al., 2004; Bodin et al., 2015). The same can be said for the $\delta^{13}C_{org}$ dataset, presenting values similar to the one reported by McAnena et al. (2013) for the DSDP site 545 offshore Morocco.

However, for the $\delta^{13}C_{carb}$ values, care must be taken for the lowermost (between **MTTK 162** and **MTTK 169**) and uppermost (between **MTTK 237** and **MTTK 249**) parts of the Tamzergout Fm. where high amplitude and sharp fluctuation of $\delta^{13}C_{carb}$ values are observed. Since similar trend and fluctuation of values cannot be observed in the $\delta^{13}C_{org}$ dataset, it can be hypothesized that these high amplitudes and sharp fluctuations of $\delta^{13}C_{carb}$ values could be linked to early diagenetic resetting, notably in the uppermost part of the Tiskatine section, close to the hiatus surface separating the Tamzergout and Oued Tidzi formations. The large negative C-isotope excursion at the top of the Tamzergout Fm. resembles a negative $\delta^{13}C$ excursion associated with subaerial exposure diagenesis due to the adjunction of ^{13}C-depleted carbon derived from soil development (Allan and Matthews, 1982). There is, however, no physical indication of subaerial exposure related to the Lower Albian unconformity at the base of the Oued Tidzi Fm. Oxidation of marine organic matter could thus be a more likely explanation for these two negative excursions. Alternatively, they may be linked to local oceanographic conditions related to water masses isolation.

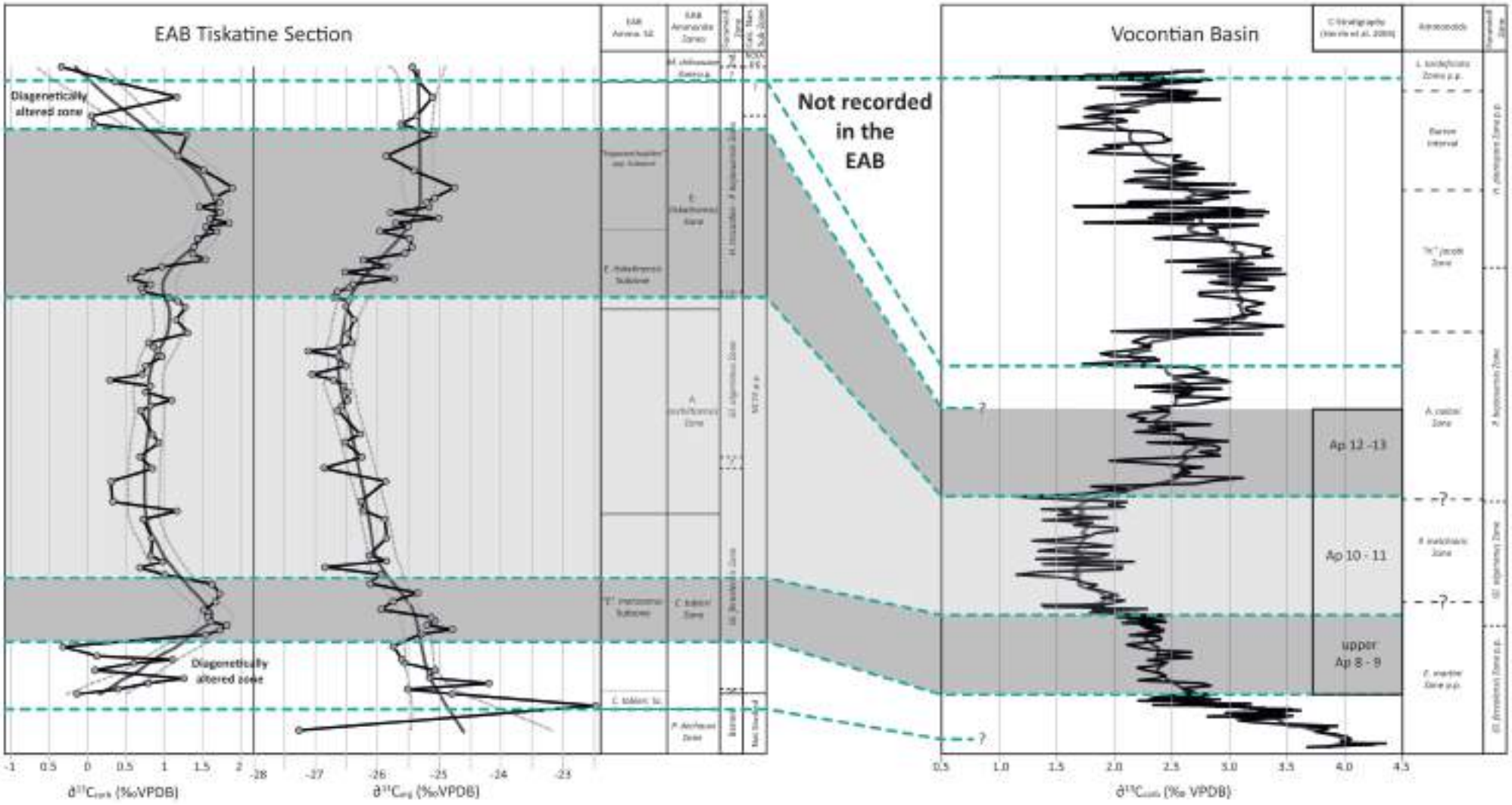
EAB Tiskatine Section
Vocontian Basin
Not recorded in the EAB
Diagenetically altered zone
Diagenetically altered zone
Ap 12 -13
Ap 10 - 11
upper Ap 8 - 9
?
?
?
-1 0.5 0 0.5 1 1.5 2
-28 -27 -26 -25 -24 -23
0.5 1.0 1.5 2.0 2.5 3.0 3.5 4.0 4.5

Figure 4.12: Comparison of lower Aptian to Lower Albian δ13 Ccarb and δ13 Corg (‰ VDPB) at Tiskatine, EAB and δ13 Ccarb (‰ VDPB) in the Vocontian Basin (data from Herrle, 2004). Two positive shifts of the succession are highlighted by grey shading bands and diagenetically altered data annotated. Data is references against the local ammonoid zonation scheme in the EAB of Luber et al. (2017), the Standard Mediterranean Ammonite Scale (SMAS) of Reboulet et al. (2011, 2014), standard planktonic foraminiferal zonation of Premoli and Verga (2004) and Lower Cretaceous NC Zones of Roth (1978, 1983) and subzones after Bralower et al. (1993).

4.6.3.2 Correlation to the Provençal and Vocontian Basin

The chemostratigraphic correlation between the EAB and the SE France reference sections established in the Provençal and Vocontian Basin (Herrle et al., 2004) has to take into account the two basin-wide hiatus recognized in the Tiskatine section, covering the 1) the upper *D. forbesi* zone to lower *E. martini* zone and 2) the whole *H. jacobi* to lowermost *L. tardefurcata* zone equivalent of the SMAS. Furthermore, it has to be taken into consideration that the sedimentary record in the EAB is far more condensed than its reference counterparts in SE France (Fig. 4.12).

Considering the hiatus in the EAB and stratigraphic gaps (see biostratigraphic discussion above), the overall $\delta^{13}C_{org}$ curve as well as the $\delta^{13}C_{carb}$ curve (excluding the lowermost and uppermost part of the latter) of the EAB (Fig. 4.5) matches the established curves of the Vocontian and Provençal Basin in SE France (e.g Fig. 4.11 and 4.12). Hence, since the lowermost and uppermost part of the Tiskatine $\delta^{13}C_{carb}$ record cannot be chemostratigraphically correlated to the French reference curve, this confirms the suspicion of diagenetic alteration raised earlier based on the high amplitude and sharply fluctuating $\delta^{13}C_{carb}$ values. These two parts of the $\delta^{13}C_{carb}$ record will thus not be further considered in the following discussion. Eliminating these data allows to clearly observe an initial negative $\delta^{13}C$ trend (minimum amplitude of ca. 1‰ for the $\delta^{13}C_{carb}$ record, and 4‰ for the $\delta^{13}C_{org}$ record) that correspond well to the upper part of the decline in $\delta^{13}C$ values spanning the lower – upper Aptian transition observed in the Vocontian Basin (in both bulk micrite and belemnite records; Herrle et al., 2004; Bodin et al., 2015), as well as in the Provençal Basin (Kuhnt et al., 2011) and elsewhere (Menegatti et al., 1998; De Gea et al., 2003; Godet et al., 2014). This decline is a global environmental signal, resulting from a return to pre-OAE 1a positive excursion values (C8 segment of Menegatti et al., 1998; see also Bodin et al., 2015). Given that the C7 segment of Menegatti et al. (1998), i.e. the

maximum of the lower Aptian positive $\delta^{13}C$, is not recorded in Tiskatine, it is difficult to assess which exact part of the C8 segment of Menegatti et al. (1998) is represented by the decreasing trend observed in our record. As the here observed decreasing trend falls within the middle to upper *E. martini* Zone equivalent of SMAS, we correlate it to the upper part of the C8 segment (Menegatti et al., 1998).

The following $\delta^{13}C$ plateau in the Tiskatine section (around 0.7‰ for $\delta^{13}C_{carb}$ and around -26.5‰ for $\delta^{13}C_{org}$) can be correlated to the Ap10 and Ap11 segments of Herrle et al. (2004), spanning most of the *G. algerianus* / *H. trochoidea* foraminifera zone. This is in agreement with our biostratigraphic zonation. Lastly, the $\delta^{13}C$ positive excursion spanning the upper part of the Tiskatine section (excluding the diagenetically altered uppermost part of the $\delta^{13}C_{carb}$ record) and the plateau of $\delta^{13}C_{org}$ in the uppermost part of the section correlates well to the Ap12 and Ap 13 segments of Herrle et al. (2004), confirming the correlation between the *E. tiskatinensis* ammonite zone in Morocco and the *N. nolani* ammonite zone in SE France (Luber et al., 2017).

Finally, it should be noted that the $\delta^{13}C_{org}$ value of -27.27‰ for the **MTTK 160** sample at the base of the section is roughly similar to the $\delta^{13}C_{org}$ values observed within the lowermost *A. aschiltaensis* Zone. This is consistent with its earliest Aptian pre-OAE 1a age attribution (*P. dechauxi* Zone, which is the equivalent to the lower part of the *D. forbesi* Zone; Luber et al., 2017). Indeed, in SE France, similar $\delta^{13}C$ values have also been observed for these two intervals (Föllmi et al., 2006; Kuhnt et al., 2011; Bodin et al., 2013, 2015)

To summarize, the comparison between both carbonate and organic matter $\delta^{13}C$ records established in the Tiskatine section (Fig. 4.5) and the Vocontian Basin reference section (Fig. 4.12) confirms the biostratigraphic scheme established in Morocco, which is based on numerous ammonites and foraminifera findings. However, it also highlights the anomalous $\delta^{13}C_{carb}$ values of the lowermost and uppermost part of this section, that are likely due to diagenetic alteration in relationship with the underlying and overlying stratigraphic boundaries of the Tamzergout Fm. Hence, it is here advised to use $\delta^{13}C_{org}$ record for further chemostratigraphic studies within the EAB.

4.6.4 Palaeoenvironmental and sequence stratigraphic interpretation Tiskatine section

4.6.4.1 Palaeoenvironmental consideration by discipline

Ammonoids: Most samples of the Aptian to Lower Albian in the Tiskatine section contain a rich and diverse fauna of ammonoids, foraminifera and calcareous nannofossils. The ammonoid assemblages show a high level of variation in abundance and diversity throughout the succession. In the upper part of the Bouzergoun Fm., the lack of mesopelagic phylloceratids and lytoceratids and the abundance of the douvilleiceratid *Procheloniceras*, interpreted as a shallow nekton-benthic form (Reboulet et al., 2005), suggest a distal neritic setting (Frau et al., 2017a). The occurrence of phylloceratids and desmoceratids in bed **MTTK 161a** indicates a brief episode of open marine conditions at the top of the Bouzergoun Fm., even so, the fauna is still largely dominated by nekton-benthic forms such as *Epicheloniceras*. Nekton-benthic forms predominate throughout the Tamzergout Fm.

Three successive evolutionary phases can be distinguished:

Phase 1 (lower part of the Tamzergout Fm.) marked by the local evolution of *Epicheloniceras* towards the endemic "*E.*" *marocanus* suggests restricted conditions during most of the *C. tobleri* Zone.

Phase 2 (middle part of the Tamzergout Fm.) characterised by the abundance of the cosmopolitan *A. aschiltaensis* (Anthula) and *P.* gr. *ramososeptatum* indicates the onset of restored open marine connections between the EAB and the Mediterranean-Caucasian Tethys.

Phase 3 (upper part of the Tamzergout Fm.) marked by the high abundance and diversity of small-sized epipelagic forms (*Elsaisabellia*, *Protacanthoplites* and "*Hypacanthoplites*") combined with spot occurrence mesopelagic desmoceratids points out to the restoration of full open-marine conditions.

It should be noted that the rich and diverse assemblages of mixed epipelagic and mesopelagic forms of the *C. tobleri* Subzone and the *E. tiskatinensis* Subzone are typical Type 2 Horizons of Faunal Uniformity (**HUF**) as defined by Bulot (1993). According to this author, the record of such horizons is connected to sea level rise and flooding events.

Foraminifera: Fig. 4.4 shows the relative proportions of the three main types of foraminifera (agglutinating, calcareous benthic and planktonic). Although planktonic foraminifera comprise the dominant component of the assemblages (usually comprising 50% or more of the total numbers), benthic foraminifera are also abundant and diverse. These include calcareous rotalid species and agglutinating species. Calcareous miliolids are very rare.

Calcareous benthic foraminifera comprise between 20-50% of assemblages in the Tamzergout Fm. They are dominated by two genera – *Gavelinella* and *Lenticulina* which are recorded consistently and in (relative) abundance throughout. Other taxa such as *Valvulineria* and *Conorotalites* are more-or-less recorded consistently through the section but in much lower numbers.

The overall nature of the assemblage, with planktonic foraminifera forming at least 50% of the assemblage, together with the occurrence of taxa such as *Gavelinella* suggests deposition in fully open-marine, deep outer shelf environments, with water depths perhaps between 50 and 200 metres below sea level (Murray, 1991). Where planktonic foraminifera are especially common (>60% of foraminiferal assemblage), somewhat deeper water depths (upper slope) may be envisaged (i.e. up to approximately 500 metres) (Armstrong and Brasier, 2005).

The presence of common to abundant planktonic and calcareous benthic foraminifera in almost all Tamzergout Fm. samples indicate a substantively well-oxygenated water column with strong open oceanic influences in the surface waters, and well-oxygenated bottom waters during deposition of these units. Nevertheless, the local abundances of agglutinating foraminifera are noteworthy. Particularly significant are common or abundant occurrences of *Tritaxia dividens* (Grabert, 1959) (Fig. 4.17.5-6) in the upper part of the Tamzergout Fm. (sample **MTTK 185a** and above, Fig. 4.4). The agglutinated foraminifera as a whole – where proportionally significant (>10%) – are often suggestive of bottom waters with lower levels of dissolved oxygen (Koutsoukos et al., 1991). In these cases, however, the continued presence of a rich and diverse calcareous benthos would seem to suggest that other reasons may be required to explain the presence of high numbers of *T. dividens*. These could include periods of relatively higher nutrient levels but this is speculative. Another possibility is the periodic encroachment of relatively oxygen-poor waters up onto the (outer) shelf which allowed suitably adapted agglutinants to thrive, but not low enough to displace the established calcareous benthic inhabitants.

The presence at local levels (**MTTK 183b**, **MTTK 229-223** inclusive, **MTTK 233**, **MTTK 237** and **MTTK 247**) of high numbers of what appear to be heavily eroded and/or damaged specimens of the genus *Epistomina* (probably *E*. ex gr. *ornata*) may also be significant. Undamaged (and therefore presumably *in situ*) specimens have not been observed in any of the analysed samples. *Epistomina* is a genus associated with shallower shelf environments than that suggested by the overall background fauna within the Tamzergout Formation (see Sikora and Olsson, 1991 for examples from the Albian to Turonian of the Atlantic Margin) and the presence of eroded, obviously transported specimens may be indicative of episodes of shelf erosion and redeposition. It is uncertain if these are the results of autocyclic processes affecting the shelf (e.g. severe storms) or of allocyclic processes such as lowering of relative sea-level.

Calcareous nannofossils: Samples **MTTK 160** to **MTTK 161** are barren of nannofloras, probably a result of proximity to the coastline. Nannofossil abundance and diversity changes between samples **MTTK 162** and **MTTK 165b** indicate a rapid transgression and deepening. Samples **MTTK 162** and **MTTK 164** are dominated by the dissolution resistant form *Watznaueria barnesae* (Black, 1959). **MTTK 165b** exhibits a varied and diverse nannoflora. The rest of the upper Aptian section does not show major nannofossil variations except for minor shallowing events associated with marked reduction in nannofossil abundance and diversity noted at samples **MTTK 186**, **MTTK 220** to **MTTK 222** and **MTTK 247**. Sample **MTTK 249** exhibits a dramatic change in palaeoenvironmental conditions compared to the underlying Aptian sediments. Both neritic dominated holococcoliths and nannoconids are rarely recorded whilst a cold water incursion of *R. parvidentatum* is recorded. A regional palaeo-oceanographic change reflected in the nannofossil assemblage appears to have occurred at the Aptian-Albian boundary.

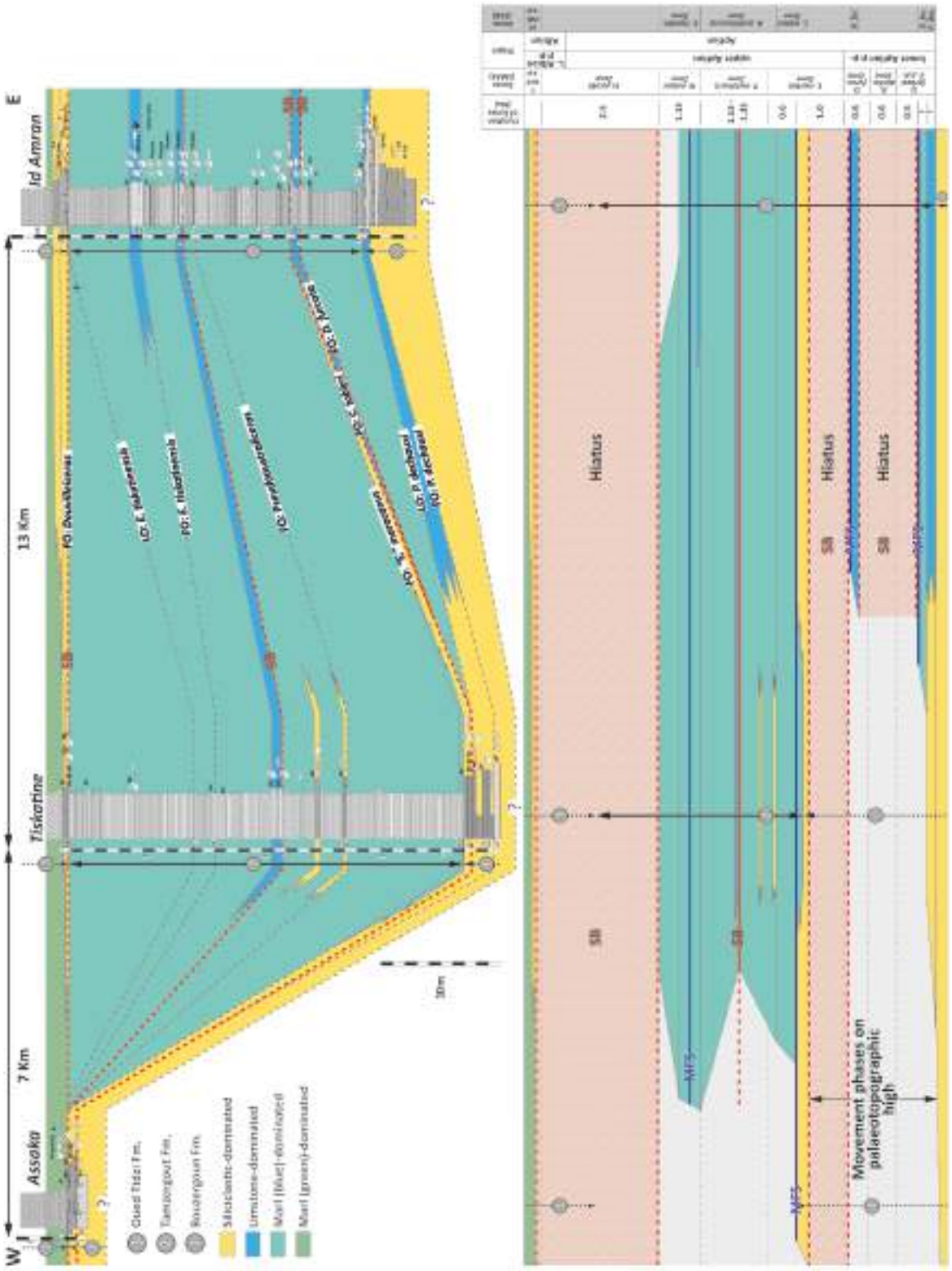

Figure 4.13: Sequence stratigraphic correlation of the Id Amran, Tiskatine and Assaka sections.

Correlation is based on ammonoid biostratigraphy with associated Wheeler Diagram. Data is referenced to the local ammonoid zonation scheme in the EAB of Luber et al. (2017), the Standard Mediterranean Ammonite Scale (SMAS) of Reboulet et al. (2011, 2014). Durations of ammonoid zones are derived from Dauphin, 2002. An A3 version is provided in appendix C6. A log of the Tiskatine section with key sequence stratigraphic surfaces is provided in appendix C14.

4.6.4.2 Sequence stratigraphic interpretation

The following depositional environments and key major and minor sequence stratigraphic intervals and surfaces, recognisable in the Tiskatine section (Fig. 4.4 and appendix C11 and C14), were identified by combining the different palaeontological disciplines and field observations. As previously noted the overall foraminiferal assemblages within the Tamzergout Fm. at Tiskatine suggest deposition in outer shelf environments. Against this background, some trends may be discernible in changing water depth, particularly as suggested by increasing and decreasing abundances of planktonic foraminifera (Fig. 4.4). This may aid recognition of, for example, flooding surfaces (Loutit et al, 1988; Armentrout, 1996).

- Shallow water conditions prevail in **MTTK 157** – **161a** and the interval is dominated by wave-influenced shoreface sedimentation transitioning into lower shoreface conditions (see App. C11). Interval **MTTK 157** – **161a** is barren in foraminifera and calcareous nannofossils.
- A 3rd order **sequence boundary** and **hiatus** around the lower / upper Aptian boundary, well constrained by ammonoid biostratigraphy (Luber et al. 2017) is recognized between **MTTK 160b** and **161a** (App. C14) and is interpreted as a surface of non-deposition in the vicinity of a topographic high experiencing multiple phases of base-level rise in the lower Aptian (see discussion below).
- A subsequent initial flooding surface (**ITS**) and condensation are recognised in **MTTK 161a** (App. C14).
- The rapid increase in water depth is suggested by first occurrence planktonic nannoflora in **MTTK 162** with the establishment of shelfal conditions indicated by an increase in foraminifera and calcareous nannofossil recovery, a lithological disconformity from sandstones to marls, and increased carbonate content in **MTTK 163.** This increase in base-level is recognized regionally and interpreted as a 3rd order **transgressive systems tract** (**TST**) starting in **MTTK 161a**.
- Between **MTTK 164** – **MTTK 232** percentage in planktonic foraminifera seldom fall below 50 % and therefore indicates water depths 50 – 200 m ranging the middle to outer shelf or even greater depth where they exceed 60 %.

- High relative abundance (65% - 81%) of planktonic foraminifera (notably *Hedbergella* spp.), a prominent increase in abundance and diversity of calcareous nannofossil from **MTTK 162** through **MTTK 165b** and increase in carbonate content suggest good open-marine conditions and are interpreted as a **lower upper Aptian maximum flooding surface** (**MFS**, see App. C14) at **MTTK 164/165** ("*E.*" *marocanus* Subzone).
- The interval from **MTTK 166** – **MTTK 191** is interpreted as multiple parasequences in third order **high stand systems tract (HST)**. This is supported by marked decrease in planktonic foraminiferal abundance (typically <50%) but variable (sample 180 contains 90% planktonic foraminifera) between **MTTK 166** – **183b**. Sample **MTTK 183b** contains common reworked *Epistomina* derived from shallow shelf environments.
- **MTTK 192** stands out in the field and has an erosive base. Further, it has higher siliciclastic content and is a barren bed for foraminifera but yields large ammonoids (*A. aschiltaensis*). Base **MTTK 192** is interpreted as a 3rd order **sequence boundary** and **MTTK 192 – MTTK 194** (*A*. *aschiltaensis* Zone, based on the occurrence of the nominate species above and below **MTTK 192**) as the associated low-stand deposits (**LST**). Further, heterogeneous infilling of the body chamber of the large *Pseudoaustraliceras* and abraded belemnites in **MTTK 192** point towards a poly-phased sedimentation.
- Top **MTTK 194** is interpreted as the **ITS**
- Foraminiferal assemblages are becoming richer than previously with *Tritaxia dividens* increasingly common and more diverse planktonic foraminifera (notably *Globigerinelloides* spp.) present to a maximum relative abundance around samples **MTTK 200** and **MTTK 201** (86% of assemblage). Rich and diverse ammonite assemblage between **MTTK 206** – **MTTK 213**, increased recovery of foraminifera and calcareous nannofossils between **MTTK 211** – **MTTK 215** suggest the presence of an **upper Aptian MFS** (App. C11) between **MTTK 206** – **MTTK 215** (*E*. *tiskatinensis* Subzone), bracketing a 3rd order transgressive systems tract between top **MTTK 194** towards this interval.
- **MTTK 216 to MTTK 247** is overall still rich in foraminifera, but the interval from **MTTK 232** to **247** is barren in ammonoids and a continuous decline of planktonic foraminifera, from 50% to <30%, is noted from bed **MTTK 233** onward. A further

reworking of shelfal *Epistomina* is particularly evident in **MTTK 223** – **MTTK 237** and likely derived from the shallow shelf. Calcareous nannofossils are still abundant in this interval with **MTTK 239** yielding the richest nannoflora of the whole section. Therefore, **MTTK 216** – **MTTK 247** is interpreted as a **HST**.

- Heralding clastic progradation is indicated by a marked reduction in diversity and abundance of calcareous nannofossils in bed **MTTK 247.** This may be an indication of the onset of a shallowing event which ultimately led to the development of a **sequence boundary** at the base of **MTTK 248** that is identified at the Tiskatine section (App. C14) but also more dramatically at DSDP boreholes 370 (Fig. 4.8) and 416A. This boundary possibly combines a 3rd and 2nd order sequence boundary. It is well constrained by ammonoids, foraminifera and calcareous nannofossils to occur between the "*Hypacanthoplites spp."* Subzone and the *M. chihaouiae* Zone and is therefore suspected of being close to the Aptian/Albian boundary.
- Further, bed **MTTK 247** shows a noteworthy increase in abundance of reworked *Epistomina* (the highest numbers recorded in any sample).

4.6.5 Local Palaeogeography – correlation Id Amran – Assaka transect

The transect from Id Amran to Assaka (Fig. 4.13, App. C6) is interpreted as a cross-section either toward the crest of a submerged fault block or toward a relative high (reduced accommodation) produced by an N-S oriented salt diapir. The following incremental tectonic movement phases are identified:

(1) *P. dechauxi* – lower *D. forbesi* Zone: Constrained by erosion of *P. dechauxi* – *C. tobleri* zones time-equivalent deposits in the distal Assaka section (erosional surface base **MTAS 121**) but preservation in Tiskatine (**MTTK 159** – **160b**) and Id Amran (**MTIA 86** – **MTIA 98**). In Id Amran preservation of the *D. forbesi* Zone time-equivalent deposits (**MTIA 98**) further constraints the timing of first movement phase.

(2) Lower *D. forbesi* – *D. furcata* Zone: Constrained by absence of the upper *D. forbesi* plus entire *Deshayesi* zones (OAE 1a-related time culmination) time-equivalent deposits and in Id Amran. *D. forbesi* and *D. furcata* zone age deposits are not recorded in Tiskatine and Assaka and form part of a composite surface including multiple unconformities (hiatus **MTTK 160b – MTTK 161a** and again erosional

surface base **MTAS 121**).

(3) *D. furcata – C. tobleri* Zone: Unconformity constrained by absence of upper *D. furcata* Zone age equivalent deposits in Id Amran

Lower Aptian tectonic movement phases (1) to (3) are expressed in the sedimentary record as disconformities, generally as surfaces of non-deposition with no or weak indication of erosion. In the Assaka section they are combined into the basal erosional surface of **MTAS 121** (App. C13). In Tiskatine they are combined into the interval top **MTTK 160b** – base **MTTK 161a** (App. C14).

Flooding within the *C. tobleri* Zone appears to be a regional event and followed by relative continuous deposition in the Tiskatine and Id Amran. The mid upper Aptian (base **MTTK 192** and **MTIA 135**) and basal Albian sequence boundaries (e.g. base **MTTK 248** and **MTIA 154**) (Figs. 4.4, 4.13, and App. C14) appear to be rather linked to relative sea level fall with differential erosion. Relating these potential sequence to published eustatic sea-level curves (e.g. Haq, 2014) is challenging given the uncertain age calibration of the Tiskatine section and needs further investigation, but the basal Albian sequence boundary is tentatively linked to KAp 7 *sensu* Haq, 2014.

Correlation of the sections allows recognition of an N – S orientated topographic high that has been active throughout the Aptian. Condensation that is apparent in the Assaka section had been previously mentioned by Peybernes et al. (2013) in the Tamri section and has further been observed in this study on the other side of the Cap Ghir Anticline in the Aghroud section.

In Assaka (Figs. 4.7, 4.13), close to the crest of the palaeotopographic high, local tectonic movement is interpreted to have caused partial erosion and reworking of the underlying stratigraphy (**MTAS 120**) and formation of localized depressions on the high. Reworked pebbles were deposited with allochthonous glauconite sandstone alongside faunal elements, including ammonites of the early late Aptian *C. tobleri* Zone. Multiple phases of reworking during the upper Aptian and basal Albian created relief on top the *C. tobleri* Zone (**MTAS 121/122**). These winnowed lenses are infilled with glauconite sand and fauna in dominantly phosphatic preservation (**MTAS 123**, App. C13). The <30 cm thick bed shows a complex assemblage of faunal elements, pointing to a poly-phased horizon and polyzonal infilling. Preserved ammonoid specimens mainly coincide with upper Aptian lowermost Albian flooding events in the basin. It is noteworthy that among the ammonoid

assemblage of **MTAS 123** open-marine fauna (*Hypophylloceras*, *Eotetragonites* and *Ephamulina*) are well represented. This suggests a localized high on the outer shelf, below storm wave base, open to the ocean in the west. The enrichment in glauconite and phosphate indicates very low sedimentation rates, further supporting this observation. Winnowing by wave-action and mixing of faunal elements with different ages in **MTAS 123** point towards a re-emerging into palaeo-water depth between the normal and storm wave base for the crest of the palaeotopographic high during this time. It is likely that several minor erosion and sedimentation events were removed and are not recorded or recorded in lenses elsewhere (App. C13). The process described above has also been observed by Gebhard (1982) and is used as an analogue here.

The transect from Id Amran to Assaka (Fig. 4.13) shows a clear trend from inner shelfal deposits towards an outer shelf environment on a palaeotopographic high. In Id Amran common bioturbation, moderate sedimentation rates, siliciclastic input and glauconite accumulation in the glauconite maximum zone are observed. In Assaka sedimentation rates are very low and laterally derived sediment still includes glauconitic material but fauna preservation is mainly phosphatic and deposition took place within phosphate maximum zone (Föllmi, 1990).

4.6.6 DSDP leg 41 borehole 370

The investigated upper Barremian to Lower Albian strata offshore (Fig. 4.8 and App. C2) have been deposited off the Mesozoic shelf on the basin floor. The coarse clastic intervals described above have been interpreted as calcareous turbidity currents (Meyer, 1978). Detailed descriptions of Meyer et al. (1978) show that most of the sand to pebble-sized material forms a mixed carbonate-clastic depositional system. Bioclastic material is mainly formed by skeletal and coated grains transported from the shallow shelf and detrital material comes from plutonic, volcanic and sedimentary onshore provenance terrains.

Based on the calcareous nannofossil data the boundary between the upper Barremian and lower Aptian is likely not preserved in the core of borehole 370 and either eroded away by the turbidity current in the upper part of core section 34-1 (872.85 – 873.26 m), or within the missing core gap above. The base of the turbidite at 873.26 m could correspond to a regional regressive phase recognized at the Barremian Aptian transition (KBa 5 *sensu* Haq, 2014) within the Bouzergoun Fm. onshore the EAB.

At DSDP borehole 370 the whole upper Aptian sequence has been eroded. The contact between the lowermost Aptian and Lower Albian sequence lies between 838.57 – 839.87 m. Onshore in the Essaouira Agadir basin the Aptian – Albian transition is marked by a regional erosive basal Albian unconformity and a distinct colour change from blue-grey marls of the Tamzergout Formation to green marls of the Oued Tidzi Formation (Fig. 4.8). This colour change is also observed in the core section 32-4 and falls within 838.57 – 839.87 m interval. Therefore, the hiatus and basal Albian unconformity is tentatively placed at the erosive surface below at 839.68 m, interpreted as a bypass surface, but could also fall at the base of the erosive turbidite at 839.87 m. The boundary is thought to correlate to the regional sequence boundary recognized onshore (Luber et al., 2017) and in borehole 370 appears to erode most of the lower Aptian and all of the upper Aptian strata. There is no indication for a time condensed interval suggesting non-deposition or concentration of the missing time interval. The interval 837.02 – 835.61 m within the Lower Albian is interpreted to represent a debris flow likely only effecting uppermost part of the Lower Albian sea floor because no contamination of older calcareous nannofossil specimen was detected.

At the adjacent DSDP Borehole 416A (approximately 5 Km West of borehole 370) the basal Albian unconformity is also recorded within core 6 (CC). Here again Lower Albian sediments yielding an influx of *R. parvidentatum*, abundant *R. achlyostaurion* and the presence of *P. columnata* rest directly with marked hiatus upon lowermost Aptian sediments yielding abundant *A. terebrodentarius*, common *C. margerelii* and common *Z. scutula*, again in the absence of nannoconids.

4.7 Conclusions

Combined high-resolution litho-, bio-, chemo- and sequence stratigraphic analysis from bed-by-bed sampling of a superbly exposed section at Tiskatine has allowed the first multi-disciplinary study for the Aptian of the NW African Atlantic margin (Figs. 4.4, 4.5). The results provide new information on ranges of foraminifera and calcareous nannofossil correlated with the local ammonoid zonation scheme for the EAB of Luber et al. (2017) and their wider correlation against type localities and species (e.g. SMAS of Reboulet et al., 2011, 2014). This study extends the growing global body of $\delta^{13}C$ data for the Lower Cretaceous against a high-resolution, biostratigraphically constrained section.

Additional sections have been analysed and reported to complement gaps in the stratigraphic record and highlight the impact of local depositional environments (Id Amran and Assaka sections, Fig. 4.6, 4.7). The study is also extended and correlated offshore, with a re-investigation of the calcareous nannofossil record of DSDP borehole 370.

The main conclusions of this study are:

Ammonoids:

- A diverse Aptian ammonoid fauna is documented from the previously unstudied Id Amran section (Fig. 4.6), including 14 genera and 20 species, correlated to the local ammonoid zonation scale of the EAB, and important specimen are fully illustrated.
- Two additional ammonoid faunas are recognized at Id Amran by comparison two the local EAB ammonoid scale of Luber et al. (2017) and correlated to the middle part of the *D. forbesi* and middle part of the *D. furcata* of the SMAS.
- A highly condensed upper Aptian to Lower Albian ammonoid collection of 12 genera and 18 species was made from the Assaka section (Fig. 4.7).

Foraminifera:

- A diverse fauna of planktonic and benthic foraminifera is recorded from the upper Aptian part of the Tiskatine section, including cosmopolitan genera and species.
- Based on the distribution of foraminifera at Tiskatine section, three widely used zones of the upper Aptian have been recognized: *G. ferreolensis* Zone*, G. algerianus* Zone and the *H. trochoidea – P. bejaouensis* Zone (Figs. 4.3, 4.4).
- This study suggests that the base of the *G. ferreolensis* Zone falls within the *E. martini* Zone and its top extends into the *P. melchioris* Zone, a modification of the correlations proposed by Ogg and Hinnov (2012).
- The occurrence of *P. cheniourensis* near the top of the Tamzergout Fm. gives further support to the absence of the "*H.*" *jacobi* Zone and supports a late Aptian age for the regional hiatus seen in the EAB**.** This observation is further supported by the carbon isotope record.

Calcareous Nannofossils:

- A diverse and abundant assemblage of upper Aptian calcareous nannofossils is identified that allows the recognition of 2 standard NC zones: NC7A Zone and NC8A Zone (Fig. 4.4).
- The two additional lower Aptian ammonite faunas (see above) recognised at Id Amran are supported by calcareous nannofossil associations.
- The local range of *Z. vanhintei* into the upper Aptian sediments extends the range of this form from its published LAD in the upper Aptian
- Calcareous nannofossil analysis of the uppermost Id Amran section provides a basal Albian age.
- Calcareous nannofossil analysis from the DSDP borehole 370 provide a latest Barremian age for core 34-1, below an uppermost Barremian to lowermost Aptian unconformity at 873.25 m (below mud line).
- Further, an earliest Aptian age (NC6) is provided for the lower half of core 32-4 and an Early Albian age (all NC8A) for core 32-3 to 31-4.
- The revised age dating of core 32-4 and 32-3 in DSDP borehole 370 (Fig. 4.8) indicates the presence of a basal Albian unconformity that can be correlated to a sequence boundary recognized onshore.

Onshore Sequence Stratigraphy and Palaeogeography:

- The following key sequence stratigraphic surfaces are identified in the transect between Id Amran and Assaka (Fig. 4.13): (*i*) a regional lower to upper Aptian (*D. furcata* Zone to *C. tobleri* Zone) third order sequence boundary, (*ii*) a regional maximum flooding surface in the lower *"E." marocanus* Subzone, (*iii*) a regional third order sequence boundary in the *A. aschiltaensis* Zone, (*iv*) a regional third order maximum flooding surface in *E. tiskatinensis* Subzone, (*v*) a regional sequence boundary at the base of the Oued Tidzi Fm, suspected as being close to the Aptian/Albian boundary in age.
- Three incremental tectonic movement phases are identified along a proposed N-S orientated palaeotopographic high with a crest in proximity of the modern coastline.

$\delta^{13}C$ Record:

- The $\delta^{13}C_{org}$ curve, as well as the $\delta^{13}C_{carb}$ curve (Fig. 4.5), can be correlated with the established curves of the Vocontian and Provençal Basin in SE France
- The C7 segment of the Menegatti et al. (1998) is absent at Tiskatine
- A clear decreasing $\delta^{13}C$ trend observed in the lower part of the Tiskatine section is linked to the upper C8 segment of Menegatti et al. (1998)
- A $\delta^{13}C$ plateau in the Tiskatine section can be correlated to the Ap10 and Ap11 segments of Herrle et al. (2004)
- A $\delta^{13}C$ positive excursion spanning the upper part of the Tiskatine section correlates well to the Ap12 and Ap 13 segments of Herrle et al. (2004)
- The $\delta^{13}C$ record established at Tiskatine further supports the biostratigraphic analysis by comparison to the Vocontian Basin (Fig. 4.12)

This study extends the global biostratigraphic and chemostratigraphic database for the Aptian in the Central Atlantic Margin, providing a high resolution well documented reference section. The results highlight existing discrepancies between the individual disciplines, which need urgent revision. The study advocates the advantage of developing multi-disciplinary local zonation schemes that greatly enhance regional application of individual stratigraphic methodologies. These regional schemes offer improvement the resolution of timing/ranges of global bio- and chemostratigraphic markers and their research and industrial application.

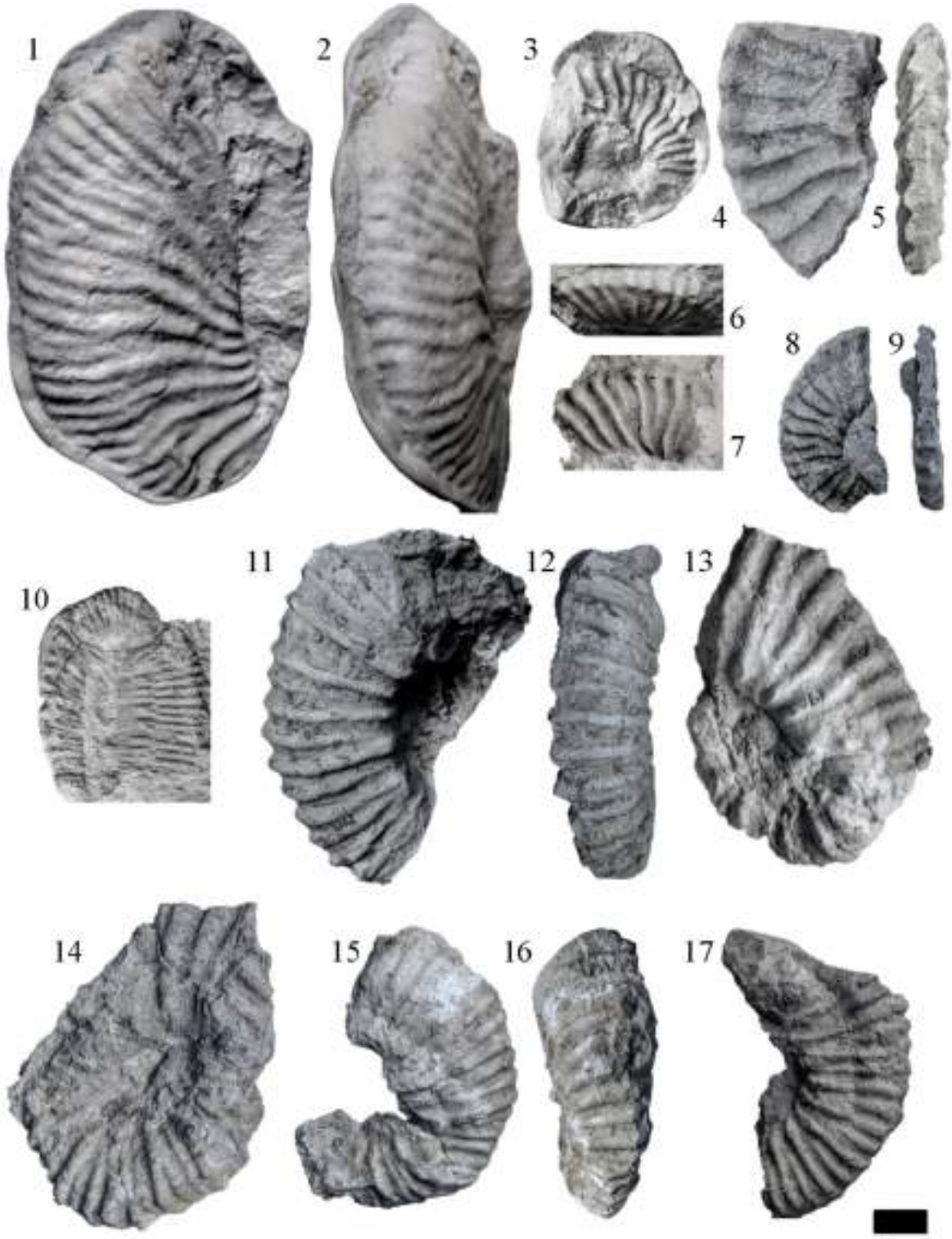

Figure 4.14: Ammonoid photographic plate of the Id Amran section.
(1-2) *Deshayesites* aff. *callidiscus* Casey, 1961a from bed **MTIA 98** ((Manch) LL. 16142); (3-9) *Dufrenoyia praedufrenoyi* Casey, 1964 from bed **MTIA 100** ((Manch) LL. 16144); (10) *Toxoceratoides rochi* Casey, 1961b from bed **MTIA 100** ((Manch) LL. 16145); (11-17) "*Procheloniceras*" sp. nov. from bed **MTIA 98** ((Manch) LL. 16143).

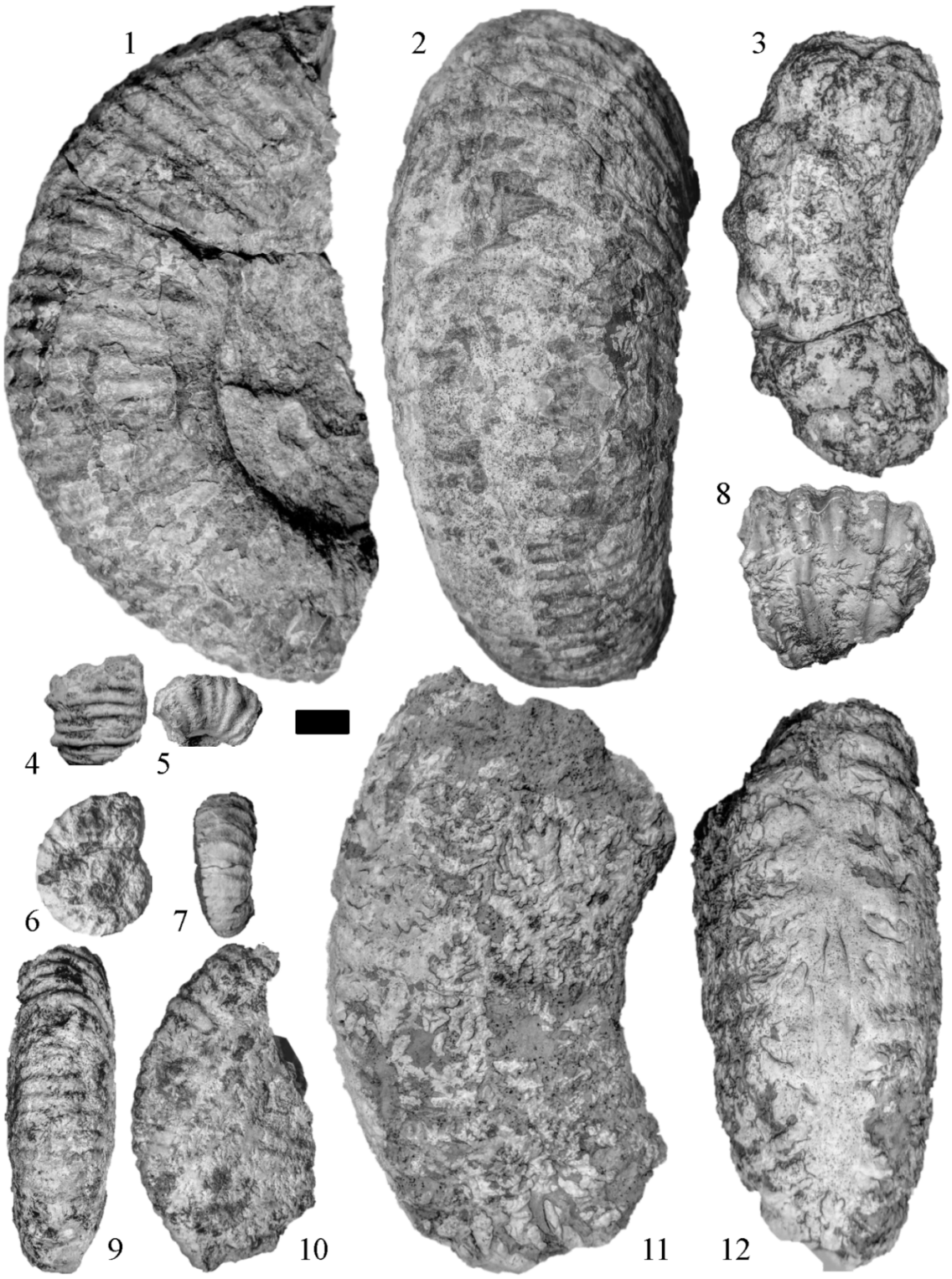

Figure 4.15: Ammonoid photographic plate of the Assaka section.
(1-2) *Epicheloniceras* gr. *waageni* (Anthula, 1900) – *tschernyschewi* (Sinzow, 1906) from bed **MTAS 122** ((Manch) LL. 16147); (3) *Pseudoaustraliceras* gr. *ramososeptatum* (Anthula, 1900) from bed **MTAS 123** ((Manch) LL. 16149); (4-5) *Epicheloniceras* gr. *gracile* Casey, 1961a from bed **MTAS 121** ((Manch) LL. 16146); (6-7) *Epicheloniceras* gr. *subbuxtorfi* – *paucinodum* (Burckhardt. 1925) from Bed **MTAS 122** ((Manch) LL. 16148); (8) "*Hypacanthoplites*" cf. *paucicostatus* (Breistroffer *in* Dubourdieu, 1953) from bed **MTAS 123** ((Manch) LL. 16150); (9-10) *Mellegueiceras* cf. *chihaouiae* Latil, 2011 from bed **MTAS 123** ((Manch) LL. 16151); (11-12) *Pseudoaustraliceras* gr. *ramososeptatum* (Anthula, 1900) from bed **MTAS 123** ((Manch) LL. 16152).

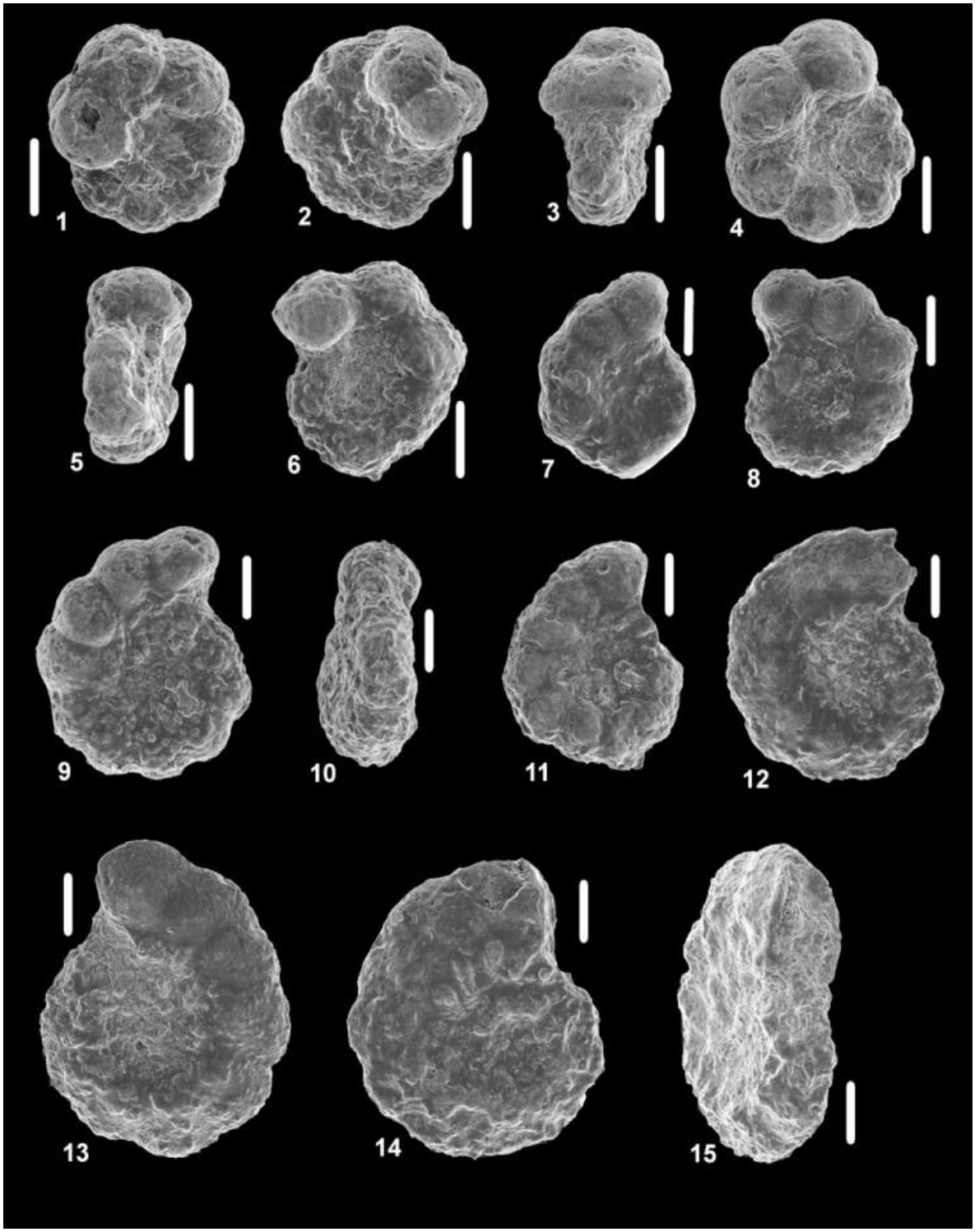

Figure 4.16: Plate 1: Scanning electron microscope images of selected planktonic foraminifera from the Tiskatine section.
All scale bars = 0.1mm. (1-3) *Globigerinelloides barri* (Bolli, Loeblich and Tappan, 1957) from **MTTK 197**; (4-6) *Globigerinelloides ferreolensis* (Bolli, Loeblich and Tappan, 1957) from **MTTK 197**; (7-8) *Globigerinelloides ferreolensis - G. algerianus* transitional form from **MTTK 185a**; (9-11) *Globigerinelloides algerianus* Cushman and Ten Dam, 1948 from **MTTK 197**; (12-13) *Pseudoplanomalina cheniourensis* (Sigal, 1952) from **MTTK 217**; (14-15) *Pseudoplanomalina cheniourensis* (Sigal, 1952) from **MTTK 237.**

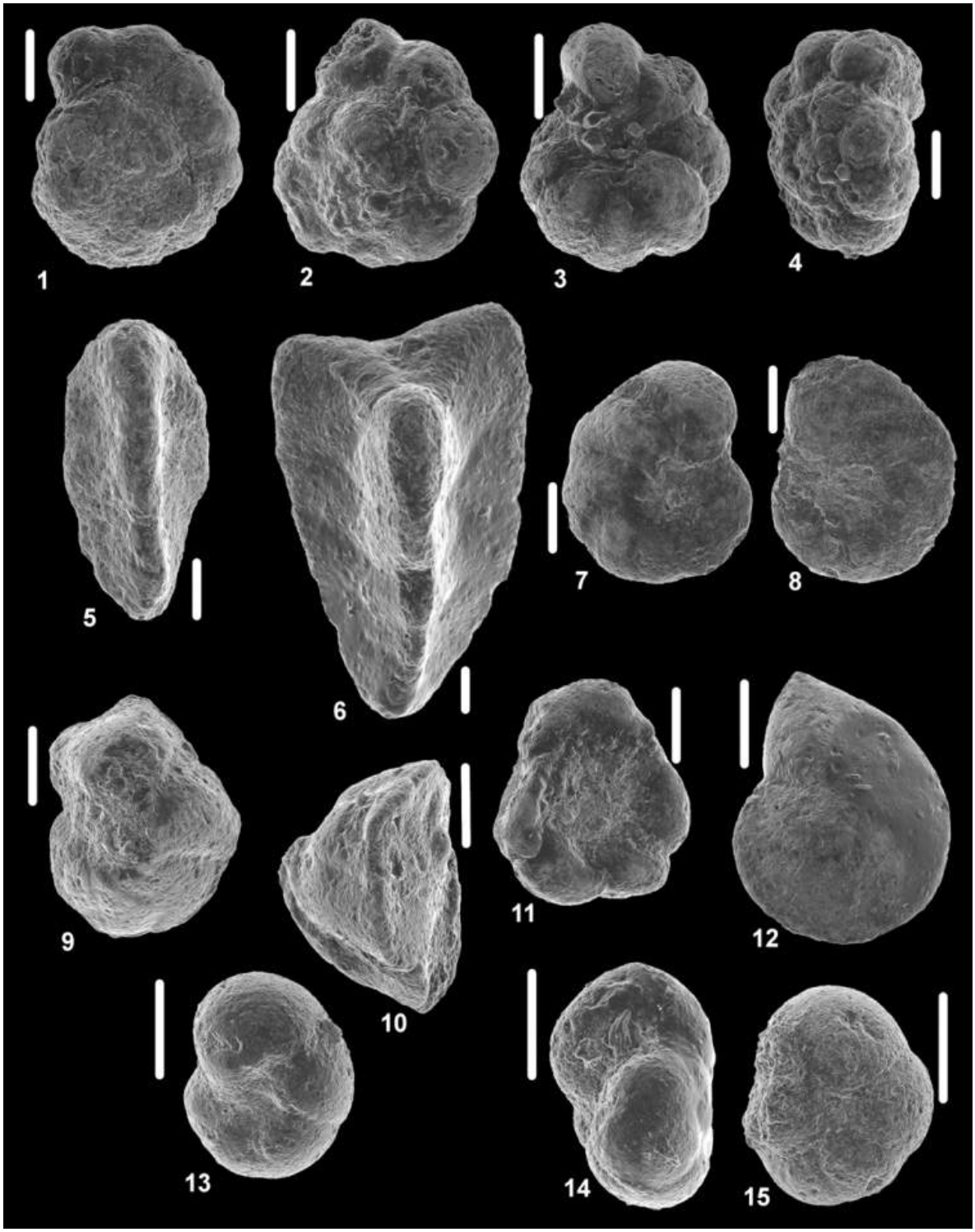

Figure 4.17: Plate 2: Scanning electron microscope images of selected planktonic foraminifera from the Tiskatine section.
All scale bars = 0.1mm. (1) ?*Paraticinella bejaouaensis* (Sigal, 1966) from **MTTK 247**; (2-4) *Hedbergella trocoidea* (Gandolfi, 1942) from **MTTK 235**; (5-6) *Tritaxia dividens* (Grabert, 1959), smaller morphotype, from **MTTK 227**; (7-8) *Gavelinella* cf. *barremiana* Bettenstaedt, 1952 from **MTTK 221**; (9-11) *Conorotalites aptiensis* (Bettenstaedt, 1952) from **MTTK 219**; (12) *Lenticulina muensteri* (Roemer, 1839) from **MTTK 215**; (13-15) *Valvulineria gracillima* Ten Dam, 1947 from **MTTK 227.**

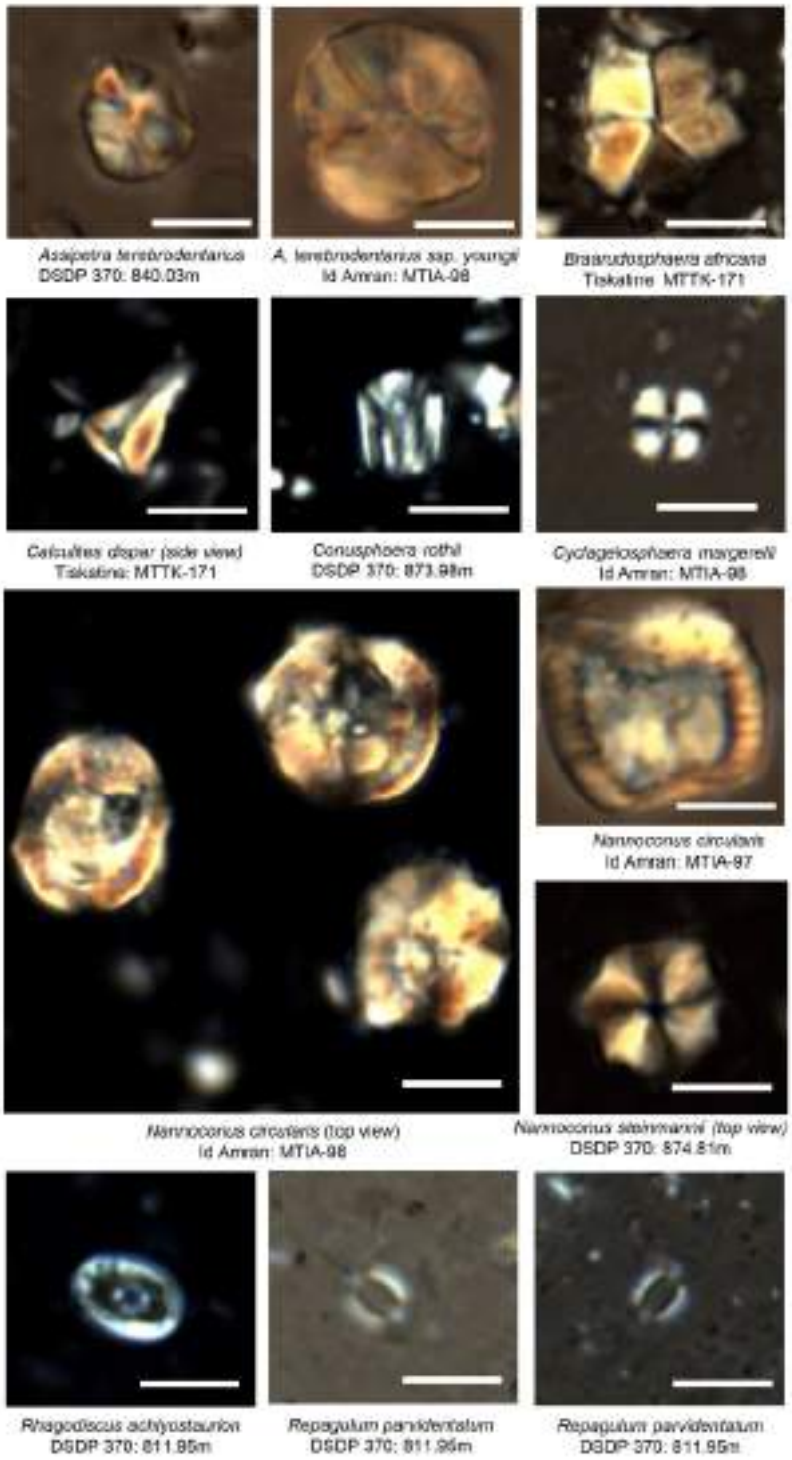

Figure 4.18: Calcareous nannofossil photographic plate.
Key specimen from the Tiskatine and Id Amran onshore sections and DSDP borehole 370. Scale bar in all photos is 5µm.

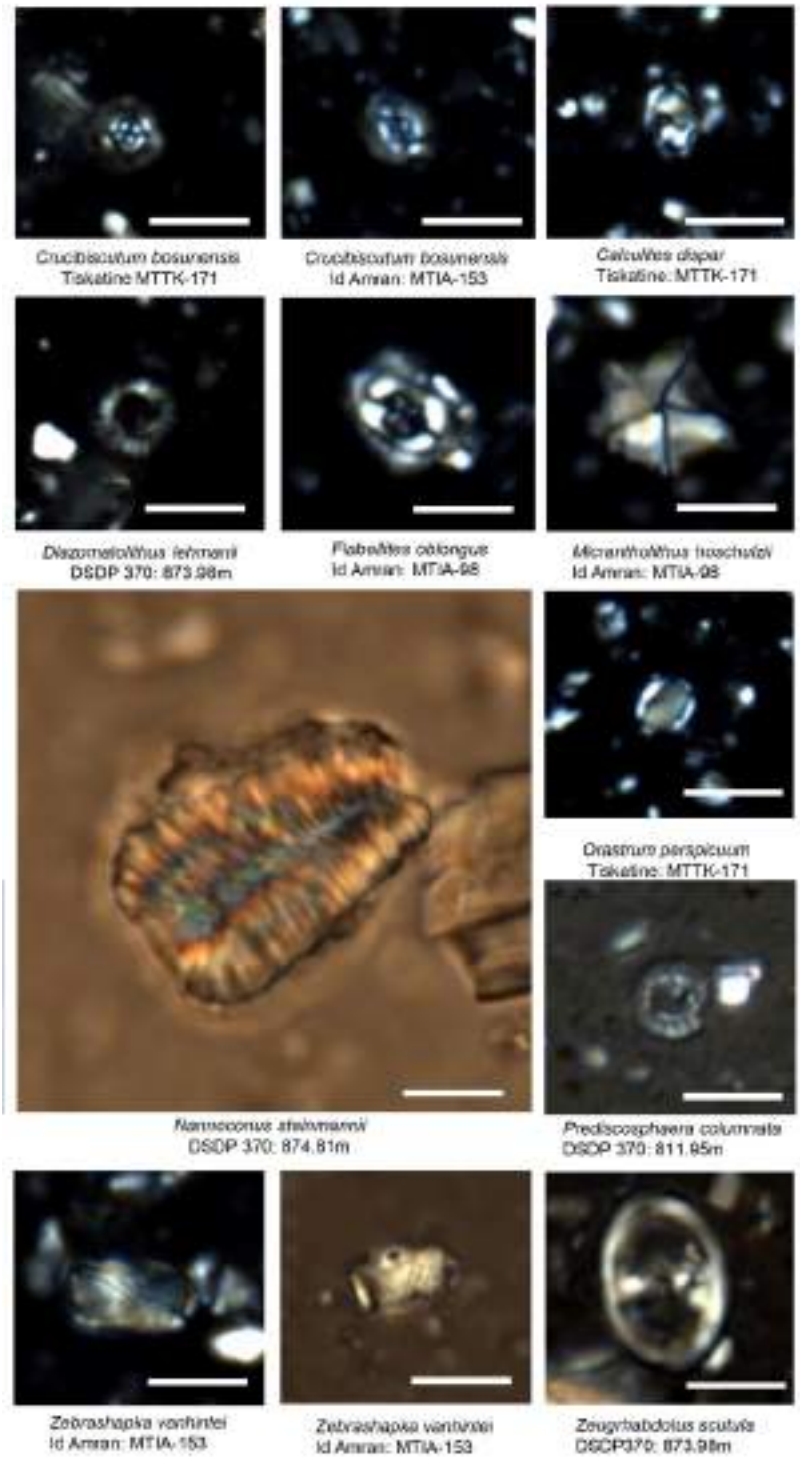

Figure 4.18 (continued): Calcareous nannofossil photographic plate.
Key specimen from the Tiskatine and Id Amran onshore sections and DSDP borehole 370.
Scale bar in all photos is 5µm.

CHAPTER 5: TECTONIC CONTROL ON THE DEVELOPMENT OF FORCED REGRESSIVE SYSTEMS ALONG A PASSIVE CONTINENTAL MARGIN.

This chapter is pending submission to Basin Research.

Authors: Luber, T.L., Redfern, J., Bulot, L. G., Bertotti, G. Charton, R.

Keywords: Forced Regression, Passive Margins, Integrated Stratigraphy, Cretaceous

5.1 Abstract

This study examines the role of post-rift tectonics in controlling accommodation and sediment routing in passive continental margins. We present an integrated high-resolution sedimentological, biostratigraphic, structural, and sequence stratigraphic assessment of a major regressive phase during the late Barremian to early Aptian along the passive Atlantic margin. Focus area of the study is the Essaouira-Agadir Basin (EAB) of Morocco

Twenty sections in the Bouzergoun Fm. have been characterised by high-resolution sedimentary logging and biostratigraphic analysis. The late Barremian to early Aptian section is dominated by shelfal mudstones interrupted by coarse clastic intervals, interpreted as regressive events. Abundant biostratigraphic markers allow high resolution correlation that shows shoreline progradation of at least 40 kilometres during the latest Barremian to Aptian.

Long-term tectonic exhumation of the provenance domains is identified from Low-T geochronology, interpreted to be a key driver in controlling sediment flux and shoreline progradation. Subsequent eustatic sea-level fall amplified the signal and led to rapid relative sea-level fall and progradation of the shoreline to the shelf edge. This is interpreted as a forced regression. During this maximum regression, the shelf became emerged and at least two west to southwest trending incised valleys have been identified.

Local tectonics also had a control on topography, with stratigraphic thinning and condensation recording east-west trending palaeohighs within the coastal plain. These are either fault or salt diaper related and form small-scale drainage divides that controlled sediment dispersal and acted as local sediment sources. North–south orientated palaeohighs along the basin margin, linked to pre-existing syn-rift faulted structures, also controlled delivery of coarse clastics, with preferential sediment routing through relays zones into the deep basin.

The results document the importance of tectonics at both large and small scale in controlling sediment delivery, routing and accommodation in passive margins.

5.2 Introduction

The Mesozoic sedimentary basins of Morocco form a key stratigraphic archive for understanding the interplay between eustasy, regional and local tectonics, and climate controls on sediment input and accommodation. This study examines the eastern portion of the Central Atlantic Margin (CAM) in the Essaouira-Agadir Basin (EAB) that contains the most expanded onshore Lower Cretaceous succession along the NW African Atlantic Margin. The Lower Cretaceous post-rift succession is dominated by shelfal mudstones with abundant biostratigraphic markers (Rey et al. 1988). The extensive mudstone succession is interrupted by two key coarse clastic regressive events, one during the early Hauterivian and one during the late Barremian to earliest Aptian. During the latter the shelf became exposed and incised valleys formed (Nouidar and Chellai, 2001). A detailed regional sequence stratigraphic interpretation of the interval has so far been lacking, studies carried out, however, indicate that this regressive sequence is linked to a forced regression.

In this paper, we examine the controls on the development of these regressive deposits along an extensive gently-dipping passive margin shelf. Integrated high-resolution biostratigraphic and sedimentological analysis have been carried out and detailed correlations allow the development of a sequence stratigraphic model and sequential palaeogeographic models. The data generated are examined to assess the relative controls of climate, eustasy and tectonics.

Recent tectonic studies indicate km-scale vertical movements of provenance areas, and the scale and timing of the regressive event are evaluated in relation to published eustatic curves to assess the importance of post-rift vertical tectonic movements and their link to the development of coarse clastic succession along passive margins.

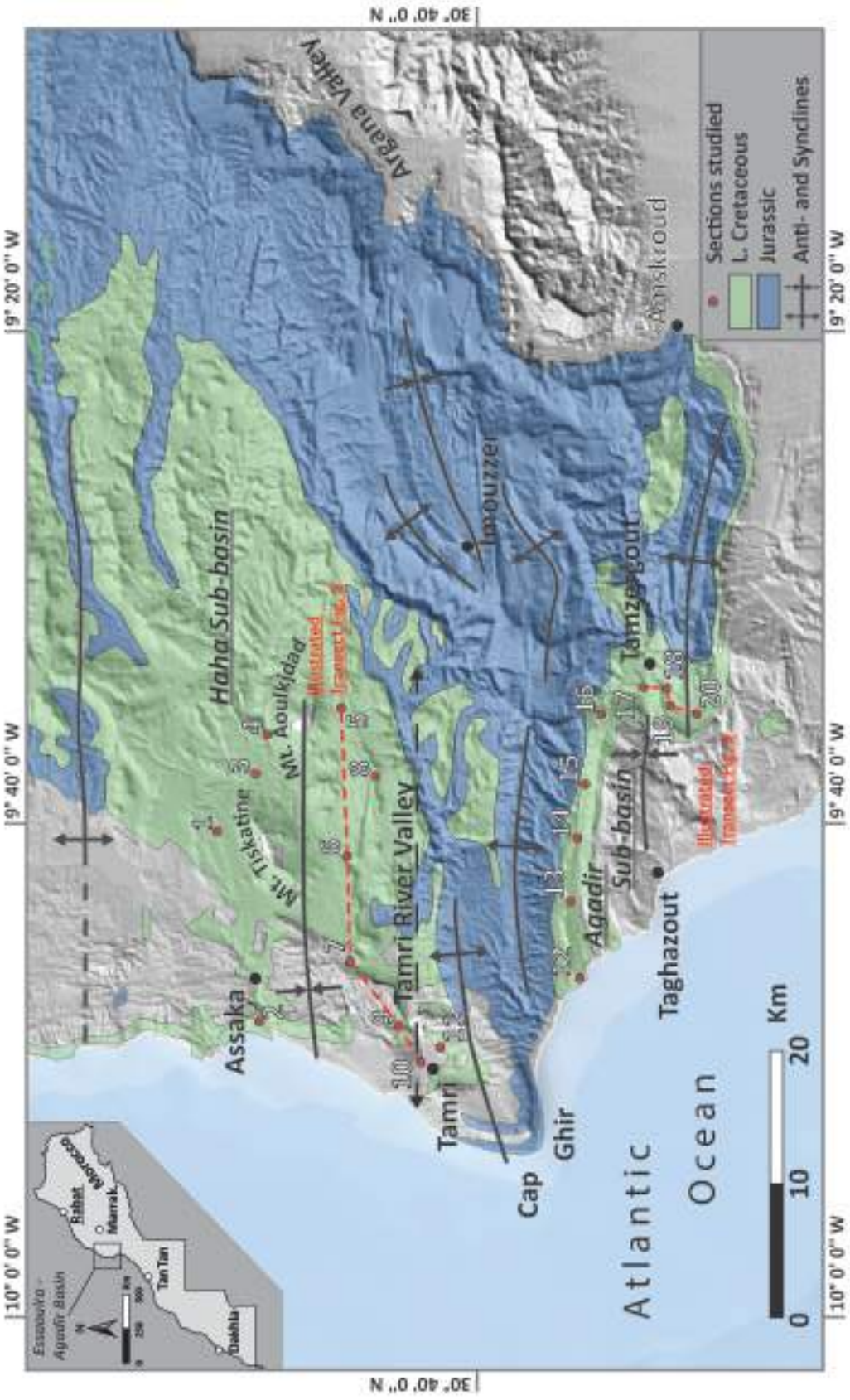

Figure 5.1: Overview map of the study area.
Inset: Location map of Morocco **Main:** Digital elevation model of the Haha and Agadir sub-basins within the Essaouira-Agadir Basin (EAB) overlain by a sub-crop of the geological map showing Lower Cretaceous and Jurassic outcrops and main anticlines and synclines. Sections studied are listed in table 5.1. For detailed maps see appendix C15 and C16.

Table 5.1: Studied locations and their geographic coordinates in decimal degrees. Numerations follow the labels in Fig. 5.1.

Location	*Lat./Long.*	*Location*	*Lat./Long.*
Tiskatine North (1)	30.843396° / -9.671297°	Tamri South (11)	30.691054° / -9.820617°
Assaka (2)	30.814370° / -9.796262°	Aghroud (12)	30.596237° / -9.772992°
Ilmer Ichemerarn (3)	30.843396° / -9.671297°	Addar (13)	30.602799° / -9.719271°
Aziar North (4)	30.807301° / -9.605719°	Adenz (14)	30.597151° / -9.675501°
Aziar South (5)	30.760975° / -9.589397°	Aouerga (15)	30.593486° / -9.642455°
Barrage (6)	30.753050° / -9.756090°	East of Aouerga (16)	30.582605° / -9.592904°
Akerkaou (7)	30.754941° / -9.687529°	Inrarne (17)	30.553390° / -9.573838°
Tinkert (8)	30.735477° / -9.633326°	Fossil Shop Road Cut (18)	30.538927° / -9.577312°
Mahmout (9)	30.720219° / -9.802239°	Alma East (19)	30.537621° / -9.586450°
Tamri Cliff (10)	30.705638° / -9.827041°	Alma (20)	30.518663° / -9.593786°

5.2.1 Geological setting

The study is located in the Essaouira-Agadir Basin (EAB). During the Lower Cretaceous, the EAB was limited to the east by the Massif Ancien de Marrakech, to the west by the Atlantic Ocean, to the north by the Jebilet and the Meseta and to the south by the Souss Basin and the Anti-Atlas (Wurster & Stets, 1982). Three sub-basins can be identified, namely the Essaouira, Haha and Agadir sub-basins. The Essaouira sub-basin lies to the north of the study area, shown in figure 5.1. This study focuses on the Haha and Agadir sub-basins in the west-central and southern part of the EAB, (Fig. 5.1). Detailed location maps of the Agadir sub-basin and the Haha sub-basin with studied sections are provided in appendix C15 and C16, respectively.

During the Lower Cretaceous, the EAB is interpreted to have been located in a tropical-equatorial climate belt (Peybernes et al. 2013) with dominantly arid climatic conditions (Daoudi & Deconinck, 1994; Pletsch et al., 1996).

The Lower Cretaceous records a change in depositional environment from the carbonate-dominated facies of the Jurassic to a clastic dominated sequence. Carbonate platform deposition prevailed into the lower Valanginian (Rey et al., 1988; Ettachfini, 1998), when subsequent flooding led to the development of the Atlas Gulf (Behrens et al., 1978), a broad, funnel-shaped embayment opening out to the west into the proto-Atlantic. Sedimentation in the Gulf was dominated by mudstones and thin interbedded limestones deposited below wave-base. Only during major regressive phases did the shoreline shift close to or beyond the position of the modern coastline (Ambroggi, 1963; Wiedmann et al., 1978, 1982; Behrens et al, 1978, 1982; Butt, 1982, Rey 1988).

Two important regressive phases in the Lower Cretaceous of the EAB were first recognised by Ambroggi (1963) and Behrens et al. (1978). The first is assigned to the lower Hauterivian and described as a regressive package thinning towards the basin, with the palaeocoastline being located inland of the modern coastline (Behrens et al. 1978). The second phase and focus of this study, the Bouzergoun Fm., was initially assigned to the lower Aptian by Ambroggi (1963), Behrens et al. (1978) and Bergner (1982), but recent high-resolution biostratigraphic investigation (Company et al., 2008; findings of this study) revised the dating, giving an upper Barremian to lowermost Aptian age. The Aptian regressive deposits thicken towards the modern coastline and down-cut into the underlying Lower Cretaceous strata.

A number of sedimentological/stratigraphic studies have been undertaken on the upper Barremian to Aptian deposits (Witam et al., 1993; Witam, 1998; Nouidar and Chellaï, 2001, 2002). Of these the most noteworthy is the work of Nouidar and Chellaï (2001), that recognized the development of an incised valley and its fill**,** and Nouidar and Chellaï (2002) that provides a description of the upper Barremian delta complex that outcrops the Tamri River Valley (Fig. 5.1).

Figure 5.2: Generalised lithostratigraphy of the upper Hauterivian to Lower Albian strata in the west-central part of the EAB.
Previous work by Witam (1998) (re-interpreted), Duffaud et al. (1966), Rey (1988) and Nouidar and Chellaï (2001) against the nomenclature and ranges used in this study. Important occurrences of key ammonoid specimen based on Company et al. (2008) and Luber et al. (2017). Main depositional environments and key sequence stratigraphic surfaces used throughout this chapter are illustrated. The legend displayed here also applies to following figures.

5.2.2 Stratigraphic framework

This study follows a modified version of the nomenclature suggested by Duffaud et al. (1966), which best applies to the west-central part of the EAB (Fig. 5.2). The main focus of this study is the Bouzergoun Fm. described below. For a description of the underlying Taboulouart Fm. the reader is referred to Company et al. (2008) and for the Tamzergout Fm. to the synthesis in Luber et al. (2017).

5.2.2.1 Bouzergoun Formation

Originally introduced by Duffaud et al. (1966) the Bouzergoun Fm. is composed of sandstones and red mudstones. Rey et al. (1986a, 1988), modified the formation to include marginal-marine deposits made of sands, varicoloured clays, dolomites and bioclastic-rich limestones with large cross-stratification. Throughout the basin, the formation is topped by a major disconformity and change to marls and limestones of the Tamzergout Formation.

Witam (1998) introduced three new formations for the west-central part of the EAB (Haha sub-basin). Company et al. (2008) highlighted that the misidentification of lower Barremian ammonoids as upper Barremian ammonoids might have led to the introduction of the Imsouane Formation as the equivalent of the Bouzergoun Fm. in the west-central part of the EAB (Haha sub-basin). This is supported by our own findings. Consequently, the Imsouane Fm. is merely the equivalent of the upper part of the Taboulouart Fm. A re-interpreted correlation of Witam (1998) is illustrated in Fig. 5.2. A detailed description in introduction of mappable members is outlined below.

5.3 Methodology

Twenty sections (Fig. 5.1, Table 5.1, and App. C15/16) covering the Bouzergoun Fm. have been characterised by high-resolution sedimentary logging and biostratigraphic analysis. Stratigraphic logs of the sections studied are illustrated in appendix B. Lithofacies description is based on field and microscopic observation (Table 5.2). Depositional environment interpretation is based on a combination of lithofacies grouped into facies

associations (Table 5.3), fossil content, and large-scale geometries through depositional profiles. To further support observations and substantiate hypotheses made on composition of sandstones in the fluvial depositional environment (FA-6), scanning electron microscope and coupled QEMSCAN analysis have been performed for selected samples (Fig. 5.4). Additional information comes from the supporting panoramic panels. Sections in the Haha sub-basin of the EAB north of the Cap Ghir anticline form two dip lines (Azziar South – Tamri and Azziar North – Assaka) respective to depositional trend. South of the Gap Ghir anticline in the Agadir sub-basin a transect from East of Aouerga to Aghroud is oblique to depositional trend and a shorter transect inland from Alma to Inrarne forms a strike line (all Fig. 5.1).

5.3.1 Lithofacies and lithofacies associations

Fifteen lithofacies have been recognized in Members 1 to 3 of the Bouzergoun Fm. (Table 5.2, App. C17 to C19). These lithofacies are grouped into seven lithofacies associations (Table 5.3). Lithofacies were defined by depositional process derived from composition, sedimentary structures and thin section petrography. Lithofacies associations (Table 5.3) are interpreted as: (1) Foreshore to upper shoreface, (2) Lower shoreface to offshore transition, (3) Offshore, (4) Terminal distributary channels and mouth bars, (5) Prodelta, (6) Fluvial trunk channel deposits, and (7) Floodplain, levee and crevasse splay deposits. Bioturbation index ranges from 1 to 5, very rare to very abundant (Table 5.3).

FA-1 within Member 3 of the Bouzergoun Fm. is dominated by a mixed carbonate-clastic system, while most other lithofacies are dominated by siliciclastics, although the coarse fraction of the fluvial deposits often includes cannibalised Cretaceous or Jurassic carbonate material as sedimentary intraclasts.

5.3.2 Mappable lithostratigraphic members

In this study, we introduce a threefold subdivision of the Bouzergoun Fm., and formally define three members. Individual members are annotated in photographic panels (Fig. 5.5 to 5.7 and App. C17 to C19).

Company et al. (2008) identified the basal bounding surface of the Bouzergoun Fm. as a regional erosive unconformity that cuts differentially into underlying strata of the uppermost Taboulouart Fm, confirmed by our observations. **Member 1** is composed of a thick succession of dark green-coloured dm- to m-sized calcareous mudstones and siltstone successions with minor sandstones in the west-central part of the EAB. Sandstone beds are cm- to dm-sized, massive or exhibit low-angle cross stratification. Mudstones and sandstones are almost free of macrofossil other than common plant debris, coal fragments and minor bivalve shell fragments. Microfossil analysis has revealed common echinoid fragments, radiolaria, gastropods, bivalves and agglutinating and benthic foraminifera. Bioturbation is common and composed mainly of *ophiomorpha* and minor *skolithos* ichnotaxa. Member 1 is truncated at the top by a regional erosive unconformity, well observed in the Assaka and Mahmout sections. Member 1 has a maximum observed thickness of 45 meters.

Member 2 is bound at the base by a sharp, erosional unconformity and is composed of coarsening and thickening-upward succession of sandstones. It includes minor bivalve- and gastropod-rich grainstones and rudstones (Fig. 5.2). Sandstones can also be rich in macrofossils, often dominated by bivalves. Sandstones at the base are interbedded with mudstones and become amalgamated to the top. They often exhibit well-developed low-angle cross-stratification, including hummocky cross-stratification, and towards the top trough cross-stratification becomes dominant. Laterally discontinuous, but observed in almost all outcrops, in-situ soft-sediment deformation is abundant in this upper part. In all sections, this succession is either incised or eroded by down cutting surfaces representing a regional unconformity. Erosional channel and valley features are commonly infilled by sandstones, conglomerates and macro fossil-free green or red-green interbedded mudstones intercalated with sandstones. These are the “Marnes lie-de-vin” of Ambroggi (1963) and “marnes rouges” of Duffaud et al. (1966). Member 2 is marked at the top by a regional sharp erosional disconformity. Member 2 has a maximum observed thickness of 40 meters.

Member 3: The base of Member 3 is defined by a regional erosional unconformity. The uppermost part of the formation is sharp-based and includes sandstones, sandy limestones and mudstone interbeds bearing marine fauna (bivalves, ammonoids, belemnites, brachiopods and gastropods), sometimes with pyritic, glauconitic or phosphatic preservation. Particularly massive oyster rudstones with a bivalve grainstone

matrix are common in the upper part of Member 3. The top of the Bouzergoun Fm. and, therefore, Member 3 is highly diachronous (see discussion below) and marked by the change to interbedded grey-blue limestones and marls of the Tamzergout Fm. Member 3 has a maximum observed thickness of 10 meters.

The Bouzergoun Fm. reaches a maximum observed thickness of 84 metres in the Assaka section. Company et al. (2008) and Luber et al. (2017) showed that the basal erosive unconformity of the Bouzergoun Fm. cuts into lower upper Barremian strata (early to middle part of the *G. sartousiana* Zone). The top of the Bouzergoun Fm. is diachronous (Luber et al., 2017) and ranges in age from early to early late Aptian (base of the *P. dechauxi* to lower part of the *C. tobleri* zones).

Table 5.2: Proposed lithofacies sorted by grain size and assigned by process of deposition.

	Lithofacies and Code		Reference Sketch	Description	Process Interpretation
>Gravel-sized Lithofacies (G)	Gcs	Clast-supported Conglomerate		Pebble- to cobble-sized clasts, poorly- to moderately-sorted, typically structureless or inversely-graded, size: dm - m	Rapid deposition from high concentration flow, **mixed fluvial lag deposits and debrites**
	Gms	Matrix-supported Conglomerate		Pebble- to cobble-sized clasts, poorly sorted, normal- to inverse-grading, sand- to clay- sized matrix, scale: dm - m	High yield strength, cohesive flow, **debrites**
	Gt	Conglomerate, cross-stratified		Pebble- to cobble-sized, moderately-sorted, normal grading, trough cross-bedding, size: dm - m	Bedload transport during sustained flow, dune/bar migration, **minor fluvial channel fill through**
	Grf	Rudstone/Floatstone		>10% of grains are >2mm, clast (>2mm)-supported (Rudstone) or matrix-supported (Floatstone), moderate- to very poor-sorting, structureless to cross-bedded, low species diversity, common detrital clasts, scale: dm - m	Reworking of bioclastic material by high-energy storm wave-dominated processes, **along shore migration of subaqueous dunes**
Sand-sized Lithofacies (S)	Sl	Low-angle cross-stratification, hummocky and swaley cross-stratification		Very fine- to fine-grained, very well- to well-sorted, cross-laminated to cross-bedded, in places forming hummocks, rare clasts, scale: cm - m	High-energy oscillatory flow, deposition during waning flow stage of **storm events** and broad bedload sheets during **dune migration** in upper flow regime
	Sh	Horizontal bedding/ lamination		Very fine- to medium-grained, very well- to moderately-sorted, laminated to bedded, scale: cm - m	Planar beds of upper flow regime, deposit during **storm events** or **crevasse splays**
	Sm	Massive		Very fine- to medium-grained, very well- to moderately-sorted, structureless to poorly-graded, often strongly bioturbated, Scale: cm - m	Rapid waning of **flows** in various environments and **destratification** by bioturbation
	St	Trough cross-bedded		Fine- to coarse-grained, well- to moderately-sorted, bedded, common clasts, scale: cm - m	Bedload transport in lower flow regime, three-dimens. **dune migration in various environments**
	Sw	Wave ripple-lamination		Very fine- to fine-grained, very well- to well-sorted, laminated, symmetrical ripples, Scale: mm - cm	Deposition through oscillatory motion in lower flow regime, **ripple migration in various environments**
	Sr	Current ripple lamination		Very fine- to fine-grained, very well- to well-sorted, laminated, asymmetrical ripples and climbing ripple, scale: mm - cm	Low-energy, unidirectional and combined flow, **ripples and climbing ripples** (high sed. rates, rapid deposition)
	Sg	Grainstone		>10% Allochems, grain-supported, well- to poorly-sorted, common detrital input, bedded, massive to cross-bedded, scale: cm - m	Reworking of bioclastic material by moderate to high-energy wave-dominated processes, **migration of subaqueous ripples and dunes**
Mud-sized Lithofacies (F)	Fm	Massive mudstones		Clay- to silt-sized, very well- to well-sorted, massive, common bioturbation and rooted horizons, rare mud cracks, scale: mm - m	Low-energy suspension fall-out, in **standing water, floodplain and channel abandonment**
	Fl	Horizontally-laminated mudstones		Clay- to silt-sized, well- to poorly-sorted, laminated, small sandstone interbeds and ripples, scale: mm - m	Suspension fall-out, **overbank deposits and crevasse splays**
	Fmc	Massive calc. mudstones (Micrite and Marls)		Clay- to silt-sized, very well- to well-sorted, massive, common bioturbation, scale: mm - m	Suspension fall-out, marine environment, **shelfal pelagic sedimentation**
	Flc	Horizontally-laminated calc. mudstone (Micrites and Marls)		Clay- to silt-sized, well- to poorly-sorted, laminated, small sandstone interbeds and ripples, scale: mm - m	Suspension fall-out with occasional sand-sized siliciclastic input, **shelfal mixed pelagic and gravity flow deposits**

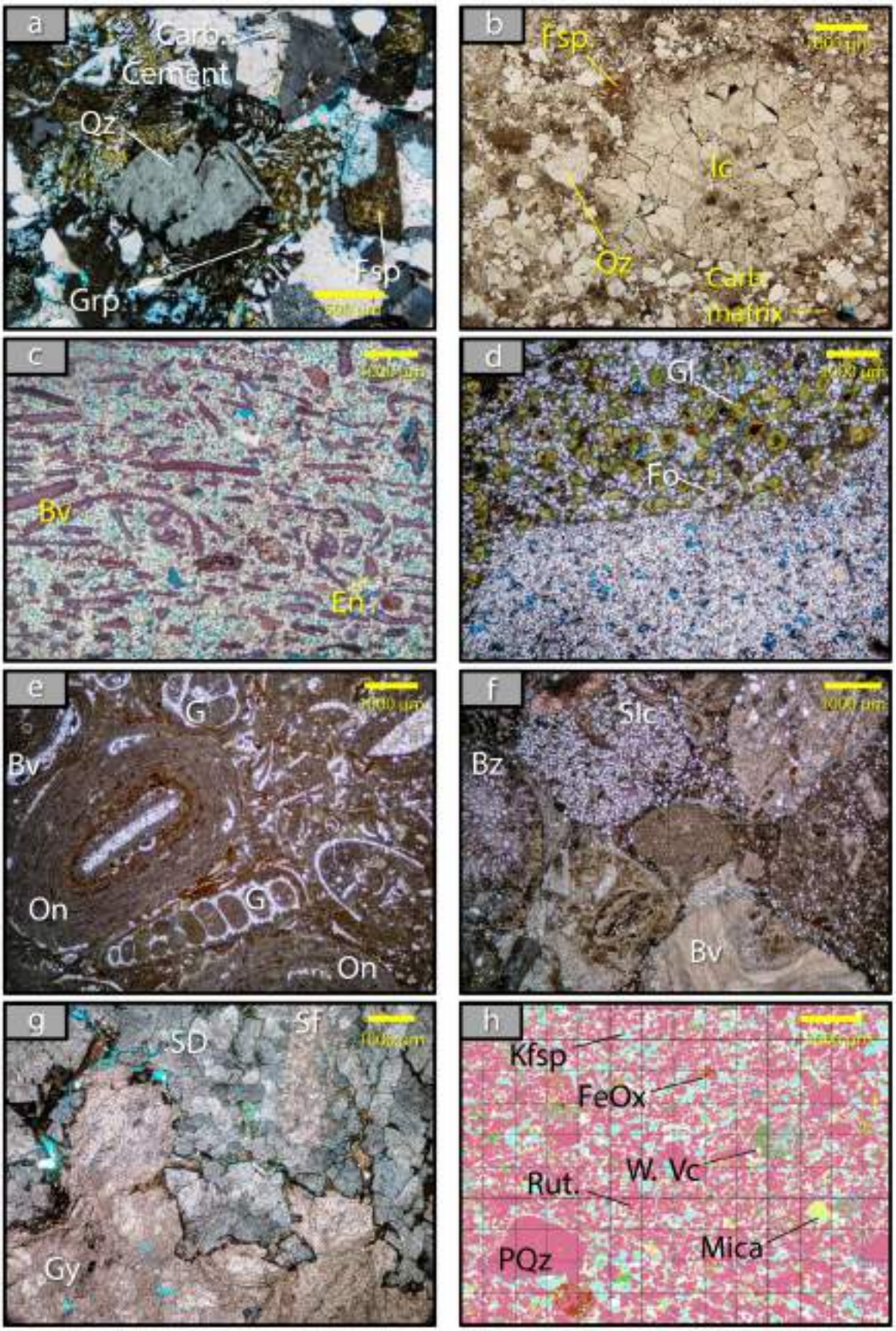

Figure 5.3: Thin section micrographs and QEMSCAN analysis of selected lithofacies.
(a) lithofacies Gms with common granophyric texture (Tinkert section, 43 m); (b) lithofacies Gms, debrite with common carbonate clast and carbonate matrix (Aouerga section, 36 m); (c) lithofacies St, shell-rich shoreface bars of the falling stage systems tract (FSST) (Assaka

section, 75 m); (d) sequence boundary SB4, reworking of clean and well-sorted sandstone(Sh) into polyphased, glauconitic sandstone above (Sm) (Assaka section, 90.5 m); (e) lithofacies Grf, shelf succession immediately below palaeosol indicating exposure of the lower Barremian shelf (Alma East section, 27.7 m); (f) fluvial fill (Gcs), note the common shelf – shallow marine carbonate intraclasts (Alma section); (g) original lithofacies likely Sg or Grf, exposure of carbonate deposits and development of a palaeosol, lateral equivalent to fluvial facies in image f (Alma East section, 28 m); (h) lithofacies Gcs, QEMScan image of fluvial channel fill with common weathered volcaniclastic material and abundant K-Feldspar (Azziar South Section, 23 m). Qz – Quartz, Grp – Granophyric texture, Ic – Intraclast, Bv – Bivalve, En – Echinoid, Gl – Glauconite, Fo – Foraminifera, G – Gastropod, On – Oncoids, SIc – Sedimentary Intraclast, Bz – Bryozoan, Sf – Shell fragment, SD – Saddle-Dolomite, Gy – Gypsum, Kfsp – K-Feldspar, FeOx – Iron oxide, W. Vc – Weathered volcanoclastics, Rut. – Rutile, PQz – Polycrystalline quartz.

5.4 Interpretation

5.4.1 Depositional model/Facies associations

The 15 lithofacies presented in Table 5.2 were grouped into 7 facies associations (FA). The interpreted depositional environments summarised in table 5.3. Examples for facies associations with detailed photographs and logs are show in appendix C17 to C19.

5.4.1.1 Foreshore to upper shoreface (FA-1)

FA-1 commonly comprises amalgamated sandstones with minor grainstones and rudstones/floatstones. These deposits are occasionally interbedded with mudstones. Sandstones are well to moderately-sorted. Individual beds are cm to m-sized, exhibit erosive bases, and contain common trough cross-bedding (see App. C17 and C19). Bioturbation is variable.

Deposition is interpreted to have taken place above storm wave-base in high-energy oscillatory flow during storm events.

5.4.1.2 Lower shoreface to offshore transition (FA-2)

FA-2 exhibits laterally-extensive successions of interbedded sandstones and mudstones. Sandstone beds are generally non-amalgamated, cm to dm-sized, with

similarly extensive mudstone interbeds. They commonly show low-angle and hummocky cross-stratification (see App. C19). Bioturbation is common to very abundant sometimes leading to destratification.

The presence of HCS suggests the main depositional process for the sandstones is high-energy oscillatory flow during waning stages of storm events below fair-weather wave-base and dune migration in upper flow regime. Mudstones are deposited through suspension fall-out on the shelf or from gravity flow deposits.

5.4.1.3 Offshore/shelf (FA-3)

FA-3 is dominated by massive to laminated, laterally-extensive, calcareous mudstones. (see App. C17 and C19) The mudstone succession are typically meters to tens of meters in thickness. Minor intercalated sandstones with thickness ranging from cm to dm-size are locally confined, typically ranging in width from decimetres to a couple of metres.

FA-3 is interpreted to record deposition on the shelf below storm wave-base. The mudstones were deposited mainly through pelagic fall out, with intercalated sandstones recording shelf gravity flows.

5.4.1.4 Terminal distributary channels (FA-4a) and mouthbars (FA-4b)

FA-4a is composed of inclined, laterally-extensive, heterolithic strata. Sandstones and mudstones are usually cm to dm-sized. Sandstone beds exhibit common low-angle and hummocky cross-stratification, can become amalgamated and occasionally include abundant plant debris (see App. C18). Mudstones are often non-calcareous and massive or laminated. Bioturbation is common to very abundant.

FA-4b is composed of through cross-bedded and massive sandstones and minor mudstones infilling concave up channel features. Sandstones often exhibit rippled, massive, or horizontal-stratified sandstones at the top, and are cm to dm-sized. Gravel-sized clasts and plant debris is abundant. Deposits are laterally confined and usually meters to tens of meters wide. Bioturbation is rare to common.

FA-4a is interpreted as mouthbar deposits. Sandstones were deposited through gravity flows and high-energy oscillatory flow during waning stages of storm events.

Mudstones were deposited through suspension fall-out and gravity flows. The mouthbars of FA-4a are linked to the terminal distributary channels of FA-4b. Here sandstones are associated with bar forms forming through dune migration and bed load transport. FA-4a and b form the distal expression of the main fluvial trunk system (FA-6).

5.4.1.5 Prodelta (FA-5)

FA-5 is composed of laterally-extensive and up to hundreds of meters thick mudstone successions with minor intercalated sandstone beds (see App. C18). Sandstones are often locally-confined and are massive or horizontal-stratified with common rippled tops. Deposits of FA-5 can exhibit large-scale soft sediment deformation features and even emplacement of proximal delta deposits as rafts. Bioturbation in the deposits is variable but common to abundant.

FA-5 is interpreted as prodelta deposits. Mudstones are laid down mainly through low-energy suspension fall-out and intercalated sandstones are deposited through shelf gravity flows triggered by coarse siliciclastic input during river floods and storm events. FA-5 is building outboard of FA-4 commonly onto the underlying shelf succession (FA-3).

5.4.1.6 Fluvial trunk channel (FA-6)

Deposits of FA-6 infill concave up erosional surfaces that are often tens to hundreds of meters wide. Internally deposits are poorly to moderately-organised. Stacked successions often include conglomerates at the base overlain by sand-sized deposits exhibiting either massive appearance or through cross-bedding, and are often topped by rippled or horizontal-laminated deposits. The gravel-sized lithofacies varies in thickness from centimetres to meters and is dominated by grainstone clasts. Sandstones are dm to m-sized and occasionally topped by massive or laminated mudstones, often reworked into the basal coarse-grained interval of the overlying stack. Concave up erosional surfaces can also become mud-plugged (Fm, Fl). Bioturbation is variable but usually rare to common.

FA-6 includes the traction-load fills and, where present, mud-plugged parts of the fluvial trunk channels. Gravel-sized lithofacies are deposited mainly through unidirectional bedload transport. Clasts are derived from provenance areas in the hinterland, but commonly include abundant intra-basinal sedimentary clasts. These clasts are likely

derived through vertical incision into underlying Lower Cretaceous and Jurassic successions (see App. C17). Sand-sized deposits form large-scale bedforms topping the gravel-sized lithofacies in the waning stages of river discharge. Mud-plugged channels are interpreted as infill of abandoned channels.

5.4.1.7 Floodplain, levee and crevasse splay deposits (FA-7)

FA-7 is composed of laterally-extensive (hundreds of meters to kilometres) mudstone deposits of alternating red and green colour. Sheet-like sands are common with variable lateral extend but usually ranging from meters to tens of meters, but can range up to hundreds of meters (see App. C17). Bioturbation is strongly variable but where present often very abundant.

Mudstones successions are interpreted as floodplain deposits to the sides of major fluvial input points laid down on vast and extensive plains. The red-green colour variation is linked to changes in the groundwater table, with red interpreted to represent times of exposure. Further, palaeosols have been identified, most commonly close to incising fluvial successions. Sheet-like sands are interpreted as crevasse splays and overbank deposits. FA-7 is wide-spread in the Agadir sub- basin and almost absent in the Haha sub-basin.

Table 5.3: Proposed lithofacies associations of lithofacies from table 5.2 and interpreted depositional environment.

(FA) Facies Associations	Lithofacies	Description	Interpretation Depositonal Environment
FA-1	Grf, Sh, Sl, Sm, St, Sw, Sr Sg, Fmc, Flc	Amalgamated beds of fine- to medium-grained sandtones (St, Sl, Sw, Sh, Sm); Lag deposits form grainstones (Sg), Storm events rework oyster beds (Grf); lateral extent: metres to hundreds of metres; thickness: metres to tens of metres; bioturbation index (BI): 0-3	**Foreshore to upper shoreface**
FA-2	Sl, Sw, Sr, Fm, Flc, Fm, Flc	Non-amalgamated to amalgamated beds of fine-grained sandstones (Sl, Sw, Sr) interbedded with mudstones (Fm, Flc, Fmc, Flc); lateral extent: metres to hundreds of metres; thickness: metres to tens of metres; BI: 1-5	**Lower shoreface to offshore transition**
FA-3	Fmc, Flc, Sh, Sr, Sm	Dominated by mudstones (Fmc, Flc) through pelagic sedimentation and minor fine- to medium-grained sandtones (Sh, Sr, Sm) deposited via shelf gravity flows; lateral extent: hundreds of metres to kilometres, sandstones locally confined; thickness: tens of metres; BI: 3-5	**Offshore, shelf**
FA-4	St, Sm, Sh, Sw, Sr, Sl, Fm, Fl,	Infilling channel features; bar forms (St, Sm) often with Sh, Sw, Sr at top; abandoned channel often mud-pluged (Fm, Fl); common plant debris; lateral extent: strongly variable, tens of metres to hundreds of metres; thickness: tens of metres; BI: 1-5	**Terminal distributary channels and mouthbars**
FA-5	Fm, Fl, Fmc, Flc, Sm, Sh, Sr	Dominated by mudstones (Fm, Fl, Fmc, Flc); occasional sand-sized lithofacies (Sm, Sh, Sr) during river floods; lateral extent: hundreds of metres to kilometres; thickness: tens of metres; BI: 1-5	**Prodelta**
FA-6	Gcs, Gms, St, Sm, Sw, St, Sh, Sr, Fm, Fl	Infilling concave-up erosional surface; basal part of channel often filled with conglomerates (Gcs, Gms); bar forms (St, Sm) often with Sh, Sw, Sr at top or to the side of bar forms; abandoned channel often mud-pluged (Fm, Fl); interbeds of locally derived debrites (Gms); common plant debris; lateral extent: strongly variable, tens of metres to hundreds of metres; thickness: metres to tens of metres; BI: 1-3	**Fluvial trunk channel**
FA-7	Fm, Fl, St, Sh, Sm, Sr	Extensive mudstone units (Fm, Fl); distinct alternating red and green colour representing exposure and changing water table; interbedded with minor laterally-variable sandstone beds (St, Sh, Sm, Sr); lateral extend: mudstones tens of metres to kilometres, sandstones metres to hundreds of metres; thickness: metres to tens of metres; BI: 0-5	**Floodplain, levee and crevasse splays deposits**

5.4.2 Biostratigraphy

The ammonite biostratigraphic framework of the EAB for the early Barremian is discussed in Company et al. (2008) and the framework of the Aptian in chapter 3 of this thesis. Important early Barremian ammonoid-biostratigraphically constrained timelines for the sequence stratigraphic interpretation are: (1) *N. pulchella* Zone, (2) *T. huggi* to *N. pulchella* zones and (3) *K. compressissima* to *C. darsi* zones; for the early late Barremian (4) *T. vandenheckii* to *G. sartousiana* zones; and for the early Aptian: (5) *P. dechauxi* Zone
Key upper Barremian ammonoids utilised in this study are illustrated in figure 5.15. A correlation of the Azziar South to Tamri South transect with key biostratigraphic surfaces is illustrated in appendix C20.

5.4.3 Sequence stratigraphic concepts, models and nomenclature

Sequence stratigraphic nomenclature used here is closely related to the depositional sequence IV of Catuneanu et al. (2009) based on Hunt and Tucker (1992 and 1995), Helland-Hansen and Gjelberg (1994), and Plint and Nummedal (2000). This is illustrated in Fig. 5.3 which defines the position of the interpreted systems tracts and key surfaces relative to base-level change. An abridged definition of the sequence stratigraphic horizons is given below, for a detailed discussion on the individual sequence stratigraphic surfaces the reader is referred to Zecchin and Catuneanu (2013).

Other widely-used depositional sequence models exist, namely depositional sequence I, II, and III (summarised in Catuneanu et al. (2009)). These models vary in placement of the sequence boundary and nomenclature used for systems tracts. For example, in depositional sequence II (Haq et al., 1987; Posamentier et al., 1988) the sequence boundary is placed at the onset of base-level fall, while in depositional sequence IV, followed in this study, the sequence boundary is placed at the end of base-level fall (see Fig. 5.3).

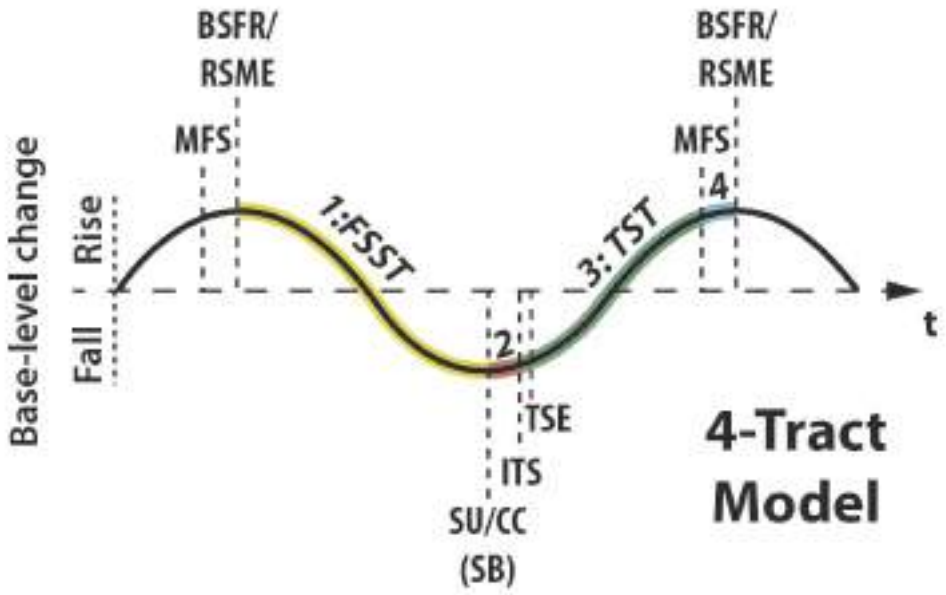

Figure 5.4: Sequence stratigraphic nomenclature.
Nomenclature followed in this study is based on Hunt and Tucker (1992 and 1995), Helland-Hansen and Gjelberg (1994), and Plint and Nummedal (2000). MFS: Maximum flooding surface, BSFR: Basal Surface of the Forced Regression, RSME: Regressive Surface of Marine Erosion, 1 - FSST: Falling Stage Systems Tract, SU: Subaerial Unconformity, CC: Correlative Conformity, 2 - LST: Lowstand Systems Tract, ITS: Initial Transgressive Surface, TSE: Transgressive Surface of Erosion, 3 – TST: Transgressive Systems Tract, 4 – HST: Highstand Systems Tract.

5.4.3.1 Maximum Flooding Surface (MFS)

The MFS is defined as the point of maximum transgression and marks the change from transgressive to normal regressive shoreline trajectories (Helland-Hansen and Martinsen, 1996; Catuneanu, 2006; Zecchin and Catuneanu, 2013). In marine locations, this surface can be expressed as a glauconite-rich hardground (Loutit et al., 1988) or an indistinguishable horizon in mudstone succession. The MFS forms the basal surface of the highstand systems tract (HST).

5.4.3.2 Basal Surface of the Forced Regression (BSFR) and Regressive Surface of Marine Erosion (RSME)

The BSFR (Hunt and Tucker, 1992) marks the onset of base-level fall and only forms if the base of the forced regression lies below the wave base and is not eroded during base-level fall. The erosion surface forming at the base of the forced regressive shorefaces and

deltaic sequences above the wave base is the RSME (Plint, 1988; Plint Nummedal, 2000). The RSME is a diachronous surface along dip and multiple RSME can be formed during stepped forced regressions.

5.4.3.3 Subaerial Unconformity and Correlative Conformity (SB)

The end of fall in base-level is marked by the development of a sequence boundary (SB) forming an erosional surface, a subaerial unconformity in the non-marine environment. In the marine environment, it can be traced into a correlative conformity (Hunt and Tucker 1992). The sequence boundary is the lower bounding surface of the low-stand systems tract (LST). As shown by Aitken and Flint (1996) and McCarthy and Plint (1998), in interfluve areas, the subaerial unconformity can be expressed by the development of palaeosols.

5.4.3.4 Initial Transgressive Surface (ITS)

The ITS has been assigned various terms in previous literature, see discussion of the maximum regressive surface in Zecchin and Catuneanu et al. (2013). We here use the nomenclature given by Nummedal et al. (1993). It represents the surface marking the change from progradation to retrogradation. This surface can be highly diachronous, depending on palaeotopography, sediment supply and subsidence. This surface might not be preserved everywhere as it can be easily be reworked by the overlying transgressive surface of erosion (TSE). The ITS is the lower bounding surface of the transgressive systems tract (TST).

5.4.3.5 Transgressive Surface of Erosion (TSE)

During base-level rise the shoreline shifts landward producing a ravinement surface along its course (Nummedal and Swift, 1987) that is often onlapped by the transgressive shoreface deposits (Catuneanu, 2002). This shoreface ravinement has the potential of reworking and removing a substantial amount of the underlying strata, e.g. the expression of the sequence boundary (Embry, 1995).

5.4.4 Key sequence stratigraphic surfaces

A sequence stratigraphic model described in 5.4.4 has been developed using detailed analysis of key sections (e.g. Fig. 5.5 to 5.7) and construction of both dip and strike correlations across the Haha and Agadir sub-basins of the EAB (Fig. 5.1). Four important 3rd order stratigraphic sequences (ranging from 1-10 Ma duration) and associated sequence stratigraphic surfaces have been identified. These are annotated in the text and figures as Sequence 1, SB1, LST1, TS1, TSE1 etc. An annotated version of the transect between Azziar South and Tamri South with key time lines and surfaces can be found in appendix C20. In the following we will describe the key sequence stratigraphic surfaces, followed by the sequence stratigraphic model in section 5.4.4.

5.4.4.1 Sequence boundary 2 (SB2)

The transect in between Azziar South to Tamri South (Fig. 5.8, App. C7 and C20) shows an erosive unconformity with the emplacement of upper shoreface to offshore transition deposits (FA-1 and FA-2) on top of shelfal deposits (FA-3). This regionally-recognisable surface forms the base of the Bouzergoun Fm and is interpreted as sequence boundary 2 (SB2), differentially cutting into the underlying upper Barremian strata (Company et al., 2008) (Fig. 5.8, App. C19).

5.4.4.2 Initial transgressive surface 2 (ITS2)

Deposits of FA-1 and FA-2 that rest upon the SB2 are followed by a regionally recognisable lithological change to a succession of shelfal mudstones (FA-3 and FA-5). The surface marking the lithological change is interpreted as the initial transgressive surface 2 (ITS 2), well exposed e.g. in the Assaka section (Fig. 5.5 and appendix C19).

5.4.4.3 Maximum flooding surface 2 (MFS 2)

The extensive shelfal mudstone successions (FA-3 and FA-5, see e.g. App. C18 and C19) overlying the ITS2 becomes increasingly fine-grained / clay rich, as shown by field gamma ray logging. The gamma ray peak in the Assaka section (24m depth location, Fig. 5.5) is interpreted as the maximum flooding surface (MFS2, see App. C20). In places this

surfaces constitutes an iron and glauconite-rich horizon with extensive bioturbation interpreted as a condensed section / hardground, e.g. in the Barrage section (Fig. 5.6).

5.4.4.4 Regressive surfaces of marine erosion (RSME)

The succession overlying MFS2 is marked by gradual coarsening- and thickening-upward succession with increasing clastic input. This is shown on gamma-ray by gradually reducing values (Fig. 5.5 and App. C19). It varies in character along the dip line (figure 5.8) from an offshore mud-rich (FA3) to prodelta environment (FA5) to more proximal prograding and aggrading mouth bars (FA4), e.g. in the Akerkaou section (Fig. 5.5). The gradually progradation and aggradation trend is followed by a package of sediments that indicate a rapid progradation and down-stepping, with emplacement of sharp-based shoreface deposits (FA-1 and 2) and mouth bar successions (FA-4) close to the modern coast in both the Haha (e.g. Assaka section, Fig. 5.5 and appendix C19) and Agadir sub-basin (e.g. Addar section, Fig. 5.7 and App. C18). The erosional bases of these sharp-based shoreface and deltaic successions are interpreted as regressive surfaces of marine erosion (RSME), formed by wave erosion of the underlying shelfal succession. Examples of similar RSME with sharp-based shoreface and deltaic succession are well-documented in the literature (e.g. Plint, 1988, 1991; Hampson et al, 1999, 2001; Hamberg and Nielsen, 2000; Plint and Nummedal, 2000; Posamentier and Morris, 2000; Plink-Björklund and Steel, 2006).

A prominent example of the RSME is well-exposed in the Assaka section where a thick sandstone tongue of shoreface deposits (FA-1 and 2) has been emplaced directly on top of offshore mudstones (FA-3) (Fig. 5.5, at 52m spot height and App.C19). This erosive surface is marked by a distinct grain size break and frequent soft-sediment deformation of the underlying mudstone succession, suggesting rapid loading. In Assaka this contact is also associated with a significant decrease in gamma ray-values (Fig. 5.5) due to the higher input of siliciclastic material.

In the Tamri South section, the RSME is characterised by a prominent erosive boundary and grain size break (Fig.5.8, 43 m spot height, and appendix C18), with a sharp erosive basal surface at the contact between mouth bars resting on top shelfal mudstones

Another shoreline and development of a second RSME advance is marked by the emplacement of proximal distributary channel deposits onto the mouth bar deposits in the

Tamri South section (appendix C18). Instabilities and slumps are commonly observed, with extensive loading and soft-sediment deformation affecting deposits above and below the second RSME (Fig. 5.8, 80 m spot height Tamri South). These features are interpreted to be caused by the loading and over steepening of the rapidly forestepping shoreface and deltaic deposits. They are prominently displayed in Tamri South and Aghroud.

5.4.4.5 Sequence Boundary 3

In the Tamri area, deltaic successions (FA-6) are overlain by an erosive contact, followed by fluvial trunk deposits (FA-6) (Fig. 5.8, Tamri South 87 m spot height and App. C18). This is correlated as a regional unconformity, marked by the incision of a fluvial system into underlying strata. A similar incised valley architecture has been described by Tesson et al. (1990) in the upper Quaternary deposits of the Rhone Delta of France and by Sydow and Roberts (1994) in Pleistocene shelf-edge deltas of the Gulf of Mexico. The degree of down-cutting varies along the studied transects, but it is more pronounced in proximal sections, e.g. in the Barrage section in the Haha sub-basin (Fig. 5.6) and also in the proximal sections of the Agadir sub-basin.

Along a strike line from the Alma to Inrarne outcrops (Fig. 5.9 and App. C20) development of this erosive unconformity leads to down-cutting into lower Barremian and as deep as upper Hauterivian strata (e.g Fig. 5.9, Alma section 23 m spot height, or Alma East 28 m spot height). Here fluvial sediments (Fig. 5.4f) and palaeosols (Fig. 5.4g) are in direct contact with shelfal deposits (Fig. 5.4e and appendix C17). Development of palaeosols as a lateral equivalent to the erosive unconformity are common (e.g. East Alma and Inrarne, Fig. 5.9) and comparable to descriptions by Aitken and Flint (1996) and McCarthy and Plint (1998). This surface is interpreted as a key regional sequence boundary (SB3) and an important sediment bypass surface, associated with a dramatic change in depositional environment and increase in grain size. The infill above SB3 is composed of coarse-grained fluvial (Fig. 5.8, Barrage section) to proximal distributary channel deposits (FA-6), e.g. in the Addar section (Fig. 5.7 and App. C18).

5.4.4.6 Initial transgressive surface 3

The coarse-grained deposits of FA-6 infill the relief created by SB3 and are overlain in the Agadir sub-basin by extensive red-green mudstone facies (see e.g. App. C17). The transition is often marked by an iron-rich and bioturbated horizon (e.g. Addar 23 m spot height, Fig. 5.7). This surface is interpreted as the initial transgressive surface 3 (ITS 3). This corroborates the observation of Amorosi and Colalongo (2005) that in the non-marine part of the system the transgressive surface can be found at the contact between fluvial and floodplain deposits. ITS3 and overlying deposits are often absent and eroded in the Haha sub-basin by the next erosive unconformity.

5.4.4.7 Transgressive surface of erosion 3 (TSE 3)

In the Agadir sub-basin shoreface deposits (FA-1 and 2) rest with a sharp, erosive contact upon the red-green non-marine mudstone successions (FA-7) (App. C17). In the Haha sub-basin this erosive unconformity is marked by either a change from poorly-sorted, coarse clastic fluvial deposits (FA6), or floodplain deposits where preserved (FA7), to siliciclastic shoreface deposits (App. C19). These deposits often include grainstones and rudstones dominated by oysters (FA1), interpreted as storm wave concentrations (Fürsich and Oschmann, 1993). This shoreface interval is well-exposed in many sections, particularly in Inrarne (Fig. 5.9, 44 m spot height), where red-green mudstones of the floodplain are overlain by fine- to medium-grained sandstones of the advancing shoreface (also see appendix C17). The basal beds of the shoreface deposits often include reworked material of the underlying stratigraphy (FA-7). This erosive unconformity is interpreted as the transgressive surface of erosion (TSE3). Shoreface retreat is interpreted to have occurred rapidly, as it is followed by the appearance of ammonites of the similar age (*P. Dechauxi* Zone) in the shelfal succession, recorded in almost all sections studied.

5.4.5 Sequence stratigraphic model

Two correlation panels (Fig. 5.8, 5.9 and App. C20) have been constructed, using the transgressive surface of erosion (TSE3) within Sequence 3 as the correlation datum. This surface can be traced across the study area. While this is diachronous by its nature, and not

a perfect time line, it is interpreted to have developed very rapidly, supported by occurrence of the same ammonoid fauna above in all sections, allowing it to be utilised. Other datum were considered (e.g. MFS3) but due to poor exposure in the field, local tectonic activity following the forced regressive phase (see chapter 4.6.5) and condensation, they were rejected.

The interval between MFS2 and SB3, two prominent and regionally mappable surfaces in the west-central EAB, is well dated as upper Barremian to lowermost Aptian, and interpreted to record a progradation of the shoreline. During highstand systems tract 2 (HST2), bound at the base by MFS2, the shoreline prograded basinward with the development of extensive deltaic successions in the west-central part of the EAB. Subsequently, rapid lowering in base-level lead to the development of sharp-based shoreface and deltaic successions (see e.g. App. C18 and C19). These deposits are bounded at the base by the RSME and at the top by a regionally-observed erosive unconformity (SB3), and are interpreted as the falling stage system tract (FSST2).

Multiple packages of sharp-based shoreface and deltaic successions are in contact with one another and separated by successive RSMEs. This architecture is interpreted to record attached forced regressive deposits (Posamentier and Morris, 2000) which have a shingled appearance that has previously been described by Hamberg and Nielsen (2000). The shoreline trajectory of the FSST2 shows a forestepping and downstepping character, typical for forced regressions (Catuneanu et al., 2011).

A constructed Wheeler diagram and associated cross section (Fig. 5.8) shows the dynamics of the systems, from aggradation and progradation in HST2 to strong progradation and down-stepping in FSST2 up to the maximum point of regression (SB3). The interpreted SB3 forms a regional unconformity marked by the development of two basin-scale incised valleys with incision of a fluvial system (Fig. 5.11). In places this cuts deeply into the underlying stratigraphy and locally erodes the deposits of FSST2 and even HST2. Coarse clastic fluvial deposits that rest on SB3 and infill the relief and are interpreted to be the low stand fill (LST3). The top of LST3 is marked by ITS3 and is overlain by floodplain deposits of the lower transgressive systems tract 3 (TST3).

Ravinement by the retreating shoreline is marked by TSE3 and transgression led to reoccurrence of shelfal deposits during the earliest Aptian in the upper TST3. In the Haha sub-basin the development of TSE3 leads to erosion of the lower part of TST3. The better preservation potential for floodplain deposits of TST3 in the Agadir sub-basin is interpreted

to have resulted from greater accommodation caused by higher rate of subsidence. This might be linked to the differences in the underlying structure of this part of the basin, as the Lower Cretaceous is generally thicker in the Agadir sub-basin than the Haha sub-basin.

NW
SE
ITS4
SB4
TSE3
SB3
ITS3
RSWE
SB2
SB1
TSE2
SB2
ITS2
RSWE
ITS1
SB1
2-3shell free/-rich conglomerate
Assaka
Gamma-Ray
Mem.
Fm.
O. Tid.
Sy. Tr.
Stage
Deposit. Environ.
Bouzergoun Fm. p.p.
HST 2
FSST2
TST2
TST3
TST4
upper Barremian
Shelf
Lower to upper Shoreface
Shoreface
Shelf

Figure 5.5: Interpretation panel of the Assaka section (GPS point: Table 5.1).
Panel showing the upper Hauterivian Talmest Fm. to Lower Albian Oued Tidzi Fm. Note the absence of the Tamzergout Fm. in this location, due to the proximity to the palaeotopographic high active in the Aptian. The regressive surface of marine erosion (RSME) is well-exposed at the base of Member 2 of the Bouzergoun Fm. See Fig. 5.2 for the legend. ^3: Lower Albian.

SW
NE
MFS1
SB1
SB2
SB3
MFS2
TSE1
Barrage
Mem.
Fm.
Sy. Tr.
Stage
Depos. System
Tab. Fm. p.p.
T5T1
HST1
lower Bar. p.p.
Carbonate Shoal
LST2
TST2
HST2
upper Bar. p.p.
Shoref.
Shelf
LST3
TST3
lower Aptian
Fluvial trunk channel
Shoreface
2
3
Bouzergoun Fm.
Tamzerg
Shelf

Figure 5.6: Interpretation panel of the Barrage section (GPS point: Table 5.1).
Panel showing the lower Barremian Taboulouart Fm. and upper Barremian – lowermost Aptian Member 1 (partially eroded), 2 and 3 (partially preserved) of the Bouzergoun Fm. Note the downcutting of Member 2, erosion of Member 1 and locally incision even into lower Barremian strata. Sequence boundary (2) is in parts of the section eroded by the advancing fluvial system, forming sequence boundary3 (SB 3). See Fig. 5.2 for the legend.

NNE
SSW
SB1
ITS1
TSE1
SB1
ITS1
MFS1
ADDAR
Member
Fm.
Syst. Tr.
Stage
Depos. Environ.
Tam.
TST3
lower Aptian
u. A.
Shoref.
Shelf
Floodplain
Distribut. Ch.
Shoreface/Mouthbar
upper Barremian p.p.
FSST2
LST3
Bouzergoun Fm. p.p.
2
3

Figure 5.7: Interpretation panel of the Addar section (GPS point: Table 5.1).
Panel showing the upper part of Member 2 and Member 3 of the Bouzergoun Fm. Sequence boundary (3) is here overlain by distributary channel deposits. Note the development of the red-green mudstone facies also displayed in the proximal strike line of Fig. 5.9. Here in the most distal location of the Agadir sub-basin the red- and green-coloured mudstones already show common marine incursions towards the top assigned to an estuarine depositional environment. See Fig. 5.2 for the legend.

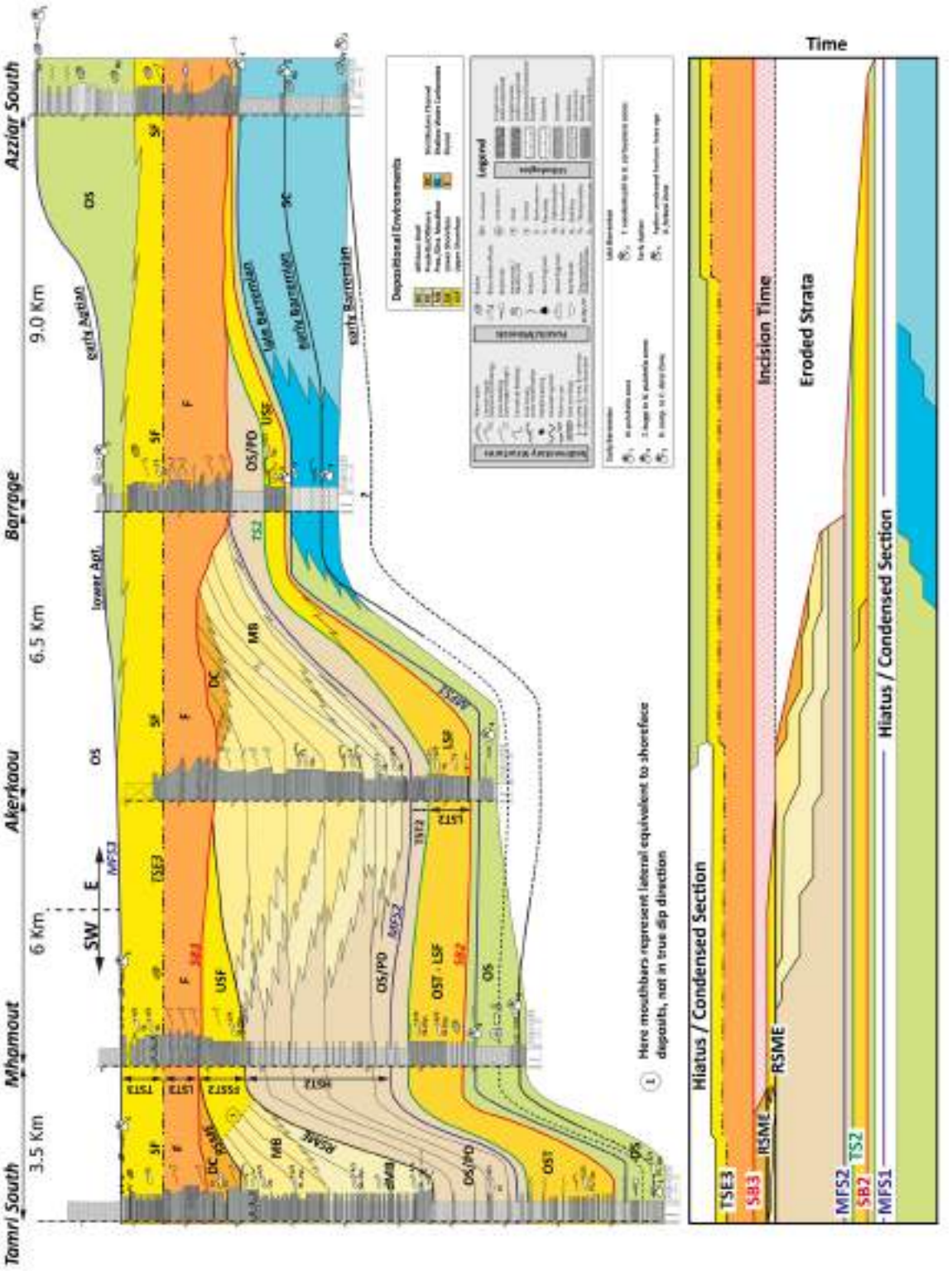

Figure 5.8: Correlation panel of a dip line from east (Azziar South) to west (Tamri).
For the location of this transect see figure 5.1. Note the increased down-cutting of the fluvial deposits in the Barrage section (also see Fig. 5.6). Above the regressive surface of marine erosion, the trend of the system changes from aggradation to strongly progradational with the establishment of attached forced-regressive deposits. During this phase the shoreline prograded beyond the modern coastline, leading to the exposure of the shelf (also see Fig. 5.9). This represents the most basinward progradation during the Cretaceous of the EAB. An A3 version is provided in appendix C7.

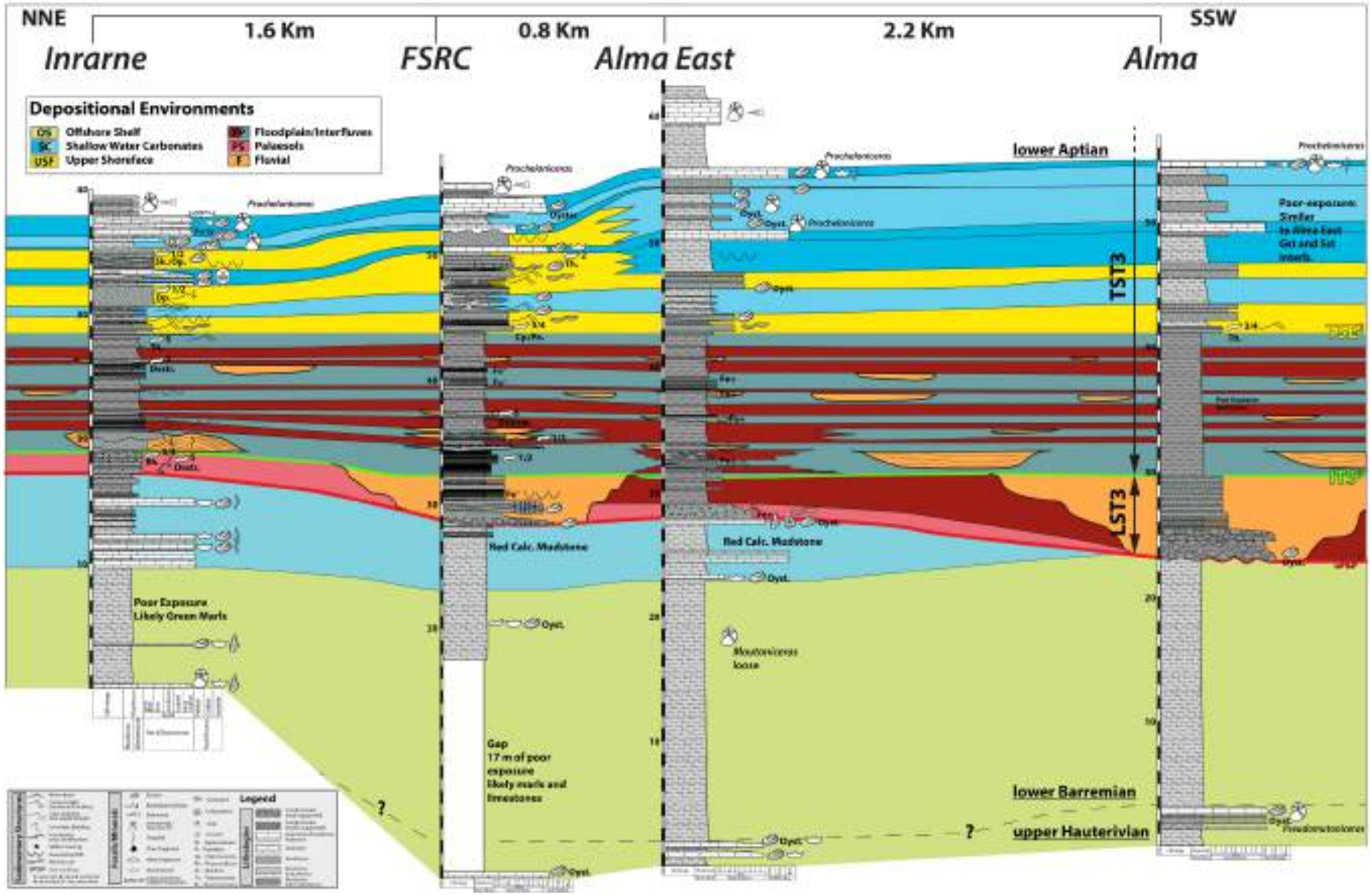
NNE
1.6 Km
0.8 Km
2.2 Km
SSW
Inrarne
FSRC
Alma East
Alma
Depositional Environments
OS Offshore Shelf
SC Shallow Water Carbonates
USF Upper Shoreface
FP Floodplain/Interfluves
PS Paleosols
F Fluvial
lower Aptian
TST3
LST3
Red Calc. Mudstone
Poor Exposure
Likely Green Marls
Gap
17 m of poor
exposure
likely marls and
limestones
lower Barremian
upper Hauterivian
Legend

Figure 5.9: Correlation panel of a strike line from north northeast (Inrarne) to south southwest (Alma).
For the location of this transect see figure 5.1. The interfluve environment of TST 3 is well-exposed along this transect. Note different expressions of the sequence boundary as erosional surfaces (FSRC and Alma) and palaeosols (Inrarne and East Alma). The contact between fluvial deposits of LST 3 and interfluve deposits of TST3 is interpreted as the ITS3. An A3 version is provided in appendix C8.

5.4.6 Palaeogeography and shoreline evolution

The seven main depositional environments identified in this study (Table 5.3) have been mapped using regional correlations of the outcrops studied and integrating all previous work, to generate a sequential series of gross depositional environment (GDE) maps, illustrated in figure 5.10-13. The GDE maps were constructed for the upper Barremian to lowermost Aptian Sequence 2 and 3: during the highstand systems tract of Sequence 2 (Fig. 5.10), during maximum regression around Sequence boundary 3 (Fig. 5.11), during the initial transgression of Sequence 3 (Fig. 5.11), during the initial transgressive systems tract of Sequence 3 (Fig. 5.12), and for the transgressive systems tract of Sequence 3 (Fig. 5.13).

5.4.6.1 Highstand Systems Tract of Sequence 2 (Fig. 5.10)

The maximum landward extension of the upper Barremian shoreline shown in Fig. 5.10 is inferred from Ambroggi (1963) and data from studied outcrops. Its exact position is uncertain, as it is located inland behind the line of preservation for Barremian to Aptian strata in the Haha and Agadir sub-basin of the EAB, but extrapolation of outcrop observations from inland sections of the Essaouira sub-basin support this interpretation. Fig. 5.10 illustrates the progradation of the shoreline during HST2 over a distance of 40 Km towards the basin to the west, approximately 15 Km to the east of the modern shoreline. This was marked by progradation and aggradation of mouth bars over shelfal mudstones, observed at outcrop in the Akerkaou section (Fig. 5.8). This migration of the littoral zone and increase in siliciclastic material was also noted by Butt (1982), and is supported by a marked decrease of nannoflora observed in samples analysed from these sections (Jeremiah pers comm.). Inland the development of extensive coastal plain and interfluve areas are hypothesised. The coast is interpreted to have been orientated approximately

north-south and wave-dominated, in accordance with observations made in shoreface successions in various locations (e.g. Assaka Fig. 5.5 and Addar Fig. 5.7), (Fig. 5.10). The deeper part of the shelf to the west was predominantly characterised by mud-rich deposits (e.g. Mahmout and Tamri South section, Fig. 5.8).

These deposits are overlain by sharp-based shoreface bodies that are interpreted as marking a forced regression (FSST2, see e.g. C18 and C19). It is a stepped process that leads to the development of several sharp-based shoreface and mouth bar successions (Fig. 5.5, 5.7and 5.8) over a minimum distance of 15 Km, prograding out to the position of the modern coastline and most-likely beyond. These deposits of the FSST are well-exposed at the base of the coarse clastic cliff in the Assaka (Fig. 5.5 and App. C19), Tamri South (App. C18), and Mahmout sections (Fig. 5.8 spot height 44 m and 53m, respectively).

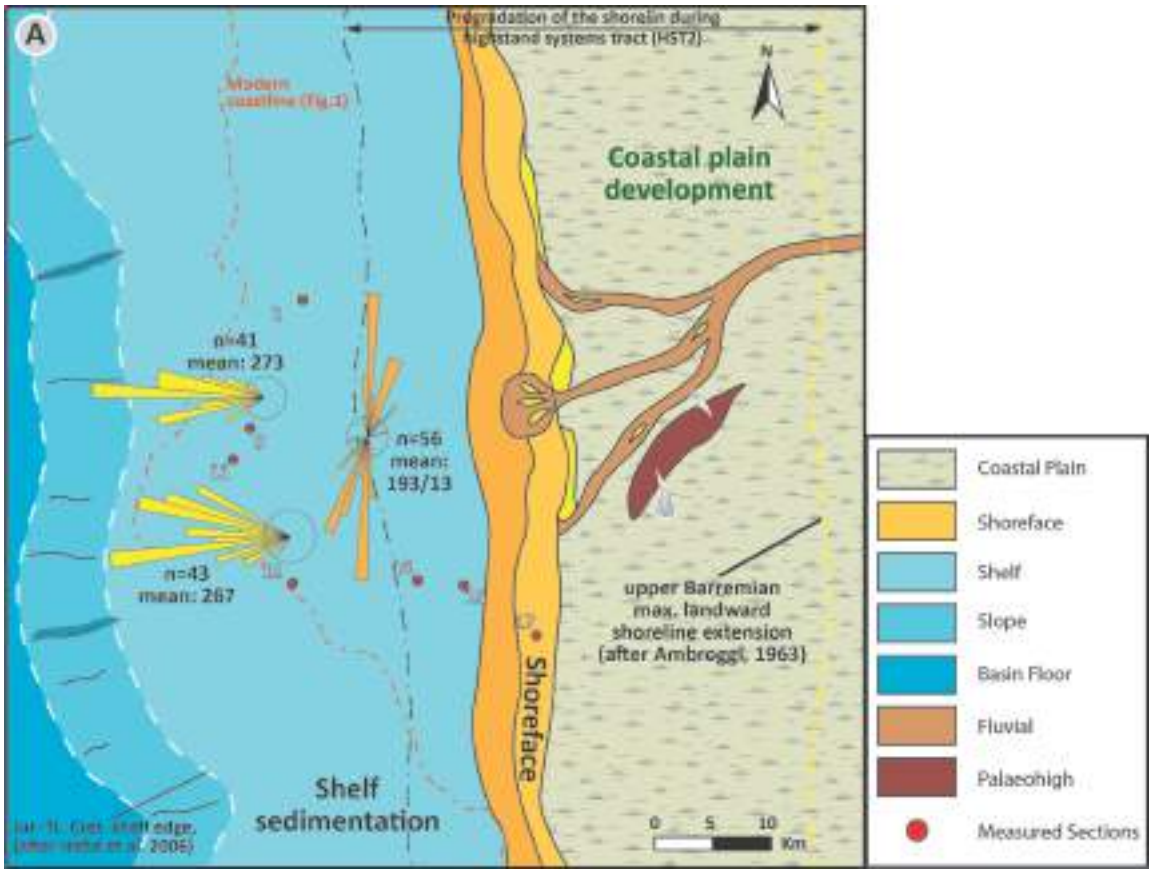

Figure 5.10: Gross depositional environment (GDE) map during HST2.
Palaeocurrent data comes from sole markings at the base of mouthbar deposits (yellow) and symmetric wave-ripples (orange) indicating shoreline orientation during HST2.

5.4.6.2 Maximum regression – Sequence Boundary 3 (Fig. 5.11)

During maximum regression, delta complexes become increasingly fluvial-dominated. Overall very few tidal indicators have been found at outcrop and the coast appears to have been wave-dominated. Frequent observation of soft-sediment deformation suggests sediment instability (e.g. Fig. 5.8, Azziar South 77-80 m and App. C18) indicating rapid progradation and oversteepening of the deltaic complex along the shelf edge. The majority of the shelf is thought to have been exposed during maximum regression (e.g. Inrarne and Alma East, Fig. 5.9), with fluvial deposits cutting into, and cannibalising the intra-Cretaceous and potentially older Jurassic sediments in more proximal locations. This is supported by common bryozoan, grainstone and rudstone fragments of shelfal deposits reworked as intraclasts in the fluvial succession (Fig. 5.4f and App. C17) and the sharp erosive contact of fluvial successions and development of palaeosol over shelfal carbonates (Fig. 5.4e-g and 5.9). This process of downcutting linked to the basinward shift in facies has previously been reported from the Gulf of Mexico by Suter and Berryhill (1985) and is often associated with base-level fall.

The shift of the shoreline beyond the modern coastline is suggested by fluvial channel-fill deposits and pedogenic horizons mapped in the most distal outcrops studied at Tamri South and Assaka (Figs. 5.5, 5.8, and App. C18/C19). A fluvial network has been mapped using studied outcrops and collected palaeocurrent data (Fig. 5.11), suggesting an overall westward transport. The active duration of each fluvial distributary is not known (i.e. whether they were coeval or represent migrating channel systems) but figure 5.11 gives an approximation on the extent of the fluvial system in the area.
Logging of an isolated section to the north of the study area suggests that this system might have extended even further into the area around Tamanar.

Palaeocurrent data, thickness variations of the correlated stratigraphy and mapping of the fluvial systems suggest the presence of multiple coeval palaeotopographic highs. Interaction with local palaeohighs is suggested by the presence of debrites with a distinctive petrography, e.g. in the Aouerga section (Fig. 5.4b). The debrites are interbedded with fluvial and floodplain deposits, and the clasts and matrix show a very different composition, with clasts almost exclusively comprising carbonate material. These debrites are thought to have been locally sourced from exposed older Cretaceous or Jurassic strata on fault-controlled or salt diapir-related palaeohighs. In the Aouerga section,

this is inferred to be the Cap Ghir high (Fig. 5.11), which is an inherited structure from the Jurassic (Martin-Garin et al., 2007). The location of the high likely led to the divergence of the fluvial system further inland into an overall westward-orientated system north of the Cap Ghir anticline and southwest-orientated system south of the anticline (palaeocurrent data Fig. 5.11).

The advance of the shoreline close to, or even beyond the shelf edge, probably allowed for the capture of rivers/shelf delta complexes along the shelf and this is interpreted to be the optimum timing for transport of coarse clastic material into slope canyons and deposition as turbidites on the basin floor during the upper Barremian to lowermost Aptian. Observations made from thin section of a coarse clastic interval overlying the uppermost Barremian mud-dominated strata (see chapter 4, figure 4.8) in DSDSP well 370, also indicates erosion and transport of shallow marine carbonate material into the deep basin (Meyer, 1978). Carbonate clasts in the DSDP well are interpreted to have been derived from either coeval erosion of the shelf or eroded material from outcropping older Cretaceous or Jurassic strata (Meyer, 1978). The succession in Borehole 370 is followed by a core gap overlain by lowermost Aptian strata. Therefore, the coarse clastic interval could correspond to the lowstand systems tract (LST3) developed following the forced regression. A significant core gap in the DSDP borehole 370 (see discussion chapter 4.6.6), as well as absence of biostratigraphic markers directly below the forced regressive package in the onshore sections, still limit a direct correlation of the events.

Previously authors have noted that the composition and transport direction of the Barremian to Aptian fluvial systems point towards a provenance from the Toubkhal-Ouzellarh massif and the Meseta (Meyer 1978; Price, 1980; Lancelot and Winterer, 1980; Behrens and Siehl, 1982). This is in agreement with collected palaeocurrent data and observations from thin sections in this study, and work in progress by the North Africa Research Group (NARG) aims to confirm provenance of this fluvial system. Thin section petrography and QEMScan analysis of the fluvial succession point towards common to abundant presence of feldspar and volcanoclastic fragments, illustrated in figure 5.4.a and 5.4.h. The presence of such clasts strongly indicates a first-order sedimentary cycle.

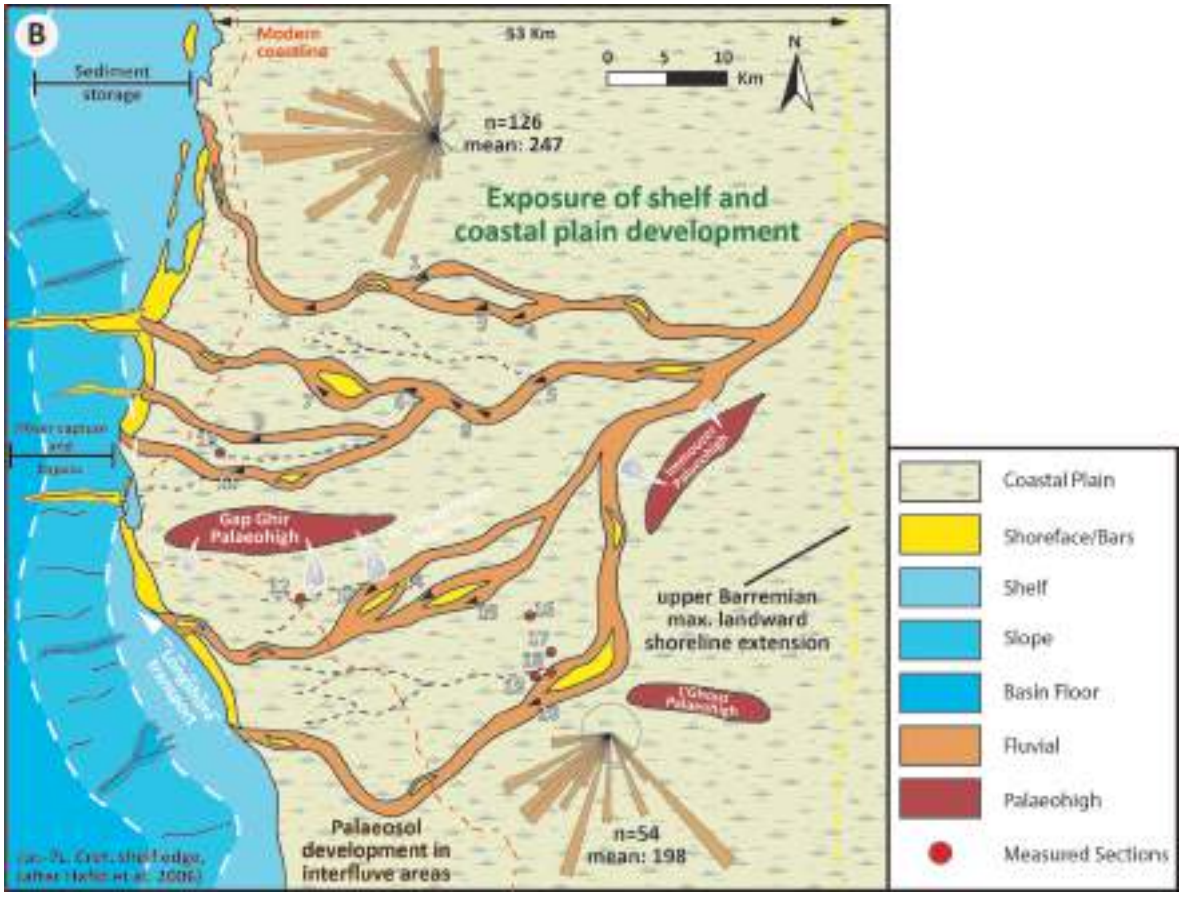

Figure 5.11: Gross depositional environment (GDE) map during the time of maximum regression of the shoreline.
Palaeocurrent data are grouped for the Haha and Agadir sub-basin (large rose diagrams). Black arrows indicate transport direction for individual sections studied.

5.4.6.3 Initial transgression – Transgressive Systems Tract 3 (Fig. 5.12)

Following maximum regression, the shoreline retreated rapidly during the subsequent transgression. In the Haha sub-basin of the EAB only few outcrops preserve of the lower TST3. In most sections studied the deposits were eroded by the TSE3 due to the ravinement of the retrograding shoreline. However, in the Agadir sub-basin, widespread prominent red-green mudstone facies developed (FA-7), interpreted to be floodplain to estuarine deposits (see also App. C17). The red-green colour change is interpreted to record variations in groundwater levels as previously mentioned by Wilson et al. (2014), supported by the lateral continuity of the mudstone facies, correlative over tens of kilometres (Fig. 5.9). The mud-rich succession includes small-scale fluvial channel features, crevasse splays and point bar features. FA-7 is macrofossil free and only the distal sections (e.g. Addar Fig. 5.7) yields rare microfossils (e.g calcareous benthic foraminifera) in the upper part. The

occurrence of calcareous benthic foraminifera identified in some smaples point towards periodic marine incursion, linked to the establishment of an estuarine environment towards the top of the FA-7 deposits. Butt (1982) also noted the occurrence of charophyta, small ostracodes and agglutinating foraminifera from the red bed facies and interpreted brackish water conditions. In the Agadir sub-basin FA-7 appears first between Addar and Aghroud and was not observed in the Aghroud section (also reported by Bergner et al., 1982). It is likely that FA-7 never developed in the westernmost sections due to the presence of a palaeotopographic high that appears to have been active during this time. Bergner et al. (1982) highlight this pre-existing relief by outlining the development of different condensed horizons throughout the Aptian along the transect from Aghroud to Inrarne, an observation also made in the Haha sub-basin to the north. Palaeohighs are interpreted to be linked to footwall uplift along basin-bounding faults, active during the post-regressive phase along a transect between Assaka and Id Amran (see chapter 4.6.5). Faults likely played a significant role in the position of the river systems developing during the regressive phase. Rivers are interpreted to migrate into the relay zones of the fault system along the modern coast (Fig. 5.12). Similar preferential drainage of rivers along these boundaries has previously been shown e.g. by Gawthorpe and Leeder (2000).

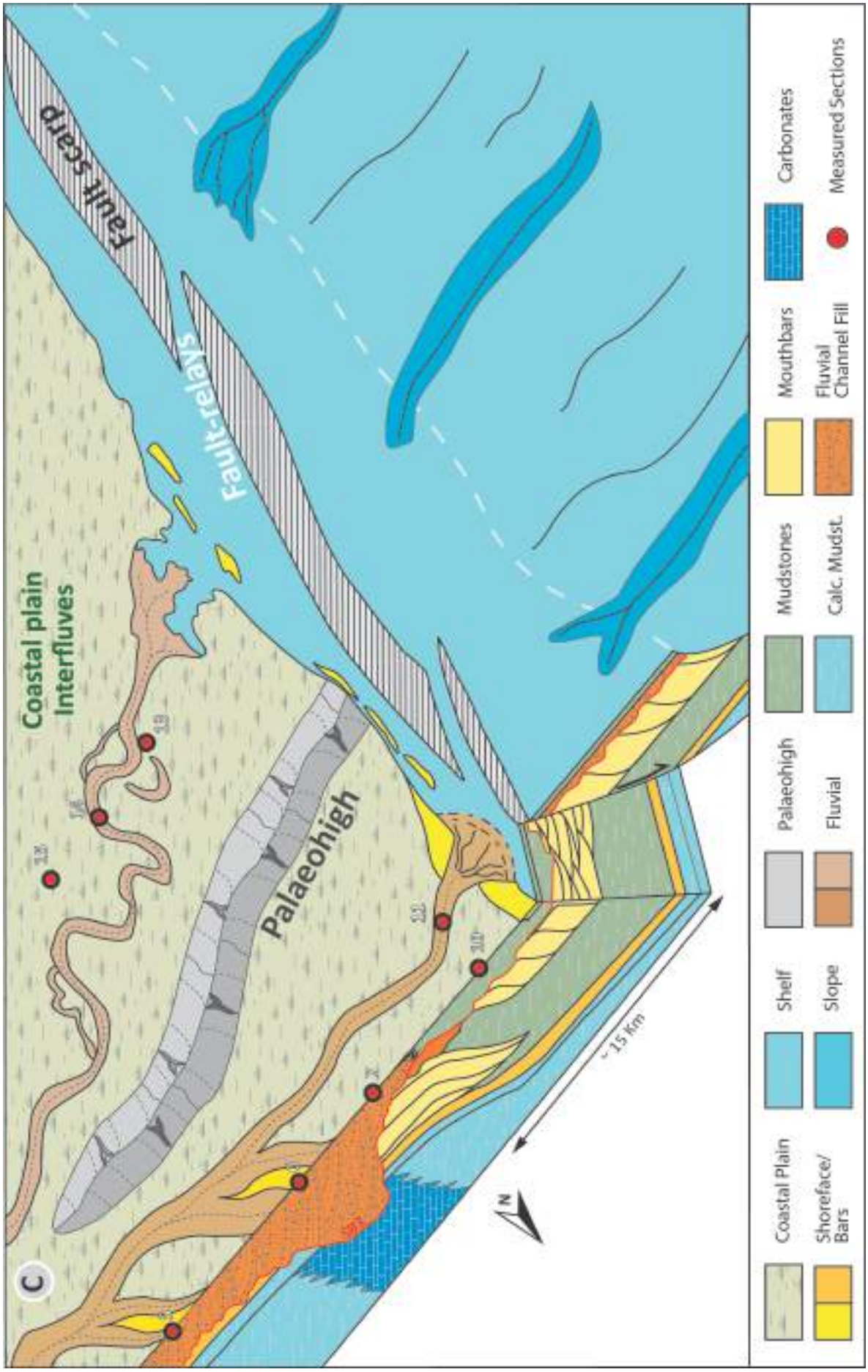

Figure 5.12: Gross depositional environment (GDE) map during initial transgression.

5.4.6.4 Continued transgression – Transgressive Systems Tract 3 (Fig. 5.13)

Transgression is thought to have occurred rapidly with the development of a widespread erosional surface, the transgressive surface of erosion (TSE3), recognised throughout the basin (Fig. 5.8). Deposits of the transgressive shoreface commonly include reworked carbonate and siliciclastic coarse-grained material.

During the lower Aptian, the EAB was dominated by shallow shelfal deposition. Open-marine fauna, e.g. ammonoids, belemnites and echinoids are common and widespread. The presence of bioclastic-rich bars points towards a high-energy environment with deposition taking place between the fair-weather and storm wave base (Fig. 5.13). This phase was followed by the establishment of mid to outer shelfal conditions and widespread deposition of monotonous marl and limestone successions during the upper Aptian (Luber et al. 2017, see also App. C11, 12 and 14) Close to the palaeohighs coarse clastic sedimentation prevailed, interpreted to be associated with erosion and reworking of the highs themselves (App. C13).

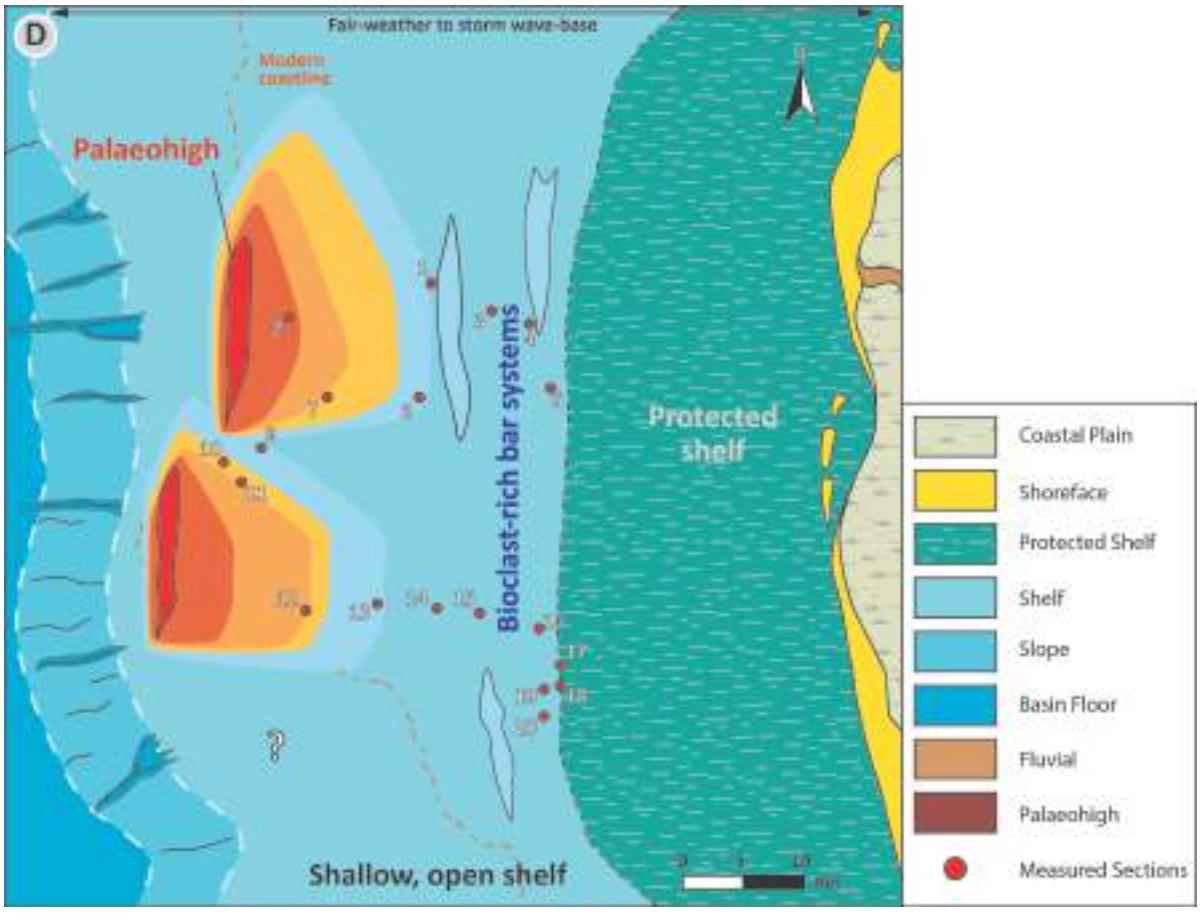

Figure 5.13: Gross depositional environment (GDE) map during the advanced transgression of the lower Aptian.

5.5 Discussion – Controls and mechanisms during the forced regressive phase

The advance of the shoreline to the edge of a shelf can be caused by changes in climate (controlling sediment discharge), local tectonics, and eustasy (controlling accommodation). In the following we assess the contribution of the individual factors.

5.5.1 Post-rift vertical movements

Km-scale vertical movements of the Moroccan margin during the Lower Cretaceous have been documented by a growing number of studies (e.g. Ghorbal et al., 2008; Ghorbal, 2009; Gouiza, 2011; Bertotti and Gouiza, 2012; Leprêtre et al., 2015). Uplift of potential provenance terranes for the EAB during the Late Jurassic to Early Cretaceous occurred along three main structural grains, the ENE-WSW-trending Anti-Atlas to the south of the study area (Gouiza et al., 2017), the Meseta to the north (Saddiqi et al., 2009; Ghorbal et al. 2008; Gouiza et al., 2010), and the NNE-SSW-trending Massif Ancien de Marrakech to the east of the study area (Gouiza, 2011; Bertotti and Gouiza et al., 2012). Exhumation rates inferred from low-temperature geochronology (Charton et al., 2017 pers. comm.) for the provenance terranes of the EAB during the Lower Cretaceous (Fig. 5.14) indicate increased rates relative to the rest of the Mesozoic post-rift phase. Time-temperature plots show a range of 0.5-2.0°C/Ma for the Meseta (based on Ghorbal et al., 2008; Ghorbal, 2009; Saddiqi et al., 2009; Barbero et al., 2011) and 1.7-2.7°C/Ma for the Massif Ancien de Marrakech (based on Ghorbal, 2009; Domenech, 2015). Assuming a geothermal gradient of 30 °C/Km and a surface temperature of 20 °C, uplift rates range from approximately 20-60 m/Ma (meters per million years) for the Meseta to 50-90 m/Ma for the Massif Ancien de Marrakech (see Fig. 5.14). Stable to slightly subsiding conditions are indicated for the Anti-Atlas. The driving mechanism for the increased exhumation in the provenance areas and the increased subsidence in the sink is still a topic of debate.

Throughout the entire Cretaceous interval in the EAB, the FSST2 in the upper Barremian to lower Aptian represents the most significant basinward shoreline shift. Preceding this, during HST2, the shoreline prograded over 40 Km basinward to the west (Fig. 5.10).

An interpreted relative exhumation curve is shown in Fig. 5.14. Times of elevated exhumation rates are predicted from Low-T Geochronology. These periods likely resulted in increased denudation of provenance terranes and subsequently more siliciclastic input to the basin (Fig. 5.14). Exhumation phases, indicated by low-temperature geochronology, have a much coarser temporal resolution than the field observations (tens of millions of years versus millions of years or less) and it is therefore hard to directly tie specific tectonic uplift phases to third and fourth order sedimentary sequences. But if sufficient siliciclastic material is introduced into the basin from the hinterland, progradation of the shoreline and deltaic systems can be predicted. The stratigraphic record of the EAB provides a high-temporal resolution and evidence for times of elevated exhumation within the Lower Cretaceous against the coarser temporal-resolution of the low-temperature geochronology data.

Small (10^0-10^1km) and large-scale (10^1-10^2km) movement in provenance areas is predicted. The larger wavelength (10^1-10^2km) exhumation along the three structural grains that control the major interior massifs are identified as a key contributor, leading to increased erosion in the provenance areas, increased sediment input, and resulting in progradation during the Barremian to Aptian. Smaller-scale features in the EAB have a wavelength of a few kilometres to maximum of 20 kilometres (see palaeohighs in figure. 5.11 and structural map in figure 5.1). The existence of local highs and their interaction with Lower Cretaceous strata have previously been noted in the literature (e.g. Duffaud et al., 1966; Rey et al., 1988). During maximum regression, the east-west trending small-scale structural features (anticlines) became exposed as palaeotopographic highs. These highs acted as small-scale drainage divides and provide a local sediment input, with immature carbonate-rich debrites interfingering with the fluvial channels and floodplains.

Subsequently, during the Aptian to Cenomanian exhumation slowed or was outpaced by eustatic sea-level rise, resulting in a regional transgression and return to carbonate sedimentation (Wurster and Stets, 1982).

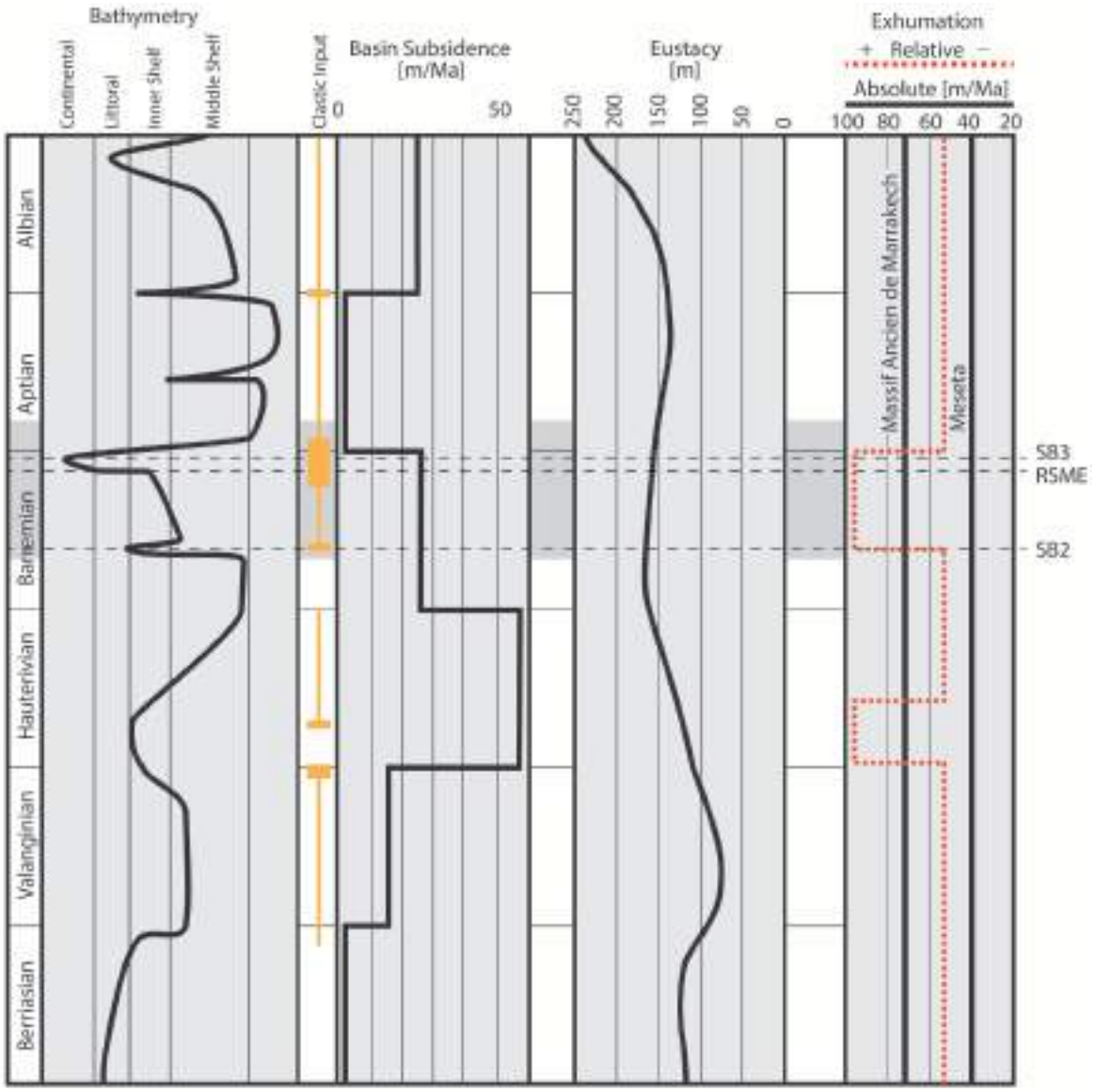

Figure 5.14: Controlling factors of sediment delivery in the Lower Cretaceous of the EAB. Bathymetry data modified from Butt (1982). Clastic input derived from field observations and regional studies (e.g. Butt, 1982). Subsidence curves represent uncompacted sediment thickness in the EAB against the time scale of Gradstein and Ogg (2012). Eustatic sea-level curve after Haq (2014). Exhumation rates for the Meseta based on Ghorbal et al. (2008), Ghorbal (2009), Saddiqi et al. (2009) and Barbero et al. (2011). Exhumation rates for the Massif Ancien de Marrakech based on Ghorbal (2009), Domenech (2015).

5.5.2 Eustatic sea-level changes

The local bathymetric curve for the EAB is shown in figure 5.2 and 5.14. This is a modified version from Butt (1982) and incorporates the work of Company et al. (2008), and this study. The lowest relative-sea level in the EAB during the Cretaceous occurred at the Barremian Aptian boundary. We interpret the observed advance of the shoreline toward

the basin as a coupled effect of exhumation and eustasy. Increased exhumation in the hinterland led to higher siliciclastic input and progradation during the highstand conditions (HST2). This was followed by a forced regression, expressed as a rapid progradation of the shoreline during FSST2 driven by a eustatic sea-level fall, ultimately leading to the development of sequence boundary 3.

No equivalent advance of the shoreline and siliciclastic-dominated system is observed throughout the Lower Cretaceous (Fig. 5.14) in the EAB. This would support an interpretation that eustasy is not the sole driver for base-level changes, as one would expect similar advances of siliciclastic systems during more pronounced global eustatic sea-level falls, e.g. during the Valanginian (Fig. 5.14). The remainder of the Lower Cretaceous is mud-dominated with only minor advances of mixed carbonate-siliciclastic depositional systems into the basin (e.g. the lower Hauterivian) but never developing coarse, siliciclastic-dominated systems and leading to the emersion of the shelf (Fig. 5.14).

Detailed biostratigraphy undertaken in this study (chapter 3 and 5) has allowed the correlation of the key surfaces identified in the study area with the sea-level curve of Haq (2014). Sequence boundary KBa4 *sensu* Haq (2014) would fall within the late Barremian *G. sartousiana* Zone and, therefore, predate the FSST2 and SB3. KAp1 *sensu* Haq (2014) straddles the early Aptian *D. forbesi* Zone and *D. deshayesi* Zone boundary and, therefore, post-dates SB3 (see Fig. 5.2). SB3 is thus correlated to sequence boundary KBa5 *sensu* Haq (2014). This is the best interpretation based on current understanding, however, it must be noted that dating of the sequence boundaries KBa5 and KAp1 (Haq, 2014) is subject to much discussion (see an alternative model for the Barremian-type section at Angles in France, Adatte et al. 2005) and has to be treated with care.

5.5.3 Climatic controls

Climate-controlled enhanced physical weathering in provenance areas could lead to greater siliciclastic input. However, there is no direct evidence in the published literature for a change in climate in the source areas during the Barremian to Aptian. In fact, the published studies addressing climatic conditions during the Lower Cretaceous of the EAB show no significant climatic changes overall (Wiedmann et al., 1978; Daoudi and Deconinck, 1994; Pletsch et al., 1996). The EAB is postulated to have been located within a broad arid equatorial climate zone (Hallam, 1985, Chumakov, 1995; Fluteau, 2007). Douadi

and Deconinck (1994) who suggest that the low percentage of kaolinite observed in Lower Cretaceous strata of the Atlantic basins, including the EAB, is linked to the absence of palaeosols in the hinterland due to a steep relief of the Meseta, High Atlas and the Anti-Atlas, preventing their development. The high percentage of illite reported by those authors is linked to erosion of exposed Precambrian and Palaeozoic strata. A significant further reduction of kaolinite is shown within the upper Barremian, likely a coupled effect of prevailing arid conditions and increased erosion during the regressive phase recognized in our study.

5.6 Conclusion

Integration of detailed sedimentary logging, structural studies, high-resolution biostratigraphy and mapping of a major regressive phase in the upper Barremian to lower Aptian has enabled the generation of detailed sequential palaeogeographic maps for the Haha and Agadir sub-basins of the EAB. Interpretation of the controls driving the forced regressive system indicate an important tectonic control for the development of sequence architecture along passive continental margins. Further this work adds to the documentation of forced regressive deposits, which come mainly from well-known examples of the Western Interior Seaway (e.g. Hampson et al., 1999, 2001) or the North Atlantic (e.g. Plink-Björklund and Steel, 2006), but published studies in the Central Atlantic Margin (CAM) are limited.

The main conclusions of this study are:

- A highstand system tract (HST2) is recognised in the upper Barremian to lowermost Aptian, where the shoreline progrades over a distance of ~ 40 Km.
- This regressive phase cannot be correlated to a major global eustatic event.
- Tectonic activity and regional exhumation of the hinterland, supported by recent low-temperature geochronology studies that identify km-scale post-rift vertical movements during the Late Jurassic to Early Cretaceous, is identified as the main control resulting in increased sediment input and shoreline progradation during the HST2.

- A subsequent further rapid progradation and down-stepping of the shoreline is interpreted as a forced regression (FSST2). This is interpreted to result from a superimposed eustatic sea-level fall, amplifying the tectonic signal and shifting the shoreline close to or beyond the modern-day shelf edge.
- During maximum regression shoreface systems along the shelf and shelf-edge delta system were most likely developed. Maximum regression led to exposure of the shelf and in many locations to the development of palaeosols next to zones of fluvial incision.
- The resultant incised valleys were subsequently infilled by mainly coarse clastic fluvial deposits during the lowstand systems tract (LST3).
- We recognise the influence of older reactivated normal faults along the margin, likely basin bounding faults, and preferential migration of the rivers into the relay zones is postulated along these north-south orientated features.
- East-west trending palaeohighs are also identified and play an important role in sediments routing and provide a provenance for locally-derived carbonate rich deposits (debrites) interacting with regional fluvial systems.
- The system was eventually drowned with re-establishment of shelfal conditions in the lower Aptian (Tamzergout Fm.).

The study provides the first integrated documentation of this major regressive phase on the Atlantic margin and highlights the role of tectonic activity on the flank of passive margins as an important control on sedimentation and sequence development.

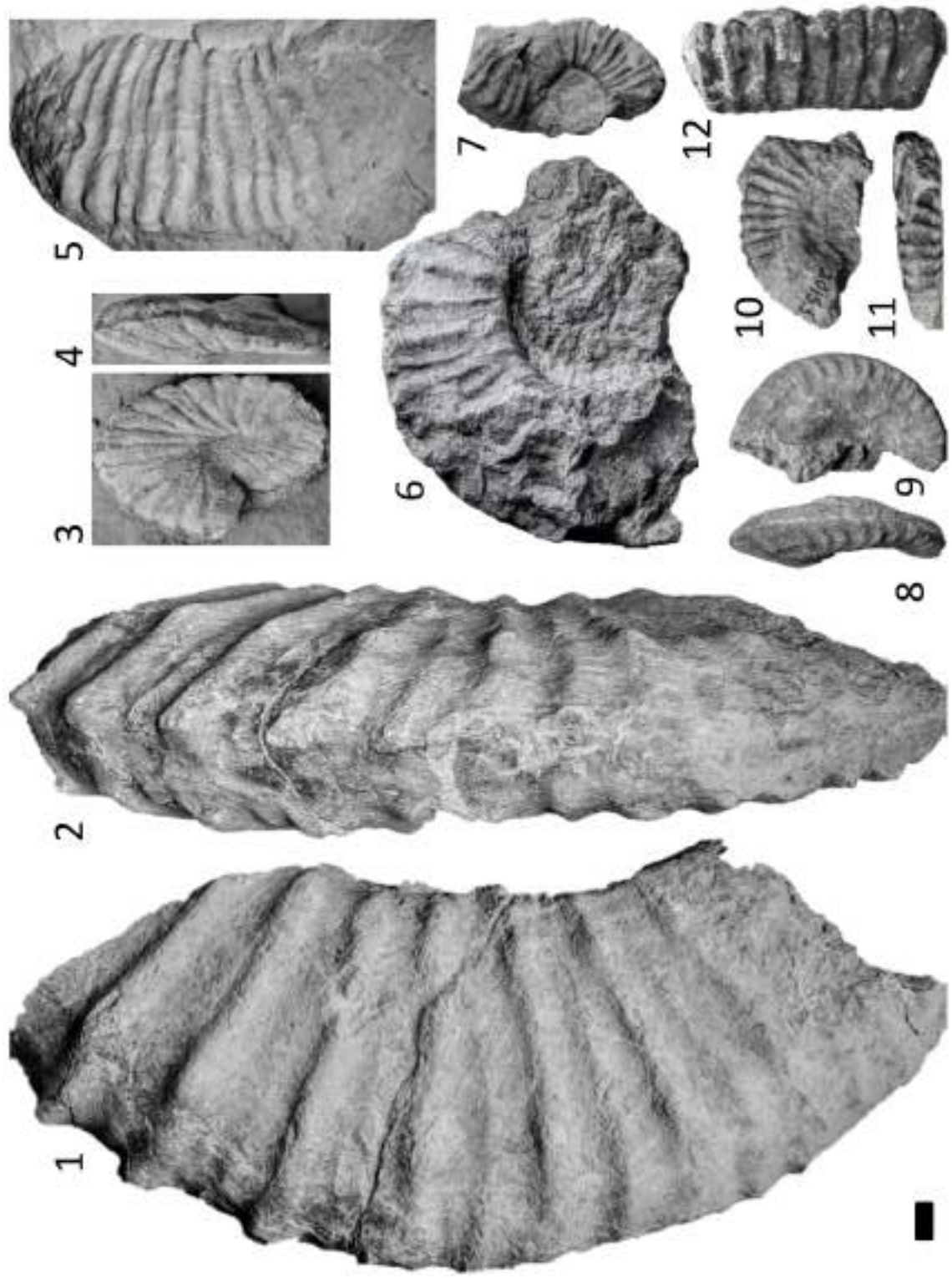

Figure 5.15: Upper Barremian ammonoid photographic plate.
Scale bar 10 mm: (1-2) *Gassendiceras* sp. cf. *multicostatum* Bert, Bersac, Delanoy and Canut, 2013 from bed **MTAS 101,** Assaka, *T. vandenheckii* Zone, *B. alpinum* Subzone ((Manch) LL. 16153); (3-4) *Gerhardtia sartousiana* (d'Orbigny, 1841), from Azziar (photographed in the field); (5) *Gassendiceras* gr. *hammatoptychum* (Douvillé, 1916 *non* Uhlig, 1883) from Tinker section, ? *T. vandenheckii* Zone, *B. alpinum* Subzone or *G. sartousiana* Zone (Silicon Cast (Manch) LL. 16154) (6) *Pachyhemihoplites* sp. cf. *dolloi* (Sarkar, 1955) from bed **MTAS 101s**, Assaka, *G. sartousiana* Zone, *G. sartousiana* Subzone ((Manch) LL. 16155); *Camereiceras limentinus* (Thieuloy, 1979) from bed **MTAS 101s**,

Assaka, *G. sartousiana* Zone, *G. sartousiana* Subzone ((Manch) LL. 16156); (8-9) *Kotetishvilia brevicostata* (Kotetishivili, 1980) from bed **MTAS 101s**, Assaka, *G. sartousiana* Zone, *G. sartousiana* Subzone ((Manch) LL. 16157); (10-11) *Janusites sp. cf. janus* (Thieuloy, 1979) from bed **MTAS 101s**, Assaka, *G. sartousiana* Zone, *G. sartousiana* Subzone ((Manch) LL. 16158);(12) *Toxancyloceras* sp. cf. *ebboi* Delanoy, 2004 from bed **MTAS 100,** Assaka, *T. vandenheckii* Zone, *B. alpinum* Subzone ((Manch) LL. 16159).

CHAPTER 6: SYNTHESIS, CONCLUSIONS AND FUTURE WORK

6.1 Synthesis

This PhD thesis is one project within a larger source-to-sink study to assess the evolution of the Moroccan continental margin during the Mesozoic and forms a collaboration between the Technical University of Delft and the University of Manchester. The source-to-sink study and this PhD commenced in January 2014.

The Lower Cretaceous post-rift succession is one of the main reservoir targets in the offshore Moroccan Atlantic margin, but commercial hydrocarbon reservoirs have so far proven elusive. This industry-sponsored project aims at improving our understanding of timing, location, and mechanisms of coarse clastic sediment delivery along the passive margin and particularly throughout the Essaouira-Agadir Basin (EAB). This main goal of the project is achieved through detailed stratigraphic investigation of specific intervals in the Lower Cretaceous.

Early in the study, it became apparent that a local high-resolution bio-chronostratigraphic framework was needed to gain control on the timing of depositional environment changes within the EAB and to enable correlation. Identification of major timelines and local marker beds was provided by a comprehensive review of the Aptian and upper Barremian ammonoid biostratigraphy. To constrain these observations further and enable detailed regional and inter-regional correlations other chronometers were integrated into the Aptian study, namely planktonic and benthic foraminifera, calcareous nannofossils and $\delta^{13}C$ analysis. Sequence stratigraphic interpretation of the regressive phase in the upper Barremian to lower Aptian was achieved by detailed sedimentological and stratigraphic logging and correlation of 20 sections in the Haha and Agadir sub-basins of the EAB.

Analysis of the Aptian to Lower Albian strata within the EAB led to the development of a new regional ammonoid biostratigraphic scale, comprising eight zones and subzones. A correlation to the Standard Mediterranean Ammonite Scale (SMAS) is proposed when possible (Fig. 6.1). Two important basin-scale hiatus are recognized, one spanning the middle part of the *D. forbesi* Zone to the lower part of the *E. martini* Zone and the other one including the *H. jacobi* Zone to the lower *L. tardefurcata* Zone (SMAS equivalent). The

Tiskatine section is recognised as the type section for the Aptian in the west-central part of the EAB.

Limitations of ammonoid biostratigraphic work come mainly from the endemism characterising the ammonoid assemblage in the EAB, the absence of key index specimens used in the SMAS and the precise definition of some zones and subzones in the SMAS. This precisely highlights the needs for local biostratigraphic and chronostratigraphic zonation schemes developed in chapters 3 and 4.

Detailed bed-by-bed analysis of the Tiskatine section has produced the first integrated, multi-disciplinary study of the Aptian in NW Africa. This study extends the global biostratigraphic and chemostratigraphic database for the Aptian of the Central Atlantic Margin, providing a high-resolution and well-documented reference section. Based on the distribution of foraminifera, three upper Aptian zones are recognised, the *G. ferreolensis* Zone, *G. algerianus* Zone, and the *H. trochoidea – P. bejaouensis* Zone. Observations from foraminifera data further support the hiatus of the *H. jacobi* Zone to *L. tardefurcata* Zone (SMAS equivalent). Two standard zones are recognized for calcareous nannofossils, NC7A and NC8A. Chemostratigraphic analysis of the Tiskatine section has yielded the first carbon isotope data from the Lower Cretaceous onshore of the NW African Atlantic Margin. $\delta^{13}C_{carb}$ and $\delta^{13}C_{org}$ curves here are correlated to the established sections in the Vocontian and Provençal Basins in SE France.

The work has greatly enhanced the regional and inter-regional application of the individual stratigraphic methods and updates timing and range of local and global stratigraphic markers. The findings of this study also highlight the need for revision of some key cosmopolitan biostratigraphic markers (e.g. ammonites versus foraminifera) and indicate further work is required on the SMAS type sections, which is being undertaken by NARG outside if this PhD.

During the upper Barremian to lowermost Aptian the littoral zone migrated up to and probably beyond the modern shelf edge. Unprecedented progradation over ~40 kilometres of the shoreface and deltaic deposits is recorded during highstand conditions. The driving mechanisms for this progradation have been evaluated. Migration of the shoreline that far into the basin has not previously been observed and is not observed later in the Cretaceous. Considering that the Cretaceous has other important eustatic sea-level falls it would be expected to see similar expressions in the stratigraphic record on the

shallow shelf. Based on the published literature in the region, the climate is interpreted to have had only a limited influence and the EAB was located in a broad and mostly arid climate belt throughout the Lower Cretaceous. However, the understanding of climate as a contributing factor remains the key risk due to the limited numbers of detailed studies carried out in the research area. A change in climate, e.g. a change to more humid conditions, could have led to signidicant increase in erosion and silicicasltic input from the provenance terrains. A growing body of studies shows unexpected post-rift exhumation of terranes in the hinterland of the study area during the Late Jurassic and Early Cretaceous. The main cause for progradation during the upper Barremian to lower Aptian is in this study attributed to exhumation in the hinterland and to the increased input of coarse siliciclastic material through denudation of the provenance terranes. Therefore, we here interpret a direct link between shoreline progradation and long-term exhumation of provenance terranes along a passive margin. A coupled effect of exhumation and change in climate can not be excluded but also not be discerned based on the currently published literature.

Within the EAB a subsequent and superimposed sea-level fall led to the exposure of the shelf, and development of attached forced regressive deposits. During this time the shoreline shifted close to or potentially beyond the Cretaceous shelf edge. Incision of fluvial systems, with a western to a southwestern mode of transport, led to the development of at least two incised valleys, one in the Haha and one in the Agadir sub-basins of the EAB. Based on palaeocurrent information, low-temperature geochronology and main structural features of the basin the catchment of the river systems established is interpreted to be located between the Western Moroccan Arch (WMA) to the east and the Meseta to the north of the study area (Fig. 6.2).

Following maximum regression, the depositional environment of the research area rapidly returned to open-marine shelfal sedimentation in the Aptian. The integrated biostratigraphic and chemostratigraphic work in the Aptian above the regressive deposits has also highlighted the presence and syn-sedimentary movement of north-south running palaeotopographic highs during the Lower Cretaceous. These highs were located close to the modern-day coastline. Highs are related to footwall uplift along pre-existing normal faults, likely basin bounding faults. At least three incremental movement phases have been identified within the lower Aptian. The rapid transgression is attributed to a eustatic sea-level rise coupled with increased subsidence indicated by fault activity in the basin. This

amplified signal leads to a significant increase in base-level along this low relief shelfal setting and rapid transgression. Another regional sequence boundary is located at the lower to upper Aptian boundary and falls within the first major hiatus identified. An uppermost Aptian tobasal Albian sequence boundary located within the second major hiatus has been interpreted onshore in the EAB and also offshore in DSDP borehole 370.

The sequence stratigraphic work carried out in this study has some limitations. The maximum inland extension of the shoreline is not known as it is located behind the limit of preservation for Lower Cretaceous outcrops in the study area. Similarly, the maximum basinward extension of the shoreline, beyond the modern coastline of Morocco, during maximum regression is also not known but might be revealed by future seismic data acquisition.

The timing, location and controls of sediment input points during the most significant regressive phase in the EAB have been greatly improved. The findings here question the validity of some of the global regressive events and if eustasy really is the sole driver of shoreline progradation along passive margins. Results of this PhD are in agreement with many recent works published showing that passive margins have a far more complex post-rift tectonic history than initially proposed.

6.2 Key findings of this thesis

The following objectives were defined to meet the aims of this thesis and are addressed with the key findings below:

Objective 1: Improving the dating resolution of the upper Barremian and Aptian strata in the Haha sub-basin of the EAB, to better constrain the coarse clastic sediment delivery phase of the upper Bouzergoun Formation.

- Upper Barremian strata investigated at the base of the Bouzergoun Fm. is constrained to the *G. sartousiana* and *T. vandenheckii* ammonoid zones.
- A synthetic figure for a local biostratigraphic framework of the upper Barremian to Lower Albian is shown figure 6.1, recognising 17 zones and subzones, of which five are newly introduced.
- The coarse clastic sediment delivery phase can be timed between the middle part of the *G. sartousiana* Zone and the lower part of the *D. forbesi* Zone.
- Additionally, offshore, the following ages have been assigned after reinvestigation of DSDP borehole 370: (*i*) a late Barremian age is established for the lower part of core 34-1 (NC6A Zone), (*ii*) an earliest Aptian age for the lower half of core 32-4 (NC6B Zone), and (*iii*) an early Albian age for core section 32-3 to 31-4 (NC8A Zone).

Objective 2: Building a bio-chronostratigraphic framework and sequence stratigraphic interpretation for the Aptian in the EAB, enabling regional and inter-regional correlation.

- The Tiskatine section is proposed as the reference section for the Aptian of NW Africa and high-resolution ammonoid, foraminifera and calcareous nannofossil biostratigraphy has been established, supplemented with chemostratigraphic data ($\delta^{13}C$).
- The top of the Bouzergoun Fm. is documented to be diachronous and ranges in age from early to early late Aptian (base of the *D. forbesi* Zone to lower part of the *C. tobleri* Zone)
- The Tamzergout Fm. is defined as ranging from the *P. dechauxi* Zone to the *E. tiskatinensis* Zone.
- An Early Albian age for the base of Oued Tidzi Fm. is established by the lowest occurrence of the genus *Douvilleiceras.*

- Three widely used foraminifera zones of the upper Aptian have been recognized in the EAB during this study: (*i*) *G. ferreolensis* Zone, (*ii*) *G. algerianus* Zone and the (*iii*) *H. trochoidea – P. bejaouensis* Zone.
- Two standard calcareous nannofossil Zones are recognized in the EAB: (*i*) NC7A and (*ii*) NC8A.
- The $\delta^{13}C_{org}$ curve, as well as the $\delta^{13}C_{carb}$ curve, can be correlated with the established curves of the Vocontian and Provençal Basin in SE France. The $\delta^{13}C$ record established at Tiskatine further supports the biostratigraphic analysis by comparison to the Vocontian Basin.
- Two basin wide hiatuses are recognized: (*i*) includes the middle part of the *D. forbesi* Zone to the lower part of the *E martini* Zone of SMAS; (*ii*) includes the *H. jacobi* Zone and the lower part of the *L. tardefurcata* Zone. These hiatuses are also supported by other bio- and chemostratigraphic markers.
- The following key sequence stratigraphic surfaces are interpreted in the transect between Id Amran and Assaka: (*i*) a regional lower to upper Aptian (*D. furcata* Zone to *C. tobleri* Zone) third order sequence boundary, (*ii*) a regional maximum flooding surface in the lower *"E." marocanus* Subzone, (*iii*) a regional third order sequence boundary in the *A. aschiltaensis* Zone, (*iv*) a regional third-order maximum flooding surface in *E. tiskatinensis* Subzone, and (*v*) a regional sequence boundary at the base of the Oued Tidzi Fm., suspected as being close to the Aptian/Albian boundary in age.

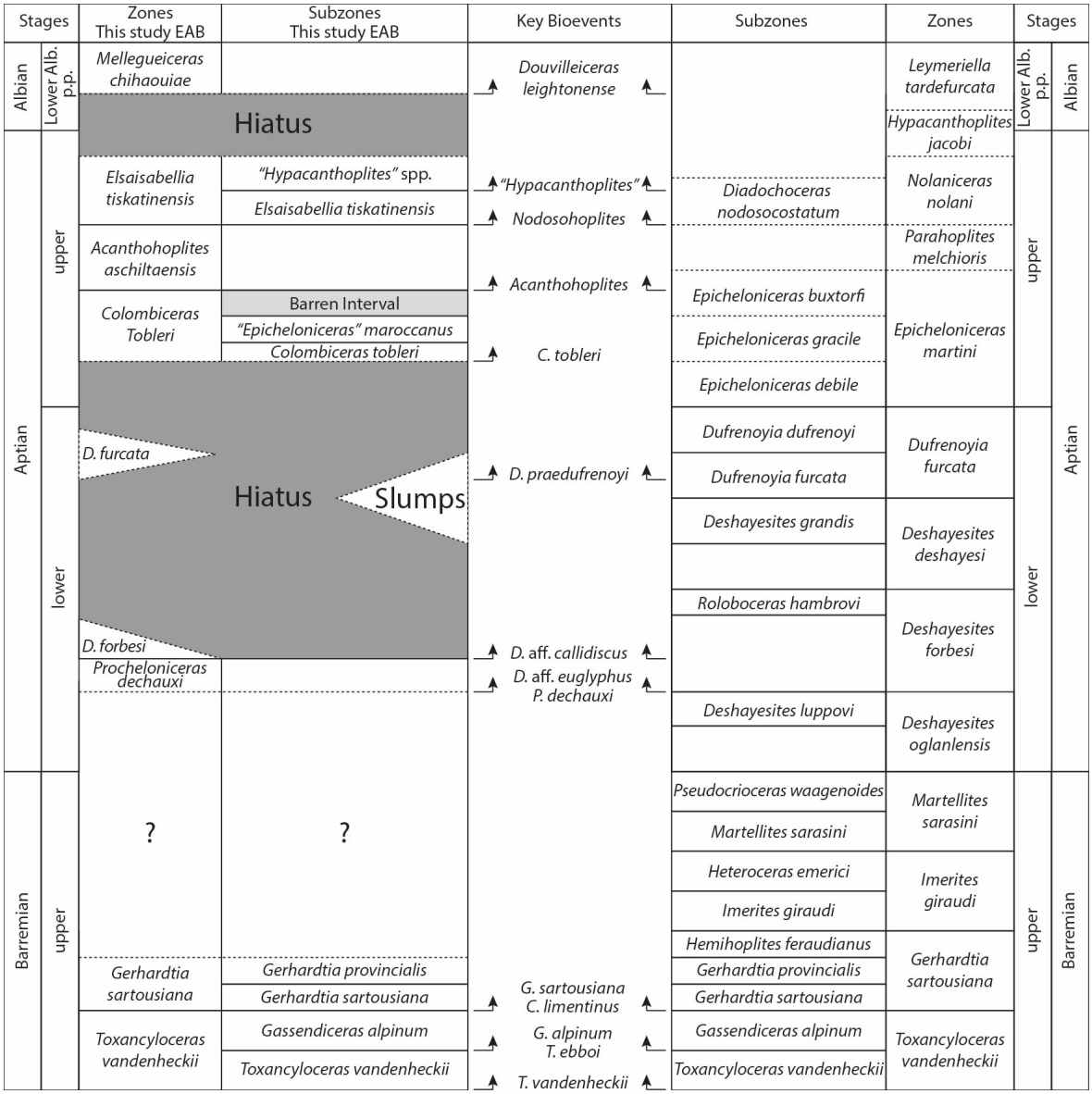

Figure 6.1 Synthetic biostratigraphic scale for the upper Barremian to Lower Albian of the Essaouira-Agadir Basin (EAB).
Comparison to the work of the Standard Mediterranean Ammonite Scale (SMAS) of Reboulet et al. (2011, 2014)

Objective 3 and 4: Investigating the coarse clastic sediment delivery system in the upper Barremian to lower Aptian through detailed and integrated stratigraphy. Reconstructing the sequence stratigraphy and palaeogeography of this key interval through field mapping and logging.

- The Bouzergoun formation has been subdivided into 3 members.
- The following key sequence stratigraphic surfaces and systems tracts have been identified around the regressive phase of the upper Barremian to lower Aptian: (*i*) a sequence boundary at the base of member 1 of the Bouzergoun Fm., (*ii*) a maximum flooding surface within Member 1, (*iii*) regressive surfaces of marine erosion below the sharp-based deltaic and shoreface deposits of Member 2, (*iv*) a sequence boundary forming during maximum regression within member 2, (*v*) initial transgressive surface separating fluvial deposits and floodplain deposits within member 2, and (*vi*) transgressive surface of erosion at the base of Member 3.
- During the falling stage systems tract the shoreline prograded close to the shelf edge and beyond the modern day coastline. This is the key time of potential coarse siliciclastic sediment delivery into the deep basin. A gross depositional environment map and interpreted catchment area during maximum regression is shown in figure 6.2.
- Subsequent transgression was rapid and followed by re-establishment of a shelfal depositional environment.
- Palaeohighs expose older Cretaceous and potentially Jurassic stratigraphy, which was eroded and their interaction with adjacent fluvial systems has been documented.
- Palaeocurrent data suggest an overall western to southwestern transport for the fluvial systems developing in the area, and approximately a north-south orientation of the shoreline during the regressive phase.
- The common presence of volcaniclastic clasts and feldspar suggest a first-order sedimentation cycle and erosion of igneous domains.

Objective 5: Identifying the mechanisms and controls on forced regressions in a passive margin setting.

- No significant climate changes can be ascertained, and thus climate is interpreted to have had only limited influence on the regressive phase during the upper Barremian to lower Aptian in the EAB.
- The main controlling factors resulting in progradation during the highstand systems tract is interpreted to be the increased sediment supply through long-term elevated exhumation in the hinterland.
- Subsequently a eustatic sea-level fall amplified the effect of continued exhumation of the hinterland and resulting progradation of the shoreline basinward by significantly lowering the base-level. It is the controlling factor leading to a forced regression, with maximum progradation of the shoreline to the shelf edge at the time and potentially beyond.
- This study documents the importance of post-rift vertical movements along passive margins and their direct influence on sediment delivery.

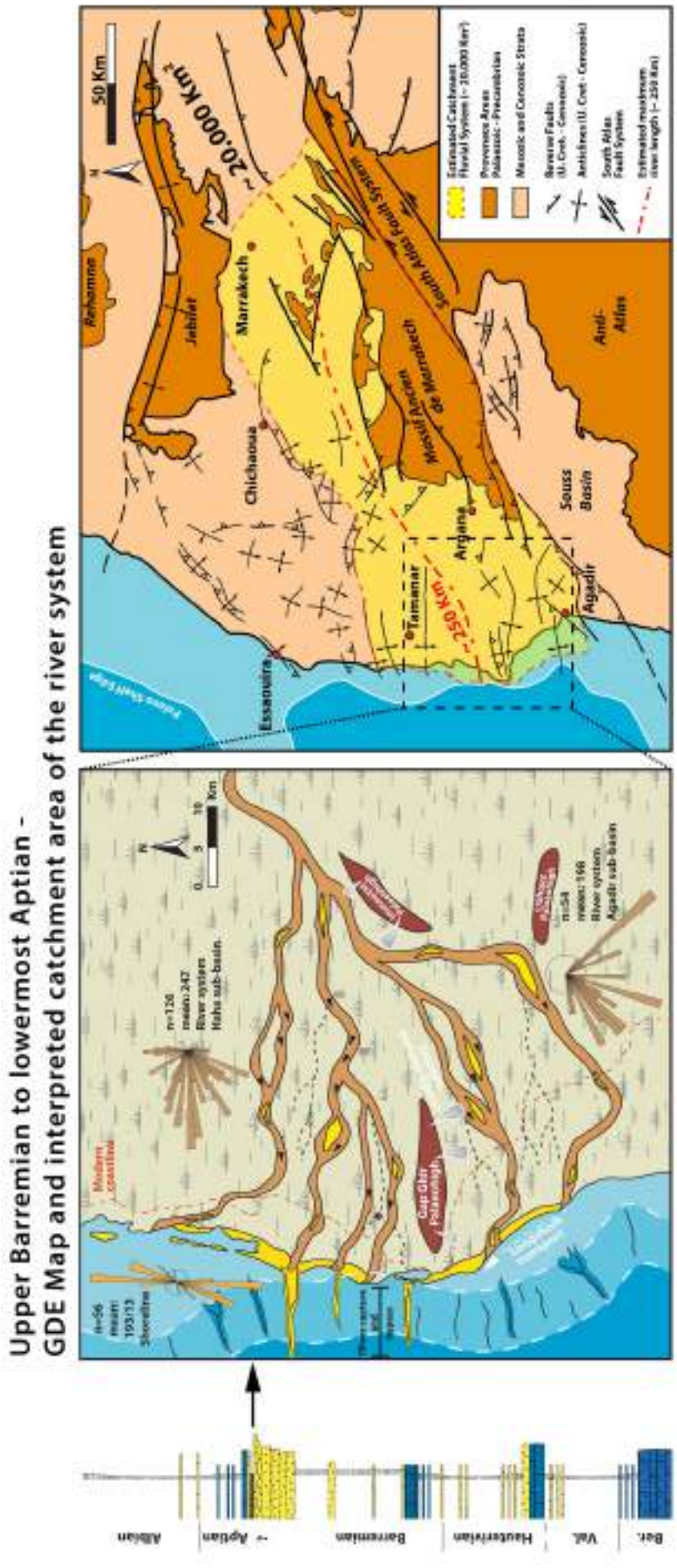

Figure 6.2: Upper Barremian to lowermost Aptian GDE map and catchment area.

6.3 Future work

Throughout the study the following main topics have been identified for future work:

6.3.1 Ammonoid biostratigraphic investigation

During the course of this PhD, many sections throughout the Lower Cretaceous were visited and presence of accessible sections with good outcrops has been documented. Abundant ammonoid fauna have been observed during reconnaissance studies, opening the potential for further biostratigraphic investigation. The Valanginian and Berriasian (Ettachfini, 1991, 2004; Ettachfini et al. 1998; Wippich, 2001) and lower Barremian (Company et al., 2008) sections have been investigated, but the Jurassic/Cretaceous boundary, the Hauterivian, and the Albian sections deserve a dedicated study. Ammonoid fauna seems to be scarce in the Albian and therefore other chronometers (e.g. calcareous nannofossils, foraminifera) should be utilised.

6.3.2 Integrated stratigraphy of the lower Aptian

During the fieldwork for chapter 4, we identified the presence of sections with lower Aptian strata where a detailed investigation for foraminifera, calcareous nannofossils and chemostratigraphy (TOC and $\delta^{13}C$) could be carried out. This would expand our work and would give further insight into the extent of the hiatus identified in the basin and the absence of the oceanic anoxic events on the shelf during the Aptian of the EAB. Additionally, an integrated study should be carried out in the Agadir segment of the EAB to further extend the local bio-chronostratigraphic framework established here and investigate similarities and potential differences of the two sub-basins.

6.3.3 The offshore record

To extend the integrated work done onshore and complement the hiatus recognised on the shallow shelf, a re-investigation of core and cuttings of the Aptian in offshore wells should be launched. This would greatly benefit the sponsoring companies and give insight into the dynamics of the various fossil groups in the Central Atlantic Margin.

Further, this could provide information on the extent and timing of oceanic anoxic events in the Central Atlantic Margin.

6.3.4 Sequence stratigraphic studies

An extension of the sequence stratigraphic work presented in chapter 5 into the Essaouira segment of the EAB is feasible. This would hold the potential to further constrain the timing of the regressive phase during the upper Barremian to lower Aptian and to map out the extent of the fluvial system developed during maximum regression.
Similarly, combined with biostratigraphy the lower Hauterivian and in particular, the Tamanar Formation with the extensive development of coral reef facies would require a re-investigation.

6.3.5 Provenance

Future work here will evaluate the provenance areas of the fluvial and shallow-marine sediments described throughout chapter 5 of this study. Adequate material was collected at various locations from fluvial outcrops of the Bouzergoun Formation. Feasibility of this study is indicated by the presence of volcanoclastic material and feldspar in thin sections pointing towards a first order sedimentation cycle. Heavy minerals have also been identified to be common in thin sections. Initial works show that distinct age populations exist in the hinterland providing the basis for detailed detrital heavy mineral studies. Ultimately this work could be extended to the lower Hauterivian and the Jurassic.

6.3.6 Quantification of the forced regressive phase

A detailed investigation into the extent of the river system discussed in chapter 5 with focus on quantifying the system (size of channels, channel belts, bar size, etc.) would be required. Combined with provenance works this could provide the size of the drainage of the river system and give information on sediment volumes being transported to the offshore.

6.3.7 Forced regressions along passive margins

Integrated stratigraphic studies of forced regressive deposits, or regressive deposits in general, along passive margins segments that document post-rift vertical movements would help to evaluate the main factors of shoreline migration and sediment delivery along passive margins. A holistic source-to-sink approach is favoured.

REFERENCES

Adams, A.E., Ager, D.V., Harding, A.G., 1980. Géologie de la région d'Imouzzer des Ida-ou-Tanane (Haut Atlas occidental). Notes et Mémoires du Service géologique du Maroc 41, 59–80.

Aguado, R., Castro, J.M., de Gea, G.A., 1999. Aptian bio-events – an integrated biostratigraphic analysis of the Almadich Formation, Inner Prebetic Domain, SE Spain. Cretaceous Research 20, 663–683.

Aitken, J.F., Flint, S.S., 1996. Variable expressions of interfluvial sequence boundaries in the Breathitt Group (Pennsylvanian), eastern Kentucky, USA. In: Howell, J.A., Aitken, J.F., Eds., High resolution sequence stratigraphy: Innovations and applications, Special Publications of the Geological Society London 104, 208-220.

Allan, J.R., Matthews, R.K., 1982. Isotope signatures associated with early meteoric diagenesis. Sedimentology, 29, 797–817.

Ambroggi, R., 1963. Etude géologique du versant méridional du Haut-Atlas occidental et de la plaine du Souss. Notes et Mémoires du Service Géologique du Maroc 157, 1–322.

Amorosi, A., Colalongo, M.L., 2005. The linkage between alluvial and coeval nearshore marine successions: evidence from the Late Quaternary record of the Po River Plain, Italy. In: Blum, M.D., Marriott, S.B., Leclair, S.F., Eds., Fluvial Sedimentology VII, International Association of Sedimentologists Special Publication 35, 257-275.

Ando, A., Woodard, S.C., Evans, H.F., Littler, K., Herrmann, S., 2013. An emerging palaeoceanographic 'missing link': multidisciplinary study of rarely recovered parts of deep-sea Santonian–Campanian transition from Shatsky Rise. Journal of the Geological Society 170, 381–84.

Andreu, B., 1989. Le Crétacé moyen de la transversale Agadir-Nador (Maroc): précisions stratigraphiques et sédimentologiques. Cretaceous Research 10, 49–80.

Anthula, D.J., 1900. Über die Kreidefossilien des Kaukasus mit einem allgemeinen Überblick über die Entwicklung der Sedimentärbildungen des Kaukasus. Beiträge zur Paläontologie und Geologie Österreich–Ungarns und des Orients 12 (1899), 55–159.

Armentrout, J.M., 1996. High resolution sequence biostratigraphy: examples from the Gulf of Mexico Plio-Pleistocene. Geological Society, London, Special Publications 104, 65–86.

Armstrong, H.A., Brasier, M.D., 2005. Microfossils. Blackwell Publishing Ltd (Wiley-Blackwell), Oxford, 296pp.

Arthur, M., Jenkyns, H.C., Brumsack, H.J., Schlanger, S.O., 1990. Stratigraphy, geochemistry and paleoceanography of organic carbon-rich Cretaceous sequences. In: Ginsburg, R.N., Beaudoin, B., (Eds.), Cretaceous Resources, Events and Rhythms, NATO ASI Series C, 304, 75–119. Springer-Verlag, Berlin.

Barbero, L., Teixell, A., Arboleya, M.-L., Río, P.D., Reiners, P.W., Bougadir, B., 2007. Jurassic-to-present thermal history of the central High Atlas (Morocco) assessed by low-temperature thermochronology. Terra Nova 19, 58–64.

Barragán-Manzo, R., Méndez-Franco, A.L., 2005. Towards a standard ammonite zonation for the Aptian (Lower Cretaceous) of northern Mexico. Revista Mexicana de Ciencias Geológicas 22, 39–47.

Barragán, R., Moreno-Bedmar, J.A., González-Arreola, C., 2016. Aptian ammonites from Mazapil, Zacatecas State (north-central Mexico) studied by Burckhardt in 1906: A revision – Carnets de Géologie 16/14, 355–367.

Baudin, F., Moullade, M., Tronchetti, G., 2008. Characterisation of the organic matter of upper Bedoulian and lower Gargasian strata in the historical stratotypes (Apt and Cassis-la-Bédoule areas, SE France). A revision – Carnets de Géologie / Notebooks on Geology 01, 1-9.

Bartenstein, H., Bettenstaedt, F., 1962. Marine Unterkreide (Boreal and Tethys). In: Simon, W., Bartenstein, H., Eds., Leitfossilen der Mikropaläontologie. Berlin: Gebrüder Borntraeger, 225–298.

Behrens, M., Krumsiek, K., Meyer, D.E., Schäfer, A., Siehl, A., Stets, J., Thein, J., Wurster, P., 1978. Sedimentationsabläufe im Atlas-Golf (Kreide Küstenbecken Marokko). Geologische Rundschau 67, 424–453.

Behrens, M., Siehl, L.A., 1982. Sedimentation in the Atlas Gulf: 1. Lower cretaceous clastics. In: Von Rad, U., Hinz, K., Samthein, M., Seibold, E. (Eds.), Geology of the Northwest African Continental Margin. 427–438. Springer-Verlag, Berlin.

Bellier, J.P., Moullade, M., 2002. Lower Cretaceous planktonic foraminiferal biostratigraphy of the western North Atlantic (ODP Leg 171B), and taxonomic clarification of key index species. Revue de Micropaléontologie 45, 9–26.

Bergen, J.A, 2000. Calcareous Nannofossils from the Lower Aptian Historical Stratotype at Cassis-La Bédoule (SE France). In: Moullade, M., Tronchetti, G., Masse, J.-P., Eds., Le stratotype historique de l'Aptien inférieur (Bédoulien) dans la région de Cassis-La Bédoule (S.E. France), Géologie méditerranéenne 25/3-4 (1998), 227–255.

Bergner, H.D., Gebhard, G., Wiedmann, J., 1982. Kondensationserscheinungen in der marokkanischen und alpinen Mittelkreide (Apt, Alb). Neues Jahrbuch für Geologie und Paläontologie. Abhandlungen 165, 102-124.

Bert, D., Bersac, S., Delanoy, G., Canut, L., 2013. Palaeontology, taxonomic revision and variability of some species of the genus Gassendiceras Bert et al., 2006 (Ammonitina, Upper Barremian) from southeastern France. Acta Geologica Polonica 63/3, 355-397.

Bettenstaedt, F., 1952. Stratigraphisch wichtige Foraminiferen-Arten aus dem Barreme vorwiegend Nordwest Deutschlands. Senckenbergiana, 33/4-6:275.

Bertotti, G., Gouiza, M., 2012. Post-rift vertical movements and horizontal deformations in the eastern margin of the Central Atlantic: Middle Jurassic to Early Cretaceous evolution of Morocco. International Journal of Earth Sciences 101, 2151–2165.

Bodin, S., Godet, A., Westermann, S., Föllmi, K. B., 2013. Secular change in northwestern Tethyan water-mass oxygenation during the late Hauterivian-early Aptian. Earth and Planetary Science Letters 374, 121–131.

Bodin, S., Meissner, P., Janssen, N.M.M., Steuber, T., Mutterlose, J., 2015. Large igneous provinces and organic carbon burial: Controls on global temperature and continental weathering during the Early Cretaceous. Global and Planetary Change 133, 238–253.

Bogdanova, T.N., 1983. *Deshayesites tuarkyricus* Zone – the lower zone of the Aptian in Turkmenia. Ezhegodnik Vsesojuznogo Paleontologischeskogo Obshchesteva 26, 128–147. [in Russian].

Bogdanova, T.N., Tovbina, S.Z., 1995. On development of the Aptian Ammonite zonal standard for the Mediterranean region. In: Bulot, L.G., Argot, M., Arnaud, H., (Eds.), Lower Cretaceous Cephalopod Biostratigraphy of the Western Tethys: Recent Developments, Regional Synthesis and Outstanding Problems, Géologie Alpine, Mémoire Hors Série 20 (1994), 51–59.

Bogdanova, T.N., Prozorovsky, V.A., 1999. Substantiation of the Barremian/Aptian boundary. Scripta Geologica, Special Issue 3, 45–81.

Bogdanova, T.N., Mikhailova, I.A., 2016. Middle Aptian Biostratigraphy and Ammonoids of the Northern Caucasus and Transcaspia. Paleontological Journal 50/8, 725–933.

Bolli, H.M., Loeblich, A.R., Jr., Tappan, H., 1957. Planktonic foraminiferal families Hantkeninidae, Orbulinidae, Globorotaliidae and Globotruncanidae. U.S. National Museum Bulletin 215, 3–50.

Bouatmani, R., Chakor Alami, A., Medina, F., 2007. Subsidence, evolution thermique et maturation des hydrocarbures dans le bassin d'Essaouira (Maroc): apport de la mode´lisation. Bull de l'Institut Scientifique, Rabat 29, 15–36.

BouDagher-Fadel, M. K., Banner, F.T., Whittaker, J.E., with a contribution from M. D. Simmons, 1997. The Early Evolutionary History of Plank tonic Foraminifera. British Micropalaeontological Society Public Series. Chapman and Hall, London, 269 pp.

Bown, P., Rutledge, D., Crux, J.A., Gallagher, L.T., 1998. Lower Cretaceous. In: Bown, P., Ed., Calcareous Nannofossil Biostratigraphy, 86-131, Chapman and Hall; Kluwer Academic.

Bown, P.R., Young, J.R., 1998. Techniques. In: Bown, Ed., Calcareous Nannofossil Biostratigraphy, 16-28.

Bown, P.R., 2005. 7. Early to Mid-Cretaceous calcareous nannoplankton from the Northwest Pacific Ocean, Leg 198, Shatsky Rise. In Bralower, T.J., Premoli Silva, I., and Malone, M.J. (eds.), Proceedings of the ODP, Scientific Results 198, 1–82.

Bralower, T.J., 1987. Valanginian to Aptian calcareous nannofossil stratigraphy and correlation with the upper M-sequence magnetic anomalies. Marine Micropaleontology 11, 293–310.

Bralower, T.J., Sliter, W.V., Arthur, M.A., Leckie, M.R., Allard, D., Schlanger, S.O., 1993. Dysoxic/Anoxic Episodes in the Aptian-Albian (Early Cretaceous). In: Pringle, M.S., Sager, W.S., Sliter, W.V., Stein, S., Eds, The Mesozoic Pacific. Geology, Tectonics and Volcanism. Geophysical Monograph Series 77, 5–37.

Bralower, T., Arthur, M.A ., Leckie, R.M., Sliter, W.V., Allard, D.J., Schlanger, S.O., 1994, Timing and paleoceanography of oceanic dysoxia/anoxia in the late Barremian to early Aptian (Early Cretaceous). Palaios 9, 335–369.

Brown, R. H., 1980. Triassic rocks of the Argana Valley, southern Morocco, and their regional structural implications. American Association of Petroleum Geologists Bulletin 64/7, 988–1003.

Bulot, L.G., 1993. Stratigraphical implications of the relationship between ammonites and facies; examples from the Lower Cretaceous (Valanginian–Hauterivian) of the Western Tethys: In: House, M.R., Ed., The Ammonoidea: Environment, Ecology and Evolutionary Change, The Systematics Association Special Volume 47, 243–265.

Bulot, L.G., 2010. Appendix. Systematic palaeontology of Aptian and Albian ammonites from southwest Iran. In: Vincent, B., van Buchem, F.S.P., Bulot, L.G., Immenhauser, A., Caron, M., Baghbani, D., Huc A.Y., Carbon–isotope stratigraphy, biostratigraphy and organic matter distribution in the Aptian-Lower Albian successions of southwest Iran (Dariyan and Kazhdumi formations). GeoArabia Special Publication 4/1, 167–195.

Bulot, L.G, Latil, J.-L., Hairabian, A., Fournillon, A., 2014. New insight on the genus *Nolaniceras* Casey, 1961 (Ammonoidea, Cretaceous) and its consequences on the biostratigraphy of the Aptian Stage. Proceedings of the Geologists' Association 125, 227–232.

Burckhardt, C., 1925. Faunas del Aptiano de Nazas (Durango). Boletín del Instituto Geológico de México 45, 7–71.

Butt, A., 1982. Micropaleontological bathymetry of the Cretaceous of western Morocco. Palaeogeography, Palaeoclimatology, Palaeoecology 37, 235–275.

Callomon, J., 1994. Palaeontological methods of stratigraphy and biochronology: some introductory remarks. GEO-BIOS 17, 16-30.

Canérot, J., Cugny, P., Peybernès, B., Rahhali, I., Rey, J., Thieuloy, J.-P., 1986. Comparative study of the Lower and Mid-Cretaceous Sequences on different Maghrebian shelves and basins – their place in the evolution of the North African Atlantic and Neotethysian margins. Palaeogeography, Palaeoclimatology, Palaeoecology 55, 213–232.

Caron, M., 1985. Cretaceous planktonic foraminifera. In: Bolli, H.M., Saunders, J.B. and Perch-Nielsen, K., Eds., Plankton Stratigraphy, Cambridge University Press, 17-86.

Casey, R., 1954. New genera and subgenera of Lower Cretaceous ammonites. Journal of the Washington Academy of Science 44/4, 106–115.

Casey, R., 1961a. The stratigraphical palaeontology of the Lower Greensand. Palaeontology 3, 487–621.

Casey, R., 1961b. A monograph of the ammonoidea of the Lower Greensand. Part II. Palaeontographical Society 114, 45–118.

Casey, R., 1962. A Monograph of the Ammonoidea of the Lower Greensand. Part IV. Palaeontographical Society, 217–288.

Casey, R., 1964. A Monograph of the Ammonoidea of the Lower Greensand. Part V. Palaeontographical Society (for 1963), 289–398.

Casey, R., Bayliss, H. M., Simpson, M. I., 1998. Observations on the lithostratigraphy and ammonite succession of the Aptian (Lower Cretaceous) Lower Greensand of Chale Bay, Isle of Wight, UK. Cretaceous Research 19, 511–535

Catuneanu, O., 2002 Sequence stratigraphy of clastic systems: concepts, merits, and pitfalls. Journal of African Earth Sciences 35, 1–43.

Catuneanu, O., 2006. Principles of Sequence Stratigraphy. Elsevier, Amsterdam,
pp. 386.

Catuneanu, O., Abreu, V., Bhattacharya, J.P., Blum, M.D., Dalrymple, R.W., Eriksson, P.G., Fielding, C. R., Fisher,W. L., Galloway, W. E., Gibling, M.R., Giles, K.A., Holbrook, J.M., Jordan, R., Kendall, C.G.St.C., Macurda, B., Martinsen, O.J., Miall, A.D., Neal, J.E., Nummedal, D., Pomar, L., Posamentier, H.W., Pratt, B.R., Sarg, J.F., Shanley, K.W., Steel, R.

J., Strasser, A., Tucker, M.E., and Winker, C., 2009. Towards the standardization of sequence stratigraphy. Earth-Science Reviews 92, 1-33.

Catuneanu, O., Galloway, W.E., Kendall, C.G.St.C., Miall, A.D., Posamentier, H.W., Strasser, A., Tucker, M., 2011. Sequence Stratigraphy: Methodology and Nomenclature. Newsletters on Stratigraphy 44/3, 173-245.

Cecca, F., Ropolo, P., Gonnet, R., 1999. The appearance of the genus *Deshayesites* (Kazansky, 1914, Ammonoidea) in the lowermost Aptian (Lower Cretaceous) of la Bédoule (SE France). Rivista Italiana di Paleontologia e Stratigrafia 105, 267–286.

Charton, R. et al., in review. Deciphering Phanerozoic vertical movements in Morocco: A qualitative and quantitative 1 study of Post-Variscan Source-to-Sink systems.

Chihaoui, A., Jaillard, E., Latil, J.-L., Zghal, I., Susperregui, A.S., Touir, J., Ouali, J., 2010. Stratigraphy of the Hameima and lower Fahdene Formations in the Tadjerouine area (Northern Tunisia). Journal of African Earth Sciences 58, 387–399.

Chumakov, N.M., Zharkov, M.A., Herman, A.B., Doludenko, M.P., Kalandadze, N.M., Lebedev, E.L., Ponomareko, A.G., Rautian, A.S., 1995. Climatic belts of the mid-Cretaceous time. Stratigraphy and Geological Correlation 3, 241-260.

Cohen, K.M., Finney, S.C., Gibbard, P.L. & Fan, J.-X., 2013 (updated). The ICS International Chronostratigraphic Chart. Episodes 36, 199-204.

Collet, L.W., 1907. Sur quelques espèces de l'Albien inférieur de Vöhrum (Hanovre). Mémoires de la Société de Physique et d'Histoire naturelle de Genève 35, 519–529.

Company, M., Sandoval, J., Tavera, J.M., Aoutem, M., Ettachfini, M., 2008. Barremian ammonite faunas from the western High Atlas, Morocco – biostratigraphy and palaeobiogeography. Cretaceous Research 29, 9–26.

Conte, G., 1981. "*Ammonites stobieskii*" d'Orbigny. Bulletin de la Société d'étude des Sciences Naturelles de Vaucluse 1979–1981, 65–70.

Cushman, J.A., Ten Dam, A., 1948. *Globigerinelloides*, a new genus of the Globigerinidae. Contributions From the Cushman Foundation for Foraminiferal Reseach 24/2, 42–43.

Damotte R., Magniez-Jannin, F. 1973. Ostracodes et foraminifères de l'Aptien inférieur du Sondage du Bois du Perchois (Aube). Bulletin d' Information des Géologues du Bassin de Paris 36, 3–47.

Daoudi, L., Deconinck, J., 1994. Contrôles paléogéographique et diagénétique des successions sédimentaires argileuses du Bassin Atlasique au Crétacé (Haut-Atlas Occidental, Maroc). Journal of African Earth Sciences 18, 123–134.

Dauphin, L., 2002. Litho–, bio–, et chronostratigraphie comparées dans le bassin Vocontien à l'Aptien. Doctoral Thesis, Université Lille 1, 451 pp. (Unpublished).

Davison, I., 2005. Central Atlantic margin basins of North West Africa: Geology and hydrocarbon potential (Morocco to Guinea). Journal of African Earth Sciences 43, 254–247.

De Gea, G.A., Castro, J.M., Aguado, R., Ruiz-Ortiz, P.A., Company, M., 2003. Lower Aptian carbon isotope stratigraphy from a distal carbonate shelf setting: the Cau section, Prebetic zone, SE Spain. Palaeogeography, Palaeoclimatology, Palaeoecology 200, 207–219.

Delanoy, G., 1995. About some significant ammonites from the Lower Aptian (Bedoulian) of the Angles-Barrême area (South-East France). Memorie Descrittive della Carta Geologica d'Italia 51, 65–101.

Delanoy, G., 1998. Biostratigraphie des faunes d'Ammonites à la limite Barrémien–Aptien dans la région d'Angles–Barrême–Castellane. Etude particulière de la famille des Heteroceratina Spath, 1922 (Ancyloceratina, Ammonoidea). Annales du Muséum d'Histoire Naturelle de Nice 12 (1997), 1–270.

Delanoy, G., Baudoin, C., Gonnet, R., Bert, D., 2008. Sur les faunes d'ammonites (Crétacé inférieur) du niveau glauconieux de la carrière des Trois–Vernes, près de Crest (Drôme, sud–est de la France). Annales du Muséum d'Histoire Naturelle de Nice 23, 11–65.

Dimitrova, N., 1967. Les fossiles de Bulgarie. IV. Crétacé Inférieur. Cephalopoda (Nautiloidea et Ammonoidea). 236 pp., Académie Bulgare des Sciences, Sofia.

Domenech, M., 2015. Rift opening and inversion in the Marrakech High Atlas: Integrated structural and thermochronological study. PhD Thesis, University Autonoma de Barcelona, 157 pp.

Doyle, P., Macdonald, I.M., 1993. Belemnite Battlefields. Lethaia 26, 65–80.

Dubourdieu, G., 1953. Ammonites nouvelles des Monts du Mellègue. Bulletin du Service de la Carte Géologique d'Algérie, Série Paléontologie 16, 1–76.

Duffaud, F., Brun, L., Planchut, B., 1966. Le bassin du Sud-Ouest marocain. In: Reyre, D. (Ed.), Bassins sédimentaires du Littoral africain, Symposium de l'Association des Services géologiques africains (New Dehli, 1964), 1ère partie, Littoral Atlantique, 5–12. Firmin Didot Publications, Paris.

Dutour, Y., 2005. Biostratigraphie, évolution et renouvellements des ammonites de l'Aptien supérieur (Gargasien) du bassin vocontien (Sud–Est de la France). Doctoral Thesis, Université Lyon 1, 302 pp. (Unpublished).

Egoian, V.L., 1965. On some ammonites of the Clansayesian from the western Caucasus. In: Fauna, stratigraphy and lithology of the Mesozoic and Caenozoic deposits of the Krasnodar region. Trudy Krasnodarskogo Filiala Vsesojuznogo Nauchno–Issledovatelskogo Instituta Neft 16, 112–160. [In Russian].

Egoian, V.L., 1969. Ammonites from the Clansayesian of western Caucasus. Trudy Krasnodaskyir Filial Vsesojuznogo Nauchno–Isslevatelskogo Neftegazovogo Instituta 19, 126–188. [in Russian].

Embry, A.F., 1995. Sequence boundaries and sequence hierarchies: problems and proposals. In: Steel, R.J., Felt, V.L., Johannessen, E.P. and Mathieu, C. (Eds), Sequence stratigraphy on the Northwest European Margin, Special Publication of the Norwegian Petroleum Society 5, 1–11.

Eristavi, M.S., 1960. Lower Cretaceous of the Caucasus and Crimea. Akademia Nauk Gruzinskoi SSR Monograph 10, 1–151. [in Russian].

Ettachfini, M., 1991. Le Valanginien de l'Atlas atlantique (Maroc): stratigraphie et ammonitofaune. Strata, Mémoire 15, 1–177.

Ettachfini, M., Company, M., Jaques, R., Taj-Eddine, K., Tavera, J.M., 1998. Le Valanginien du bassin de Safi (Maroc atlantique) et sa faune d'ammonites. Implications paléobiogéographiques. Comptes Rendus de l'Académie des Sciences de Paris, Sciences de la Terre et des Planètes 327, 319–325.

Ettachfini, M., 2004. Les ammonites néocomiennes dans l'Atlas atlantique (Maroc): biostratigraphie, paléontologie, paléobiogeographie et paléoécologie. Strata, Mémoire 43, 1–223.

Fallot, P., Termier, H., 1923. Ammonites nouvelles des Îles Baléares. Trabajos del Museo Nacional de Ciencias Naturales de Madrid, Serie Geológica 32, 1–83.

Fluteau, F., Ramstein, G., Besse, J., Guiraud, R., Masse, J.P., 2007. Impacts of palaeogeography and sea level changes on Mid-Cretaceous climate. Palaeogeography, Palaeoclimatology, Palaeoecology 247, 357-381.

Föllmi, K.B.,1990. Condensation and phosphogenesis: example of the Helvetic mid Cretaceous (northern Tethyan margin). In: Notholt, A.J.G., Jarvis, I., Eds., Phosphorite Research and Development, Geological Society Special Publication 52, 237–252.

Föllmi, K.B., Godet, A., Bodin, S., Linder, P., 2006. Interactions between environmental change and shallow water carbonate buildup along the northern Tethyan margin and their impact on the Early Cretaceous carbon isotope record. Paleoceanography 21, 1–16.

Föllmi, K.B., 2012. Early Cretaceous life, climate and anoxia. Cretaceous Research 35, 230–257.

Frau, C., Delanoy, G., Hourquieg, E., 2015. Le genre *Macroscaphites* Meek, 1876 (Ammonoidea) dans l'Aptien inférieur de Cassis-La Bédoule (Bouches-du-Rhône, France). Proposition d'un nouveau schéma zonal pour la série stratotypique. Revue de Paléobiologie 34, 45–57.

Frau C., Delanoy G., Masse J.-P., Lanteaume C., Tendil, A.J.B., 2016. New Heteroceratidae (Ammonoidea) from the late Barremian deepening succession of Marseille (Bouches–du–Rhône, France). Acta Geologica Polonica 66/2, 179–199.

Frau C., Pictet, A., Spangenberg, J., Masse J.-P., Tendil, A.J.B., Lanteaume C., 2017a. New insights on the age of the post-Urgonian marly cover of the Apt region (Vaucluse, SE France) and its implications on the demise of the North Provence carbonate platform. Sedimentary Geology, in press. doi:10.1016/j.sedgeo.2017.08.003

Frau, C., Bulot, L.G., Delanoy, G., Moreno-Bedmar, J.A., Masse, J.-P., Tendil, A.J.-B., Lanteaume, C., 2017b. The candidate Aptian GSSP at Gorgo a Cerbara (Central Italy): an alternative interpretation of the bio-, litho- and chemostratigraphic markers. Newsletter on Stratigraphy, in press.

Fritel, P. .-H.,, 1906. Sur les variations morphologiques d'*Acanthoceras Milletianum* d'Orb. sp. Le Naturaliste 28 (472), 245–247.

Frizon de Lamotte, D., Zizzi, M., Missenard, Y., Hafid, M., El Azzouzi, M., Maury, R.C., Charriere, A., Taki, Z., Benammi, M., Michar, A., 2008. The Atlas System. In: Michard, A., Saddiqi, O., Chalouan, A., Frizon de Lamotte, D., Eds., Continental Evolution: The Geology of Morocco. Lecture Notes of Earth Science, 133-202.

Fürsich, F.T., Oschmann, W., 1993. Shel beds as tools in basin analysis: the Jurassic of the Kachchh, western India. Journal of the Geological Society, London 150, 169-185.

Gandolfi, R., 1942. Ricerche micropaleontologiche e stratigraphfiche sulla Scaglia e sul flysch Cretacici dei Dintorni di Balerna (Canton Ticino). Rivista Italiana Paleontologia 48, 1–160.

Gauthier, H., Busnardo, R., Combémorel, R., Delanoy, G., Fischer, J.-C., Guérin-Franiatte, S., Joly, B., Kennedy, W.J., Sornay J., Tintant, H., 2006. Volume IV. Céphalopodes crétacés. In: Fischer, J.-C., (Ed.), Révision critique de la Paléontologie Française d'Alcide d'Orbigny, incluant la réédition de l'original. 982 pp. Backhuys Publishers, Leiden.

Gawthorpe, R.L., Leeder, M.R., 2000. Tectono-sedimentary evolution of active extensional basin. Basin Research 12, 195-218.

GEBCO (2014), Gridded bathymetric data sets, British Oceanographic Data Centre (BODC).

Gebhard, G., 1982. Glauconitic condensation through high-energy events in the Albian near Clars (Escragnolles, Var, SE-France). In: Einsele, G., Seilacher, A., Eds., Cyclic and Event Stratification, 286–298. Springer-Verlag, New York.

Ghorbal, B., Bertotti, G., Foeken, J., Andriessen, P., 2008. Unexpected Jurassic to Neogene vertical movements in 'stable' parts of NW Africa revealed by low temperature geochronology. Terra Nova 20, 355–363.

Ghorbal, B., 2009. Mesozoic to Quaternary thermo-tectonic evolution of Morocco (NW Africa): PhD Thesis, Vrije Universiteit Amsterdam, 231 pp.

Gill, T., 1871. Arrangement of the Families of Mollusks. Smithsonian Miscellaneous Collections 227, 49 p.

Glazunova, A.E., 1953. Ammonites of the Aptian and Albian of Kopet–Dag, Lesser and Greater Balkhans and Mangyshlak. Trudy VSEGEI, 156 pp. Moscow. [In Russian].

Godet, A., Hfaiedh, R., Arnaud-Vanneau, A., Zghal, I., Arnaud, H., Ouali, J., 2014. Aptian palaeoclimates and identification of an OAE1a equivalent in shallow marine environments of the southern Tethyan margin: Evidence from Southern Tunisia (Bir Oum Ali section, Northern Chott Chain). Cretaceous Research 48, 110–129.

Gouiza, M., Bertotti, G., Hafid, M., Cloetingh, S., 2010. Kinematic and thermal evolution of the Moroccan rifted continental margin: Doukkala-High Atlas transect. Tectonics 29, 1-22.

Gouiza, M., 2011. Mesozoic source-to-sink systems in NW Africa: Geology of vertical movements during the birth and growth of the Moroccan rifted margin: PhD Thesis, Vrije Universiteit Amsterdam, 192 pp.

Gouiza, M., Charton, R., Bertotti, G., Andriessen, P. and Storms, J.E.A., 2017. Post- Variscan evolution of the Anti-Atlas belt of Morocco constrained from low-temperature geochronology. International Journal of Earth Sciences 106, 593–616.

Grabert, B., 1959. Phylogenetische Untersuchungen an *Gaudryina* und *Spiroplectinata* (Foram.) besonders aus dem nordwestdeutschen Apt und Alb. Senckenberg. Gesellschaft für Naturforschung, Abhandlung 498, 1–71.

Gradstein, F.M., Ogg, J.G., 2012. In: Schmitz, M.D., Ogg, G.M., Eds., The Geological Time Scale 2012, 1176 pp.

Hafid, M., Aït Salem, A., Bally, A.W., 2000. The western termination of the Jebilet–High Atlas system (Offshore Essaouira Basin, Morocco). Marine and Petroleum Geology 17, 431–443.

Hafid, M., Zizi, M., Bally, A.W., Aït Salem, A., 2006. Structural styles of the western onshore and offshore termination of the High Atlas, Morocco. Comptes Rendus Geoscience 338, 50–64.

Hamberg, L., Nielsen, L.H., 2000. Shingled, sharp-based shoreface sandstones: depositional response to stepwise forced regression in a shallow basin, Upper Triassic Gassum Formation, Denmark. In: Hunt, D., Gawthorpe, R.L., Eds., Sedimentary Responses to Forced Regressions, Special Publications Geological Society London 172, 69-89.

Hampson, G.J., Howell,J.A., Flint, S.S., 1999. A sedimentological and sequence stratigraphic re-interpretation of the Upper Cretaceous Prairie Canyon Member (''Mancos B'') and associated strata, Book Cliffs area, Utah, U.S.A. Journal of sedimentary research 69/2, 414–433.

Hampson, G.J., Burgess, P.M., Howell, J.A., 2001. Shoreface tongue geometry constrains history of relative sea-level fall: examples from Late Cretaceous strata in the Book Cliffs area, Utah. Terra Nova 13/3, 188-196.

Hallam, A., 1985. A review of Mesozoic climates. Journal of the geological society, London 142, 433-445.

Haq, B.U., Hardenbol, J., Vail, P.R., 1987. Chronology of fluctuating sea levels since the Triassic. Science 235, 1156-1167.

Haq, B.U., 2014. Cretaceous eustasy revisited. Global and Planetary Change 113, 44–58.

Hardenbol, J., Thierry, J., Farley, M.B., Jacquin, T., de Graciansky, P.C., Vail, P.R., 1998. Mesozoic and Cenozoic sequence chronostratigraphic framework of European basins. In: De Graciansky, P.C., Hardenbol, J., Jacquin, T., Vail, P.R. (Eds.), Mesozoic and Cenozoic Sequence Stratigraphy of European Basins, SEPM, Special Publications 60, 3–13.

Helland-Hansen, W. and Gjelberg, J.G., 1994. Conceptual basis and variability in sequence stratigraphy: a different perspective. Sedimentary Geology 92, 31-52.

Helland-Hansen, W., Martinsen, O.J., 1996. Shoreline trajectories and sequences: description of variable depositional-dip scenarios. Journal of Sedimentary Research 66, 670-688.

Herrle, J.O., 2002. Mid-Cretaceous paleoceanographic and paleoclimatologic implications on black shale formation of the Vocontian Basin and Atlantic. Evidence from calcareous nannofossils and stable isotopes. Tübinger Mikropaläontologische Mitteilungen 27, 1–114.

Herrle, J.O., Mutterlose, J., 2003. Calcareous nannofossils from the Aptian-Lower Albian of southeast France: palaeoecological and biostratigraphic implications. Cretaceous Research 24, 1–22.

Herrle, J.O., Kössler, P., Friedrich, O., Erlenkeuser, H., Hemleben, C., 2004. High-resolution carbon isotope records of the Aptian to Lower Albian from SE France and the Mazagan Plateau (DSDP Site 545): a stratigraphic tool for paleoceanographic and paleobiologic reconstruction. Earth and Planetary Science Letters 218, 149–161.

van Hinte, J.E., 1976. A Cretaceous time scale. AAPG Bulettin 60, 498-516

Hoedemaker, P. J., Bulot, L.G. (reporters) 1990. Preliminary ammonite zonation of the Lower Cretaceous of the Mediterranean Region. Géologie Alpine 66, 123–127.

Hoedemaeker, P. J., Company, M. (reporters), Aguirre-Urreta, M.B., Avram, E., Bogdanova, T.N., Bujtor, L., Bulot, L.G., Cecca, F., Delanoy, G., Ettachfini, M., Memmi, L., Owen, H.G., Rawson, P. F., Sandoval, J., Tavera, J. M., Thieuloy, J.-P., Tovbina, S.Z., Vašíček, Z., 1993. Ammonite zonation for the Lower Cretaceous of the Mediterranean region; basis for the stratigraphic correlations within IGCP-Project 262. Revista Española de Paleontología 8, 117–120.

Hofmann, A., Tourani, A., Gaupp, R., 2000. Cyclicity of Triassic to Lower Jurassic continental red
beds of the Argana Valley, Morocco: implications for palaeoclimate and basin evolution. Palaeogeography, Palaeoclimatology, Palaeoecology 161, 226–266.

Huck, S., Heimhofer, U., Rameil, N., Bodin, S., Immenhauser, A., 2011. Strontium and carbon-isotope chronostratigraphy of Barremian-Aptian shoal-water carbonates: Northern

Tethyan platform drowning predates OAE 1a. Earth and Planetary Science Letters 304, 547–558.

Humphrey, W.E., 1949. Geology of the Sierra de los Muertos area, Mexico (with descriptions of Aptian cephalopods from the La Peña Formation). Geological Society of America, Bulletin 60, 89–176.

Hunt, D. and Tucker, M.E., 1992, Stranded parasequences and the forced regressive wedge systems tract: deposition during base-level fall. Sedimentary Geology 81, 1-9.

Hunt, D. and Tucker, M.E., 1995, Stranded parasequences and the forced regressive wedge systems tract: deposition during base-level fall - reply. Sedimentary Geology 95, 147-160.

Hyatt, A., 1900. Cephalopoda. In: Zittel, K.A., von, 1896–1900, Textbook of Palaeontology, pp. 502–604. Macmillan, London and New York (translation C. R. Eastman).

Immenhauser, A., Kenter, J.A.M., Ganssen, G., Bahamonde, J.R., Van Vliet, A., Saher, M.H., 2002. Origin and Significance of Isotope Shifts in Pennsylvanian Carbonates (Asturias, NW Spain). Journal of Sedimentary Research 72, 82–94.

Jacob, C., 1905. Étude sur les ammonites et sur l'horizon stratigraphique du gisement de Clansayes. Bulletin de la Société Géologique de France 5ème Série 4, 399–432.

Jacob, C., Tobler, A., 1906. Étude stratigraphique et paléontologique du Gault de la vallée de la Ellenberger Aa (Alpes calcaires suisses, environs du Lac des Quatre Cantons). Mémoire de la Société Paléontologique de Suisse 33, 3–26.

Jansa, L.F, Wiedmann, J., 1982. Mesozoic-Cenozoic Development of the Eastern North American and Northwest African Continental Margins: A Comparison. In: von Rad, U., Hinz, K., Samthein, M., Seibold, E., (Eds.), Geology of the Northwest African Continental Margin, 215–269. Springer-Verlag, Berlin.

Jarvis, I., Gale, A.S., Jenkyns, H.C., Pearce, M.A., 2006. Secular variation in Late Cretaceous carbon isotopes: a new δ13C carbonate reference curve for the Cenomanian-Campanian (99.6-70.6 Ma). Geological Magazine 143, 561–608.

Jeremiah, J.M., 1996. A proposed Albian to Lower Cenomanian nannofossil biozonation for England and the North Sea Basin. Journal of Micropalaeontology 15, 97–129.

Jeremiah, J., 2000. Lower Cretaceous turbidites of the Moray Firth: sequence stratigraphical framework and reservoir distribution. Petroleum Geoscience 6, 309-328, Supplementary Publication No. SUP 18155, 1-19.

Jeremiah, J.M., 2001. A Lower Cretaceous nannofossil zonation for the North Sea Basin. Journal of Micropalaeontology 20, 45–80.

Jeremiah, J.M., Duxbury, S., Rawson, P., 2010. Lower Cretaceous of the southern North Sea Basins: reservoir distribution within a sequence stratigraphic framework. Netherlands Journal of Geosciences / Geologie en Mijnbouw 89, 203–237.

Kazansky, P.A., 1914. Description d'une collection des céphalopodes des terrains Crétacés du Daghestan. Izvestiya Tomskogo Tekhnicheskogo Instituta 32/4, 1–127. [in Russian].

Kennedy, W.J., Gale, A.S., Bown, P.R., Caron, M., Davey, R.J., Gröcke, D., Wray, D.S., 2000. Integrated stratigraphy across the Aptian-Albian boundary in the Marnes Bleues, at the Col Pré-Guittard, Arnayon (Drôme), and at Tartonne (Alpes-de-Haute-Provence), France: a candidate Global Boundary Stratotype Section and Boundary Point for the base of the Albian Stage. Cretaceous Research 21, 591–720.

Kennedy, W.J., Gale, A.S., Huber, B.T., Petrizzo, M.R., Bown, P., Barchetta, A., Jenkyns, H.C., 2014. Integrated stratigraphy across the Aptian/Albian boundary at Col de Pré-Guittard (southeast France): A candidate Global Boundary Stratotype Section. Cretaceous Research 51, 248–259.

Kilian, W., Gentil, L., 1906. Découverte de deux horizons crétacés remarquables au Maroc. Comptes rendus sommaire de l'Académie des Sciences de Paris 142, 603–605.

Kilian, W., Reboul, P., 1915. La faune de l'Aptien inférieur des environs de Montélimar (Drôme) (Carrière de l'Homme d'Armes). In: Kilian, W. (Ed.), Contribution à l'étude des faunes paléocrétacées du Sud–Est de la France, Mémoires pour servir à l'Explication de la Carte Géologique détaillée de la France 14, 1–221.

Klein, J., Bogdanova, T., 2013. Lower Cretaceous Ammonites VI Douvilleiceratoidea and Deshayesitoidea. In: Riegraf, W., (Ed.), Fossilium Catalogus I: Animalia 151, pp. 1–299, Backhuys Publishers; Leiden.

Kotetishvili, E., 1980. Semeystvo Pulchellidae H . Douvillé (iznishnemelovykh otlosheniy Yuga SSSR) (The Family Pulchelliidae H . Douvillé (from the Lower Cretaceous of South USSR)). — Trudy. Geol. Inst. Akad . Nauk. Gruz . SSR, 67:1110 (in Russian).

Kotetishvili, E., 1986. Zonal'naya stratigrafiya Nishnemelovykh otlosheniy Gruzi i i paleozoogeogrfiya Pannemelovykh basseynov Sredizemnomorskoy oblasti. (The zonal stratigraphy of the Lower Cretaceous deposits of Georgia and palaeozoogeography of the Mediterranean Early Cretaceous bassins). — Trudy. Geol. Inst. Akad . Nauk Gruz . SSR, 91:1-160 (in Russian).

Koutsoukos, E.A.M., Mello, Azambuja Filho, M.R.N.C., Hart, M.B., Maxwell, J.R. 1991. The Upper Aptian-Albian Succession of the Sergipe Basin, Brazil: An Integrated Palaeoenvironmental Assessment. American Association of Petroleum Geologists, Bulletin 75, 479-498.

Kuhnt, W., Moullade, M., 2007. The Gargasian (Middle Aptian) of La Marcouline section at Cassis-La Bédoule (SE France): Stable isotope record and orbital cyclicity. Carnets de Geologie, Article 2007/02, 9 p.

Kuhnt, W., Holbourn, A., Moullade, M., 2011. Transient global cooling at the onset of early Aptian oceanic anoxic event (OAE) 1a. Geology 39, 323–326.

Kump, L.R., Arthur, M.A., 1999. Interpreting carbon-isotope excursions: carbonates and organic matter. Chemical Geology 161, 181–198.

Kvantaliani, I.V., 1971. Aptian ammonites of Abhakazia. Gruzinski Politekhnicheskii Institut, Tbilisi 98, 1–175. [in Russian].

Kvantaliani, I.V., 1972. Some new species of the Clansayesian of Abkhazia. Journal of the Georgian Geological Society, Academy of Sciences 8(1/2), 10–27.[in Russian].

Larson, R.L., Erba, E., 1999, Onset of the mid-Cretaceous greenhouse in the Barremian-Aptian: Igneous events and the biological, sedimentary, and geochemical responses. Paleoceanography 14, 663–678.

Lancelot, Y., Winterer, E.L., 1980. Evolution of the Moroccan Oceanic Basin and Adjacent Continental Margin—A Synthesis. In: Lancelot, Y., Winterer, E.L., Eds., Initial Reports Deep Sea Drilling Vol. L, 801-821

Latil, J.-L., 2011. Early Albian ammonites from Central Tunisia and adjacent areas of Algeria. Revue de Paléobiologie 30/1, 321–429.

Laville, E., Pique, A., Amrhar, M., Charroud, M., 2004. A restatement of the Mesosoic Atlasic Rifting (Morocco). Journal of Africa Earth Sciences 38, 145–153.

Leckie, R., Bralower, T.J., Cashman, R., 2002. Oceanic anoxic events and plankton evolution: Biotic response to tectonic forcing during the mid-Cretaceous. Paleocenography 17, 1–29.

Lehmann, J., Heldt, M., Bachmann, M., Hedi Negra, M.E., 2009. Aptian (Lower Cretaceous) biostratigraphy and cephalopods from north central Tunisia. Cretaceous Research 30, 895–910.

Lehmann, J., Friedrich, O., von Bargen, D., Hemker, T., 2012. Early Aptian bay deposits at the southern margin of the lower Saxony Basin: Integrated stratigraphy, palaeoenvironment and OAE 1a. Acta Geologica Polonica 62/1, 35–62.

Lehmann, J., von Bargen, D., Engelke, J., Claßen, J., 2016: Morphological variability in response to palaeoenvironmental change – a case study on Cretaceous ammonites. Lethaia 49, 73–86.

Leprêtre, R., Missenard, Y., Barbarand, J., Gautheron, C., Saddiqi, O. and Pinna-Jamme, R., 2015. Post-rift history of the eastern Central Atlantic passive margin: insights from the Saharan region of South Morocco. Journal of Geophysical Research: Solid Earhth 120/6, 1–58.

Le Roy, P., Piqué, A., 2001. Triassic–Liassic Western Moroccan synrift basins in relation to the Central Atlantic opening. Marine Geology 172, 359–381.

Loutit, T.S., Hardenbol, J., Vail, P.R., Baun, G.R., 1988. Condensed sections: the key to age determination and correlation of continental margin sequences. In: Wilgus, C.K., Hastings, B.S., Kendall, C.G.S.C, Posamentier, H., Ross, C.A., Van Wagoner, J.C., Eds., Sea-Level Changes: An Integrated Approach. SEPM Spec. Publ. 42, 183-213.

Luber, T.L., Bulot, L.G., Redfern, J., Frau, C., Arantegui, A., Masrour, M., 2017. A revised ammonoid biostratigraphy for the Aptian of NW Africa: Essaouira-Agadir Basin, Morocco. Cretaceous Research 79, 12–34.

Marshall, J.D., 1992. Climatic and oceanographic isotopic signals from the carbonate rock record and their preservation. Geological Magazine 129(2), 143–160.

McAnena, A., Flögel, S., Hofmann, P., Herrle, J. O., Griesand, A., Pross, J., Talbot, H. M., Rethemeyer, J., Wallmann, K., and Wagner, T., 2013. Atlantic cooling associated with a marine biotic crisis during the mid-Cretaceous period. Nature Geoscience 6, 558–561.

McCarthy, P.J., Plint, A.G., 1998. Recognition of interfluve sequence boundaries: Integrating paleopedology and sequence stratigraphy. Geology 26, 387-390.

Menegatti, A.P., Weissert, H., Brown, R.S., Tyson, R.V., Farrimond, P., Strasser, A. and Caron, M., 1998. High-resolution δ13C stratigraphy through the early Aptian "Livello Selli" of the Alpine Tethys. Paleoceanography 13, 530–545.

Meyer, D., 1978. Microfacies and microfabrics of Early Middle Cretaceous sediments selected from site 370, DSDP Leg 41 (deep basin off Morocco). In: Gardner, J. and Herring, J., Eds., Initial reports of the deep sea drilling project 41, 961–981.

Miall., A.D., 1983. Basin analysis of fluvial sediments. In: Collinson, J. D.,Lewin, J., Eds., Modern and Ancient Fluvial Systems, Spec. Publ. int. Ass. Sediment. 6, 279-286.

Michard, A., Frizon de Lamotte, D., Saddiqi O., Chalouan, A., 2008. An outline of the Geology of Morocco. In: Michard, A., Saddiqi, O., Chalouan, A., Frizon de Lamotte, D., Eds., Continental Evolution: The Geology of Morocco. Lecture Notes of Earth Science, 1-31.

Mikhailova, I.A., 1963. On the systematic position and scope of the genus *Diadochoceras.* Paleontologicheskyi Zhurnal 1963-3, 65–77.[in Russian].

Miller, M.C., McCave, I.M., Kosar, P.D., 1977. Threshold of sediment action in unidirectional currents. Sedimentology 24, 507-528.

Mitchum, R.M. Jr, Vail, P.R. , Thompson, S. III, 1977. Seismic stratigraphy and global changes of sea level, part 2: The depositional sequence as a basic unit for stratigraphic analysis. In: Payton, C.E., Ed., Seismic Stratigraphy - Applications to Hydrocarbon Exploration, Mem. Am. Ass. Petrol. Geol. 26, 53-62.

Moullade, M., 1961. Quelques Foraminifères et Ostracodes nouveaux du Crétacé inférieur des Baronnies (Drome). Revue de Micropaléontologie 3, 213–216.

Moullade, M., 1966. Étude stratigraphique et micropaléontologique du crétacé inférieur de la "fosse vocontienne". Documents des Laboratoires de Géologie de la Faculté des Sciences de Lyon 15, 1–369.

Moullade, M., Tronchetti, G., Busnardo, R., Masse, J.-P., 2000. Description lithologique des coupes types du stratotype historique de l'Aptien inférieur dans la région de Cassis-La Bédoule (SE France). In: Moullade, M., Tronchetti, G., Masse, J.-P., Eds., Le stratotype historique de l'Aptien inférieur (Bédoulien) dans la région de Cassis-La Bédoule (S.E. France), Géologie méditerranéenne 25/3-4 (1998), 15–29.

Moullade,M., Bellier, J.P., Tronchetti, G., 2002. Hierarchy of criteria, evolutionary processes and taxonomic simplification in the classification of Lower Cretaceous planktonic foraminifera. Cretaceous Research 23, 111–148.

Moullade, M., Tronchetti, G., Bellier, J.P., 2005. The Gargasian (Middle Aptian) strata from Cassis-La Bédoule (Lower Aptian historical stratotype, SE France): planktonic and benthic foraminiferal assemblages and biostratigraphy. Carnets de Géologie, Article CG2005_A02.

Mordvilko, T.A., 1960. Lower Cretaceous Deposits of the Northern Caucasus and Ciscaucasia). Part 1. 238 pp. Akademia Nauka SSSR, Moscow – Leningrad. [In Russian].

Moreno-Bedmar, J.A., Bulot, L.G., Company, M., Sandoval, J., Tavera, J.M., 2008. Estudio bioestratigráfico de los ammonites del Aptiense medio de la sección de Aigües (Prebético alicantino, SE de España). Datos preliminares. In: Ruiz-Omeñaca, J.I., Piñuela, L., García-Ramos, J.C. (Eds.), XXIV Jornadas de la Sociedad Española de Paleontología, Libro de resúmenes, Museo del Jurásico de Asturias (MUJA), Colunga, 156–157.

Moreno-Bedmar, J.A, Company, M., Bover-Arnal, T., Salas, R., Delanoy, G., Martínez, R., Grauges, A., 2009. Biostratigraphic characterization by means of ammonoids of the lower Aptian Oceanic Anoxic Event (OAE 1a) in the eastern Iberian Chain (Maestrat Basin, eastern Spain). Cretaceous Research 30, 864–872.

Moreno-Bedmar, J.A., Company, M., Bover-Arnal, T., Salas, R., Delanoy, G., Maurasse, J.F.-M.R., Grauges, A., Martínez, R., 2010. Lower Aptian ammonite biostratigraphy in the Maestrat Basin (Eastern Iberian Chain, Eastern Spain). A Tethyan transgressive record enhanced by synrift subsidence. Geologica Acta 8/3, 281–299.

Moreno-Bedmar, J.A., Company, M., Sandoval, J., Tavera, J.M., Bover-Arnal, T., Salas, R., Delanoy, G., Maurrasse, F.J.-M.R., Martínez, R., 2012a. Lower Aptian ammonite and carbon isotope stratigraphy in the eastern Prebetic Domain (Betic Cordillera, southeastern Spain). Geologica Acta 10/4, 333-350.

Moreno-Bedmar, J.A., Bover-Arnal, T., Barragán, R., Salas, R. 2012b. Uppermost Lower Aptian transgressive records in Mexico and Spain: chronostratigraphic implications for the Tethyan sequences. Terra Nova 24 (4), 333–338.

Moreno-Bedmar, J.A., Barragán Manzo, R., Company Sempere, M., Bulot, L.G., 2013. Aptian (lower Cretaceous) ammonite biostratigraphy of the Francisco Zarco Dam stratigraphic section (Durango State, northeast Mexico). Journal of South American Earth Sciences 42, 150–158.

Moreno-Bedmar, J.A., Barragán, R., Delanoy, G., Company, M., Salas, R. 2014. Review of the early Aptian (Early Cretaceous) ammonoid species Deshayesites deshayesi (d'Orbigny, 1841). Cretaceous Research 51, 341–360.

Moreno-Bedmar, J.A., Mendoza-Rosales, C.C., Minor, K.P., Delanoy, G., Barragán, R., González-Léon, O., 2015. Towards an Aptian (Lower Cretaceous) ammonite biostratigraphy of the Mina Texali section, Central Atlantic province (Puebla State, Central Mexico). Cretaceous Research 54, 203–211.

Murphy, M.A., Salvador, A., 1999. International Stratigraphic Guide — An abridged version. Episodes 224, 255-271.

Murray, J.W., 1991. Ecology and palaeoecology of Benthic Foraminifera. Wiley, 397 pp.

Mutterlose, J., Bornemann, A., Luppold, F.W., Owen, H.G., Ruffell, A., Weiss, W. and Wray, D., 2003. The Vöhrum section (northwest Germany) and the Aptian/Albian Boundary. Cretaceous Research 24, 203–252.

Navarro-Ramirez, J.-P., Bodin, S., Immenhauser, A., 2016. Ongoing Cenomanian — Turonian heterozoan carbonate production in the neritic settings of Peru. Sedimentary Geology 331, 78–93.

Nikchitch, I.I., 1915. Representatives of the genus *Douvilleiceras* from the Aptian beds on the northern slope of the Caucasus. Mémoires du Comité Géologique, Nouvelle série 121, 1–53. [in Russian].

Nouidar, M., Chellai, H., 2001. Facies and sequence stratigraphy of a Late Barremian wave-dominated deltaic deposit, Agadir Basin, Morocco. Sedimentary Geology 150, 375-384.

Nouidar, M., Chellai, H., 2002. Facies and sequence stratigraphy of an estuarine incised-valley fill: Lower Aptian Bouzergoun Formation, Agadir Basin, Morocco. Cretaceous Research 22, 93-104.

Nummedal, D., Swift, D.J.P., 1987. Transgressive stratigraphy at sequence-bounding unconformities: Some principles derived from Holocene and Cretaceous examples. In: Nummedal, D., Pilkey, O.H., Howard, J.D. (Eds.), Sea-level Fluctuation and Coastal Evolution, SEPM Special Publication, 41, 241-260.

Nummedal, D., Riley, G.W., and Templet, P.L., 1993. High-resolution sequence architecture: A chronostratigraphic model based on equilibrium profile studies. In: Posamentier, H.W., Summerhyes, C.P., Haq, B.U., Allen, G.P. (Eds.), Sequence stratigraphy and facies associations, International Association of Sedimentology Special Publication 18, 55–68.

Obata, I., 1975. Lower Cretaceous Ammonites from the Miyako Group. 5. *Diadochoceras* from the Miyako Group. Bulletin of the National Science Museum, Série C, Geology 1/1, 1–10.

Ogg, J.G., Hinnov, L.A., 2012. Cretaceous. In: Gradstein, F.M, Ogg, J.G., Schmitz, M., Ogg, G., Eds., The Geologic Time Scale 2012, Elsevier, 793–853.

Orbigny, A., d'. 1840–1842. Paléontologie française: Terrains crétacés. 1. Céphalopodes. 1–120 (1840); 121–430 (1841); 431–662 (1842). Masson, Paris.

Orbigny, A., d'. 1850. Prodrome de Paléontologie stratigraphique universelle des animaux Mollusques et rayonnés faisant suite au cours élémentaire de Paléontologie et de Géologie stratigraphiques, 2ème volume, 427 pp. Masson, Paris.

Owen, H.G., 1996. Boreal and Tethyan late Aptian to late Albian ammonite zonation and palaeobiogeography. Mitteilungen aus dem Geologisch-Paläontologischen Institut der Universität Hamburg 77, 461–481.

Parona, C.F., Bonarelli, G., 1897. Fossili Albiani d'Escragnolles del Nizzardo e della Liguria Occidentale. Palaeontographica Italica 2 (1896), 53–112.

Perch-Nielsen, K., 1985. Mesozoic calcareous nanofossils. In: Bolli, H.M., Saunders, J.B., Perch-Nielsen, K., Eds., Plankton Stratigraphy. Cambridge University Press, Cambridge, 329-426.

Peybernes, C., Giraud, F., Jaillard, E., Robert, E., Masrour, M., Aoutem, M., Içame, N., 2013. Stratigraphic framework and calcareous nannofossil productivity of the Essaouira-Agadir Basin (Morocco) during the Aptian-Early Albian: Comparison with the north-Tethyan margin. Cretaceous Research 39, 149–169.

Phelps M. R., Kerans C., Da-Gama, R.O.B.P., Jeremiah, J., Hull, D, Robert G., Loucks, R.G., 2015. Response and recovery of the Comanche carbonate platform surrounding multiple Cretaceous oceanic anoxic events, northern Gulf of Mexico. Cretaceous Research 54, 117–144 (Supplementary Data).

Pictet, A., 2012. Evolution of the Cheloniceratinae: an alternative to Deshayesitidae for the Lower Aptian biozonation? Preliminary observations. In: Bert, D., Bersac, S., (Eds.), First

Meeting of the Research Group for Paleobiology and biostratigraphy of the ammonites, Boletín del Instituto de Fisiografía y Geología 82, 34–36.

Pletsch, T., Daoudi, L., Chamley, H., Deconinck, J.F. and Charroud, M., 1996. Palaeogeographic controls on the palygorskite occurrence in mid-Cretaceous sediments of Morocco and adjacent basins. Clay Minerals 31, 403-416.

Plink-Björklund, P., Steel, R., 2006. Deltas on falling-stage and lowstand shelf margins, Eocene Central Basin of Spitsbergen. In: Giosan, L., Bhattacharya, J., Eds., River Deltas: Concepts, models and examples: SEPM Special Publication 83, 179-206.

Plint, A. G., 1988. Sharp-based shoreface sequences and “offshore bars” in the Cardium Formation of Alberta; their relationship to relative changes in sea level. In: Wilgus, C. K., Hastings, B. S., Kendall, C. G. St. C., Posamentier, H. W., Ross, C. A., Van Wagoner, J. C., Eds., Sea Level Changes – An Integrated Approach. SEPM Special Publication 42, 357–370.

Plint., A.G., 1991. High-Frequency Relative Sea-Level Oscillations in Upper Cretaceous Shelf Clastics of the Alberta Foreland Basin: Possible Evidence for a Glacio-Eustatic Control? In: Macdonald, D.I.M., Ed., Sedimentation, Tectonics and Eustasy: Sea-Level Changes at Active Margins, Special Publications international Association of Sedimentologists 12, 409-428.

Plint, A.G. and Nummedal, D., 2000. The falling stage systems tract: recognition and importance in sequence stratigraphic analysis. In: D. Hunt and R. L. Gawthorpe (Eds.), Sedimentary Response to Forced Regression, Special Publications of the Geological Society of London 172, 1–17.

Porebski, S., Steel, R.J., 2003. Shelf-margin deltas: their stratigraphic significance and relation to deepwater sands. Earth Science Reviews 62, 283-326.

Posamentier, H.W., Jervey, M.T., Vail, P.R., 1988. Eustatic controls on clastic deposition I — conceptual framework. In: Wilgus, C.K., Hastings, B.S., Kendall, C.G.St.C., Posamentier, H.W., Ross, C.A., Van Wagoner, J.C. (Eds.), Sea Level Changes — An Integrated Approach.

Special Publication Society of Economic Paleontologists and Mineralogists (SEPM) 42, 110–124.

Posamentier, H.W., Morris, W.R., 2000. Aspects of the stratal architecture of forced regressive deposits. In: Hunt, D., Gawthorpe, R.L., Eds., Sedimentary Responses to Forced Regressions. Geological Society of London, Special Publication 172, 19–46.

Premoli Silva, I., Verga, D., 2004. Practical Manual of Cretaceous Planktonic Foraminifera. In: Verga, D., Rettori, R., Eds., International School on Planktonic Foraminifera, Universities of Perugia and Milano, Tipografia Pontefelcino, Perugia, 462 p.

Price, I., 1980. Provenance of the Jurassic-Cretaceous flysch, deep sea drilling project sites 370 and 416. In: Lancelot, Y., Winterer, E.L., Eds., Initial Reports Deep Sea Drilling Vol. L, 751-757.

von Rad, U., Hinz, K., Sarnthein, M., Seibold, E. (Publ.), 1982. Geology of the Northwest African Continental Margin, Springer, Berlin, 703p.

Raisossadat, S.N., 2004. The ammonite family Deshayesitidae in the Kopet Dagh Basin, north-east Iran. Cretaceous Research 25, 115–136.

Raisossadat, S.N., 2006. The ammonite family Parahoplitidae in the Sanganeh Formation of the Kopet Dagh Basin, north-eastern Iran. Cretaceous Research 27, 907–922.

Raspail, F.V., 1831. Histoire des ammonites suivie de la description des ammonites des Basses–Alpes et des Cévennes. Le Lycée, des sciences et des sociétés savantes 27, 115. Librairie Hachette, Paris.

Reboulet, S., Giraud F., Proux O., 2005.Ammonoid abundance variations related to changes in trophic conditions across the Oceanic Anoxic Event 1d (Latest Albian, SE France). Palaios 20, 121–141.

Reboulet, S., Rawson, P.F., Moreno-Bedmar, J.A. (reporters), Aguirre-Urreta, M.B., Barragán, R., Bogomolov, Y., Company, M., González-Arreola, C., Idakieva Stoyanova, V., Lukeneder, A., Matrion, B., Mitta, V., Randrianaly, H., Vašíček, Z., Baraboshkin, E.J., Bert, D., Bersac, S., Bogdanova, T.N., Bulot, L.G., Latil, J.-L., Mikhailova, I.A., Ropolo, P., Szives, O., 2011. Report on the 4th International Meeting of the IUGS Lower Cretaceous Ammonite Working Group, the "Kilian Group" (Dijon, France, 30th August 2010). Cretaceous Research 32, 786-793.

Reboulet, S., Szives, O., Aguirre-Urreta, B., Barragán, R., Company, M., Idakieva, V., Ivanov, M., Kakabadze, M.V., Moreno-Bedmar, J.A., Sandoval, J., Baraboshkin, E.J., Çağlar, M.K., Főzy, I., González-Arreola, C., Kenjo, S., Lukeneder, A., Raisossadat, S.N., Rawson, P.F., Tavera, J.M., 2014. Report on the 5th International Meeting of the IUGS Lower Cretaceous Ammonite Working Group, the Kilian Group (Ankara, Turkey, 31st August 2013). Cretaceous Research 50, 126–137.

Reineck, H.E., Singh, I.B., 1980. Depositional Sedimentary Environments, 2nd edn. SpringerVerlag, Berlin.

Rey, J., Canérot, B., Peybernès, B., Taj-Eddine, K., Rahhali, I., Thieuloy, J.-P., 1986a. Le Crétacé inférieur de la région d'Essaouira: données biostratigraphiques et évolutions sédimentaires. Revue de la Faculté des Sciences de Marrakech, Numéro spécial 2, 413-411.

Rey, J., Canérot, B., Rocher., A., Taj-Eddine, K., Thieuloy, J.-P., 1986b. Le Crétacé inférieur sur le versant nord du Haut-Atlas (région d'Imi n'Tanout et Amizmiz) données biostratigraphiques et évolutions sédimentaires. Revue de la Faculté des Sciences de Marrakech, Numéro spécial 2, 393-441.

Rey, J., Canérot, J., Peybernès, B., Taj-Eddine, K., Thieuloy, J.-P., 1988. Lithostratigraphy, biostratigraphy and sedimentary dynamics of the Lower Cretaceous deposits on the northern side of the western High Atlas (Morocco). Cretaceous Research 9, 141–158.

Robaszynski, F., Caron, M., 1995. Foraminiferes planctoniques du Crétacé: commentaire de la zonation Europe-Méditerranée. Bulletin de la Société Géologique de France 166, 681–692.

Robert, E., Peybernès, B., Bulot, L.G., 2001. Caractérisation d'une nouvelle sous-zone d'ammonites au passage Aptien-Albien dans les 'Marnes noires à *Hypacanthoplites*' des Pyrénées espagnoles. Geobios 34/1, 53–62.

Roch, E., 1930. Etudes géologiques dans la région méridionale du Maroc Occidental. Notes et Mémoires du Service des Mines et de la Cartes Géologiques Maroc 9, 1–542.

Roemer, F.A., 1839. Die Versteinerungen des Norddeutschen Oolithen-Gebirges. Hannover, Deutschland Hahnsche Hofbuchhandlung, p. 47.

Roman, F., 1938. Les ammonites Jurassiques et Crétacées. Essai de Genera. 554 pp. Masson Editeur, Paris.

Ropolo, P., Gonnet, R., Conte, G., 1999. The '*Pseudocrioceras* interval' and adjacent beds at La Bédoule (SE France): implications to highest Barremian/lowest Aptian biostratigraphy. In: Rawson, P.F., Hoedemaeker, P.J., (Eds.), Proceedings 4th International Workshop Cephalopod Team (IGCP-Project 362), Scripta Geologica, Special Issue 3, 159–213.

Ropolo, P., Cecca, F., Gonnet, R., 2000a. The stratigraphic position of "*Ammonites*" *consobrinus* d'Orbigny (Deshayesitidae, Ammonoidea) in the Lower Aptian of Cassis – La Bédoule (SE France). In: Moullade, M., Tronchetti, G., Masse, J.–P. (Eds.), Le stratotype historique de l'Aptien inférieur (Bédoulien) dans la région de Cassis–La Bédoule (S.E. France), Géologie méditerranéenne 25/3–4 (1998), 159–165.

Ropolo, P., Gonnet, R., Conte, G., 2000b. Les *Deshayesites* de la zone à *D. tuarkyricus* dans l'Aptien inférieur de Cassis - La Bédoule. In: Moullade, M., Tronchetti, G., Masse, J.–P., (Eds.), Le stratotype historique de l'Aptien inférieur (Bédoulien) dans la région de Cassis–La Bédoule (S.E. France), Géologie méditerranéenne 25/3–4 (1998), 125–148.

Ropolo, P., Conte, G., Gonnet, R., Masse, J.-P., Moullade, M., 2000c. Les faunes d'Ammonites du Barrémien supérieur – Aptien inférieur (Bédoulien) dans la région stratotype de Cassis – Le Bédoule (SE France): état des connaissances et propositions pour une zonation par ammonites du bédoulien-type. In: Moullade, M., Tronchetti, G., Masse, J.–P., (Eds.), Le stratotype historique de l'Aptien inférieur (Bédoulien) dans la région de Cassis–La Bédoule (S.E. France), Géologie méditerranéenne 25/3–4 (1998), 167–176.

Ropolo, P., Moullade, M., Gonnet, R., Conte, G., Tronchetti, G. 2006. The Deshayesitidae Stoyanow, 1949 (Ammonoidea) of the Aptian stratotype region at Cassis–la Bédoule (SE France). Carnets de Géologie / Notebooks on Geology, Memoir 2006/01 (CG2006_M01), 1–46.

Ropolo, P., Conte, G., Moullade, M., Tronchetti, G., Gonnet, R., 2008a. The Douvilleiceratidae (Ammonoidea) of the Lower Aptian historical stratotype area at Cassis–La Bédoule (SE France). Carnets de Géologie / Notebooks on Geology, Memoir 2008/03 (CG2008_M03), 1–60.

Ropolo, P., Moullade, M., Conte, G., Tronchetti, G., 2008b. About the stratigraphic position of the Lower Aptian *Roloboceras hambrovi* (Ammonoidea) level. Carnets de Géologie / Notebooks on Geology, Letter 2008/03 (CG2008_L03), 1–7.

Rossi, A., Rey, J., Andreu, B., Taj-Eddine, K., 2003. Apport des ostracodes à l'interprétation séquentielle du Crétacé inférieur (Berriasien–Valanginien) du bassin d'Essaouira–Agadir (Maroc). C. R. Palevol 2, 133-141.

Roth, P. H., 1978. Cretaceous nannoplankton biostratigraphy and oceanography of the northwestern Atlantic Ocean: Initial Reports of the Deep-Sea Drilling Project 44, 731–759.

Roth, P. H., 1983. Jurassic and Lower Cretaceous calcareous nannoplankton in the western North Atlantic (Site534): biostratigraphy, preservation and some observations on biogeography and palaeoceanography. In: Winterer, E.L., Ewing, J.I., Eds., Initial Reports of the Deep Sea Drilling Projects 76, 587-621.

Rückheim, S., Bornemann, A., Mutterlose, J., 2006. Planktic foraminifera from the mid-Cretaceous (Barremian-EarlyAlbian) of the North Sea Basin: Palaeoecological and palaeoceanographic implications. Marine Micropalaeontology 58, 83–102.

Saadi, M., Hilali, E.A., Bensaid, M., Boudda, A., Dahmani, M., 1985. Carte Geologique du Maroc (1: 1000 000). Mémoires de la service géologique du Maroc 260.

Saddiqi, O., El-Haimer, F.Z., Michard, A., Barbarand, J., Ruiz, G.M.H., Mansour, E.M., Leturmy, P., Frizon de Lamotte, D., 2009. Apatite fission-track analyses on basement granites from south-western Meseta, Morocco: Paleogeographic implications and interpretation of AFT age discrepancies. Tectonophysics 475/1, 29-37.

Sakar, S. S., 1955. Révision des Ammonites déroulées du Crétacé inférieur du SE de la France. Mémoires de la Société géologique de France 34 (72), 1-176.

Sayn, G., 1891. Description des ammonitidés du Barrémien du Djebel Ouach prés Constantine. Annales de la Société d'Agriculture, Histoire Naturelle et Arts Utiles de Lyon 6/3 (1890), 135–208.

Schlager, S., Jenkyns, H., 1976. Cretaceous Oceanic Anoxic Events: Causes and consequences. Geologie en Mijnbouw 55, 179–184.

Scholle, P. A., Arthur, M.A., 1980. Carbon isotope fluctuations in Cretaceous pelagic limestones: potential stratigraphic and petroleum exploration tool. American Association of Petroleum Geologists Bulletin 64, 67–87.

Scotese, C.R., Dreher, C., 2012. GlobalGeology, http:/www.GlobalGeology.com.

Scott, R.W., 2016. Barremian-Aptian-Albian carbon isotope segments as chronostratigraphic signals: Numerical age calibration and durations. Stratigraphy 13 (1), 21–47.

Seunes, J., 1887. Sur quelques ammonites du Gault. Bulletin de la Société Géologique de France, Série 3 15, 557–571.

Seyed-Emami, K., Wilmsen, M., 2016. Leymeriellidae (Cretaceous ammonites) from the lower Albian of Esfahan and Khur (Central Iran). Cretaceous Research 60, 78–90.

Sigal, J., 1952. Aperçu stratigraphique sur la micropaléontologie du Crétacé. XIX Congrès Géologique International. Monographies régionales: Algérie 26, 1–47.

Sigal, J., 1966. Le concept taxinomique de spectre. Exemples d'application chez les foraminiferes. Propositions de règles de nomenclature, Société géologique de France Mémoires hors-série 3, 5–126.

Sigal, J., 1977. Essai de zonation du Crétacé du Méditerrannéen a l'aide des foraminiféres planctoniques. Géologie Méditerranéenne 4, 99–108.

Sikora, P.J., Olsson, R.K., 1991. A paleoslope model of late Albian to early Turonian foraminifera of the western Atlantic Margin and North Atlantic basin. Marine Micropaleontology 18, 25–72.

Sinzow, I., 1906. Die Beschreibung einiger Douvilleiceras–Arten aus dem oberen Neokom Russlands. Verhandlungen der Russisch–Kaiserlichen Mineralogishen Gesellschaft zu St.–Petersburg 44, 157–197.

Sinzow, I., 1908. Untersuchung einiger Ammonitiden aus dem Unteren Gault Mangyschlaks und des Kaukasus. Verhandlungen der Russisch–Kaiserlinghen Mineralogishen Gesellschaft zu St–Petersburg 45 (1907), 455–519.

Sinzow, I., 1913. Beiträge zur Kenntnis der unteren Kreideablagerungen des Nord-Kaukasus. Travaux du Musée Géologique Pierre le Grand près l'Academie Impériale des Sciences de St. Petersbourg 7, 93–117.

Spath, L.F., 1923. Ammonoidea of the Gault. Part I. Paleontographical Society Monograph 75/353 (1921), 1–72.

Steel, R.J., Crabaugh, J., Schellpeper, M., Mellere, D., Plink-Björklund, P., Deibert, J., Loseth, T., 2000. Deltas vs. Rivers on the Shelf Edge: Their Relative Contributions to the Growth of Shelf-Margins and Basin-Floor Fans (Barremian and Eocene, Spitsbergen). In: Weimer, P., Eds., Deep-water Reservoirs of the World. Proceedings of the GCSSEPM Foundation 20th Annual Research Conference, 981-1009.

Steel, R., Porebski, S., Plink-Björklund, P., Mellere, D., Shellpeper, M., 2003, Shelf-edge delta types and their sequence stratigraphic relationships. SEPM, Gulf Coast Section Foundation, 23th Annual Research Conference, Special Publication, CD, p. 205–230.

Stoyanow, A., 1949. Lower Cretaceous stratigraphy in southeastern Arizona. Geological Society of America, Memoirs 38, 1–169.

Stow, D.A.A., 1986. Deep clastic seas. In: Reading, H.G., Ed., Sedimentary Environments and Facies, 2nd Edn., 399-444.

Strasser, A., Hillgaertner, H., Hug, W., Pittet, B., 2000. Third-order depositional sequences reflecting Milankovitch cyclicity. Terra Nova 12, 303-311.

Street, C., Bown., P.R., 2000. Palaeobiogeography of Early Cretaceous (Berriasian-Barremian) calcareous nannoplankton. Marine Micropaleontology 39, 265–291.

Suter, J.R., Berryhill, H.L. Jr., 1985. Late Quaternary Shelf-Margin Deltas, Northwest Gulf of Mexico. AAPG Bulleting 69/1, 77-91.

Sydow, J., Roberts, H.H., 1994. Stratigraphic Framework of a Late Pleistocene Shelf-Edge Delta, Northeast Gulf of Mexico. AAPG Bulletin 78/8, 1276-1312.

Szives, O., Csontos, L., Bujtor, L., Főzy, I., 2007. Aptian-Campanian ammonites of Hungary. Geologica Hungarica, Series Palaeontologica, Fasciculus 57, 1–187.

Tari, G., Jabour, H., 2013. Salt tectonics along the Atlantic margin of Morocco. Geological Society, London, Special Publications 369, 337–353.

Taj-Eddine, K., 1992. Le Jurassique terminal et le Crétacé basal dans l'Atlas atlantique (Maroc): biostratigraphie, sédimentologie, stratigraphie séquentielle et géodynamique. Strata 16, 1–285.

Tedeschi, L.R., Jenkyns, H.C., Robinson, S.A., Sanjinés, A.E.S., Viviers, M.C., Quintaes, C.M.S.P., Vazquez, J.C., 2017. New age constraints on Aptian evaporites and carbonates from the South Atlantic: Implications for Oceanic Anoxic Event 1a. Geology 45, 543–546.

Ten Dam, A., 1947. On Foraminifera of the Netherlands; No. 9-Sur quelques especes nouvelles ou peu connues dans le Cretace inferieur (Albien) des Pays-Bas. Geologie en Mijnbouw 9/2, p. 29.

Tesson, M., Gensours, B., Allen, G.P., Ravenne, Ch., 1990. Late Quaternary Deltaic Lowstand Wedges on the Rhône Continental Shelf, France. Marine Geology 91, 325-332.

Thieuloy, J.-P., 1972. Biostratigraphie des lentilles à pérégrinelles (Brachiopodes) de l'Hauterivien de Rottier (Drôme, France). Géobios 5/1, 5-53.

Tietze, E., 1872. Geologische und paläontologische Mitteilungen aus dem südlichen Teil des Banater Gebirgsstockes. Jahrbuch der Kaiserlich–Königlichen Geologischen Reichsanstalt 22, 35–142.

Tixeront, M., 1973. Lithostratigraphie et minéralisations cuprifères et uranifères stratiformes syngenetiques et familières des formations detritiques permo-triassiques du couloir d'Argana, Haut Atlas occidental (Maroc). Notes du Service Géologique du Maroc 33, 147–177.

Tovbina, S.Z., 1968. On the Zone of *Acanthohoplites prodromus* in the boundary deposits of the Aptian and Albian of Turkmenia. Izvestiia Akademii Nauk Turkmenistana. Seriia

fiziko–matematicheskikh, tckhnicheskikh, khimicheskikh i geologicheskikh nauk 2, 100–109. [in Russian].

Tovbina, S.Z., 1970. A new Aptian genus of the family Parahoplitidae. Paleontologicheskyi Zhurnal 1970/3, 56–65 [in Russian].

Tovbina, S.Z., 1982. New representatives of the family Parahoplitidae of Turkmenia. Ejegodnik Vsesojuznogo Nauchno Paleontologischeskogo obtchestva 25, 60–79. [in Russian].

Trecalli, A., Spangenberg, J., Adatte, T., Föllmi, K.B., Parente, M., 2012. Carbonate platform evidence of ocean acidification at the onset of the early Toarcian oceanic anoxic event. Earth and Planetary Science Letters 357-358, 214–225.

Tremolada, F., Erba, E., 2002. Morphometric analysis of the Aptian *Rucinolithus terebrodentarius* and *Assipetra infracretacea* nannoliths: implications for taxonomy, biostratigraphy and paleoceanography. Marine Micropaleontology 44, 77–92.

Uhlig, V., 1883. Die Cephalopodenfauna der Wensdorferschichten. Denkschriften der Kaiserlichen Akademie der Wissenschaften Wien, Mathematisch–Naturwissenschaftliche Klasse 46, 127–290.

USGS (2004), Shuttle Radar Topography Mission, Global Land Cover Facility.

Vail, P.R., Mitchum, R.M. Jr, Thompson, S. III, 1977. Seismic stratigraphy and global changes of sea level, part 4: Global cycles of relative changesof sea level. In: Payton, C.E., Ed., Seismic Stratigraphy – Applications to Hydrocarbon Exploration, Mem. Am. Ass.Petrol. Geol. 26, 83-97.

Vail, P.R., Audemard, F., Bowman, S.A., Eisner, P.N., Perez-Cruz, C., 1991. The stratigraphic signatures of tectonics, eustasy and sedimentology - an overview. In: Einsele G. et al., Eds. Cycles and Events in Stratigraphy, pp. 617-659.

Vašiček, Z., Michalík, J. 1986. The Lower Cretaceous ammonites of the Manín unit (Mt. Butkov, West Carpathians). Geologica carpathica 37/4, 449-481.

Verati, C., Rapaille, C., Féraud G., Marzoli, A., Bertrand, H.; Youbi, N., 2007. 40 Ar/ 39 Ar ages and duration of the Central Atlantic Magmatic Province volcanism in Morocco and Portugal and its relation to the Triassic–Jurassic boundary. Palaeogeography, Palaeoclimatology, Palaeoecology 244/1–4, 308–325.

Verga D., Premoli Silva, I., 2003a. Early Cretaceous planktonic foraminifera from the Tethys: the large, many–chambered representatives of the genus *Globigerinelloides*. Cretaceous Research 24, 661–690.

Verga D., Premoli Silva, I., 2003b. Early Cretaceous planktonic foraminifera from the Tethys: small few–chambered representatives of the genus *Globigerinelloides*. Cretaceous Research 24, 305–334

Vincent, B., van Buchem, F.S.P., Bulot, L.G., Immenhauser, A., Caron, M., Baghbani, D., Huc, A.Y., 2010. Carbon-isotope stratigraphy, biostratigraphy and organic matter distribution in the Aptian – Lower Albian successions of southwest Iran (Dariyan and Kazhdumi formations). In: van Buchem, F.S.P., Al-Husseini, M.I., Maurer, F., Droste, H.J. (Eds.), Barremian - Aptian Stratigraphy and Hydrocarbon Habitat of the Eastern Arabian Plate, GeoArabia Special Publication 4, Gulf PetroLink, Bahrain 2, 139–197.

Weissert, H., 1989. C-isotope stratigraphy, a monitor of paleoenvironmental change: a case study from the Early Cretaceous. Surveys in Geophysics 10, 1–61.

Weissert, H., Lini, A., Föllmi, K.B., Kuhn, O., 1998. Correlation of Early Cretaceous carbon isotope stratigraphy and platform drowning events: a possible link? Palaeogeography, Palaeoclimatology, Palaeoecology 137, 189–203.

Wenke, A., Zühlke, R., Jabour, H., Kluth, O. 2011. High-resolution sequence stratigraphy in basin reconnaissance: example from the Tarfaya Basin, Morocco. First Break 29, 85–96.

Westermann, G.E.G, 2000. Marine faunal realms of the Mesozoic: review and revision under the new guidelines for biogeographic classification and nomenclature. Palaeogeography, Palaeoclimatology, Palaeoecology 163, 49–68.

Wiedmann, J., 1966. Stammesgeschichte und System der posttriadischen Ammonoideen: Ein Überblick (2. Teil). Neues Jahrbuch für Geologie und Paläontologie Abhandlungen 127, 13–81.

Wiedmann, J., Butt, A., Einse1e, G., 1978. Vergleich von marokkanischen Kreide-Küstenaufschlüssen und Tiefseebohrungen (DSDP): Stratigraphie, Paläoenvironmnent und Subsidenz an einem passiven Kontinentalrand. Geologische Rundschau 67, 454–508.

Wiedmann, J., Butt, A., Einsele, G., 1982. Cretaceous Stratigraphy, Environment, and Subsidence History at the Moroccan Continental Margin. In: von Rad, U., Hinz, K., Samthein, M., Seibold, E., (Eds.), Geology of the Northwest African Continental Margin, 366–395. Springer-Verlag, Berlin.

Wilson, A., Flint, S., Payenberg, T., Tohver, E., Lanci, L., 2014. Architectural styles and sedimentology of the fluvial lower Beaufort Group, Karoo Basin, South Africa. Journal of Sedimentary Research 84, 326-348.

Wippich, M.G.E., 2001. Die tiefe Unter-Kreide (Berrias bis Unter-Hauterive) im Südwestmarokkanischen Becken: Ammomnitofauna, Bio- und Sequenzstratigraphie. Unpublished PhD thesis, Ruhr-Universität, Bochum, 142 pp.

Wippich, M.G.E., 2003. Valanginian (Early Cretaceous) ammonite faunas from the western High Atlas, Morocco, and the recognition of western Mediterranean ‘standard’ zones. Cretaceous Research 24, 357–374.

Witam, O., Rey, J., Aadjour, M., Magniez-Janin, F., Delanoy, G., 1993. Nouvelles données biostratigraphiques et séquentielles sur la série barrémienne et aptienne du bassin d’Agadir (Maroc). Revue de Paléobiologie 12, 193–202.

Witam, O., 1998. Le Barrémien-Aptien de l'Atlas Occidental (Maroc) : lithostratigraphie, biostratigraphie, sédimentologie, stratigraphie séquentielle, géodynamique et paléontologie. Strata 30, 1–421.

Wright, C.W., Callomon, J.H., Howarth, M.K., 1996. Cretaceous ammonoidea. In: Moore, R. C., Kaesler, K.L. (eds.), Treatise on invertebrate palaeontology, Part L, Mollusca 4 revised, 362 pp. Geological Society American and University Kansas Press, New York.

Wurster, P. and Stets, J., 1982. Sedimentation in the Atlas Gulf II: mid-Cretaceous events. In: von Rad, U., Hinz, K., Samthein, M., Seibold, E., (Eds.), Geology of the Northwest African Continental Margin, 439–459. Springer-Verlag, Berlin.

Yamina, B., Ali Nabiha, B. H., Saloua, R., Kamal, T., 2002. Etude biostratigraphique du Crétacé inférieur (Barrémien supérieur- Albien) du Haut Atlas occidental (MAROC). Estudios Geologicos 58, 105–112.

Young, K., 1974. Lower Albian and Aptian (Cretaceous) ammonites of Texas. Geoscience and Man 8, 175–228.

Young, K., 1986. Cretaceous, marine inundations of the San Marcos Platform, Texas. Cretaceous Research 7, 117–140.

Zecchin, M., Catuneanu, O., 2013. High-resolution sequence stratigraphy of clastic shelves I: Units and bounding surfaces. Marine and Petroleum Geology 39, 1-25.

Zecchin, M., Catuneanu, O., Caffau, M. 2017. High-resolution sequence stratigraphy of clastic shelves V: Criteria to discriminate between stratigraphic sequences and sedimentological cycles. Marine and Petroleum Geology 85, 259-271.

Zittel, K.A., von 1884. Cephalopoda. In: Zittel, K.A., von, Handbuch der Paläontologie, Band 1, Abt. 2, Lief 3, pp 329–522. R. Oldenbourg, Munich and Leipzig.

Zittel, K.A., von 1895. Grundzüge der Paläontologie (Paläozoologie). vii + 972 pp. R. Oldenbourg, Munich and Leipzig.

Zühlke, R., Bouaouda, M.-S., Ouajhain, B., Bechstädt, T., Reinfelder, R., 2004. Quantitative Meso-/Cenozoic development of the eastern Central Atlantic continental shelf, western High Atlas, Morocco. Marine and Petroleum Geology 21, 225–276.

APPENDICES

A) Taxonoamic list calcareous nannofossils

B) Stratigraphic logs

B1: Addar and Agroud

B2: Adenz and Aouerga

B3: Akerkaou and Tinkert

B4: Alma

B5: Azziar South and Barrage

B6: East of Aouerga and Inrarne

B7: Fossil Shop Road Cut and Alma East

B8: Ilmer Ichemerarn and Azziar North

B9: Mahmout and Tamri South

B10: Tiskatine North and Assaka

C) Correlation panels and charts – oversize

C1: Integrated biostratigraphic chart of the Tiskatine Section

C2: DSDP borehole 370: Lithostratigraphic log and calcareous nannofossil distribution

C3: Distribution of key ammonoid, foraminifera and calcareous nannofossils of the Vocontian Basin of SE France.

C4: Distribution of key ammonoids, foraminifera and calcareous nannofossils of the Marcouline section, Provençal Basin.

C5: Distribution of key ammonoid, foraminifera and calcareous nannofossil specimen from the Cassis section, Provençal Basin.

C6: Sequence stratigraphic correlation of the Id Amran, Tiskatine and Assaka section based on ammonoid biostratigraphy with associated Wheeler Diagram.

C7: Correlation panel Azziar South to Tamri

C8: Correlation panel Inrarne to Alma

C9: Biostratigraphic correlation panel Mramer to Tiskatine

C10: Detailed location map of studied sections in chapter 4

C11: Tiskatine section with field photographs

C12: Id Amran section with field photographs

C13: Assaka section with field photographs

C14: Tiskatine section - Key Surfaces

C15: Detailed location map Agadir segment of the Essaouira-Agadir Basin

C16: Detailed location map Haha segment of the Essaouira-Agadir Basin

C17: Depositional environments with supporting logs and field photographs of the Fossil Shop Road Cut section

C18: Depositional environments with supporting logs and field photographs Tamri South section

C19: Depositional environments with supporting logs and field photographs Assaka section

C20: Key timelines and sequence stratigraphic surfaces Azziar South to Tamri South

Appendix A: Taxonomic list calcareous nannofossils

A full list of all taxa cited in the text, figures, and range charts is given below. Most bibliographic references can be found in Perch-Nielsen (1985) and Bown (1998).

Ansulasphaera sp. Grün and Zweili, 1980

Assipetra terebrodentarius (Applegate et al. in Covington and Wise, 1987) Rutledge and Bergen in Bergen, 1994, ssp. *terebrodentarius* emend.

Assipetra terebrodentarius (Applegate et al. in Covington and Wise, 1987) Rutledge and Bergen in Bergen, 1994, ssp, *youngii* Tremolada and Erba, 2002, emend.

Axopodorhabdus dietzmannii (Reinhardt, 1965) Wind and Wise, 1983

Biscutum constans (Górka, 1957), Black, 1959

Biscutum gaultensis (Mutterlose, 1992) Bown in Kennedy et al., 2000

Braarudosphaera africana Stradner, 1961

Braarudosphaera batilliformis Troelson and Quadros, 1971

Braarudosphaera primula Black, 1973

Broinsonia galloisii (Black, 1973) Bown in Kennedy et al., 2000

Broinsonia viriosa (Jeremiah, 1996) Bown in Kennedy et al., 2000

Bukrylithus ambiguus Black, 1971

Calcicalathina alta Perch-Nielsen, 1979

Calculites dispar Varol *in* Al-Rifaiy *et al.*, 1990

Calculites percernis Jeremiah, 1996

Calciosolenia fossilis (Deflandre in Deflandre and Fert, 1954) Bown in Kennedy et. al., 2000

Chiastozygus litterarius (Górka, 1957) Manivit, 1971

Conosphaera rothii (Thierstein, 1971) Jakubowski, 1986

Corollithion exiguum Stradner, 1961

Corollithion signum Stradner, 1963

Crepidolithus burwellensis Black, 1972

Cretarhabdus conicus Bramlette and Martini, 1964

Cretarhabdus inaequalis Crux, 1987

Cretarhabdus loriei Gartner, 1968

Crucibiscutum bosunensis Jeremiah, 2001

Crucibiscutum neuquenensis Bown and Concheyro 2004

Cyclagelosphaera margerelii Noël, 1965

Cyclagelosphaera rotaclypeata Bukry, 1969

Diazomatolithus lehmanii Noël, 1965

Discorhabdus ignotus (Gorka, 1957) Perch-Nielsen, 1968

Eiffellithus hancockii Burnett, 1998

Eprolithus floralis (Stradner, 1962) Stover, 1966

Farhania varolii (Jakubowski, 1986) Varol, 1992

Flabellites oblongus (Bukry, 1969) Crux in Crux et al., 1982

Glaukolithus diplogrammus (Deflandre *in* Deflandre and Fert, 1954) Reinhardt, 1964

Gorkaea operio Varol and Girgis, 1994

Grantarhabdus coronadventis (Reinhardt, 1966a) Grün in Grün and Allemann, 1975

Haqius circumradiatus (Stover, 1966) Roth, 1978

Haqius ellipticus (Grün in Grün and Allemann, 1975) Bown, 1992

Hayesites albiensis Manivit, 1971

Hayesites irregularis (Thierstein in Roth and Thierstein, 1972) Applegate et al. in Covington and Wise, 1987

Helenea chiastia Worsley, 1971

Helicolithus leckiei Bown, 2005.

Helicolithus trabeculatus (Górka, 1957) Verbeek, 1977

Hemipodorhabdus gorkae (Reinhardt, 1969) Grün in Grün and Allemann, 1975

Laguncula dorotheae Black, 1971

Lapideacassis mariae Black, 1971

Lithraphidites carniolensis Deflandre, 1963

Lithraphidites houghtonii Jeremiah, 2001

Lithraphidites moray-firthensis Jakubowski, 1986

Lordia xenota (Stover, 1966) Varol and Girgis, 1994

Manivitella pecten Black, 1973

Manivitella pemmatoidea (Deflandre, 1965) Thierstein, 1971, emend. Black, 1973

Micrantholithus hoschulzii (Reinhardt, 1966) Thierstein, 1971

Micrantholithus obtusus Stradner, 1963

Nannoconus Kamptner, 1931

Nannoconus circularis Deres and Achéritéguy, 1980

Nannoconus fragilis Deres and Achéritéguy, 1980

Nannoconus globulus Brönnimann, 1955

Nannoconus quadriangulus Deflandre and Deflandre-Rigaud, 1962

Nannoconus steinmannii Kamptner, 1931

Nannoconus truitti Brönnimann, 1955, *rectangularis* Deres and Achéritéguy, 1980

Nannoconus truitti Brönnimann,1955) *frequens* Deres and Acheriteguy, 1980

Nannoconus vocontiensis Deres and Achéritéguy, 1980

Octocyclus magnus Black, 1972

Octocyclus reinhardtii (Bukry, 1969) Wind and Wise *in* Wise and Wind, 1977

Orastrum perspicuum Varol in Al-Rifaiy *et al.*, 1990

Owenia hilli Crux, 1991

Owenia partitum (Varol *in* Al-Rifaiy et al., 1990) Bown *in* Kennedy et al., 2000

Percivalia fenestrata (Worsley, 1971) Wise, 1983

Pickelhaube furtiva (Roth, 1983) Applegate et al. in Covington and Wise, 1987

Prediscosphaera columnata (Stover, 1966) Perch-Nielsen, 1984

Prediscosphaera spinosa (Bramlette and Martini, 1964) Gartner, 1968

Repagulum parvidentatum (Deflandre and Fert, 1954) Forchheimer, 1972

Rhagodiscus achlyostaurion (Hill, 1976) Doeven, 1983

Rhagodiscus angustus (Stradner, 1963) Reinhardt, 1971

Rhagodiscus asper (Stradner, 1966) Reinhardt, 1967

Rhagodiscus infinitus (Worsley, 1971) Applegate et al. in Covington and Wise, 1987

Rhagodiscus robustus Bown, 2005

Rhagodiscus splendens (Deflandre, 1953) Verbeek, 1977

Rotelapillus crenulatus (Stover, 1966) Perch-Nielsen, 1984

Seribiscutum primitivum (Thierstein, 1974) Filewicz et al. in Wise and Wind, 1977

Sollasites horticus (Stradner et al., 1966) Black, 1968

Staurolithites crux (Deflandre and Fert, 1954) Caratini, 1963

Staurolithites gausorhethium (Hill, 1976) Varol and Girgis, 1994

Staurolithites glaber (Jeremiah, 1996) Burnett, 1998

Staurolithites mutterlosei Crux, 1989

Stoverius achylosus (Stover, 1966) Perch-Nielsen, 1986

Tegumentum stradneri Thierstein in Roth and Thierstein, 1972

Tranolithus gabalus Stover, 1966, emend. Köthe, 1981

Tubodiscus Thierstein, 1973

Watznaueria barnesae (Black, 1959) Perch-Nielsen, 1968

Watznaueria britannica (Stradner, 1963) Reinhardt, 1964

Zebrashapka vanhintei Covington and Wise, 1987

Zeugrhabdotus clarus Bown, 2005

Zeugrhabdotus diplogrammus (Deflandre in Deflandre and Fert, 1954) Burnett in Gale et al., 1996

Zeugrhabdotus embergeri (Noël, 1958) Perch-Nielsen, 1984

Zeugrhabdotus fissus Grün and Zweili, 1980

Zeugrhabdotus howei Bown in Kennedy et al., 2000

Zeugrhabdotus moulladei Roth and Bowdler, 1981

Zeugrhabdotus scutula (Bergen, 1994) Rutledge and Bown, 1996

Appendix B: Stratigraphic logs

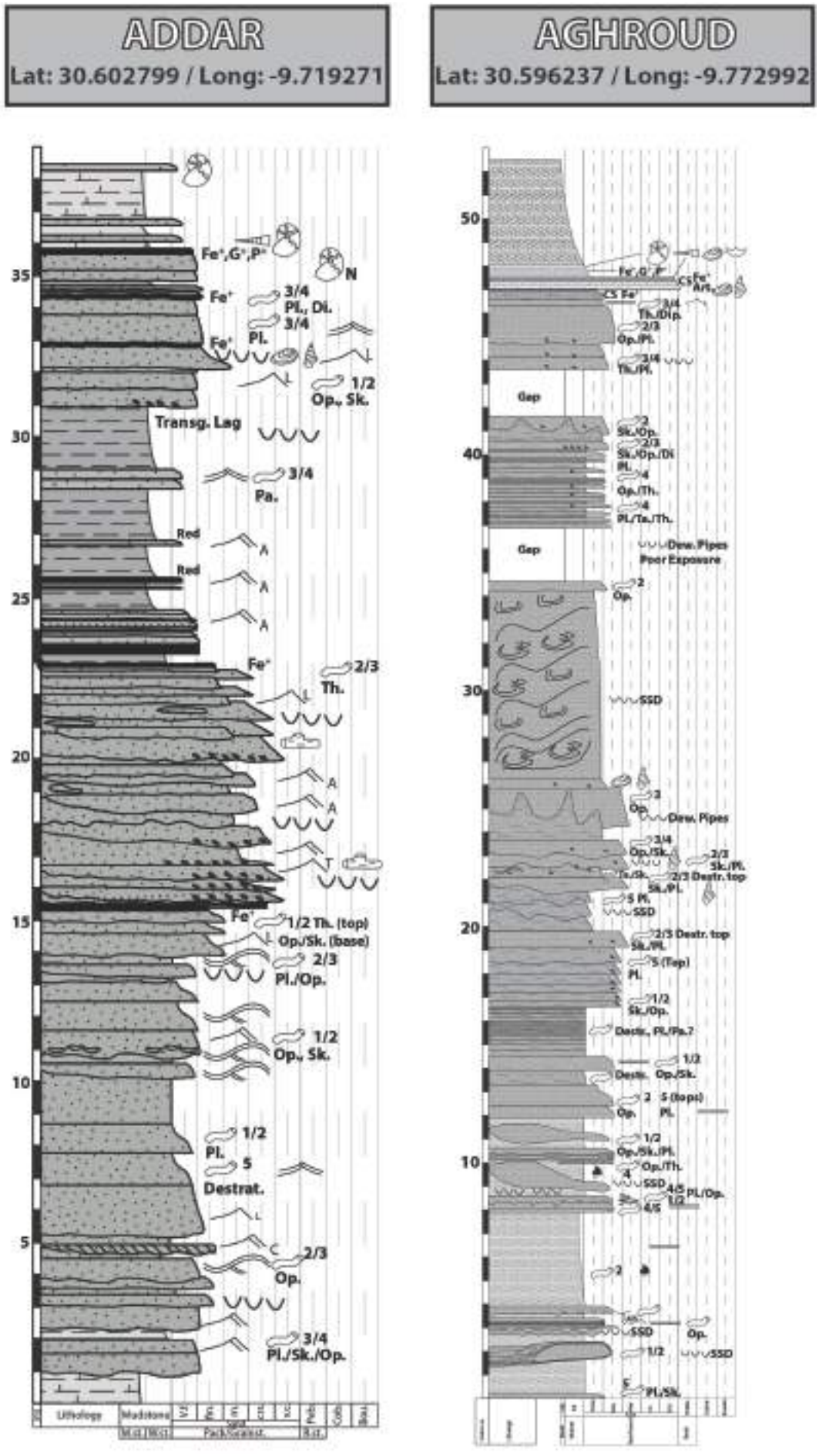

B 1: Stratigraphic Logs Addar and Aghroud

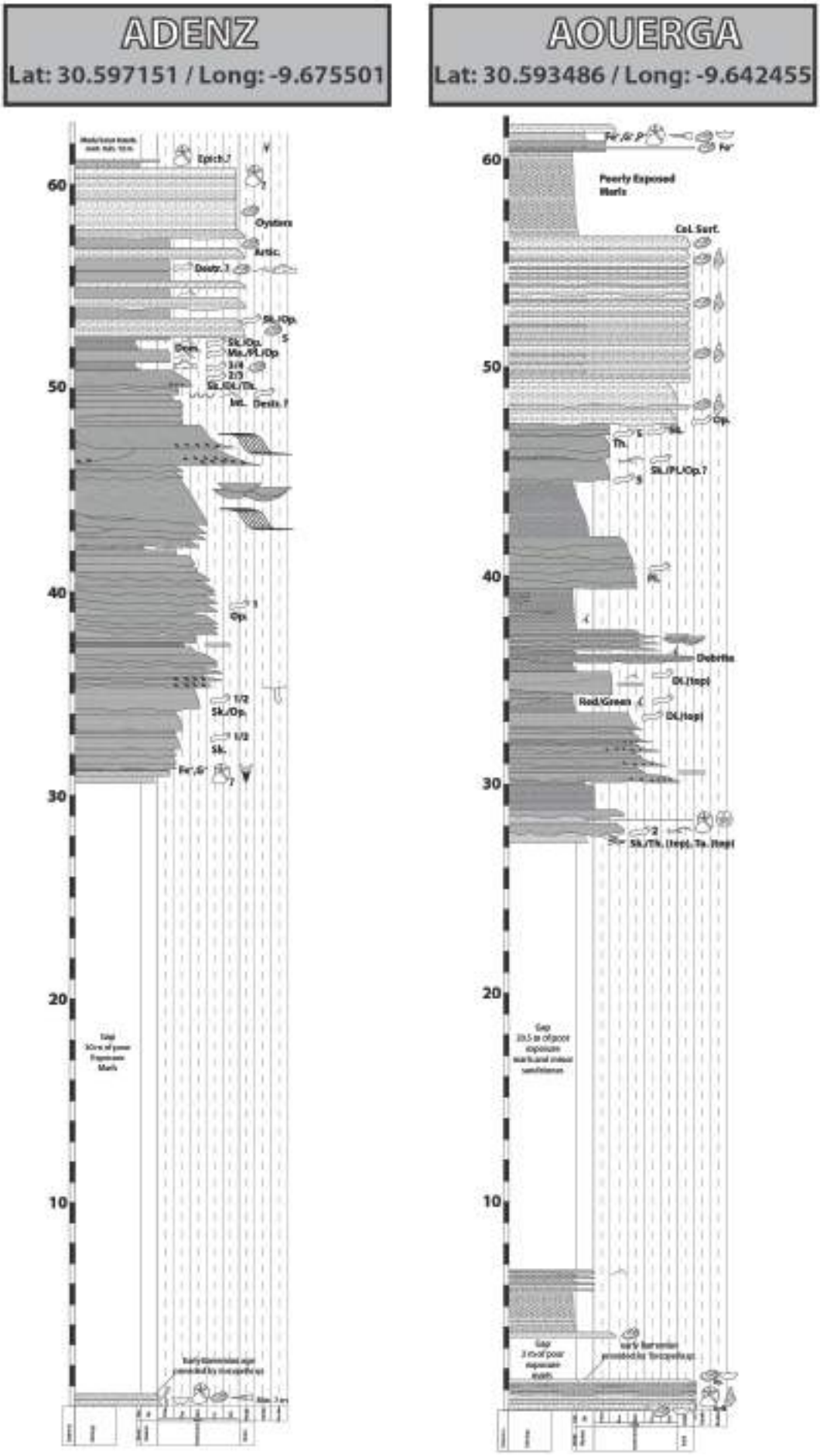

B 2: Stratigraphic Logs Adenz and Aouerga

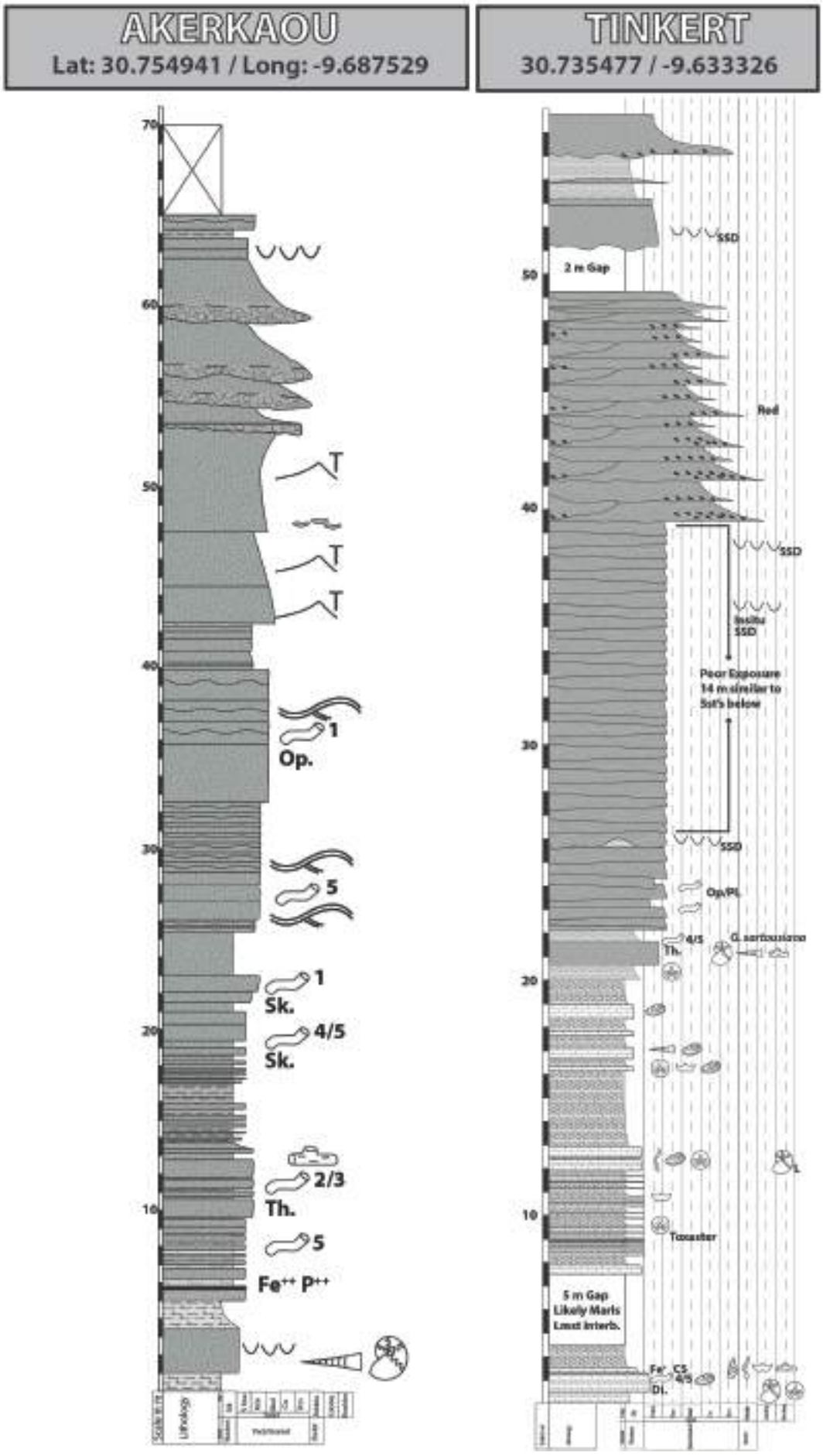

B 3: Stratigraphic Logs Akerkaou and Tinkert

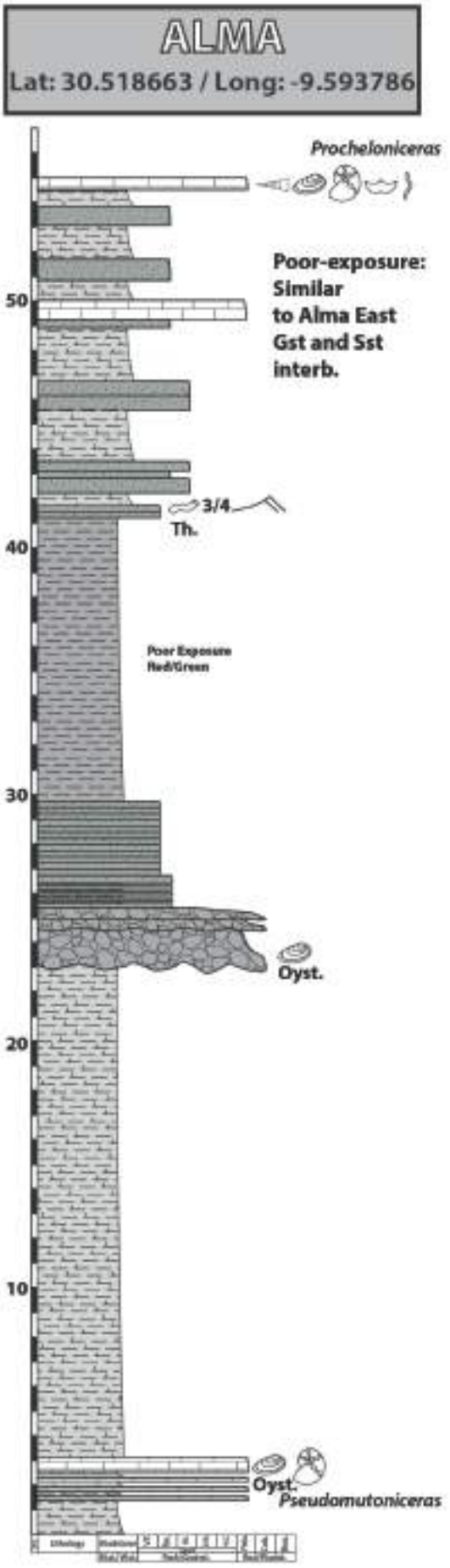

B 4: Stratigraphic Logs Alma

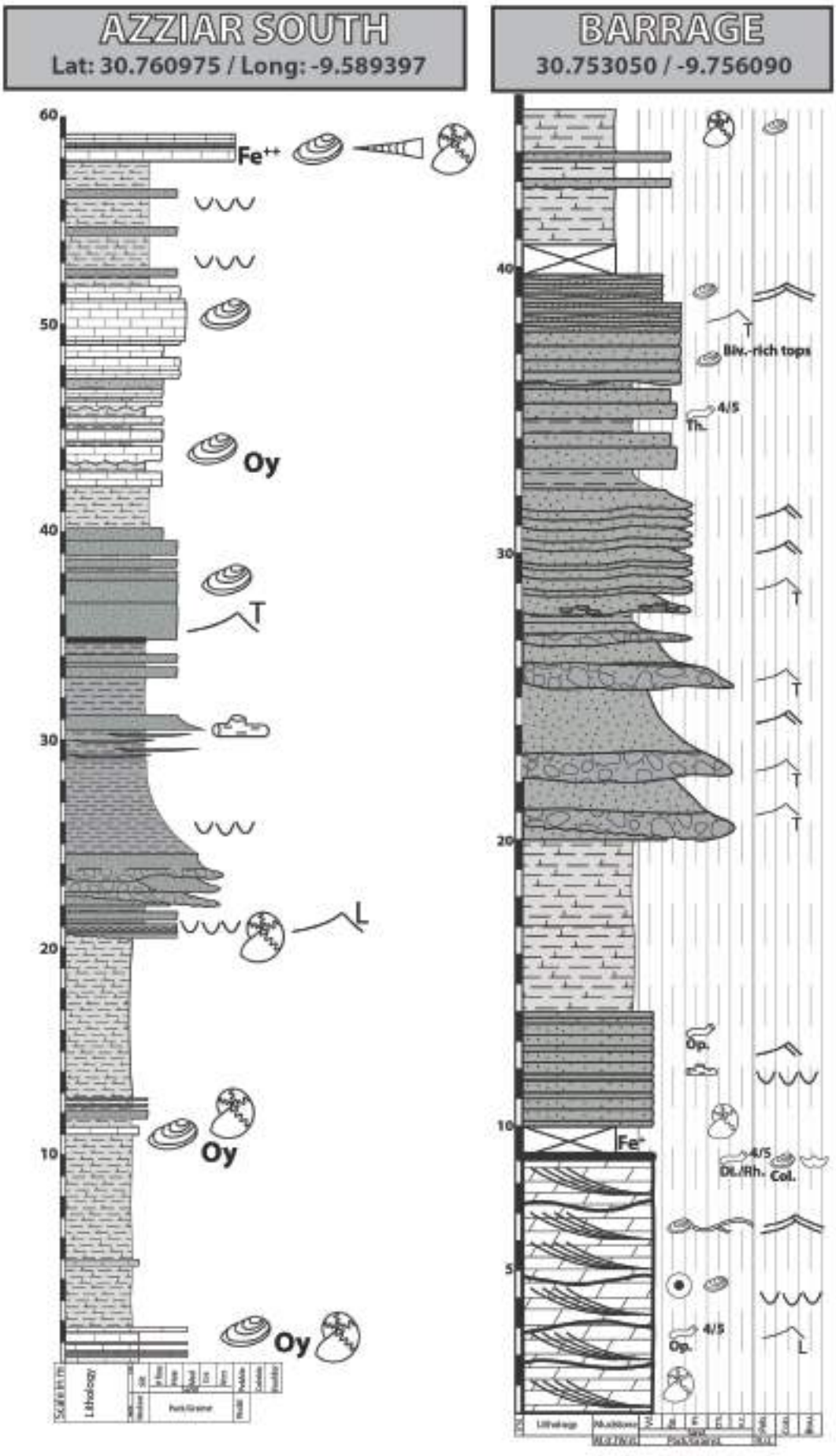

B 5: Stratigraphic Logs Azziar South and Barrage

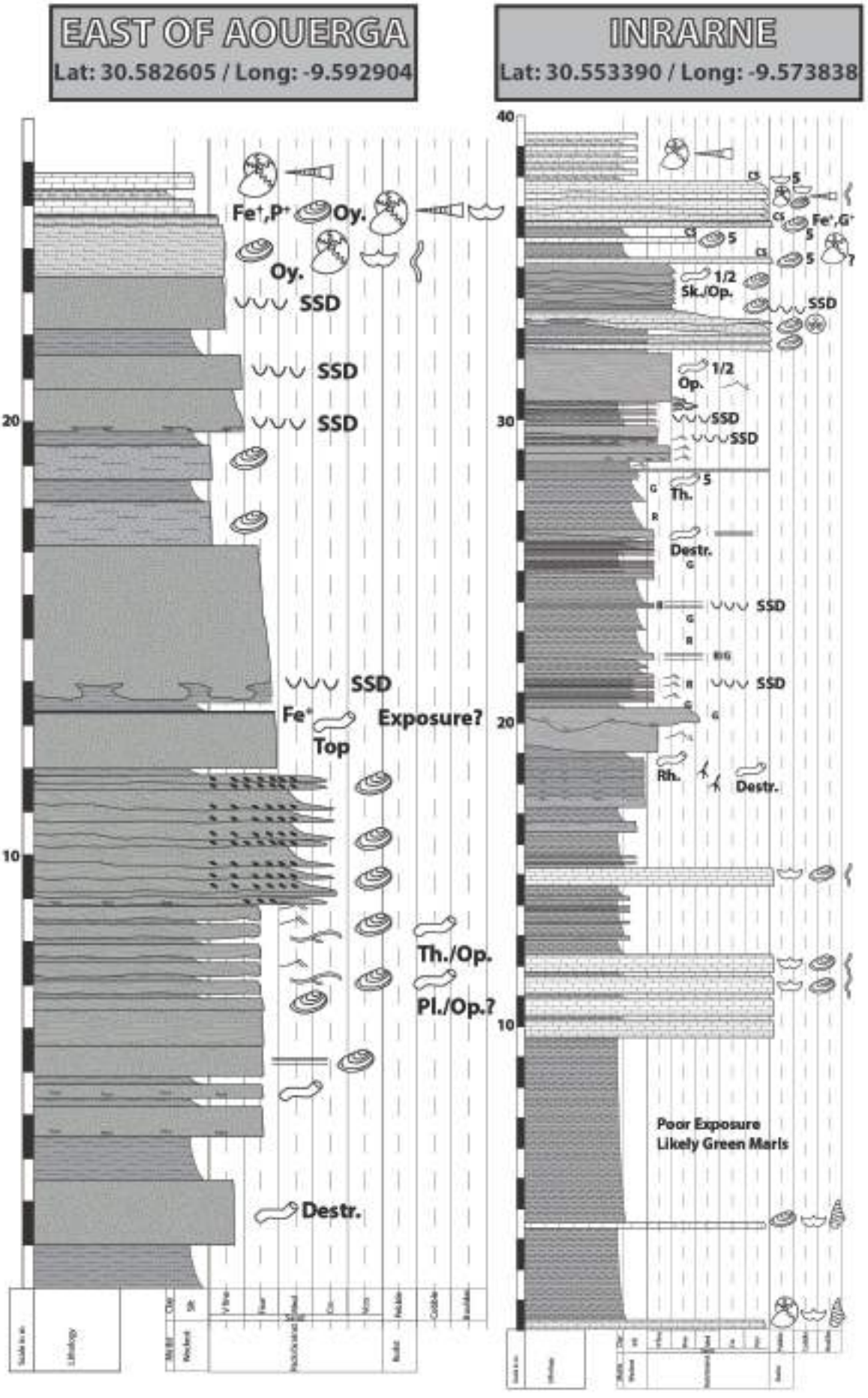

B 6: Stratigraphic Logs East of Aouerga and Inrarne

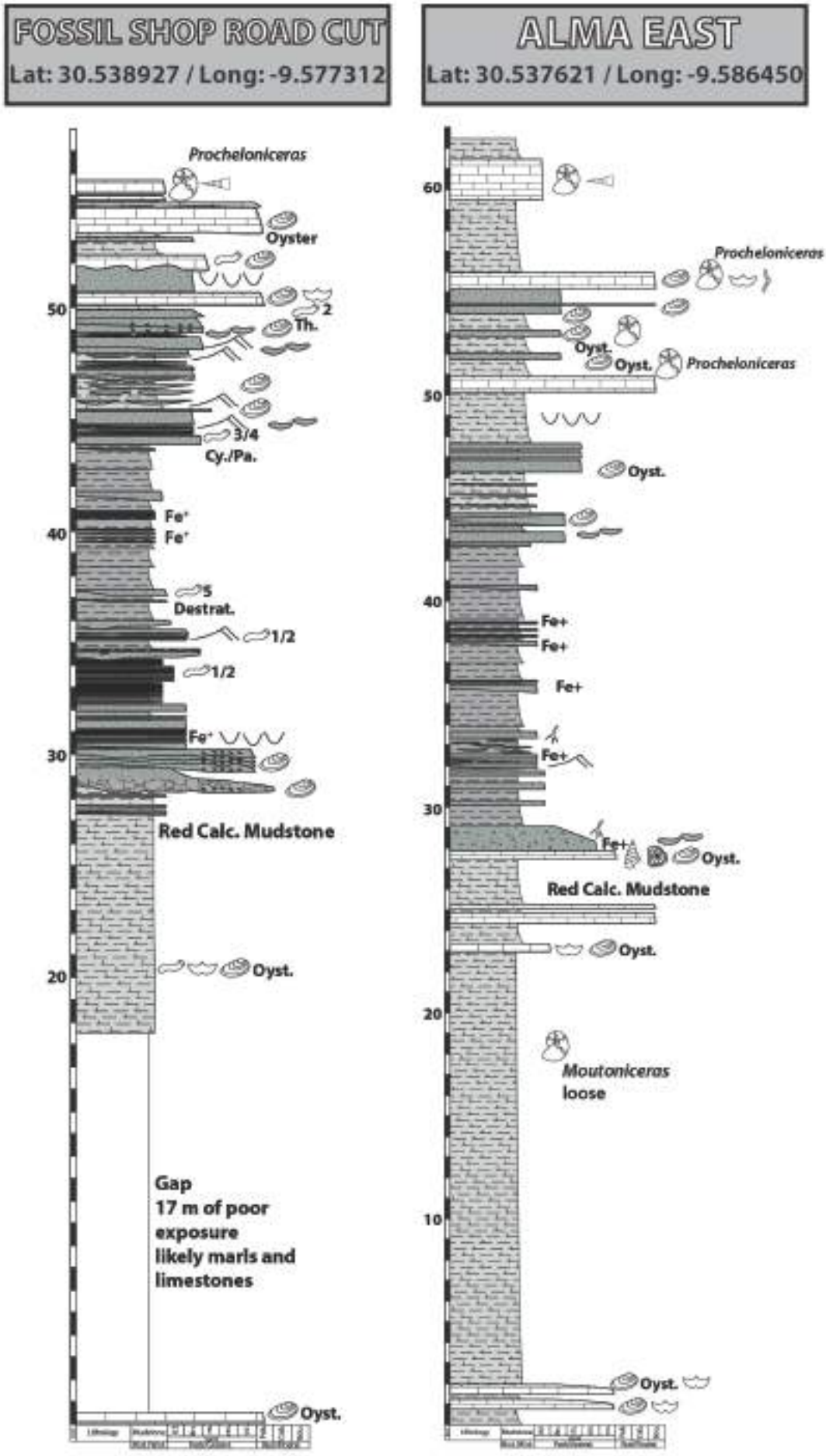

B 7: Stratigraphic Fossil Shop Road Cut and Alma East

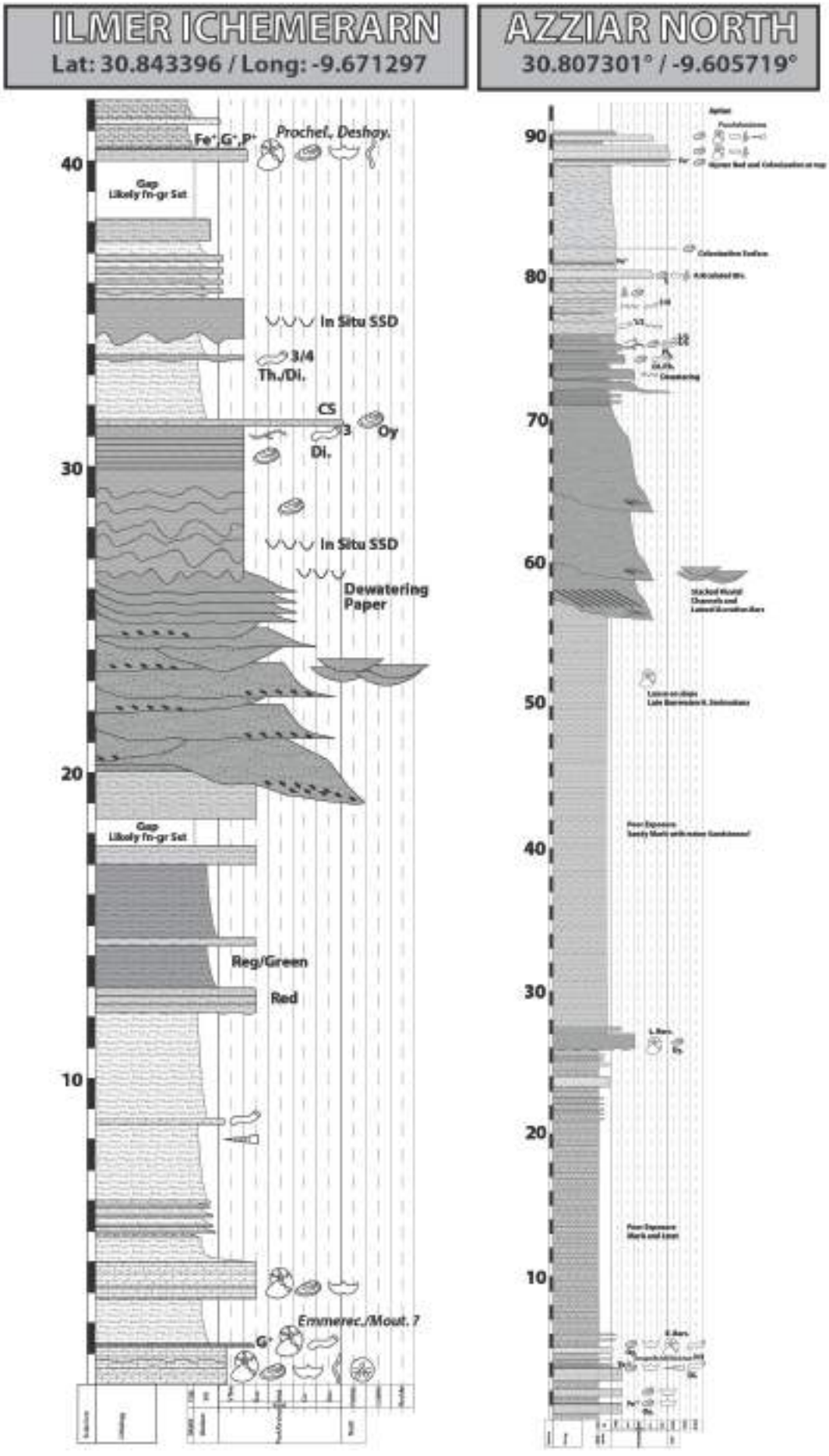

B 8: Stratigraphic Logs Ilmer Ichemerarn and Azziar North

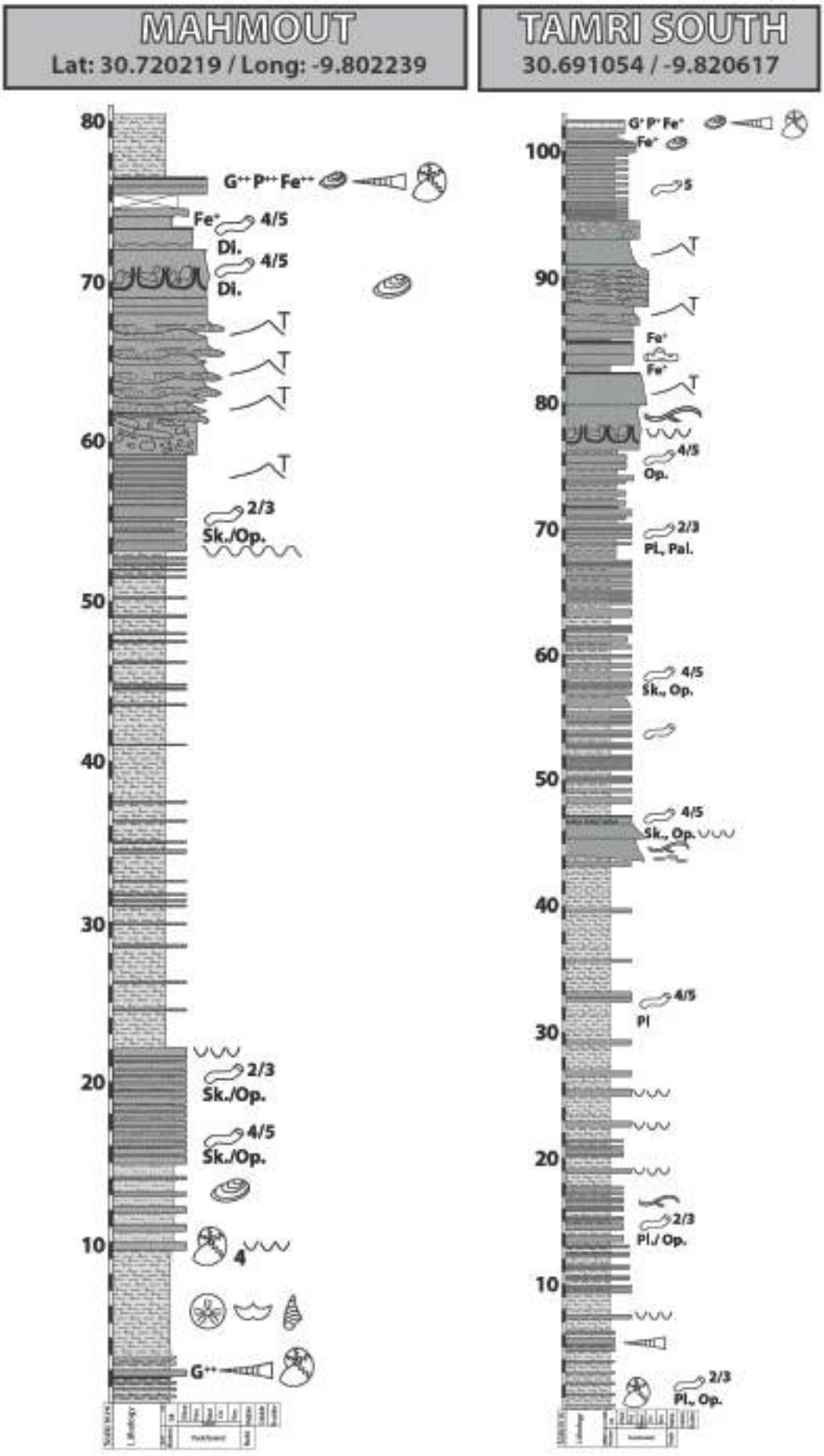

B 9: Stratigraphic Logs Mahmout and Tamri South

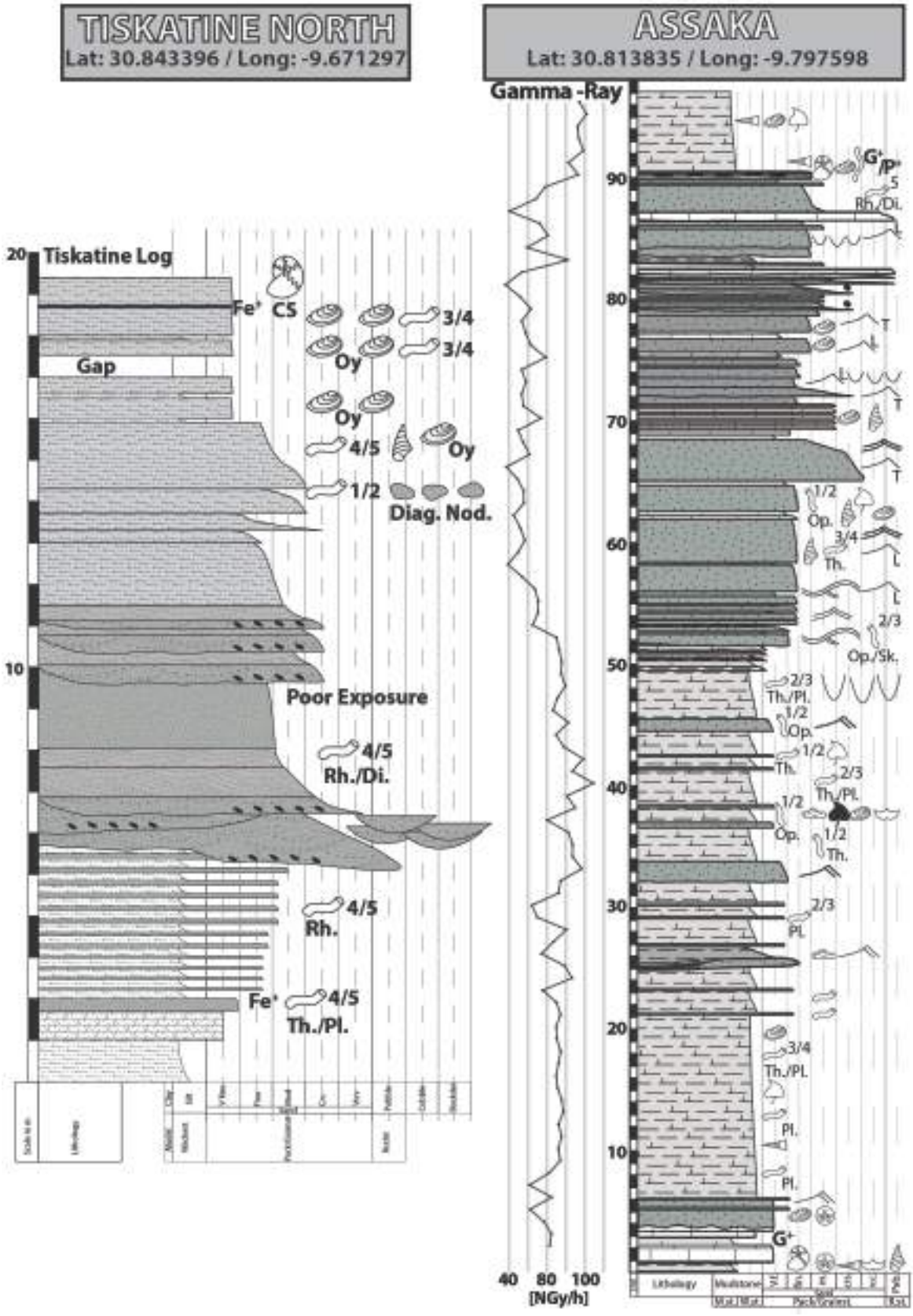

B 10: Stratigraphic Logs Tiskatine North and Assaka

Appendix C: Correlation panels and charts